Chris Magombedze

Geochemical Processes Controlling the Generation and Environmental Impacts of Acid Mine Drainage in Semi Arid Conditions

A Case Study based on Sulphide Metal Mines in Zimbabwe

Thesis for the Philosophiae Doctoral Degree (PhD)

Trondheim, August 2006

Norwegian University of Science and Technology
Faculty of Engineering Science and Technology
Department of Geology and Mineral Resources
Engineering

NTNU
Innovation and Creativity

NTNU
Norwegian University of Science and Technology

Thesis for the degree Philosophiae Doctor (PhD)

Faculty of Engineering Science and Technology
Department of Geology and Mineral Resources Engineering

ISBN 82-471-8244-0 (printed version)
ISBN 82-471-8243-2 (electronic version)
ISSN 1503-8181

Doctoral theses at NTNU, 2006:231

Printed by NTNU-trykk

Acknowledgement

This thesis is based on studies carried out at the Department of Geology and Mineral Resources Engineering (IGB), NTNU and the University of Zimbabwe (UZ) Department of Metallurgical Engineering between February 2002 and August 2006.

I would like to express my profound gratitude to my Supervisor, Professor Knut Lyng Sandvik, for introducing me to NTNU and mostly for his guidance and critical reviews throughout this work. His vast knowledge, experience and availability to visit project sites in Zimbabwe and discuss issues onsite will be most appreciated. I am also grateful to Dr Francis Pedzana Gudyanga, Chairman Research Council of Zimbabwe, who started as co-supervisor in the project and for his support and encouragement during the formulation and early stages of this work. I sincerely thank Dr Ndabezinhle Dube for the fruitful discussions we had while on his sabbatical leave at NTNU and Dr. Ing. Rolf Arne Kleiv for reviewing my thesis at short notice.

This work would not have been possible without the financial support from The Norwegian Research Council's Quota and NUFU Programs. I sincerely thank the coordinators for these programs, Ragnhild Brakstad and Guri Eggan for all the administrative and logistical arrangements pertaining to my studies at NTNU, stay in Norway, and fieldwork in Zimbabwe. I also acknowledge most heartily, the support from University of Zimbabwe, especially the Dean of the Faculty of Engineering – Eng. Wilson Nyemba, for his recommendations to the Vice Chancellor so that I could get study leave to complete this work. A lot of thanks go to my colleagues in the Department of Metallurgical Engineering for shouldering extra responsibilities during my absence. I thank the following people for their support with managing the NUFU cooperation project which enabled me to participate at conferences and attend advanced professional courses during my tenure at NTNU: Professor Terje Malvik, Irene By and Aina Myrvold.

I also want to thank the management of Trojan Nickel Mine, Iron Duke Pyrites and Mazowe Mine for their permission to allow me to carry out fieldwork study at their mine sites. The Concentrator Manager - Stanely Matutu; Plant Manager – Badnock Manda; Plant Engineer – Clifford Mutevhe; Reduction Officer – Paul Mekani; Plant Metallurgist - Richard Chatikobo and Environmental Officers Tsuro and Blessing are appreciated for their fruitful discussions and assistance with sampling, monitoring program and facilitating laboratory analysis at their works.

Technical staff at the Zimbabwe National Water Authority Laboratory, UZ Institute of Mining Research, UZ Department of Metallurgical Engineering and IGB is thanked for handling some of the analytical work for the many samples generated and investigated throughout this study.

To all Doctoral Research Fellows sitting and sharing office space in the F-Block of the 2nd Floor at IGB, thanks for all the technical and moral support. I will remember the informal discussions during our tea time & lunch breaks for many years to come. Special thanks go to Knut Olav Solem and Trinh Quoc Nghia for their assistance with trouble shooting computing problems.

Finally, I want to give thanks to Almighty God for my wife Liliosa Magombedze for her love, patience and encouragement; my daughters Komborero & Lisa Gundani for their cheerfulness; and all the Gundani -Mushandu, Magombedze and Zezai families, relatives and friends for their encouragement, social and moral support over the years. I dedicate this thesis to my distinguished supporters who are unfortunately not there to celebrate my accomplishment: my late 'mother' Agnes Magombedze and my sister Blessing Zivurawa, who both passed away tragically in 2005. May their souls rest in peace!

Abstract

This study evaluates the geochemical processes that control the geochemistry of acid mine drainage in semi arid conditions. The central objective is to characterise and understand the evolution of acid mine drainage and its potential environmental impacts on the Mazowe River sub-catchment, in north east Zimbabwe. The work is based on a case study at three neighbouring metal sulphide mines, namely Trojan Nickel Mine, Mazowe Gold Mine and Iron Duke Pyrites.

The methodology used in this research includes site assessment & characterisation of tailings dumps; waste rock samples; drainage from dumps; surface water and groundwater in the vicinity of the selected mine sites. Geochemical modelling with Phreeqc was used to evaluate pollutant attenuation mechanisms and thereby interpret the environmental effects of over 6 years of acidic seepage infiltration into the groundwater at the most acidic mine in the country, Iron Duke Pyrites. It was also used to predict the seasonal variation in drainage chemistry along Yellow Jacket & Mazowe Rivers due to mixing with other waters or drainage and reaction with bedrock downstream.

The study shows that during the wet season surface water is more prone to acidification than groundwater because the residence time of acidic drainage passing through the soil and shallow bedrock into streams is generally much shorter than that of drainage percolating through the unsaturated zone into the deeper groundwater flowpaths associated with the semi arid climate. During the hot dry season, water flow conditions are greatly reduced and may even stop. This is a favourable condition which limits the rates of sulphide oxidation, acid release and pollutant loadings to the environment. The study discusses several complex mechanisms which act simultaneously on the drainage as it migrates from the source minerals into water and soil changing its chemistry, viz: dilution, precipitation, hydrolysis, adsorption, desorption, complexation, cation exchange, diffusion and evaporation to dryness. These processes play an essential role in the natural attenuation and lowering of toxic concentrations of potentially harmful heavy metals in polluted water draining from the mine sites.

The study has also shown that prediction tests using the standard Sobek humidity cell procedure can overestimate the rates of sulphate generation for semi arid conditions by a factor of four, predicts a shorter time to acidity, and also estimates rather high chemical loadings to the environment than those actually measured when simulated rainfall conditions at a site are used.

Phreeqc geochemical modelling predicts that the resultant environmental effects of more than 6 years of acidic seepage infiltration into Yellow Jacket River at Iron Duke is ‘a pollution time bomb’. A sulphate saturation front of 1795.2 mg/l is progressing through the subsurface at an estimated rate of 6.67 m per year towards the banks of the river. Considering that most of the metal pollutants are associated with sulphate as the dominant anion, a major pollution breakthrough is predicted to occur within 7.5 years when the sulphate saturation front reaches the river. However, simulation prediction shows that the situation could be abated by injecting unpolluted streamwater into the presently polluted aquifer, and shift equilibrium in favour of desorption of pollutants from the currently saturated cation exchangers to the water phase. This is expected to freshen sorption sites of the soil matrix, while allowing a slow dilution process from the injected water to clean up the polluted aquifer.

Organisation of the Thesis

This thesis is organized as a Monograph although chapters 2, 4 and 6 have been published as indicated in the reference section and also from the list of scientific pubications given below.

Chapter 1 gives background information to the research project and justification for the study. The key research issues being addressed, the objectives of the study, methodology, and limitations of the research study are presented in this chapter.

Chapter 2 provides a brief profile of the Zimbabwe Mining Industry and how the nature of mining and mineral processing operations impact on the environment, especially water quality. The problem of AMD in Zimbabwe is introduced in general. The overview is intended to give the reader an overall picture of the state of mining and environment in the country. An overview of mining and the physical environment, size, geographic distribution, employment, production, and economic condition of the metal mining industry are included to give the reader an appreciation of the basic data for the mineral sector of Zimbabwe as in December 2005.

The main objectives of Chapter 3 are to provide a review of acid mine drainage production mechanisms as well as present the current school of thought and practice on methods and techniques used to control and treat AMD. The discussion focuses on the environmental geochemistry of AMD, the applicability of assessment techniques, the shortcomings and reproducibility of control and treatment methods under specific environmental conditions such as semi arid climates. Current industry practice on managing reactive sulphide mine waste and the relevance of such technologies to semi arid climates are also reviewed.

Chapter 4 describes the location, general geology and environmental setting of the case study sites. Most of the data from the field work program is discussed in this chapter, such as field measurements, methods used for solids and water sampling, and the analytical techniques employed to characterise and quantify sample compositions. The environmental conditions at mine sites, potential for metal leaching and risk of AMD to the Mazowe River watershed are assessed from drainage chemistry and discussed with comparison to regulated and background levels.

Chapter 5 describes standard geochemical methods and the proposed modifications to the standard protocols for predicting acid generation for waste materials in semi arid climates. The laboratory tests investigate rates of sulphate generation, estimated time to acidity and correction to field weathering rates.

In Chapter 6 a detailed discussion is given for a full scale study of the geochemical controls on AMD using equilibrium analysis methods and Eh – pH diagram with measurements at plant and field scale for the most acidic mine in the country, Iron Duke Pyrites. The chapter focuses on the effect of geochemical processes on: leachate chemistry; acid neutralisation with lime treatment; and the observed patterns and mechanisms of natural attenuation of acid and metal bearing solutions in the evaporation ponds, shallow aquifer and in sediments & water along the Yellow Jacket River.

The application of Phreeqc geochemical modelling code in predicting water chemistry after AMD – fresh water – mineral interactions at Iron Duke is explored in Chapter 7. The geochemical processes contributing to contaminant transport, retardation and attenuation are evaluated using the model. Predictions are discussed regarding the risks of a major pollution breakthrough from the contaminated aquifer to stream water and a possible remedial option suggested. The supporting data for the modelling is from chapters 4 to 6.

Finally, Chapter 8 gives the conclusions and some recommendations for further study.

List of Scientific Publications from the Thesis – Not Appended

i) Magombedze, C. and Brattli, B, (2003). The Role of Acid Mine Drainage in Heavy Metal Dispersion, in *Proceedings of the 6th International Conference on Acid Rock Drainage 2003*, Cairns, Australia, pp. 1079 – 1084.

ii) Magombedze, C and Sandvik, K.L, (2006). Profile of the Zimbabwe Metal Mining Industry and its Impact on the Environment, in *African Journal of Environmental Impact Assessment and Management*, vol. 11, pp. 42 – 63.

iii) Magombedze, C, Sandvik, K.L, Manda, B & Musiwa, K, (2006). Geochemical Controls on Acid Mine Drainage Neutralization Treatment and Attenuation at Iron Duke Mine, in *Proceedings of Metallurgical Plant Design and Operating Strategies (MetPlant 2006),* Perth, Australia, 18 – 19 September 2006, pp. 440 - 463.

iv) Magombedze, C., Sandvik, K.L., Dube, N., & Mutevhe, C., (2006). Geochemical Mass Balance & Characterisation of Pollutants Draining from a Nickel Mine Site, in *Proceedings of Metallurgical Plant Design and Operating Strategies (MetPlant 2006),* Perth, Australia, 18 – 19 September 2006, pp. 415 - 439.

Table of Contents

CHAPTER 1

GENERAL INTRODUCTION

1.1 Background

There is a growing concern in Zimbabwe among the mining industry, government and researchers that if left unchecked, acid generation from past and present sulphide mining operations poses a significant risk to surface and groundwater pollution. The problem is that the acidic drainage from mineralised areas has a high capacity to dissolve metals, accelerating their turbidity and mobilisation. It is deemed that metals and metal containing substances can accumulate to toxic concentration levels in water or can become bio-magnified in the food chain.

The adoption of the 'Polluter Pays' principle under the Zimbabwe National Water Authority Guidelines (1998) for Effluent Discharge limits and the Environmental Management Act (2003), has put the mining industry under great pressure to control the quality of drainage from mine sites. The perception of government policy makers and the general public is to categorise effluents from mine sites as 'very dangerous'. Inevitably, such generalisation calls for regulation of pollutant concentrations in discharged effluents, but sometimes to unattainable levels in mineralised environments. The mining industry argues that such strict measures being imposed without a scientific basis may place limitations on expansion programs and the general viability of operations. Therefore, the challenge is to harmonise regulatory policies with supporting scientific information, and establish a technical framework that will guide sustainable environmental stewardship.

Studies on acid mine drainage issues in Zimbabwe have not yet realised the high profile in the national public perception that it has in some developed mining countries like USA, Australia, Canada, South Africa, etc. This research was formulated on the basis that there is currently no sufficient scientific information on case studies in Zimbabwe to guide the ways government and industry operate in controlling and managing pollution from sulphide metal mines. An integral part of the control or the management of AMD is the understanding of the physical, chemical, biological, hydrological and geographical aspects of the problem. The input of many disciplines in minerals engineering is required to address the research needs and challenges we face in environmental protection and achieving sustainability in the mining industry as a developing country.

The Nature of Acid Mine Drainage

Acid mine drainage (AMD) results from the oxidative dissolution of sulphide minerals contained in mine waste materials with subsequent release of acidity, dissolved metals and sulphate to the environment. It is considered the single most important environmental problem world wide facing the mining industry in recent years, (White *et al.,* 1999; Jambor *et al.,* 2002). By its acidic nature, AMD poses a significant threat to ecosystem functioning around mine sites and to the sustainability of the metal mining industry itself, (Miller *et al.,* 1991 and Weatherel, *et al.,* 1997).

More than 90% of Zimbabwe’s operating mines process sulphide metal bearing minerals and hence, pollution of natural water sources is a major concern to the industry, government, scientific community and the general public. The generation of AMD is a natural phenomenon occurring in sulphide bearing rock materials and resulting in the production of acidic discharge. The sulphide minerals are oxidised when exposed to oxygen and water. The low pH drainage seeps through waste rock piles, tailing dumps, and country rocks, dissolving metals along its flow path, which then find their way into surface and ground waters. Elevated concentrations of metals can include typical major rock constituents (Ca, Mg, Na, K, Fe, Mn & Al) as well as trace elements such as Cu, Cd, Pb, Ni, As & Zn. These contaminated waters have a negative impact on public health, life of aquatic organisms, animal health, vegetation, soil quality and lead to the impairment of engineering materials.

Global Challenges with AMD Control and Management

Control technologies are applied where AMD formation has already taken place or is anticipated. At source control methods aim to stop or retard pyrite oxidation by reducing the volume of water and/or oxygen infiltrating into the waste piles. Treatment methods add neutralising chemicals such as limestone, lime, sodium hydroxide, etc, directly to the acidified water or direct the acidic drainage through passive systems for treatment. Chemical treatment is often a long term prospect, expensive and with liabilities. Re-vegetation over waste piles stabilises the piles with respect to air and water erosion, but does little to prevent or curtail sulphide oxidation and the subsequent discharge of polluted acidic water. Selection and design of an AMD abatement technology is largely site specific and based on water chemistry, flow rate, local conditions and site characteristics, (Faulkner and Skousen, 1994).

Some of the control techniques have been very successful while others have achieved very poor results. The Løkken mine, in Norway, operated for 333 years as a copper mine, then a pyrite mine and finally a copper-zinc mine. It became the most acidic mine in the country, with mine water having the following composition: pH - 2.3; 530 mg/l Cu; 870 mg/l Zn and 1529 mg/l Fe, averaged over 15 years, (Arnesen, 1999). The mine was closed in 1987, flooded and plugged, leading to less sulphates and metals in the water for almost 15 years. Sandvik and Ese (2002) have recently observed a resurgence in metal concentrations and a sharp drop in pH to around 2.9, in the mine water. Presumably a lot of equipment was left in the adits at the time of closure, but besides the probable iron reaction from this, it is still very difficult to account for the observed changes.

There can be a lag period between waste placement and sulphide oxidation, and between sulphide oxidation and the appearance of acidic drainage. The actual times associated with these phases are at present very ill defined, (Miller *et al.*, 2003). High sulphur waste may generate acid a few days after exposure whereas low sulphur (<2%) waste with some carbonate may not release acid for several years or decades, (Jampor *et al.,* 2002). After pyrite oxidation it is usually not possible to stop subsequent acid production. As the acidic drainage is transported or dispersed away from the source, it is not clear whether there is a general decay in the pollution profile or remobilisation and regeneration (resurgence) in terms of pollutant loads. It is widely accepted that once discharge of contaminated acidic water occurs from a mine waste dump, it becomes a 'perpetual pollution machine'.

Scope of the Current Study

The geochemical environment that exits in mine waste/tailings piles provides a basis for assessing the equilibrium and kinetic controls on factors which affect the major processes in the system such as sulphide oxidation, acid production and transport and fate of contaminants. Such controls include lithology (rock types, porosity and accessory minerals); mineralogy; acid/base balance; reaction rates; depositional environment; microbiological and mine site hydrology, which limit or accelerate the overall acidification process. A detailed evaluation of the mechanisms by which these controls regulate the fate and distribution of contaminants in specific environs may provide an insight on how to manipulate some of the controls in order to effectively manage AMD.

1.2 Research Issues being addressed in this Study

a) Hydro-geochemical Characterisation of Mine site Drainage in the Mazowe Catchment

About 90% of the 150 metal-related mines across Zimbabwe contain sulphide rock materials that are either currently producing acid drainage or have the potential to do so if exposed to oxidising conditions. The full extent of the impact of acid drainage and heavy metal contamination on the environment has never been assessed in Zimbabwe. There is lack of detailed hydro-geochemical characterisation, as well as baseline data on mass loadings and environmental parameters at mine sites. There is need for an assessment to establish the contribution of each mine to acid mine drainage pollution on a watershed basis. Such an assessment requires evaluation of geochemical processes over time and analysis of specific parameters not always measured in routine water quality analyses.

b) Geochemical Controls Governing the Environmental Geochemistry of AMD in Semi Arid Environments

The interactive nature of the composition of mine waste, geochemical controls and predominant mechanisms in the generation of acid mine drainage play a critical role in acid dispersion patterns, attenuation and fate. Evaluating and understanding these controls and their mechanisms at selected sites would allow the design of a systematic environmental assessment procedure for all the potential and current acid producing sites. The discharge of AMD into soil and natural water systems results in numerous physical, chemical and biological responses in which the environment can be modified detrimentally.

Water plays a significant role in heavy metal mobilisation. It acts as a storage buffer for the pollutants, as the medium in which most of the reactions take place, and is undoubtedly the most significant transport vector in the pollution process, (Salomons, 1995). In wetter cold environments, dilution reduces metal concentration of acidic discharges. However, in arid and semi arid climates such as Zimbabwe, acidic leachates can be highly concentrated with toxic heavy metals, and dispersion is largely affected by seasonal variations in the hydrologic cycle. The exact effects of the dry and wet cycles on drainage quality and metal transport, dispersion and attenuation are not known and need to be investigated.

1.3 Problem Statement

Sulphide wastes from metal mining in Zimbabwe are disposed without any measures to prevent or control acid generation. Contrary to a previously accepted view that in this semi arid climate, prolonged dry spells and re-vegetating mine waste piles will prevent AMD, several mine locations are indicating pollution problems from acid mine drainage and heavy metals contamination. The water quality of the Mazowe River sub-catchment in north east Zimbabwe is strongly influenced by naturally mineralised and polluted waters draining from mine sites and discharged to the surficial flows, (Magombedze and Brattli, 2003; Lupankwa *et al.,* 2004; Ravengai *et al.,* 2005).

It is commonly understood that the quality of drainage is primarily a function of mine waste composition and the availability of water & oxygen, and also widely accepted that the drainage quality varies with time and distance along its flow path. These conditions are variable even within a mine site. The evolution in the geochemistry of AMD as it disperses from the primary source minerals until final attenuation is subject to site specific influences and necessitates site specific evaluation. Information on the propagation of the acid flux, exact causes & effects of secondary minerals, and the mechanisms by which the master variables of pH and redox potential continue to influence acid attenuation and resurgence profiles under conditions of aridity is missing from the literature.

Generally, pollution is a localised phenomenon, decreasing with distance from the pollution source. This means that there are natural processes that act to reduce metal concentration fluxes in aquatic environments downstream of impacted mine sites. Such processes help to mitigate the effects of water borne pollutants on the receiving environment and can be taken advantage of to find natural and cost effective solutions to the control and management of AMD. The fundamental questions being addressed in this research work are as follows:

a) What is the magnitude of the risk of AMD, potential for metal leaching and impact on water quality draining from mine sites?
b) How do the geochemical processes change in response to dry and wet weather conditions and what are the effects of such changes on drainage chemistry?
c) How do the seasonal changes in geochemical processes impact the acid flux, profile of AMD and management control measures with time and in space?
d) If a real threat from acid mine drainage related pollution on the Mazowe River sub-catchment exists, when can this reach catastrophic levels?

e) Is natural attenuation a possible remedial option at some sites, and can it be exploited sufficiently and reliably to achieve regulatory compliance in an acceptable time frame?

In order to answer the above questions, and to choose and implement cost effective technologies in alleviating the problems of AMD under semi arid environments, it is necessary that the quality of the present drainage be determined and that of the future be predicted. The extrapolation of laboratory test data to prediction of field behaviour over time is not well defined in the literature. Furthermore, there is insufficient laboratory prediction data and corresponding field behaviour to define a general correlation between the two. These comparisons must be made on a site specific basis, influenced by the mine plan, geology, climate, topography and hydrology of the area. Materials of particular concern are those for which there is a long lag time until the onset of acid generation.

1.4 Hypothesis and Research Objectives

It is hypothesised that drainage characteristics and environmental impact are time and flow path dependent. The main objective of this study is to evaluate the geochemical controls responsible for changes in the geochemical signature of acid mine drainage under semi arid conditions. This requires site assessment and geochemical investigations (on a seasonal basis) of AMD potential, impact on fresh water recipients, geochemical modelling prediction of long term leachate chemistry and pollutant loadings to a watershed impacted by several mines. The broad objective encompasses four specific goals which are interrelated, namely:

- To identify mine wastes susceptible to AMD generation and metal leaching, and ascertain the potential risk in degrading water quality
- To evaluate the reliability of some of the prediction techniques in forecasting actual field behaviour of mine site drainage quality under wet and dry weather cycles
- To determine the effect of geochemical controls on the environmental geochemistry or evolution of AMD under semi arid conditions
- To predict the levels and variability of drainage pollutants in a watershed impacted by neighbouring mines over time

1.5 Research Methodology

The strategy adopted in this research is to use an integrated, multidisciplinary approach that recognises that there are four key areas associated with control and management of AMD, namely: identification/assessment; prediction; treatment and mitigation. The case study involves three neighbouring mine sites located in the Mazowe River watershed, in north east Zimbabwe. The mines are Trojan Nickel Mine, Mazowe Gold Mine and Iron Duke Pyrites. The approach in this study involves three elements:

i) Field Site Assessment and Characterisation
ii) Laboratory Geochemical Prediction Tests and
iii) Geochemical Modelling. Both the field and laboratory data are used to support geochemical modelling.

1.5.1 Site Assessment and Characterisation

The specific goals of site assessment and characterisation are to:

- Identify the types and quantities of mine waste materials and determine period of exposure
- Assess the sources and path ways for acid and metal release, quality of drainage from waste piles, mine water, and determine the extend of AMD pollution in water streams draining from mine sites
- Study observed patterns in terms of pollutant load distribution from point source, direction (preferential flow paths), decay and resurgence profiles
- Monitor parameters which control acid flux and chemical character of the drainage
- Assess waste handling procedures at the mine sites and how they influence observed drainage quality
- Ascertain hydrological data, climate and topography from current measurements and historical mine records
- Establish a sampling and monitoring program based on the site plan drainage pattern

1.5.2 Geochemical Prediction Tests

The purpose of geochemical prediction tests are to:

- Ascertain the mineralogy and chemical composition with a view to establish neutralising and acid generating minerals
- Conduct acid base balance through static prediction tests in order to determine the acid generation and neutralisation potentials
- Carry out kinetic tests for assessment of the reactivity of waste materials and mode of acid generation, change of drainage quality with time, and determination of potential pollutant loads and behaviour during dry and wet seasons

1.5.3 Geochemical Modelling

It is well known that pollution from mining sources can take place during mine operation or after mine closure. The long term nature of mining impacts requires predictive tools and monitoring of any negative changes in the geochemistry of the mine waste material over time, (Lappako, 2002). Predictive tools can help mitigate potential problems by factoring control measures into facility designs and operating plans, while design or operation can be modified based on monitoring. Models allow a maximum number of interactive input variables and quick calculations. This greatly improves the ability to predict impacts resulting from a given mine site for which the model calibration is valid, allowing for reliable, technically supported decision making on AMD control and management.

Geochemical modelling is an invaluable tool for predicting future water quality in catchments impacted by acid mine drainage. The principal modelling goal is to evaluate AMD attenuation mechanisms and thereby predict variation in pollutant characteristics at Iron Duke Mine (the most acidic site) and downstream environments. It is intended to address the question of transport and dispersion of the acid flux, the nature and result of its interactions with clean water, soil and rock along its flow paths. Because geochemical reactions affect solute concentrations in space and in time, geochemical modelling is intended to answer some of the following questions.

- What geochemical reactions take place to enhance or attenuate AMD pollution along its flowpath and what processes retard the migration of pollutants?

- How fast do the contaminants progress downstream and through the groundwater aquifer, and if variables such as pH or pe or P_{CO2} changes, how does the system equilibrium change?
- Will the concentrations of the contaminants be above regulatory thresholds, and what happens if the AMD is mixed with fresh water?
- What happens to the resultant water chemistry when an acidic solution is reacted with minerals A, B and/or C, and what minerals are saturated in the system?
- Is natural attenuation a possible option for control and mitigation?

A geochemical modelling program called PHREEQC, developed by Parkhurst and Appelo (1999), has been selected for the purpose. It is a program designed to model geochemical reactions, based on ion pairing and can calculate pH, redox potential, and mass transfer based on reaction progress. The composition of solutions in equilibrium with multiple phases can be calculated.

1.6 Data Quality Control, Analysis and Graphical Methods

Field Measurements and Instruments Calibration

A variety of special sampling and preservation techniques were employed for the analysis of major and trace species in water samples and leachates measured during the study. All natural water samples were filtered through a 0.45 micron pore diameter filter to remove all suspended clays and most bacteria. The filtering was required to ensure that the laboratory analysis represents dissolved species and not suspended constituents which may be contributed from erosion. The dissolved species are the ones which take part in most geochemical reactions and are used in chemical equilibrium equations. Samples for cation analysis were acidified with 65% nitric acid to pH < 2 in order to keep the metals in solution. Samples for anion analysis were filtered but not acidified.

Geochemical studies are based on the measurement of the inorganic constituents in a water sample and a series of parameters that control the interactions of these constituents. Certain parameters are difficult to preserve during storage and were measured in the field using the Myron Ultrameter Model 6P (1999), viz: Temperature; pH; EC; TDS; Redox potential (ORP); and Alkalinity (by titration). The instrument was calibrated with reference buffer solutions of pH 4, 7 and 10; the EC and Redox potential electrodes were also checked against the manufacture's supplied solution.

Chemical Data Criteria Limits

Accurate analysis of environmental samples for their total or partial elemental content is a simple routine task but numerous problems must be addressed to assure a high quality analysis (Crock and others, 1999). The following accuracy checks were used to assess the analytical quality of the chemical data for purposes of this study.

a) Major ion charge balance % error

Chemical analysis of all water samples were tested for charge balance (Freeze and Cherry, 1979).

$$\%CB = \frac{\sum z.m_c - \sum z.m_a}{\sum z.m_c + \sum z.m_a}.100 \qquad (1.1)$$

where %CB is the charge balance error, z is the absolute value of the ionic valence, m_c the molality of cationic species and m_a is the molality of anionic species.

b) Measured total dissolved solids (TDS) versus specific conductance (EC)
c) Calculated TDS versus measured TDS
d) Anions or cations versus specific conductance

The limits for the above criteria are summarised in Table 1.1.

Table 1.1: Data Quality Control Criteria limits

Rating	Action	Charge Balance % error	Measured TDS:EC	Calculated TDS: Measured TDS (% difference)	Anions or Cations : EC (% difference)
Good	Accept Analysis	< 10	0.55 – 0.75	< 10	< 10
Marginal	Repeat/Duplicate	10 - 15	0.50-0.49 or 0.76-0.90	10 – 20	10 – 20
Poor	Reject Analysis	> 15	< 0.50 or >0.90	> 20	> 20

Censored Data

Water chemistry data is frequently censored, meaning that concentrations of some elements are reported as non-detected, less than or greater than. These values are created by the lower or upper detection limit of the instrument or method used. Censored data are not appropriate for statistical analysis and therefore must be replaced with unqualified values, (Farnham *et al.,* 2002). In this study, there were no censored values for the upper detection limit for the 21 variables used (Temperature, pH, TDS, EC, ORP, DO, Acidity, Alkalinity, SO_4^{2-}, NO_3^-, Cl^-, Fe, Mn, Al, Ni, Cu, Zn, Ca, Mg, K

& Na). However, there were censored values for the lower detection limits on trace elements and half the value of the lower detection limit was used in those cases for statistical calculations, (Jin *et al.,* 2001).

Application of Statistics on Drainage Composition Data

When dealing with environmental geochemical data, many questions may be encountered such as probability distribution, mean calculation, correlation, outlier detection and differentiation of anthropogenic from natural background values, (Zhang and Selinus, 1998). Identification of a probability distribution is useful to differentiate between sample populations and to provide basic information for the subsequent statistical analysis. Statistical associations do not necessarily establish cause-and-effect relationships, but do present the information in a compact format as the first step in the complete analysis of the data. This can assist in generating hypothesis for the interpretation of hydro-chemical processes, (Guler *et al.,* 2002).

The application of statistics in this study is limited to evaluating the distribution characteristics of individual variables measured or analysed. The physical and chemical properties are evaluated using central tendency (mean, median, dispersion or standard deviation, skewness and kurtosis) assuming the data were normally distributed or log-normally distributed. Statistical and graphical analyses are done using Microsoft Excel 2003 (Microsoft Corporation, 1985), Sigma Plot 9.0 (STATCON, 2001) and Phreeqc (Parkhurst & Appelo, 1999) commercial software packages to show graphical displays of the data as histograms, scatter plots, probability plots and box plots.

1.7 Limitations of the Research

Ores are valued chiefly for the metals they contain, which are recovered for use as constituents of alloys, chemicals, pigments, or other products. In the context of this report, the metal mining industry is defined to include facilities engaged primarily in exploring for metallic minerals, developing mines, ore mining, ore dressing and beneficiation operations. Environmental impacts from coal mining, small scale operations, riverbed gold panning and ore or concentrate smelting operations are not covered in this report. Background minerals that result from pre-mining weathering could not be assessed since all sample locations were from operating mine sites. Biota such as crops, vegetation, livestock, fish or other aquatic organisms were not sampled as this was beyond the scope of this study. The study does not cover nor include any investigations on air pollution, organic pollutants, toxicity or uptake of pollutants by organisms and their behaviour in the food chain.

CHAPTER 2

PROFILE OF THE ZIMBABWE METAL MINING INDUSTRY AND ITS IMPACT ON THE ENVIRONMENT

2.1 Introduction

This chapter seeks to present an overview of the metal mining and mineral processing operations in Zimbabwe as a basis for understanding the nature of these operations and how they impact the biophysical environment. The specific requirements of the legal framework or legislation on mining and the environment are presented. The chapter also seeks to highlight the problem of acid mine drainage in Zimbabwe and its impact on water quality. The problem of AMD, its potential threat to human health & the environment are discussed in light of the new legislation on environment (Environmental Management Act, 2003), and requirements on Waste Water & Effluent Discharge Regulations (1998).

Mining of minerals is an essential economic activity that provides the raw materials for our industrialised society and is driven by the need to make profit. The extraction and beneficiation of these minerals generate large amounts of wastes which become exposed to accelerated weathering leading to increased metal loading to the environment, (Arnesen, 1999). Unless adequate precautions are taken, mining can be accompanied by serious negative impacts on the environment and human health. Mining can change the landscape, alter water tables, disrupt the local ecology, generate serious air and water pollution, and permanently degrade large areas of land. Exposure to toxic chemicals, dusts, heat and noise can seriously affect the health of workers.

Zimbabwe produces over forty metals and minerals including precious metals, platinum group metals (PGM's), base metals, industrial minerals, iron & steel, diamond, asbestos, ferrochromium alloys and coal. Gold and platinum contribute over 70% of foreign earnings from mineral production. The industry is dominated by large scale multinational companies but small scale miners in the gold and chrome sectors also make significant contributions to minerals production, (Maponga & Mutemererwa, 1995). Despite this socioeconomic importance, effluent discharges from mining point sources represent a significant threat to water quality with implications to human health via consumption of contaminated drinking water & fish. Aquatic ecosystem integrity is also impaired through toxicity and poisoning from pollutants, leading to changes in ecosystem structure and function and overall aquatic biodiversity, (Zelmanowitz, *et al.*, 1995).

The typical life cycle of a mining operation consists of sequential phases such as prospecting, development, operation, decommissioning and eventually closure. Each phase is associated with different environmental impacts which have the potential to drive environmental change in several different ways and at various scales, (Ashtorn *et al.,* 2001). The environmental impacts of mining and metal processing in Zimbabwe originate from the two sections characteristic of the industry, namely: the large scale formal mining operations and small scale informal miners involved in gold panning, including riverbed and chrome mining.

Some of the serious environmental damage from small scale operators includes river siltation and land disturbance, mercury poisoning, deforestation, health & safety due to unprotected mine shafts and poor housing and sanitation conditions. The large mines extract ore with sulphide mineralization and sulphides oxidize in the presence of water and oxygen resulting in acidic drainage high in sulphate and toxic metal concentrations. Most of the currently known methods that deal with acidic drainage and toxic residual process chemicals have largely revolved around containing the mine waste in structures such as tailings dams. Though tailings dam failure is not a common occurrence in Zimbabwe, acidic seepage from the dams & waste rock piles often find its way to fresh water recipients around mine locations.

2.2 Overview of Mining in Zimbabwe

Geological Outline

Zimbabwe is a landlocked country in central Southern Africa. It consists predominantly of Precambrian rocks, which can be divided into five major geological units:

a) *The Archean Craton - granite/greenstones:* cover about half of Zimbabwe and form the central part of the country.
b) *The Archean Limpopo Mobile Belt:* located between the Archean Craton and the Kapvaal Cratons in the south. It is characterised by high grade metamorphic rocks that have undergone polyphase deformation.
c) *The Paleoproterozoic Umkondo and Lomagundi Group:* low grade metasediments of the Umkondo group which are exposed in the east - southeast along the border with Mozambique.
d) *The Neoprotorozoic Makuti, Rushinga and Sijarira Groups:* metasedimentary successions in the northwest part of the country.
e) *The Great Dyke*: a massive intrusive body with similarities to the Bushveld Complex of South Africa, hosts most of the gold, PGM's, base metal and

chromite mines. The Great Dyke is one of the longest mafic and ultramafic layered intrusions in the world, crossing the country for about 550km in a north-north easterly direction. It varies in width from 4 km to 12 km, and age is estimated at 2,586 $^{+}/_{-}$ 16 million years (Mukasa *et al.,* 1998). Figure 1 shows a map of the geology of Zimbabwe, adapted from Batholomew (1994).

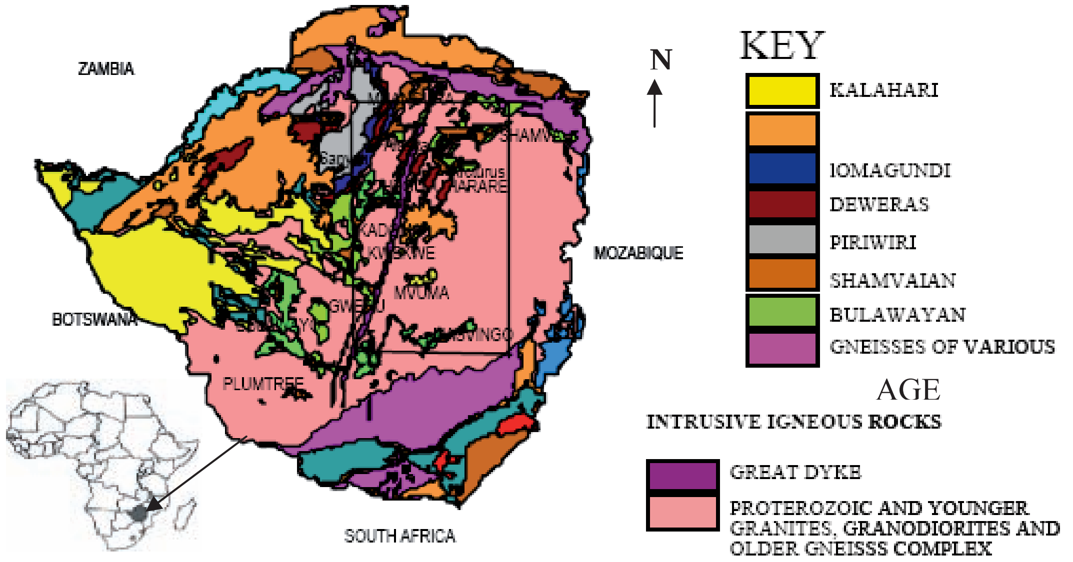

Figure 2.1: Geological map of Zimbabwe

Geographic Distribution and Structure of the Industry

The country is divided into four mining districts or regions as depicted in Table 2.1. and Figure 2.2. Harare Mining Region covers mines located in Mashonaland East, Mashonaland Central and some parts of Mashonaland West provinces. The Midlands Mining Region covers all the platinum producing mines (Zimplats, Ngezi mine in Mhondoro, Unki mine, & Mimosa), all of the gold mines around Kadoma, Chakari, Sanyati Copper Mine in Gokwe, chrome & iron ore mines in central Midlands and asbestos and diamond mines in the Zvishavane and Mberengwa districts. Renco and Penhalonga gold mines are the only notable large scale gold mines which lie in the MasvingoRegion.

Bulawayo Region hosts River Ranch Diamond in Beit Bridge, How mine & Vubachikwe gold mines, as well as Wankie Colleiry, the only coalmine in the country. Though mining operations are performed throughout Zimbabwe, the concentration of metal mining is located around the Great Dyke.

Table2.1: Geographical spread of operating mines in Zimbabwe

Region/Mining District	Large Formal Mines*		Small Scale & Syndicates**		Riverbed gold panning
	Gold	*Base Metals & Other*	*Gold*	*Base Metals & Other*	*km of rivers affected*
Harare	7	21	11	25	55
Midlands	8	5	30	12	80
Bulawayo	18	4	21	0	80
Masvingo-Mutare	2	9	2	0	120

*More than 50 people labour force & mechanised; **More than 20 but less than 50

Source: Extracted from schedule of mining claims registered at the Office of the Mining Commissioner, Harare, 2003.

Fig.2.2: Zimbabwe Mining Districts & Major Mineral Locations

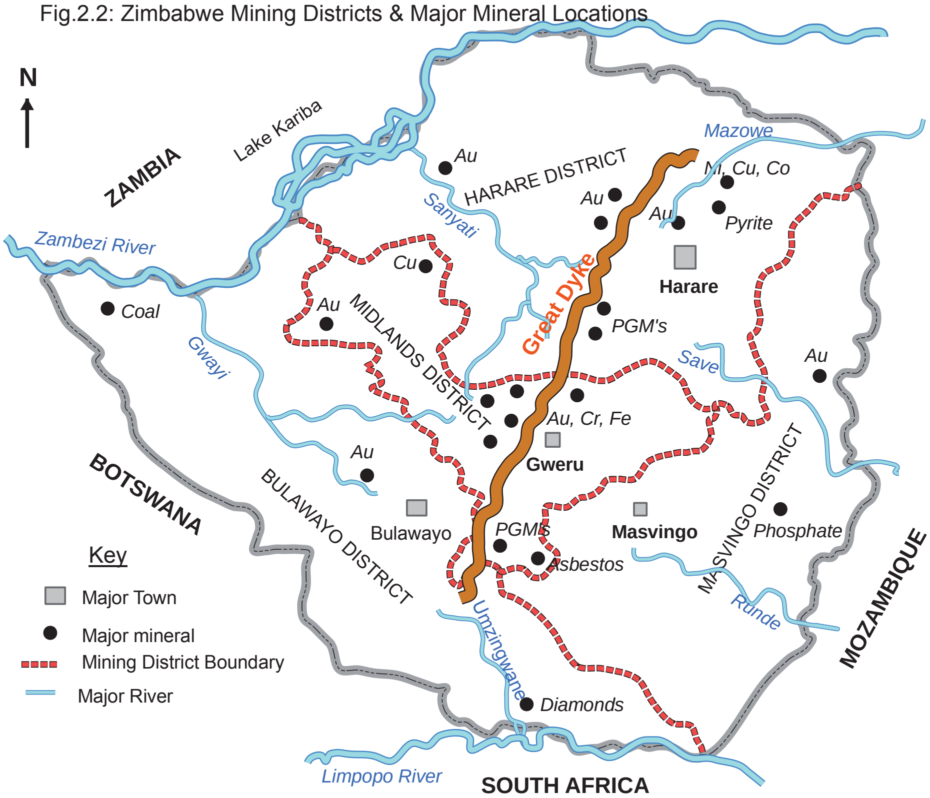

The industry is dominated by few large multinational mining companies which are predominantly foreign owned, and which produce the bulk of the mineral output. Besides the major foreign companies that dominate mining, there is a growing informal sector, particularly in gold panning and chrome mining. There are approximately 1,000 operating mines (mainly gold) worked by small companies, syndicates and individuals, (Larson and Guyette, 2002). The large number of panners, estimated at between 50,000 and 500,000, coupled with the enormous geographic expanse of the activity, makes gold panning currently difficult to regulate. These comprise mainly registered and unlicensed operators from an individual to a syndicate, working on small gold reefs, chrome seams and gold panning along rivers. Group numbers are usually less than 50 and mostly characterised by poor methods of ore extraction due to lack of mechanised equipment. Operations are not continuous and depend heavily on seasonal rainfall/drought patterns and alternative employment.

2.3 Minerals Production and Waste Generation

Open Pit and Underground Mining Methods

There are two mining methods most commonly used at mines in Zimbabwe. Surface mining is favoured when the characteristic of the ore deposit (e.g. location, size & grade) make it cost effective to remove the overburden. This is the most economical way to mine highly disseminated low grade deposits but has more physical impacts on the environment than underground mining. For the large ore bodies at Ngezi Platinum Mine, Ripple Creek Iron Ore Mine, Freda Rebeca Gold Mine, Sanyati Copper Mine & Eureka Gold Mine, the ore bodies are typically mined in benches by drilling vertical holes from the top of the bench and blasting the ore onto the adjacent lower level. At Wankie Colliery, the less resistant coal materials are excavated by scraping machinery without the use of explosives. For primary blasting, virtually all open pit mines use fertiliser grade ammonium nitrate (ANFO) explosives mixed with 6% fuel oil.

Underground mining is the major method for the production of metals from sulphide deposits. Typically it has less visual impact on the environment compared to surface mining in that there is reduced surface disturbance and lower quantities of materials that must be removed and disposed as waste. Table 2.2 shows extraction methods for major metals mined in Zimbabwe and the nature of waste materials generated.

Table 2.2: Metal Extraction Processes and Waste Materials

Metal	**Mining Method**	**Beneficiation Method**	**Primary Waste Materials**
Gold & Silver	Surface & Underground	➢ Milling ➢ Cyanidation (CIP, CIL, CIS) ➢ Elution ➢ Electrowinning/zinc precipitation ➢ Smelting	➢ Mine water ➢ Overburden ➢ Waste rock ➢ Dust ➢ Tailings ➢ Spent solutions
Alluvial Gold	Riverbed	➢ Panning (small scale) ➢ Sluice Box ➢ Gravity concentration	➢ Process water ➢ River silt & bedrock ➢ Mercury
Platinum Group Metals (Platinum, Paladium, Rhodium, Iridium & Rhuthenium*)*	Surface & Underground	➢ Milling ➢ Flotation ➢ Smelting	➢ Mine water ➢ Overburden ➢ Waste rock ➢ Dust ➢ Tailings ➢ Slag
Base Metals (Nickel, Copper & Cobalt)	Surface & Underground	➢ Milling ➢ Acid Heap Leaching ➢ Solvent Extraction & Electrowinning ➢ Flotation ➢ Smelting	➢ Mine water ➢ Overburden ➢ Waste rock ➢ Spent ore ➢ Tailings ➢ Spent Leach solution ➢ Slag
Chromite	Surface & Underground	➢ Milling ➢ Briquetting ➢ Smelting Arc Furnace	➢ Waste Rock ➢ Overburden ➢ Slag
Iron	Surface	➢ Milling ➢ Magnetic separation ➢ Sintering ➢ Blast Furnace	➢ Waste rock ➢ Overburden ➢ Dust ➢ Slag
Pyrites	Underground	➢ Gravity concentration ➢ Roasting	➢ Mine water Waste rock; SO_2

Beneficiation Techniques

After the ore is extracted from the mine, the first step in beneficiation is *comminution* (crushing & grinding) to liberate the valuable minerals from the less valuable rock. Beneficiation or ore dressing includes physical separation techniques such as gravity concentration, magnetic separation, heavy media separation, electrostatic separation and flotation. Generally no chemical changes occur in the mineral during beneficiation which simply utilises the differences in physical properties between valuable mineral and gangue to achieve separation. Such properties include: specific gravity, magnetic susceptibility and surface affinity for certain chemicals.

Ore dressing and milling operations serve to separate and concentrate the mineral values from waste material, remove impurities, or prepare the ore for further refinement. Gravity concentration, which exploits the density difference between valuable and gangue minerals, is a common part of the milling circuit at most gold mines in Zimbabwe. The Shaking Table in conjunction with amalgamation and Knelson Concentrators are used to recover almost 50% of the gold production. The gold is usually found in quartzite veins hosted in mildly sulphide material. The remaining gold is usually recovered by cyanidation employing the technology of carbon in pulp (CIP) as at Jumbo, Acturas, Shamva & How mines) or carbon in leach (CIL) as at Ashanti Goldfields and Renco mines).

Flotation, the most versatile mineral separation technique in mineral processing, utilises the physico-chemical surface properties of sulphide minerals to effect separation. After treatment with reagents, surface properties of finely ground ore change, causing some minerals to become air avid (hydrophobic) while others become water ‘loving’ (hydrophilic). The technique is used to produce base metals at Trojan Nickel Mine and platinum group metals at the Makwiro Metallurgical complex.

Heap leaching is applied to the dissolution of soluble minerals such as copper at Sanyati Copper Mine and gold at Chaka Mine near Kwekwe. The ore material to be leached is placed on the ground and a leaching solution is applied. As the liquid percolates through the ore, it leaches out metals, and impermeable liners under the leach material assist in recovery of the leachate. Leaching can take place from several months to years, and the spent ore is left in place after rinsing or some other detoxification.

Waste Generation Volumes

In metal mining in general, there is a high volume of waste to product ratio, implying that the waste volumes generated during the recovery of a target mineral can be very high, a feature which distinguishes mining from other waste generating industries. 'Waste' is defined as rock that must be broken and disposed of in order to gain access to and excavate the ore. Most of the waste rock generated is disposed of in piles near the mine site. Tailings are the valueless material generated from beneficiation activities.
Conventional beneficiation processes generate tailings which generally leave the plant as slurry consisting of 30 to 60% solids, and are disposed of in onsite impoundments such as tailings ponds.

Table 2.3 shows waste generation volumes at prominent mines in Zimbabwe. The extraction and beneficiation of metals produce significant amounts of waste and by-products. Total waste produced can range from 10 percent of the total material mined to well over 99 percent. The volume of total waste can be enormous. At mining sites, the major sources of pollution include waste rock, overburden disposal, tailings, and mine water, much of which is introduced directly or indirectly to rivers and streams. Pollution from mining sources can take place during mine operation or after mine closure.

2.4 Basic Economic Data on the Mineral Sector

Mining Industry's Contribution to National Economy

The Zimbabwean economy depends heavily on mining and the processing of metals, non-metal minerals, coal and industrial minerals. Most of Zimbabwe's modern day cities and towns owe their origin to the discovery and development of mining or agricultural activity at these locations. The country is relatively well endowed with mineral resources. Over 40 different types of minerals are mined in Zimbabwe. The country is the world's third largest known source of high grade chromite, second largest source of platinum group metals and significant reserves of nickel are located in Zimbabwe's Great Dyke craton. Furthermore, significant attention has been focused on diamonds in recent years, following a country-wide aero-magnetic survey that drew attention to several potential diamond deposits. Zimbabwe is the fourth largest producer and exporter of asbestos, after the Russian Federation, Canada, and Brazil.

Table 2.3: Waste generation volumes at major metal mines

Mine District	**Mine**	**Mineralogy**	**Production ore tons/yr**	**Waste on surface million tons**		**Mining Method**
				Waste rock	Tails *(Mine H_2O)*	
Harare	*Ashanti*	Au in S^{2-}	1 020 000	2 .4	11.5	Open pit & Underground
	Jumbo	"	79 200	0.7	1.2	Underground
	Acturus	"	132 000	1.1	2.3	Open pit & Underground
	Shamva	Au in S^{2-}	90 000	1.2	2.1	"
	Trojan	Ni, Cu & Co in S^{2-}	972 000	5.2	110.8	"
	Iron- Duke	FeS_2	70000	0.25	*($180m^3/day$)*	Underground
Midlands	*Zimplats*	Pt, Cu, Ni, & Co in S^{2-} Fe as Fe_2O_3	2 200 000	6.5	9.5	Open pit & Underground
	Ripple-Creek	Cr	600 000	24.4	0	Open pit
	Zimasco		700 000	15.8	3.5	Open pit
Bulawayo	*How*	Au in S^{2-}	150 000	1.7	3.2	Underground
	Wankie	Coal	5 000 000	9.5	6.7	Open pit & underground
Masvingo-Mutare	*Penhalonga*	Au in S^{2-}	120 000	0.8	1.7	Underground
	Dorowa Phosphate	P_2O_5 in CO_3^{2-} & Fe_3O_4	110 000	1.6	2.5	Open pit

The mining sector contributes:

- Approximately 5% towards the country's GDP
- Between 35 - 44% of the country's foreign earnings
- About 60 000 jobs in formal direct employment and between 300 000 - 400 000 jobs as informal miners in the small to medium scale mining activities
- Directly supports supplies to the agro-industry and manufacturing sector

- Mineral products generate half the export tonnage carried by the National Railways of Zimbabwe, about 45 percent of internal rail traffic and 16 percent of railed imports.
- Mines and smelters purchase about one-third of all of Zimbabwe's electrical energy supplies.

However, mineral production has weak linkages with the manufacturing sector resulting in less value-addition. Gold and other base metals, which are produced for export, are in semi-processed form and therefore are exposed to risks associated with commodity price fluctuations on the world market.

Challenges and Future Outlook

Despite its strong minerals base, production in Zimbabwe has been depressed as a result of the macro-economic problems being experienced since 2000. The mining sector has great potential for investment with huge unexplored deposits on the Great Dyke. However, the country is facing its worst economic and political crisis since independence from Britain in 1980. Low commodity prices, unhealthy macro and micro economic policies, shortage of foreign currency and fuel, and a severe drop in direct foreign investment, among other factors, have all contributed to significant job losses, mine closures, run away inflation pegged at 1180% in May 2006, and a shrinking economy in general.

Platinum production started in 1995 and was set to be the leading mineral export but suffered a serious setback with suspension of production from 1999 to 2002 at the Hartley platinum mine. The mine faced viability problems due to unsafe mine design conditions underground and a huge drop in the world prices of platinum caused by the Russian Federation’s offloading of huge stockpiles onto the market.

2.5 Major Mineral Products

Precious metals, PGM’s and base metals

a) Gold

In value terms, gold is the principal mineral produced in Zimbabwe, with annual production rising from 14tons in 1980 to 27tons in 1999. Production is on decline in recent years, as shown in Figure 2.3, down to 18tons per year in 2001 and 14 tons per year in 2002, due to a weakened economy and unfavourable government policies.

All gold is sold to the central Reserve Bank of Zimbabwe with payment in local currency at a fixed exchanged rate, which is much lower than companies have to buy the foreign currency on the parallel market. This puts the gold sector at a disadvantage compared to other companies whose commodities are exported for hard currency. Gold used to contribute about half the value of annual mineral production but production is declining and platinum group metals are more likely to top the list as the major contributor in value terms.

Notable mine closures impacted by the hostile conditions in 2002 included the operations of Consolidated Trillion Resources Ltd., Delta Gold NL (now Aurion Gold NL), Falcon Gold Ltd., and First Quantum Minerals Ltd. Surviving operations include the major gold producers namely, Freda Rebecca Mine owned by Ashanti Goldfields of Ghana; Renco Mine, Patchway Mine & Cam Reprocessing Dump owned by Rio Tinto Zimbabwe (Pty) Ltd; and Metallon Gold's Mazowe, Shamva, Blanket, Muriel and Acturus Mines.

Figure 2.3: PGMs & Precious Metals

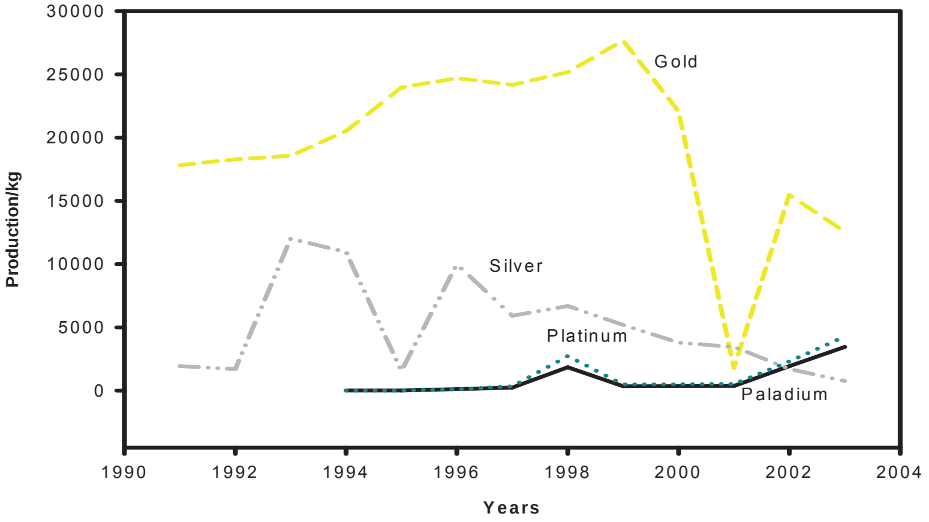

b) Platinum Group Metals (PGMs)

The mining of PGMs dates back to 1969 when Union Carbide successfully undertook pilot plant scale production at Wedza culminating in refined metals being sold, (Mobbs, 1998, Coakley, 2003). In 1994, Zimasco started production at Mimosa mine (at the southern end of the Great Dyke), now owned by Aquarius Platinum of Australia and Implats of South Africa. Concentrates are sent to Impala Refining Services in South Africa.

Makwiro Platinum Mines, a joint venture between Zimbabwe Platinum mines (Zimplats) and Impala Platinum, has taken over the much publicised and failed Hartley operation developed by BHP and Delta Gold in the mid 1990's. An underground operation, Hartely was brought into production in 1997 at a cost of some US$289 million, but shut down within two years due to operational problems. In early 2001, Zimplats announced the development of Ngezi into a 2.2 Mt/y open pit operation producing 208 000 oz/y of PGMs, plus nickel, copper and cobalt. Ore from Ngezi is treated in the Selous Metallurgical Complex at Hartley, thus reviving part of the original project, although the refinery section remains closed. An output of 3400 t/y of smelter matte is targeted. Plans by Anglo American to develop the Unki Project also along the Great Dyke are at an advanced stage and production is expected to start in 2007. With these developments the platinum sector in Zimbabwe is geared for rapid expansion and it is anticipated that platinum will soon overtake gold as the principal mineral produced and the main foreign currency earner.

c) Base Metals

Nickel dominates in tonnage and value terms, Figure 2.4, with national production amounting to 12000 tons annually. Bindura Nickel Corporation (BNC), which was owned by Anglo American until mid 2003 when ownership changed to Mwana Africa (Pty) Ltd., operates the Madziwa, Shangani, and the Trojan Nickel Mines as well as a smelter and refinery.

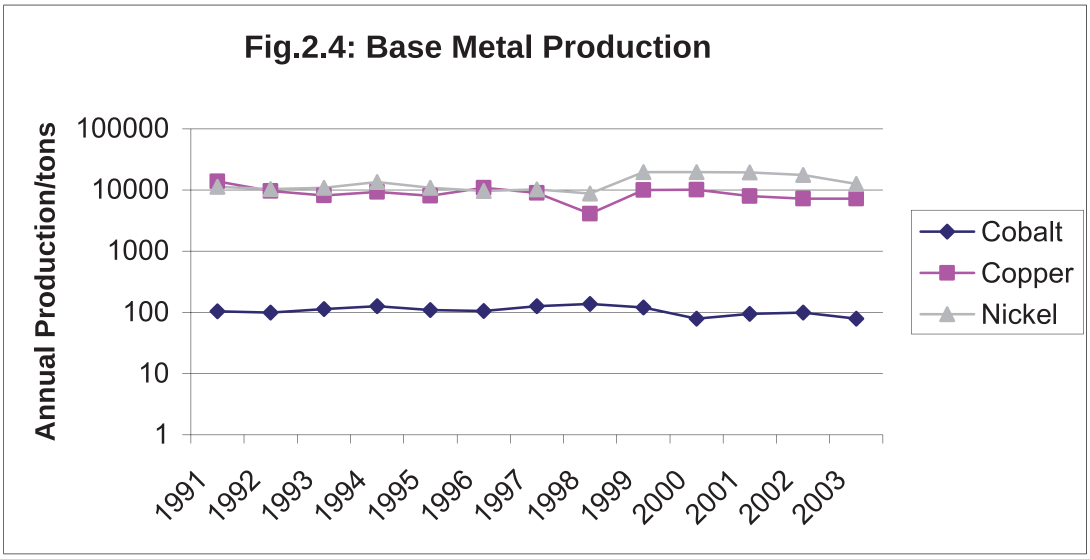

Rio Tinto operates the Empress Nickel Refinery, which processes matte from Botswana on a toll basis. A small proportion of the production also comes from PGM processing as a by product together with cobalt. Copper production has declined in recent years following the closure of Mhangura Copper mines owned by the Zimbabwe Mining Development Corporation (ZMDC) and also the closure of Sanyati mine owing to high cost and dwindling oxide deposits. Lack of sufficient concentrates to feed the Alaska smelter and Refinery has led to its closure.

Iron and Steel, Ferroalloys and Fuel Minerals

The country has huge iron ore resources estimated at approximately 30 billion tons and grading ±40% Fe. Production of crude steel is at Ziscosteel with a capacity to produce 1million tons per year following an extensive rehabilitation program of the steel works in 1999. Production of iron & steel and ferro alloys is shown in Figure 2.5. Ferroalloys are processed from the chrome ore resource along the Great Dyke. Zimbabwe Alloys Limited (a subsidiary of Anglo American) and Zimasco, have the major stakes in the production of low carbon and high carbon ferrochrome.

Zimbabwe has no domestic reserves of oil or gas and depends on coal, hydropower and petroleum imports to meet its energy requirements. Coal has been the dominant energy mineral and the country has adequate capacity to meet its energy requirements in terms of domestic heating, agricultural heating, industrial energy and power stations. However, the quality of coal in terms of sulphur and phosphorus content is not suitable for metallurgical purposes and therefore such coal is imported from South Africa.

Figure 2.5: Ferro Alloys & Fuel Minerals

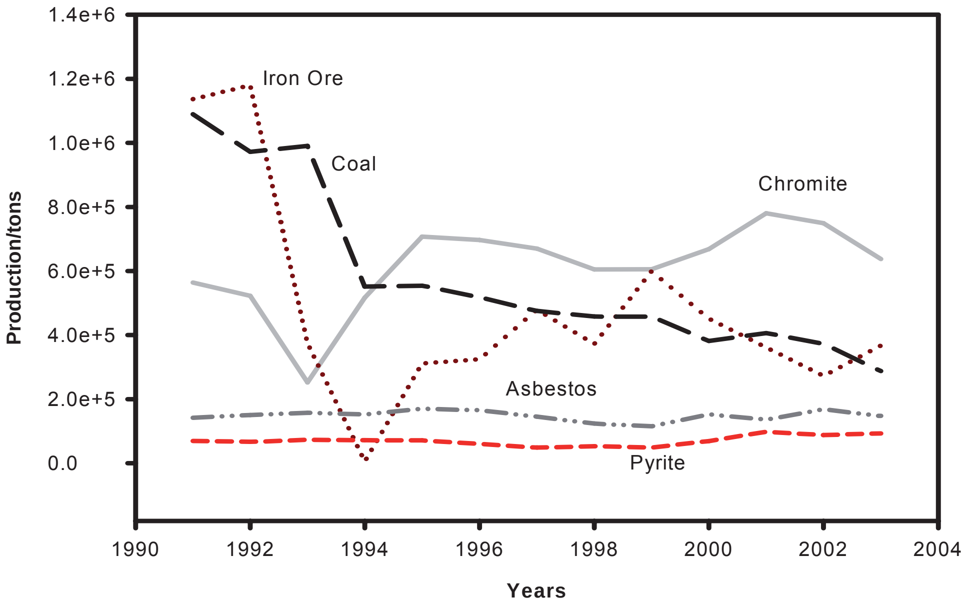

2.6 National Environmental Policy and Regulatory Framework on Mining

Minerals are valuable national assets and adequate supplies are essential for the sustainable development of a modern economy. Zimbabwe, along with other developing nations of the world are signatory to international conventions which seek to find the best ways of avoiding undue environmental impact through the systematic application of preventive technologies, processes and legislative procedures. With the severe decline in production in Zimbabwe's agricultural sector since the land reform program instituted by government in 2002, and agriculture's bleak outlook for the next few years, economists suggest that the burden now falls on mining to resuscitate the economy. Zimbabwe's National Environmental Policy is closely linked to its overall development policy and plans. Environmental issues in mineral exploitation are given due attention at project inception and development stages. Zimbabwe's Environmental Management Act of 2003 provides that Environmental Impact Assessments should be undertaken for major development projects. Environmental awareness is generally high and increasing.

Statutory instruments which regulate mining and the environment in Zimbabwe include the Mines & Minerals Act, the Water Act, Hazardous Substances Act, Atmospheric Pollution Prevention Act, Stream Bank Prevention Regulations, Mining & Safety Regulations, Mining (Alluvial Gold) Public Streams Regulations, and the Environmental Management Act (2003).

Mineral Legislation

Zimbabwe's general mining policy is to sustain development of the country's mineral resources and create employment opportunities. There is no prioritisation of minerals for exploration and development. The Mines and Minerals Act was enacted in 1961 and a number of amendments have been made since then. All minerals are vested in the President and one requires rights to work mineral deposits through an application to the Mining Commissioner. Mining activity is open to both local and foreign individuals and companies. An amended version of The Mines and Minerals Act, 1992, has become quite controversial. Exploration for mining purposes supersedes the right of the land owner for farming without any compensation to the farmer. Once a mining claim is pegged, all other acts can not be considered. Mining is depended upon non-renewable resources and it has proved difficult to enforce land reclamation after mining operations have ceased.

Recognising that there are mineral resources that can be worked profitably by small workers the Government has put in place facilities that are geared towards the development of this sub-sector which in turn would yield great benefits in terms of employment creation and alleviation of poverty among the indigenous Zimbabweans.

Prospecting License

Prospecting license holders are entitled to peg and register claims. The claim then becomes a registered mining location where mining activity can take place. A Prospecting license is valid for two years. A fee for processing a prospecting license is levied. Mining claims which are worked continuously do not have expiry dates.

Exclusive Prospecting Order (EPO)

An EPO confers the exclusive right to prospect for specified minerals in any defined area in Zimbabwe. The EPO is obtained through an application made to the Mining Affairs Board (MAB) and on payment of a deposit fee. Areas cannot normally exceed 130,000 hectares for coal, mineral oils or natural gas; 2 600 hectares for precious stones other than diamonds and 65,000 hectares for any other mineral.

The maximum possible period for operating an EPO is six years, initially for three years and possible extension for a maximum of three years. License holders are obliged to submit from time to time work programmes to be carried out in the next 6 to 12 months and work done in the past six to 12 months.

Mining Claims

The permit to mine is called a Mining Claim. Since a Claim covers a small area, usually several claims are grouped to form a block of claims. Ordinary claims are up to 25hectares and special claims are between 26 and 150 hectares. A block of claims may be transformed into a Mining Lease for simplicity of administration. There are two types of claims: precious metal/mineral claims and base mineral claims. There is fees payable on registration of claims. The claim confers on the holder the exclusive right to mine the mineral resource for which the claim was registered and of prospecting for other minerals on the claim. The claim must be inspected annually and inspection fees are applicable. The holder is required to fulfil minimum conditions. These are commitment to development work programs or production or capital expenditure. Landowners' fees are paid in respect of a producing mining location and any registered block, mining lease or special grant.

These payments are made when the owner makes an application to the Mining Commissioner. The owner may also make an application to the Mining Affairs Board (MAB) for an order authorising increased payment in respect of his location. The Government of Zimbabwe does not participate in managing the projects of local or foreign firms in the private sector. Presently Government participation in mining is through Zimbabwe Mining Development Corporation (ZMDC) and through the Minerals Marketing Corporation of Zimbabwe (MMCZ). The ZMDC was formed in 1982 for Government to participate in the mining sector and to save companies that were being threatened to close. It is active in exploration, mining and giving assistance to co-operatives and small-scale miners.

The MMCZ was formed in 1992, and is responsible for marketing all the country's minerals and metal products except gold and silver which are sold through the Reserve Bank of Zimbabwe following the enactment of the Gold Trade Act (1982). The MMCZ finances its operations by a commission charge of 0.875% on sales conducted for its clients.

2.7 Environmental Management Act (2003) and implications for Mining

Tailings Disposal

Tailings must be disposed of in a manner that optimizes protection of human safety and the environment. On-land tailings impoundment systems must be designed and constructed in accordance with internationally recognized engineering practices, local seismic conditions, and prevailing rainfall conditions. On-land disposal systems should be designed to isolate acid leachate-generating material from oxidation or percolating water. Direct discharge of tailings into a stream is not acceptable and the project owners are responsible for any negative effects on aquatic resources and on downstream users of the water resources. If the mining operation involves a series of open pit operations, project sponsors must evaluate the feasibility of using abandoned open pits for tailings disposal.

Water Quality Criteria

One of the most immediate threats posed by mineral development is water pollution. Mining impacts on water quality through mine water discharges; acid mine drainage; heavy metals contamination; discharges from waste rock, tailings & overburden; and through erosion and sedimentation. Pollution of surface and ground waters by these sources is a major cause for concern in Zimbabwe. Residual toxic chemicals used during mining and beneficiation are also a potential source of water contamination. Common types of reagents include cyanide, sulphuric acid, mercury, ammonia, sodium hydroxide, hydrogen peroxide and lime. Significant quantities of residual chemicals are left in the process water and even after dewatering the stockpiled tailings may still contain a significant proportion of residual reagents. Most of the reagents used in beneficiation processes are extremely toxic and lethal on ingestion. It is not clear from current literature studies if these residual chemicals have an enhancement effect or curtailing effect on AMD.

Water is the most significant casualty of mining. Water quality is composed of the physical, chemical and biological characteristics of water and the abiotic and biotic interrelationships. The designation of unacceptable and acceptable water quality is entirely based on the intended specific uses of the water resource. Major water uses include human consumption, irrigation, recreational, fish culture, industrial processing, energy production, transportation and fire fighting. Across the whole world, water quality standards differ as they are set out by the respective controlling authorities, but the quality parameters laid out are essentially the same. In Zimbabwe, the criteria set out by the Zimbabwe National Water Authority, (ZINWA), are used as the benchmarks to monitor & control the country's water quality in rivers, dams and ground water. These criteria are also used to develop wastewater discharge permits and determine pollution loads in water bodies situated around mine sites, municipalities and irrigated farmlands. Tables A1 and A2 in Appendix A, show the permissible discharge limits for pollutant concentrations in effluent in comparison to the Zimbabwean Standard Specification for Water for Domestic Supplies (Standards Association of Zimbabwe, SAZ 1997: 7 – 9) and WHO (2003) guidelines for drinking water quality.

A considerable challenge to address water quality issues and environmental sustainability, especially in developing countries, is the lack of capacity at the country or regional level to provide effective water governance. This is characterized by fragmented responsibility over water resources, including multiple government agencies responsible for water management, which typically operate in isolation and in competition for funds. Unfortunately, water quality problems around mine locations have not been adequately addressed in the past and Moyo (1999) admits that there is death of information on the quality of the country's waters. Deteriorating water quality has become one of the most critical issues affecting the mining industry in Zimbabwe. While most of the big mines have the technical, administrative and financial capability to support advanced technologies to treat effluent from their operations, many simply don't give sufficient consideration to environmental sustainability issues, while small scale to medium operators lack the capabilities to do so.

Water pollution is defined as the decline in the quality of natural water due to man's activities, causing it to become unsuitable for use by humans and/or some other life form. Thus, it involves the alteration of the biological, chemical, or physical properties of the water. In general, the quantity of discharges and the range of pollutants reaching the rivers have increased due to population growth, intensive urbanisation, mining activities and increased industrial activities. Thus water is considered a limiting resource in Zimbabwe and as such the Government is taking measures to manage the quality of the country's water more effectively, (Zimba, 1999). The Water Pollution Control Section takes the sensitivity of a receiving water body into account when deciding to issue a permit for discharge of wastewater that does not comply with the set standards, and has adopted the 'Pollute and Pay' principle. This implies that all effluent discharged to receiving waters from tailings impoundments, waste rock drainage, mine water, process water and any spillage effluent from mining sites should be covered by a permit.

The waste disposed can be placed in the category termed Blue, Green, Yellow or Red according to the quality as explained below. All categories attract disposal fees: ranging from US$80 - Blue; US$150 – Green; US$240 – Yellow; to US$350 – Red (as of December 2004). In addition, effluent in the green, yellow and red bands are levied environmental fees, 40, 100, & 200 US cents respectively, per mega litre of effluent.

- **Blue:** The quality of the effluent meets the standards set for this category and is considered environmentally safe. The method of waste disposal does not result in significant environmental risk.
- **Green:** The effluent pollutant concentrations are more than those of the Blue standards in one or more parameters, risk to water resources and environmental hazard is low.
- **Yellow:** The effluent is of poor quality in one or more parameters, above the standards set for the Green band, and there is medium risk to the water quality.
- **Red:** The effluent is of very poor quality, and disposal presents significant risk of water pollution and environmental damage.

The classification is based on the quality of effluent and the potential environmental risk as submitted by the permit applicant and as assessed by the Water Pollution Control Section. The categories are according to the sensitivity of the area in which the receiving water bodies occur that is either sensitive or non-sensitive as adopted from the old Water Act (1976). The zones specified as *Zone I* and *Zone II* are those found to be sensitive and not so sensitive areas respectively. Zone I is in most of the eastern part of the country where there is fish breeding, especially trout.

Non compliance by permit applicants can result in any of the following decisions being applied:

(a) Issuing a short duration permit (6 months), whilst pollution abatement works are being installed;
(b) Propose alternative methods of disposal;
(c) Refuse to issue the permit;
(d) Advise on installation of pollution control facilities.

Table 2.4 shows the recommended target guidelines below which no risk is expected or significant adverse impact on aquatic biota or human use. The figures are compared with AMD discharge from one of the metal mines in Zimbabwe and also to a polluted stream passing through the mine site. In cases where natural background concentrations exceed these levels, the discharge may contain concentrations up to natural background levels. Concentrations up to 110% of natural background can be accepted if no significant adverse impact can be demonstrated.

Mining operations use water mostly for cooling, underground drilling operations and mineral processing such as grinding, flotation and leaching. Larger mines also frequently use water to supply nearby residential areas attached to the mines. In arid and semi-arid areas such as Zimbabwe, the quantity of water used by a mining operation places it in direct competition for water with other water users, especially domestic and agriculture. This “competition” becomes heightened when the mining operation is also responsible for any deterioration in water quality as a result of effluent discharges.

An unexpected or chronic decline in water supply and deterioration in water quality can significantly jeopardize business operations, or raise the cost of operations, especially for mines that are water intensive. Fees are levied by ZINWA for water abstraction rights and effluent discharge. These factors can result in production delays, place limits on expansion programs, cause negative publicity or total failure of downstream industries. This, in turn, affects the company’s financial performance at a facility level, and ultimately at a corporate level.

Table 2.4: Comparison of AMD to recommended effluent discharge levels (mg/l)

Parameter	**Recommended Level**		**Yellow**	**Red**	**AMD**	**Polluted Stream**
	WHO	**ZINWA**				
pH	6 – 9	5.5 – 9	≤6& >9.5	>10.5	0.95	3.56
Temperature °C	≤5°C above ambient	≤25	≤40	≤40	32	23
DO	8	≥6.0	<4	<4	3.2	4.8
Oil & Grease	5	≤2.5	<7.5	>7.5	ND	ND
TSS	50	≤25.0	≤100	>100	456	210
TDS	1000	≤500	≤1500	>1500	10600	1180
SO_4^{2-}	300	≤250	≤400	>400	28700	1560
As	0.1	≤0.05	≤0.15	>0.15	<1	<1
Cd	0.1	≤0.01	≤0.1	>0.1	0.04	<0.01
Cr (VI)	0.1	≤0.05	≤0.2	>0.2	ND	ND
Cu	0.3	≤0.5	≤3.0	>3.0	0.56	0.62
Fe	2.0	≤1.0	≤5.0	>5.0	4480.17	58.74
Pb	0.1	≤0.05	≤0.2	>0.2	0.87	0.33
Ni	0.6	≤0.3	≤0.9	>0.9	1.54	0.46
Zn	0.5	≤0.3	≤0.9	>0.9	4.88	0.65
Hg	0.02	≤0.01	≤0.03	>0.03	ND	ND
Total Cyanide	0.01	≤0.05	≤0.15	>0.2	0.02	ND

2.8 Effluent Quality and Environmental Impacts

By far and large the biggest impacts of mining on water quality are acid mine drainage, heavy metals leached from wastes, residual or spillage flotation chemicals, cyanide & mercury used in the process for recovering gold, arsenic, suspended solids and sediment runoff. Derelict equipment left underground may also undergo severe corrosion leading to high metal concentrations in pumped mine water.

The type of water contamination produced by a mining operation depends to a large extent on the nature of the mineralization, mining method and on the processing chemicals used to extract the valuable minerals from the host rock. Open cast and underground mining and the subsequent beneficiation of base metal sulphide deposits, precious metal deposits and chromite ore along the Great Dyke has led to generation of poor quality leachates draining from the mine sites. Extensive vegetation death, yellow, brown and white salt crusts on the soil surface and pale blue, green and cloudy appearance of surface water can be observed in the vicinity of processing mills, waste rock and tailings dumps, a situation depicted by plates (a) to (d) in Figure 2.6.

(a) Ponded AMD at Shamva Gold Mine (b) Heavy metal deposition in stream sediments from Athens gold mine tailings dam (c) Secondary mineral precipitates at Mhangura copper mine tailings dam (d) Dried trees and oxidation salts (white) at the jig tailings dump at Iron Duke Mine.

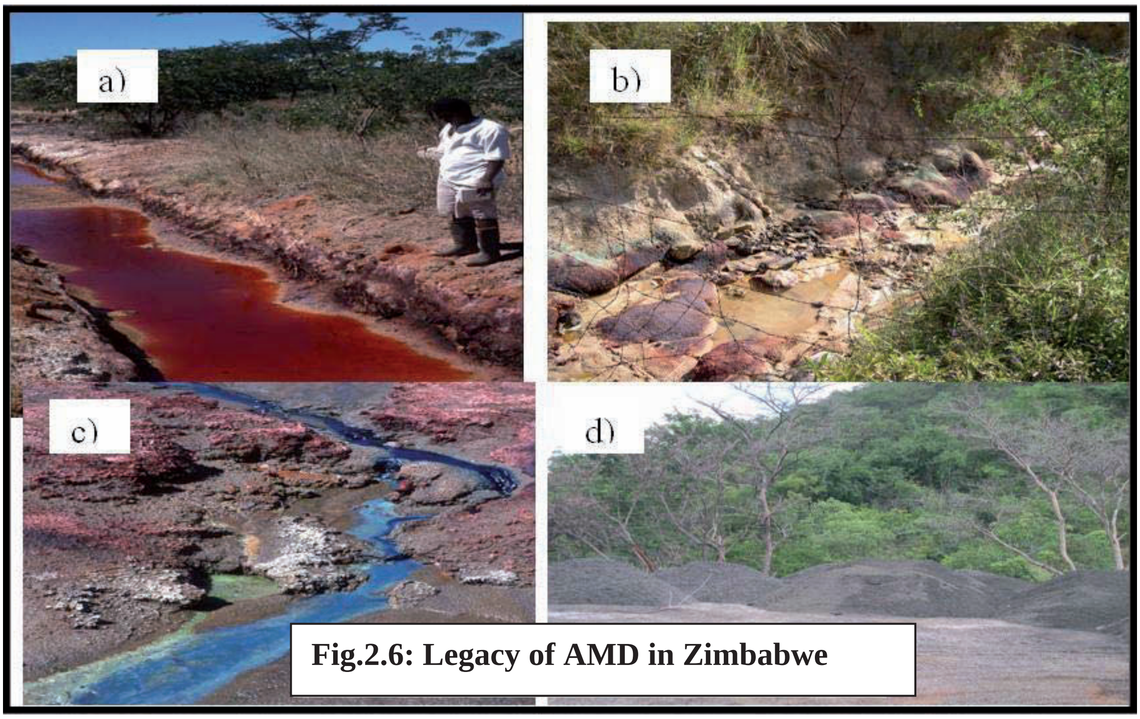

Fig.2.6: Legacy of AMD in Zimbabwe

Flotation reagents, mainly xantahtes, used to concentrate sulphide minerals, cyanide used in the extraction of gold, heavy metal ions such as antimony, cadmium, lead, copper, nickel and zinc are present in high concentrations in process water and seepage streams. Table 2.5 shows the average chemistry of leachates and stream water samples from mine locations in the Midlands and Harare mining districts during a survey of water quality around mine sites in July 2003. The worst case of acid mine drainage occurs at the Iron Duke Pyrites underground mine which must cope with 180m^3/day of acid mine water with pH < 2.5, about 14000mg/l in sulphate, 9500mg/l iron and other dissolved metals. Several other mines are also affected. The acidic waters drain through the waste rock piles dissolving metals accelerating their turbidity and mobilisation.

Table 2.5: Characteristics of Leachate from selected mines (July 2003)

Site Name	**Type of Sample**	**pH**	**E.C**	**TDS**	**Alkalinity**	**Fe**	**SO_4**	**DO**
			uS/cm	**mg/l**	**mg/l**	**mg/l**	**mg/l**	**%Sat.**
Cam & Motor Dump	Tailings drainage	8.5	2341	3783	287	0.12	2021.74	13.8
Athens Mine	Tailings drainage	4.3	3456	4160	(acidic)	0.46	4289.07	5.8
Trojan Nickel Mine	Waste rock seepage	7.76	3310	4950	145	0.74	221.43	54.7
	Dam stream	8.44	1524	1300	240	0.34	650.51	80.6
	South Effluent (at V-Notch)	8.85	1170	1200	105	3.85	305.48	77.0
Jumbo Mine	Mine water	8.12	1750	1480	90	3.2	1000.77	76.2
	Effluent from old heaps	2.85	3050	4300	21	46.81	8089.33	16.7
Iron Duke Pyrites	Mine water	2.90	15460	30570	(acidic)	9783.72	25600.45	ND
	Ground water(BH1)	3.25	6786	5670	(acidic)	1580.86	28400.67	ND
	Yellow Jacket Stream water (downstream)	3.57	3762	2789	(acidic)	10.89	3986.23	2.5
Freda-Rebecca Mine	Tailings drainage	5.85	2564	2034	16	1.87	234.65	13.5

The extremely low pH drainage is a big problem to the environment, and can find its way into surface and ground waters, severely degrading both habitat and water quality, (Kimmel, 1983).

Heavy Metals Mobilisation

The discharge of AMD into soil and natural water systems results in numerous physical, chemical and biological responses in which the environment can be modified detrimentally. Water plays a significant role in heavy metal mobilisation. It acts as a storage buffer for the pollutants, as the medium in which most of the reactions take place, and is undoubtedly the most significant transport vector in the pollution process.

The intrinsic properties of the acidic drainage such as chemical composition, speciation of key mineral components, redox potential and pH are master variables controlling metal release, transport, deposition, reactivity and availability to biota. The mobility of heavy metals is strongly increased by acidification from acid mine drainage, and the discharge of these metals into the receiving waters results in numerous physical, chemical and biological responses in which the environment can affect the metal and vice versa, (Magombedze & Brattli, 2003). The result is an overwhelming number of association/dissociation, substitution, and adsorption or desorption reactions, giving rise to a complex migration pattern as seen in Figure 2.7.

Figure 2.7: Schematic diagram of Pollutant Emission and Migration through the Geosphere.

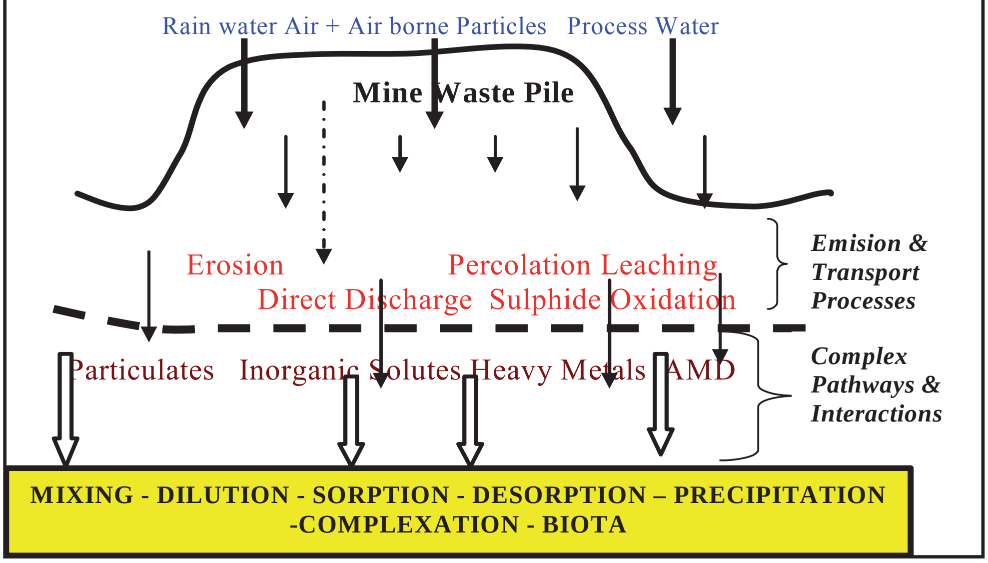

Residual Mining Chemicals

Chemicals used in mining and beneficiation are also a potential source of water contamination. Common types of reagents used include cyanide, flotation xanthates, sulphuric acid, mercury, ammonia, sodium hydroxide, hydrogen peroxide and lime. Significant quantities of residual chemicals are left in the process water and even after dewatering the stockpiled tailings may still contain a significant proportion of residual reagents. These residual reagents can form complexes with metal ions from acid mine drainage, posing great danger to human health and aquatic systems. The impact of metals on aquatic life within a water system is dependant on the specific complex that the metal is in, the ligands it is associated with, and the thermodynamic and kinetic stability of the complex (Fernando, 1995). Different metal species have different bio-availabilities, and some metal species are more toxic than others.

Discharges of process water, mine water, storm runoff and seepage are the primary transport mechanisms to surface water and ground water. Most of the reagents used in beneficiation processes are extremely toxic and lethal on ingestion. In 1993, 16 soldiers of the Zimbabwe National Army who had settled at an abandoned mine location in Kwekwe, died after drinking water contaminated by leachate from a tailings dump. In 1998, How Mine tailings dam failure occurred, resulting in several million tons of tails contaminated with cyanide, heavy metals and other toxicants spilling into the nearby river. Massive fish deaths were observed in Lake Chivero which supplies Harare with drinking water in 2001.

2.9 Concluding Remarks

The mining industry is backbone to Zimbabwe's economic growth. However, lack of environmental stewardship, economically affordable abatement technology, poor environmental monitoring, and a harsh economic climate, have resulted in the pollution of surface and ground waters by mine effluents and acid mine drainage. Re-vegetation stabilizes the dumps in relation to geotechnical stability but can not prevent the sulphide bearing waste material from oxidation. In semi - arid environments, sulphide waste disposal options are very limited, leading to unsustainable costly treatment options. The analysis given in this chapter justifies the need to assess the nature and magnitude of the problem of AMD in Zimbabwe and thereby dispel the myths regarding pollution from metal mines, especially in light of the new legislation concerning effluent discharges.

CHAPTER 3

REVIEW OF THE GEOCHEMISTRY OF AMD AND METHODS USED FOR ITS KINETIC CONTROL AND TREATMENT

3.1 Introduction to Environmental Geochemistry

Environmental Geochemistry involves the development and application of chemical principles to understand the processes that control the fate, transport and distribution of contaminant elements in geologic systems. Contaminant elements may cause acute human health effects as well as economic and resource damage. As mineral deposits continue to be mined, their associated waste rock and tailings piles continue to be exposed to weathering, large concentrations of metals and sulphate will continue to be found in surface and ground waters (Nordstrom and Alpers, 1998). Aqueous geochemistry is the application of chemistry to reactions between rock and natural water. Its major goals are to provide answers as to how the elements are distributed between the primary mineral sources, soil (vadose zone), surface water and groundwater, why the elements are distributed that way, and what principles or processes govern the distribution of the elements? Knowledge of such principles helps to understand the geochemical processes governing the changes to AMD over time and space.

To have a common base of understanding, some basic theoretical aspects of practical significance must be reviewed. The review starts with a discussion on mineral dissolution reactions that influence mine waste drainage quality. The reactions presented result in acidic drainage, acid neutralisation, and trace metal release. A detailed discussion of the geochemistry of AMD is presented by Morrin and Hutt, (1997); Nordstrom and Alpers, (1999), Smith and Huyck, (1999). This chapter continues with a review of current state of understanding and technology on AMD control and treatment. The rationale for implementation of present methods used in the characterisation and kinetic control of AMD is discussed in light of their applicability under different environmental conditions, simplicity, resources required, ease of interpretation, value of data, and time constraints.

3.2 The Problem with Acid Mine Drainage

Acid mine drainage is a low pH, sulphate and metal bearing solution usually formed when rocks containing sulphide minerals (essentially pyrite & pyrrhotite) are exposed to the atmosphere or an oxidising environment, and subsequently leached by water.

AMD ranges widely in quality from alkaline (pH ~10) to strongly acidic (pH ~ -3), usually corrosive, and contains dissolved solids ranging from about 100 to 100 000 mg/l (Hyman and Watzlaf, 1995; Rose and Cravotta, 1998; Nordstrom *et al.,* 2000). AMD is a major issue affecting the metal mining and coal industry throughout the world. Dissolved metals and other constituents of AMD can be toxic to aquatic organisms and can precipitate forming ochreous encrustations that degrade the aquatic habitat (Winland *et al.,* 1991; Bingham and Nordstrom, 2000). The pH and concentrations and loadings of alkalinity, acidity, and metals such as Fe, Cu, Ni, Cd, Zn, Al and Mn in mine effluent and receiving water bodies are commonly measured to identify potential for environmental effects and to plan appropriate treatment methods to remove metals and produce near neutral effluents. Many old mining sites have a legacy of acid drainage long after the completion of mining.

The problem of acid mine drainage begins with sulphide oxidation (mainly pyrite oxidation) and is accompanied by the dissolution and precipitation processes of metals and minerals. It has been a major focus of investigation over the last 60 years (Sato, 1960; Bryner *et al.,* 1967; Nordstrom, 1977 and 1982; Nordstrom *et al.,* 1979; Ritcey, 1989; Jambor and Blowes, 1994 & 1998; Alpers and Blowes, 1994; Evangelou, 1995; Morin and Hutt, 1997; Nordstrom and Alpers, 1999). The problem is multifaceted as AMD forms within a complex environmental system where several factors need to be considered. The presence of pyrite in the mineral assemblage, and the availability of water and oxygen constitute the principal recipe. Where different sulphides are in contact with each other, electrochemical processes are likely to occur and influence the reactivity of sulphides (Kwong, 1993). Furthermore, factors such as microbial catalysis, neutralization reactions, sorption reactions, and climatic effects have an important influence on pyrite weathering.

There are many sources of acidic drainage, both natural and anthropogenic. Natural sources include volcanic eruptions, hydrothermal activity (visible as hot springs), formation of limestone caverns, stalactites and stalagmites, brine formation from soluble minerals, and acid rock drainage from activities such as highway construction, civil engineering works and logging. Drainage from such sources is commonly referred to as Acid Rock Drainage (ARD) as opposed to AMD which emanates from mined out areas. The oxidation of sulphide minerals such as pyrite and pyrrhotite is responsible for the bulk of acid production by mine wastes (Stumm and Morgan, 1996). Other sources of acid release from mine wastes include dissolution of soluble iron sulphate minerals, and the dissolution of less soluble sulphate minerals of the alunite/jarosite series.

3.3 Oxidation of Sulphide Minerals and the Chemistry of AMD Generation

Acidity is measured in terms of H^+ and other dissolved species (e.g. Fe, Al, Mn) capable of producing acid. Acidity generally increases as pH decreases and it is possible to have water with a high acidity but neutral pH values. pH is a measure of H^+ only, and technically it is the negative logarithm of the hydrogen ion activity, {pH =-log [H^+]}. pH is a function of the balance between acid-generating and acid-consuming reactions, the relative rates of these reactions, and accessibility (liberated grains) of minerals that contribute to these reactions. Most reactions in geologic systems are pH driven because of the hydrogen ion's great potential to react with aqueous chemical species and/or mineral surfaces. This is due to its small size and high electron accepting capacity.

The acid production processes can be split into three categories. The first is the oxidation of sulphide minerals by oxygen and ferric iron. The second involves bacteria assisted oxidation and the third is hydrolysis of mainly Fe(III) and subsequent precipitation of ferric oxy-hydroxides or oxy-hydroxide sulphates.

3.3.1 Abiotic Oxidation of Sulphides

The most common sulfide mineral is pyrite (FeS_2). A complex interaction of physical, chemical and microbiological processes can influence the generation of acidic drainage and typically these factors vary on a site specific basis. The initiator reaction in AMD generation from mine sites is the oxidation of pyrite, (Singer and Stumm, 1970; Forstner and Wittmann, 1979).

1) Pyrite oxidation by oxygen

When pyrite is exposed to water and oxygen, it decomposes into water soluble components, acid is produced. Oxidation of the disulphide according to reaction 3.1 releases Fe^{2+} and 2 protons.

$$FeS_2 + \frac{7}{2}O_2 + H_2O \Rightarrow Fe^{2+} + 2SO_4{}^{2-} + 2H^+ \qquad (3.1)$$

The relatively reduced water soluble components (ferrous iron) are further oxidised at low and circum-neutral pH, and acid is consumed, (reaction 3.2), (Moses & Herman, 1991).

$$Fe^{2+} + \frac{1}{4}O_2 + H^+ \Rightarrow Fe^{3+} + \frac{1}{2}H_2O \qquad (3.2)$$

The conversion of ferrous (Fe^{2+}) by oxidation to ferric (Fe^{3+}), reaction 3.2, is followed by hydrolysis of Fe^{3+} to form ferric hydroxide (insoluble at pH>3.5) releasing 3 more protons in the process, (reaction 3.3).

$$Fe^{3+} + 3H_2O \Rightarrow Fe(OH)_3 + 3H^+ \qquad (3.3)$$

Thus, in sufficiently aerated/oxidised environments, the formation of ferric iron in water resulting in the precipitation of ferric hydroxide is a key acid producing stage. Once sulphides have been oxidised, it is extremely difficult to avoid ferric hydroxide precipitation.

2) Pyrite oxidation by ferric iron (Fe^{3+})

With the formation of soluble ferric iron (Fe^{3+}) in the presence of fresh iron sulphide, further sulphide oxidation is accelerated, as represented in reaction 3.4, (Alpers and Nordstrom, 1999).

$$FeS_2 + 14Fe^{3+} + 8H_2O \Rightarrow 15Fe^{2+} + 2SO_4{}^{2-} + 16H^+ \qquad (3.4)$$

Equation (3.1) describes the initial step of pyrite oxidation in the presence of atmospheric oxygen. Once ferric iron is produced by oxidation of ferrous iron, Fe^{3+} will be the primary oxidant of pyrite (equation 3.4) (Nordstrom, 1979; Moses *et al.,* 1987; Ehrlich, 1996). Under abiotic conditions the rate of oxidation of pyrite by ferric iron is controlled by the rate of oxidation of ferrous iron (reaction 3.2), which decreases rapidly with decreasing pH. Therefore pyrite continues to oxidize as long as ferric iron is regenerated. The ferric iron is reduced by the pyrite itself (Singer & Stumm, 1970) according to reaction (3.4). A simplified diagram illustrating reaction pathways is depicted in Figure 3.1.

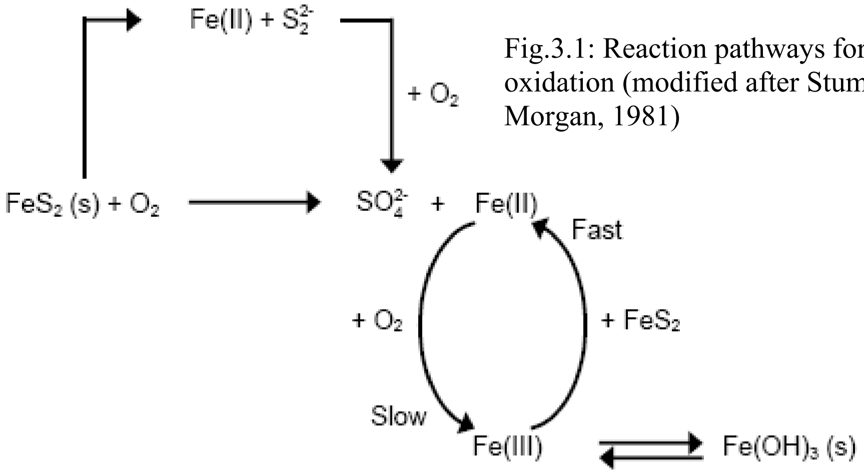

Fig.3.1: Reaction pathways for pyrite oxidation (modified after Stumm & Morgan, 1981)

3) Oxidation of other sulphides

(a) *Pyrrhotite ($Fe_{(1-x)}S$) Oxidation*

Pyrrhotite oxidizes much more rapidly than pyrite (Robertson *et al.,* 1997; Nicholson and Scharer, 1994). The amount of acid produced or consumed by pyrrhotite weathering depends on the particular oxidation path followed and the pyrrhotite composition. The general chemical formula for pyrrhotite is $Fe_{(1-x)}$ S, where x can vary from 0.125 to 0. Reactions that have been proposed to describe pyrrhotite oxidation are as follows (from Jambor and Blowes, 1994):

- Complete reaction as represented by equation 3.5. The amount of acid produced depends on pyrrhotite stoichiometry.

$$Fe_{(1-x)}S + (2 + x/2)O_2 + xH_2O \Rightarrow (1-x)Fe^{2+} + SO_4{}^{2-} + 2xH^+ \qquad (3.5)$$

- Partial reaction to produce native S:

$$Fe_{(1-x)}S + (2-2x)Fe^{3+} \Rightarrow (3-3x)Fe^{2+} + S^o \qquad (3.6)$$

- Rapid oxidation to pyrite/marcasite (FeS_2) in which acid is consumed:

$$2Fe_{(1-x)}S + (1/2 - x)O_2 + (2-4x)H^+ \Rightarrow FeS_2 + (1-2x)Fe^{2+} + (1-2x)H_2O \qquad (3.7)$$

Nicholson and Scharer (1994) propose that the stoichiometry of the pyrrhotite affects the relative production of acid. At one extreme, if x = 0 and the formula is FeS, no protons are produced in the oxidation reaction; at the other extreme, the maximum amount of acid will be produced by the iron-deficient Fe_7S_8 phase. The role of pyrrhotite in the acidifying process is similar to that of pyrite, but it is very important at early weathering stages because its oxidation rate is 20 to 100 times higher than that of pyrite in atmospheric concentrations of O_2 and at 22°C (Nicholson and Scharer, 1994). The oxidation of pyrrhotite can also involve the formation of elemental sulphur (Ahonen and Tuovinen, 1994), marcasite (Jambor, 1994), or the formation of pyrite (Burns and Fischer, 1990).

(b) Chalcopyrite ($CuFeS_2$) Oxidation

Chalcopyrite, together with molybdenite, are known as some of the most resistant sulfides to oxidation (Plumlee, 1999). Walder and Schuster, (1998), propose that complete oxidation of chalcopyrite may proceed according to reaction 3.8 without acid production:

$$2CuFeS_2 + 4O_2 \Rightarrow 2Cu^{2+} + Fe^{2+} + 2SO_4{}^{2-} \qquad (3.8)$$

However, the combination of ferrous iron oxidation and ferrihydrate hydrolysis will be the main acid producing process, reaction 3.9.

$$2CuFeS_2 + {}^{17}\!/_{2}\,O_2 + 5H_2O \Rightarrow 2Cu^{2+} + 2Fe(OH)_3 + 4SO_4{}^{2-} + 4H^{+} \quad (3.9)$$

Rimstidt and Newcomb (1993) reported that the oxidation rate of chalcopyrite increases with increasing ferric iron concentration, but with an oxidation rate of 1-2 orders of magnitude less than pyrite. Jambor (1994), reported a general sequence for the oxidation tendency of most important sulphides from readily attacked to increasingly resistant as follows:

Pyrrhotite > galena – sphalerite > pyrite – arsenopyrite > chalcopyrite

The high resistance of chalcopyrite to weathering is due to the fact that the grains are often encapsulated in silicate grains and thereby may escape the dissolution process, (Jambor, 1994).

(c) Arsenopyrite (FeAsS) Oxidation

Arsenopyrite may be oxidized by the following reaction path (Mok and Wai, 1994):

$$4FeAsS + 13O_2 + 6H_2O \Rightarrow 4Fe^{2+} + 4SO_4{}^{2-} + 4H_2AsO_4{}^{-} + 4H^{+} \qquad (3.10)$$

Combined with ferrous iron oxidation and ferrihydrate precipitation, the overall arsenopyrite oxidation reaction can be written as in equation 3.11:

$$FeAsS + {}^{7}\!/_{2}\,O_2 + 4H_2O \Rightarrow Fe(OH)_3 + SO_4{}^{2-} + H_2AsO_4{}^{-} + 3H^{+} \qquad (3.11)$$

If ferric iron is the oxidant, the oxidation rate of arsenopyrite is similar to the oxidation rate of pyrite. If the oxidant is oxygen, the oxidation rate of arsenopyrite is somewhat lower than that of pyrite (Mok and Wai, 1994).

4) Oxidation of non-acid producing sulphide minerals

Sphalerite (ZnS), galena (PbS), Covelite(CuS) and Chalcocite(Cu_2S)

Sphalerite and galena are the most important base metal bearing minerals. Though Zn is toxic only at very high concentrations, sphalerite may contain environmentally dangerous amounts of Cd and Thallium (Tl). In addition, Fe may significally substitute for Zn, in some cases up to 15 mole %, in sphalerite. If iron substitutes for zinc, sphalerite will be an acid generator in a similar way as pyrrhotite due to hydrolysis of ferric phases, (Walder and Schuster, 1998).

Galena is the main source of Pb contamination in mine areas. The common result of the wet oxidation of galena is secondary anglesite ($PbSO_4$) in equilibrium with a Pb^{2+} and SO_4^{2-} solution according to equation 3.12:

$$PbS + 2O_2 \Rightarrow Pb^{2+} + SO_4{}^{2-} \qquad (3.12)$$

Secondary anglesite coating on galena may increase the apparent resistance because anglesite has a low solubility and protects the sulphides from direct contact with oxidizing reagents (Jambor and Blowes, 1998). The oxidation process does not give rise to acidity when oxidation from O_2 is considered, as is also the case with sphalerite and Cu-sulphide minerals covellite, chalcocite, digenite and djurleite which may occur as hypogene, supergene, as well as secondary phases (Dold, 1999). In the presence of Fe^{3+}, the oxidation of divalent metal sulphides (MeS) produces acidity according to reaction schemes where part of the oxidation capacity of the system is derived from Fe^{3+} as, e.g.

$$2MeS + 4Fe^{3+} + 3O_2 + 2H_2O \Rightarrow +2Me^{2+} + 4Fe^{2+} + 2SO_4{}^{2-} + 4H^{+} \qquad (3.13)$$

In the absence of ferric iron at pH 2.5-3.0, sulphuric acid will dissolve some heavy metal carbonate and oxide minerals, but has little reactive effect on heavy metal sulphides. However, ferric ion is capable of dissolving many heavy metal sulphide minerals, including those of lead, copper, zinc, and cadmium, by the above general reaction. It is by this process that significant amounts of heavy metals may be solubilised by AMD. In addition, many metallic elements are often present at trace levels within the minerals pyrite and pyrrhotite. Oxidation of these minerals can therefore release and mobilize trace elements.

3.3.2 Microbial Assisted Pyrite Oxidation

Stumm and Morgan, (1970) pointed out that conversion of ferrous to ferric is the rate limiting step in pyrite oxidation. Under low pH conditions (pH<3), oxidation of Fe^{2+} to Fe^{3+} may be strongly accelerated by microbiological activity. The half life is estimated to be in the order of 100days in the pH range around 3, thus oxidation of pyrite would be extremely slow unless catalyzed by some microorganisms. Jaynes *et al.,* (1984), Nordstrom and Alpers, (1999), showed that sulphur oxidizing bacteria such as Thiobacillus thiooxidans and Thiobacillus ferrooxidans can rapidly oxidise ferrous iron to ferric iron in the pH range 2.5 – 3.5, and sometimes can substitute for the role of ferric iron when in the presence of oxygen and some organic substrate. Below pH 3 the oxidation of pyrite by ferric iron (reaction 3.4) is increased by up to a factor 105 over abiotic oxidation (Singer and Stumm, 1970), and Ritchie, (1994) showed that the rate can be up to about 10 to 100 times faster than by oxygen.

It is commonly thought that in the absence of bacteria, equations (3.1), (3.2) and (3.4) predominate, while in the presence of bacteria the mechanisms of pyrite oxidation are best described by the reactions 3.14 to 3.18, (Singer and Stumm, 1970, Stumm and Morgan, 1981, Nordstrom and Alpers, 1999):

$$FeS_2 + \frac{7}{2} O_2 + H_2O \Rightarrow FeSO_4 + H_2SO_4 \qquad (3.14)$$

$$4FeSO_4 + O_2 + 2H_2SO_{4\ bacteria} \Rightarrow 2Fe_2(SO_4)_3 + 2H_2O \quad (3.15)$$

$$FeS_2 + Fe_2(SO_4)_3 = 3FeSO_4 + 2S \qquad (3.16)$$

$$2S + 3O_2 + 2H_2O_{bacteria} \Rightarrow 2H_2SO_4 \qquad (3.17)$$

$$S + 3Fe_2(SO_4)_3 + 4H_2O \Rightarrow 6FeSO_4 + 4H_2SO_4 \qquad (3.18)$$

Equations 3.15 and 3.17 contain the term "bacteria" in addition to chemical formulae. The bacteria, which are usually site-specific strains of Thiobacillus ferro-oxidans, utilize the sulphur present as their source of energy. They are autotrophic (can transform carbon dioxide to organic carbon) and heterotrophic (can mineralise organic carbon to inorganic carbon), obtaining their nutritional needs from the atmosphere (nitrogen, oxygen, carbon dioxide and water) and from minerals (sulphur and phosphorus), (Ledin and Pedersen, 1996; Madigan *et al.,* 2000). While these bacteria are not catalysts by true definition, they do act as accelerating agents if their habitat conditions are at or close to optimal and they are a most important factor in the generation of AMD. They are also capable of adaptation by mutation if their habitat is markedly changed. For their growth, the optimal pH levels are 2.0 – 3.5, but they can survive from pH 0.5 – 5.5, become inert in temperatures below -20^{o}C and may die when temperatures exceed 60^{o}C, (Nordstrom and Alpers, 1999).

It may be seen that in addition to pyrite, the presence of oxygen, water and sometimes bacteria, is required for process progression. This has important ramifications for AMD control technologies in that removal of the oxygen source (e.g. by total submersion under water) or the water source (e.g. conditions of aridity) will halt AMD production. AMD production would also be considerably slowed or halted by the termination of Thiobacillus ferro-oxidans reproduction by a bactericidal agent.

3.3.3 Dissolution of Iron Sulphate Minerals Resulting in Acid Production

a) Dissolution and Transformation of secondary minerals

Dissolution and precipitation of secondary minerals is an important mechanism for recycling metals and acidity (H^+) in surficial environments. Processes that can lead to precipitation include evaporation, oxidation, reduction, dilution, mixing, and neutralization (Alpers and others, 1994). Secondary minerals include efflorescent sulphate salts, metal oxide, hydroxide, hydroxysulphate, and sulphide minerals.

Secondary minerals found within a given deposit type can vary dramatically with climate. Many of the hydrated efflorescent salts such as that shown in Figure 3.2, are stable within only relatively narrow ranges of temperature and relative humidity. Soluble salts may form upon evaporation of acidic waters and these salts store acid and metals until released by rainfall or snowmelt.

Fig. 3.2: Oxidation salts from Iron Duke mine's jig tailings dump

Iron sulphate minerals are the most common secondary minerals found in the oxidizing environment of the mine waste, due to the wide distribution of pyrite and pyrrhotite as a sulphur source. They are also common in the oxidized portions of weathering zones from ore deposits (e.g. gossans). They may be composed of Fe(II), Fe(II) & Fe(III), or only Fe(III). Examples are melanterite, roemerite, and coquimbite, respectively. A detailed overview of these secondary minerals is given in Alpers *et al.,* (1994) and Nordstrom and Alpers (1999). In general they have a high solubility, whereas supergene jarosite shows relatively low dissolution kinetics. Baron and Palmer (1996) conducted a series of dissolution experiments with jarosite from 4 to 35°C and at pH values between 1.5 and 3. Equilibrium was established in the experiment after approximately 3 to 4 months. It is important to notice that this mineral group is meta-stable with respect to more stable iron hydroxides and oxides and may liberate acidity by the following transformations, (Alpers and others, 1994):

Jarosite » goethite:

$$KFe_3(SO_4)_2(OH)_6 \Rightarrow 3FeO(OH) + K^+ + 2SO_4{}^{2-} + 3H^+ \qquad (3.19)$$

Schwertmannite » goethite:

$$Fe_8O_8(OH)_6(SO_4) + 2H_2O \Rightarrow 8FeO(OH) + SO_4{}^{2-} + 2H^+ \qquad (3.20)$$

An extended group of highly water-soluble sulphates, as for example gypsum or chalcanthite ($CuSO_4.5H_2O$), formed under oxidizing conditions and high evaporation rates, can release significant amounts of metals and acid with rain. This mineral group is an important factor that could lead to seasonal fluctuations in contamination levels of ground and surface waters, especially in semi-arid and arid climates, (Alpers *et al.,* 1994, Dold, 1999).

b) Hydrolysis of Metal Cations

There are two factors that affect the acidity of metal ions, viz: the charge on the metal ion, (thus acidity increases with charge) and the size of the metal ion (ionic radius) (thus acidity decreases as size increases). The *charge: size ratio* can be used to predict the relative acidities of metal ions: highly charged, small cations are the strongest acids in aqueous solution. This is because the greater the power of the metal ion to attract electron density from the oxygen atom of a co-ordinated water molecule, the weaker the O–H bond of this molecule, and the easier it is to break so releasing an H^+ ion. When a divalent metal aqua-ion is placed in water, the following equilibrium is set up:

$$[M(H_2O)_6]^{2+} + H_2O \Leftrightarrow [M(H_2O)_5]^+ + H_3O^+ \qquad (3.21)$$

The equilibrium position lies to the left and the equilibrium constant, K_a values lie between 10^{-6} and 10^{-11}, with a pH of about 6, (Langmuir, 1997). Thus a small amount of acid is generated due to the production of oxonium ions (H_3O^+). Similar equilibrium is established for trivalent metal cations with K_a values between 10^{-2} and 10^{-5}, producing a pH of about 3, equation (3.22).

$$Fe^{3+} + 3H_20 \Leftrightarrow Fe(OH)_3 + 3H^+ \qquad (3.22)$$

The process of hydrolysis of Fe(III) has been reviewed by Schneider and Schwyn (1987), Stumm and Morgan (1996), and Cornell and Schwertmann (1996). Metal ions undergo hydrolysis because coordinated water is a stronger acid than free water. This results from the effect that the metal-oxygen bond weakens the O-H bonds in a way that in aqueous systems the free water molecules behave as proton acceptors. So the hydrolysis of metal ions is the result of the de-protonation of the coordinated water molecules.

3.4 Acid Neutralization Mechanisms

3.4.1 Acid Consuming Reactions

Rates and mechanisms of dissolution reactions are important in terms of predicting the neutralisation potentials of minerals that are commonly present in waste rock and tailings. Many rock forming minerals have the capacity to neutralise acid upon dissolution, and these include:

a) Calcium and Magnesium bearing carbonates
b) Oxides, hydroxides oxyhydroxides of Calcium, Magnesium and Aluminium
c) Soluble, non-resistant silicate minerals, and
d) Phosphates, primarily apatite.

Table 3.1 shows the maximum neutralisation capacity of some minerals based on stoichiometric considerations assuming that the mineral dissolves completely and not accompanied by precipitation of secondary phases, (Paktunc, 1999). Incongruent dissolution behaviour of some minerals will have an effect on these values.

Table 3.1: Maximum Neutralisation Capacity of some Minerals, (Paktunc, 1999).

Neutralising Mineral	**Formula**	**Moles to neutralise 1 mole H_2SO_4**
Calcite	$CaCO_3$	1
Dolomite	$Ca_{0.5}Mg_{0.5}CO_3$	1
Ankerite	$Ca_{0.5}Fe_{0.2}Mg_{0.3}CO_3$	1.25
Chlorite	$Mg_5Al_2Si_3O_{10}(OH)_8$	0.125
Muscovite	$KAl_2(Si_3Al)O_{10}(OH)_2$	0.2
Kaolinite	$Al_2Si_2O_5(OH)_4$	0.67
Olivine (Fo100)	Mg_2SiO_4	0.5
Hornblende	$Ca_{1.7}Mg_{3.5}Fe_{1.3}Al_{1.3}Si_7O_{22}(OH)_2$	0.11
K-feldspar	$KAlSi_3O_8$	0.5
Plagioclase (Ano)	$NaAlSi_3O_8$	0.5
Plagioclase (An100)	$CaAl_2Si_2O_8$	0.25
Goethite	$Fe(OH)_3$	0.67
Brucite	$Mg(OH)_2$	1
Gibbsite	$Al(OH)_3$	0.67

Most weathering reactions consume acid and can be grouped into the following categories:

i) Dissolution of carbonate minerals consumes acid while releasing Ca, Mg, H_2CO_3 or HCO_3^- or CO_3^{2-}, reaction 3.23. In the case of carbonates, 2 moles are required to neutralise the acid generated by the oxidation of a single mole of pyrite. However, with iron bearing carbonates such as siderite, the situation is different. Although the acid neutralisation capacity of siderite is the same as that of calcite, the oxidation of ferrous iron to ferric iron and its precipitation as ferric hydroxide produces acidity and this eventually cancels the neutralisation, resulting in a net zero effect contribution by siderite, equation 3.23.

$$CaCO_3 + 2H^+ = Ca^{2+} + H_2CO_3 \qquad (3.23)$$

The solubility of carbonate minerals depends on whether the system is *open or closed* to the atmosphere. Calcite is more soluble in an open system relative to a closed system at 25°C (Stumm and Morgan, 1981). Conversely, tailings water migration studies by Morin *et al.,* (1988), indicate that below the water table (in a closed system), the principal pH buffering is due to calcium carbonate dissolution. Acidic plumes are neutralised in different regions based on mineral equilibrium pH. The base pH above which precipitation occurs is as follows:

$Fe(OH)_3$ = (3.0 - 3.7); $Al(OH)_3$ = (4.3 - 5.0); $FeCO_3$ = (5.1 - 6.0) & $CaCO_3$ = (5.5 - 5.9).

ii) Dissolution of alumino-silicate minerals in acid releases Al, Ca, Fe, K, Mg, Mn, Na, & Si, reaction 3.24. In nature the primary sink for acidity is silicate weathering, hence, chemical weathering results in the dissolution of species that determine the alkalinity of water as in the dissolution of muscovite, (Lasaga, 1981), e.g. dissolution of muscovite increases pH:

$$KAl_3Si_3O_{10}(OH)_2 + H^+ + 9H_2O = K^+ + 3H_4SiO_4 + 3Al(OH)_3 \qquad (3.24)$$

iii) Dissolution of hydrous Fe and Al oxide minerals releases Fe, Al, and sorbed elements.

iv) Sorption of H^+ onto mineral surfaces releases sorbed elements.

3.4.2 Buffering of Acidity by Aluminosilicates

The role of silicates in the neutralisation process is less well understood than that of carbonates. Buffer intensity calculations predict that the acid neutralising capacity of silicate minerals is greater than carbonates. However, silicate minerals tend to dissolve slower. Thus most buffering in near surface natural waters is achieved by carbonates, (Sherlock *et al.,* 1995). Secondary amorphous silica and goethite have also been identified within waste rock piles by Alpers and Nordstrom (1990). They found out that acid neutralisation was the result of albite, chlorite, sericite, epidote and calcite dissolution (determined by computer speciation analysis) with the largest pH increase due to chlorite dissolution. Within AMD waters, once the carbonate minerals have been depleted, the silicate minerals may play a role in long term neutralisation of sulphide oxidation products.

Kwong, (1993) listed a hierarchy of minerals and their generalised relative reaction rates, Table 3.2, on a scale from 0 (no contribution to acid neutralisation) to 1 (dissolving minerals with maximum contribution to acid neutralisation), although in reality they are site specific.

Table 3.2: Relative Reaction Rates of Minerals contributing to Acid Neutralisation (Kwong, 1993)

Group Name	Typical Minerals	Relative Reactivity
Dissolving	Calcite, aragonite, dolomite, magnesite, brucite	1
Fast weathering	Anorthite, nepheline, olivine, garnet, jadeite, leucite, spodumene, diopside, wollastonite	0.6
Intermediate weathering	Epidote, zoisite, enstatite,hypersthene, augite, hedenbergite, hornblende, glaucophane, tremolite, actinolite, anthopyllite, serpentine, chrysotile, talc, chlorite, biotite.	0.4
Slow weathering	Albite, Oligoclase, labradorite, vermivulite, montmorllonite, gibbsite, kaolinite	0.02
Very slow weathering	K-feldspar, muscovite	0.01
Inert	Quartz, rutile, zircon	0.004

It can be seen that although kaolinite and gibbsite will provide additional capacity to neutralise acidity, their dissolution rates are much slower than their parent minerals, therefore the overall contribution to the neutralisation potential may be insignificant. Thus, depending on the kinetics of the oxidation and neutralisation reactions, most rock forming minerals may be effective in terms of providing additional long term buffering capacity.

3.5 Kinetic Control of Drainage Chemistry

There are two basic approaches to drainage chemistry control, namely proactive and reactive. Proactive control focuses on minimising concentrations leaving a mine site using ‘solid covers’ such as water covers, dry covers or other techniques like back filling, blending and segregation. The concept behind the covers is that the prevention of one or more reactants from entering the mine waste will affect subsequent concentrations in the drainage. Reactive control involves collection and treatment of the drainage, and will be discussed in section 3.6. These sections address the concepts and techniques behind control of drainage chemistry rather than detailed design and engineering which is site depended.

3.5.1 Water Covers

Background Chemistry

Research has demonstrated that the oxidation of sulphides in mine tailings and waste rock is inhibited by placing the mine wastes under a water cover, (MEND, 2000). Arguments for under water disposal arose from the premise that acid generation from sulphides could be suppressed when submerged underwater where oxygen concentrations are greatly diminished relative to the atmosphere. In other words, lowering the concentration of one of the principal reaction ingredients (oxygen) would lower the oxidation reaction rate, hence the rate of generation of acid and dissolved metals.

Sulphides are formed in reducing environments (in the absence of oxygen), and they are unstable and susceptible to chemical reaction in the oxygen-rich environment of the earth’s surface. Accordingly the most stable environment in which to store sulphide-rich mine tailings is one devoid of oxygen, one that mimics their environment of genesis. The maximum concentration of dissolved oxygen found in natural waters is at a minimum 30 fold lower than that in the atmosphere, (Hollings *et al.,* 2000). Because the rate of sulphide oxidation is in part dependent on the concentration of oxygen, it is readily apparent that the generation of acid and dissolved metals can be dramatically minimized underwater.

The flux of oxygen across the water cover/tailings interface depends on the oxygen concentration at the top of the diffusive boundary layer that separates the tailings from the water column and on the thickness of the boundary layer, (Hollings *et al.,* 2000). The researchers also report that the oxygen flux can be estimated, assuming steady state conditions, using Fick’s First Law:

$$F = -D_{eff}\frac{(C_l - C_o)}{L} \qquad (3.25)$$

F is the mass flux of oxygen (mass/unit area/time); C_o is the atmospheric concentration of oxygen, C_l is the concentration of oxygen below the cover; L is the cover thickness; and D_{eff} is the effective diffusion coefficient of the cover.

More importantly, however, is the rate at which oxygen is replenished to the reaction site. Once the small inventory of dissolved oxygen in the water is consumed, it is typically replaced by processes of molecular diffusion and small-scale turbulence; the transfer of oxygen in water is nearly 10,000 times slower than similar transfers in air, (Li *et al.,* 1997). Consequently, storage under permanent water cover is perhaps the single most effective measure that may be taken to inhibit acid generation from sulphidic tailings. The chemical loadings balance assuming diffusion only allows calculation of the minimum allowable thickness of the inert cover Δz that will not exceed the maximum permissible concentration in water, C_{H_2O}:

$$C_{H_2O} = D\left(\frac{C_t - C_{H_2O}}{\Delta z}\right)T_R\frac{A_t}{V_w} \qquad (3.26)$$

C_t is the measured concentration in tailings (mg/L); D is the diffusion coefficient of the inert cover (m^2/s); T_R is the residence time in water (s); A_t is the area of tailings (m^2) and V_w is the volume of water (L).

Limitations

The practice of disposing of sulphide rich tailings under water is based on inhibiting oxidation, and acid generation and the potential for the release of metals into the aquatic system. Primary concerns that have been addressed are the potential deterioration of receiving water quality and the impact on biological resources from excessive concentrations of dissolved metals.

Previously oxidized wastes can in some instances be disposed under a water cover, but only after the wastes have been well-characterized and the potential effects of the oxidation products on tailings pore waters, containment structure seepage, groundwater recharge, and impacts to the quality of the water cover and effluent treatment requirements have been thoroughly assessed. This is to allow measures to be planned in advance and taken to deal with the possible release of contaminated pore water and oxidation by-products to seepage, the water cover and subsequently to the environment.

MEND (2000), indicates that it is apparent from laboratory and field experiments that subaqueous disposal represents the most successful method presently known for preventing and controlling acidic drainage. However, in many cases the water covering the oxidized tailings may require treatment prior to discharge to meet regulatory standards. It is not currently possible to accurately predict either the nature or duration of treatment prior to actual deposition and observation. One of the key physical processes affecting submerged tailings especially in lakes is that sufficiently large waves can generate velocities along the bed that can mobilize the bed material. The generic minimum depth (d_{min}) of water cover required to maintain a physically stable submerged bed can be calculated as follows, (Atkins *et al.,* 1997):

$$d_{\min} = 1.58x10^{-3} g (U_w F)^{\frac{2}{3}} \ln\left[5.14x10^{-2}\left(\frac{R(FU_w{}^4)}{V_b}\right)\right] \qquad (3.27)$$

where: g is force of gravity (m/s^2); F is the fetch length (m); U_w is wind speed (m/s); R is the wave height coefficient (R= 1, for significant wave height); and V_b is the critical bed velocity (m/s).

The suitability of the water cover method is subject to site specific factors, and as such is not universally applicable. For instance in semi arid climates, water covers are not feasible due to various technical factors such as water scarcity, surface topography, hydrological conditions, and long-term stability of retaining structures, as well as various social and economic factors. However, for sites where water covers can be used, the method offers one of the best solutions for preventing sulphide oxidation and acid generation over the long term, (Devos *et al.,* 1997). Additional enhancement is accomplished at some tailings ponds through the use of substrate covers over the submerged tailings using oxygen consuming materials to reinforce reducing conditions in the sediments, or the use of a non-acid generating sand layer to form a diffusion barrier.

3.5.2 Dry Covers

Dry cover systems as a closure option for management and decommissioning of waste rock and tailings is a common prevention and control technique used at numerous sites around the world. They are an alternative where underwater disposal is not possible or feasible. The two principal design objectives of dry cover systems are:

a) To function as an oxygen ingress barrier for the underlying waste material by maintaining a high degree of saturation within a layer of the cover system, thereby minimizing the effective oxygen diffusion coefficient and ultimately controlling the flow of oxygen across the cover system; and

b) To function as a water infiltration barrier for the underlying waste material as a result of the presence of a low permeability layer and/or a moisture storage and release layer.

Apart from these functions, dry covers are expected to be resistant to erosion and provide support for vegetation. Dry covers can be simple or complex, ranging from a single layer of earthen material to several layers of different material types, including native soils, non-reactive tailings and/or waste rock, geosynthetic materials, and oxygen consuming organic materials. Multi-layer cover systems utilize the capillary barrier concept to keep one (or more) of its layers near saturation under all climatic conditions. This creates a blanket of water over the reactive waste material, which reduces the influx of atmospheric oxygen and subsequent production of acidic drainage.

The influx of atmospheric oxygen to reactive waste material can also be limited by incorporating oxygen consuming materials in dry cover systems. The primary function of these barriers is to reduce the ambient oxygen concentration at the waste material/cover interface by consumption of oxygen. Almost invariably, the cover systems contain organic matter, primarily lignocellulosics such as wood chips, wood wastes, peat, sewage sludge, compost, hay, straw, silage, and paper mill sludge. Oxidation of an organic layer material will eventually decline as the remaining material becomes more humidified and more resistant to further decomposition. As a result, the long-term efficiency of oxygen consumption barriers is a key element in the design of cover systems that incorporate such barriers.

Limiting the Influx of Atmospheric Water

The net infiltrative flux through a cover system is also an important consideration in the design of a closure system for a mine waste disposal facility. The objective is to control/limit the quantity of water that flows downward through the cover to the underlying waste material because the infiltrating water ultimately contributes to subsequent production of acidic drainage. The net infiltrative flux is a function of the total rainfall, evaporative flux, transpiration, change in soil moisture storage, and runoff. Each of these factors is in turn influenced by a variety of conditions. For example, runoff and infiltration rates are a function of rainfall intensity, surface topography, vegetation, soil properties, and soil moisture conditions. Evaporation or evapo-transpiration from the cover surface is a strongly coupled process that depends on atmospheric conditions, soil/waste properties, and soil/waste conditions. In addition, it is clear that runoff, as well as run-on, are site-specific considerations. The water balance equation for any site is given by:

$$\text{Rainfall} - \text{Evapo-transpiration} = \text{Flow}_{\text{runoff}} + \text{Flow}_{\text{seepage}} = \text{Flow}_{\text{drainage}} \quad (3.28)$$

Which can be rewritten as:

$$R \quad - \quad ET \quad = \quad F_r \quad + \quad F_s \quad = \quad F_d$$

The chemical loadings balance can be computed to find the minimum allowable ratio of $\text{Flow}_{\text{runoff}}$ to $\text{Flow}_{\text{seepage}}$ (F_r:F_s) that will not exceed the maximum permissible regulatory concentration, C_d:

$$C_d = \frac{C_r F_r + C_s F_s}{F_r + F_s} \qquad (3.29)$$

C_r and C_s are the measured concentrations in runoff and seepage, respectively.

It is difficult and usually not economically feasible in arid and semi-arid climates to construct a cover system, which contains a layer that remains highly saturated, thereby reducing the influx of atmospheric oxygen. The cover system will be subjected to extended dry periods and therefore, the effect of evapo-transpiration will be significant. However, subjecting the cover system to evaporative demands can be beneficial in arid climates and result in a reduction of infiltration to the underlying waste material. A cover surface layer possessing sufficient storage capacity can be used to retain water during a rainfall event. Subsequent to the increase in moisture storage in this layer, it would release a significant portion of pore water to the atmosphere by evapo-transpiration during extended dry periods, thereby reducing the net infiltration across the soil cover system. The objective is to control acidic drainage as a result of controlling the transport mechanism (i.e. water) into the waste material.

An issue that arises with respect to a dry cover system designed to only limit net moisture percolation to the underlying waste is the question of decreasing seepage only, leading to higher concentrations and ultimately the same loading to the environment. In general, there is not complete agreement as to whether very low net percolation rates will lead to the same loading or a reduced loading. It is argued that the low percolation rates associated with a properly designed store and release cover system (with no oxygen control) will eventually lead to contaminant release, (Morin *et al.,* 1988). Conversely, it can be argued that there must be a reduction in loading for a percolation rate given that: zero flow corresponds to zero loading release. In addition, at lower percolation rates the leachable areas of waste rock, for example, will be greatly reduced (albeit the finer textured material will contain higher concentrations of leachable contaminants).

Climate Conditions

The climate conditions at the mine site are a key factor in determining the dry cover system objectives. Generally the site is considered a dry site if potential evaporation greatly exceeds annual rainfall, and generally a wet site if annual rainfall meets or exceeds annual potential evaporation. In most parts of Zimbabwe, evaporation exceeds rainfall on an annual basis. However, the sites typically experience hot, dry months from September to mid November, where evaporation greatly exceeds rainfall; hot, wet conditions from mid November to March, where rainfall exceeds evaporation; and dry cool months from April to August. These conditions can make it difficult to design a cover system that meets all objectives throughout the year, (Magombedze *et al.,* 2006).

3.6 Reactive Control

3.6.1 Active Treatment

The principal objectives in treating AMD are to neutralize free acidity and reduce the concentrations of contaminants of concern (i.e. metals, total dissolved solids) to very low levels so that the effluent quality is acceptable for release to the natural environment or recycle. The active chemical treatment of acidic drainage is typically accomplished using lime-based processes which vary in application from the batch treatment of ponded acidic water to continuous treatment using a high density sludge type treatment plant, (Zinck, 2004). In these processes, lime is used to raise the pH of the acidic streams and remove dissolved metals through precipitation and co-precipitation. These processes result in the formation of a gypsum/metal hydroxide/carbonate sludge which requires disposal. Lime/limestone treatment is the most common and preferred method because of the following reasons:

a) It is adaptable to a large range of concentrations
b) It is adaptable to a large range of flow
c) It has moderate capital and operating costs, and
d) It is generally considered best practical technology.

Some researchers report that even the simple spreading of lime in catchment basins can be beneficial. Other alkalis are used for pH adjustment to a lesser degree (i.e. sodium hydroxide, and sodium carbonate) along with other metallic salts for the removal of specific contaminants (i.e. iron salts for arsenic removal and barium salts for radium removal). Lime treatment depends on the general reaction:

Aqueous metals + aqueous sulphate + lime = metal hydroxides + gypsum (3.30)

The resulting precipitates are often collectively referred to as ‘treatment sludge’, and gypsum is desirable in the sludge because it improves chemical stability. The presence of metal hydroxides such as $Fe(OH)_3$ formed during treatment assist in scavenging other metals from the drainage, (Morin and Hutt, 1997). However, the primary problem with sludge is that it is composed mainly of water, sometimes less than 3% solids that can not be disposed of in a compact form. As a result, sludge requires anomalously large storage areas and is difficult to handle. The design, operation, and maintenance of chemical treatment systems consist of four principal components: AMD collection, AMD treatment, treated water release or recycle, and treatment sludge disposal. Figure 3.3 shows a general flowsheet diagram for the high density sludge treatment process used at most plants in the world.

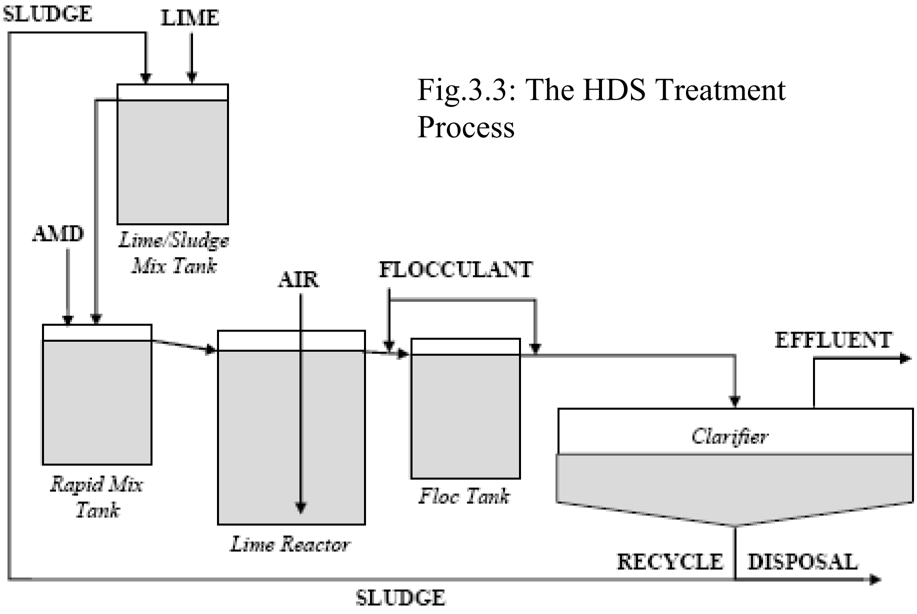

Fig.3.3: The HDS Treatment Process

The HDS process shown in Figure 3.3 is the standard in the AMD treatment industry today, (Aube, 2004). While conventional treatment processes contact lime directly to the AMD, this system contacts recycled sludge with the lime slurry for neutralisation. This is achieved by pumping sludge from the clarifier bottom to a ‘Lime/Sludge Mix Tank’ where sufficient lime to neutralise the AMD to the desired pH setpoint is also fed. This forces contact between the solids and promotes coagulation of lime particles onto the recycled precipitates.

Applications

At active mine sites, the stream flow or ponded water that requires treatment often consists of a mixture of AMD and diverse flows such as mine water, process water, tailings area decant, seepage, and runoff. The cessation of mining or metallurgical activities typically reduces the volume of water to be treated and alters influent contaminant concentrations. There are three types of lime-based treatment processes:

a) Batch treatment of ponded AMD by the addition of alkali material to the ponded water;
b) Conventional treatment of acidic water flows by continuous addition of lime; and
c) The high density sludge (HDS) type chemical treatment process.

The best application of these processes is site-specific, however, Murdock *et al.,* (1994), reported that as a guide:

- Batch treatment is most suitable for the treatment of low flows of acidic water that can be collected, stored and treated on an infrequent basis (e.g. every three to six months);
- A conventional treatment plant is most suitable for continuous treatment where suitable conditions and sufficient space are available for the disposal of the low density sludge; and
- A HDS-type treatment plant is most suitable for continuous treatment and where sludge disposal space/conditions present a challenge. HDS plants produce significantly smaller volumes of sludge in comparison to conventional plants.

Neutralisation and Precipitation

The principle of lime neutralisation of AMD lies in the insolubility of heavy metals in alkaline conditions. By controlling pH to a typical set point of 9.5, metals such as Fe, Zn and Cu are precipitated as in Figure 3.4, (Aube and Zinck, 1999). Other metals such as Ni and Cd require a higher pH, in the range of 10.5 to 11 to effectively precipitate the hydroxides.

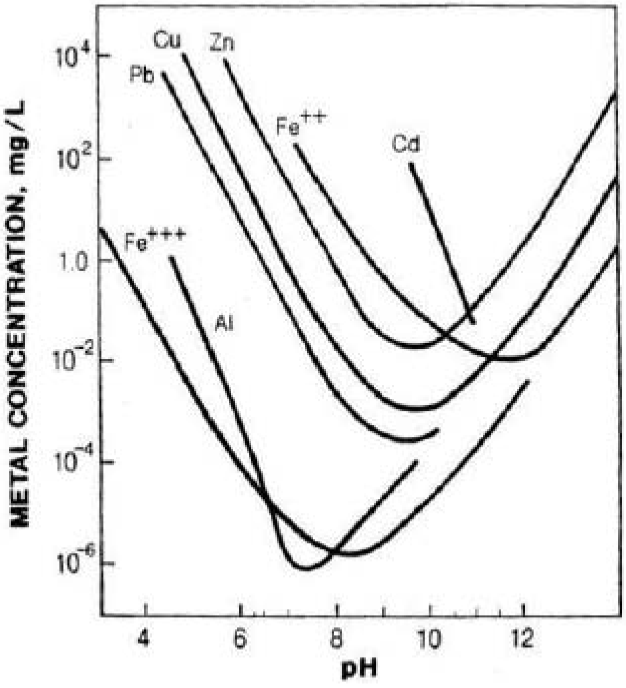

Fig. 3.4: Metal Hydrolysis with pH (after Aube & Zinck, 2003)

$Al^{3+} + 3OH^{-} \rightarrow Al(OH)_3$

$Cu^{2+} + 2OH^{-} \rightarrow Cu(OH)_2$

$Fe^{2+} + 2OH^{-} \rightarrow Fe(OH)_2$

$Fe^{3+} + 3OH^{-} \rightarrow Fe(OH)_3$

$Ni^{2+} + 2OH^{-} \rightarrow Ni(OH)_2$

$Pb^{2+} + 2OH^{-} \rightarrow Pb(OH)_2$

Limitations

Concerns have been raised about the long-term chemical stability of treatment sludges and about potential liability arising from the dissolution of heavy metals contained in sludge. Literature studies to date largely indicate that sludge will remain stable if properly disposed of and if geochemical conditions are maintained. The volume of sludge requiring disposal can be quite large at some mine properties. In extreme conditions, the cumulative volume of sludge produced over the long term from the conventional lime-based chemical treatment of AMD from tailings can exceed the volume of the stored tailings. As part of chemical treatment system planning, provisions need to be made to provide for adequate and suitable sludge storage space, or consideration of methods to reduce sludge volume. Increasing the solids content of sludge can have a very significant impact. For instance, increasing the sludge solids content from 1% to 10% produces about one tenth the total sludge volumes. An increase in solids content from 15% to 30% reduces sludge volume by roughly half.

Conventional lime-based treatment plants produce a low density sludge typically in the range of 1 to 5% solids, Morin & Hutt, 1997; Aube, 2004). These sludge tend to be fluffy, gelatinous voluminous flocs and difficult to dewater. HDS treatment plants can produce treatment sludge with solids contents in excess of 25%. Price and Errington (1998) indicate that while long-term chemical treatment can be effective in protecting the off-site environment, its use can result in significant long-term environmental risk, liability and land alienation.

3.6.2 Passive Treatment

By definition, passive treatment includes methods of neutralizing AMD and removing metal contaminants that require minimal inputs of labour, energy, or raw materials following the initial capital construction phase. Passive treatment technologies include both physical/chemical and biological treatment methods. The passive technologies discussed in this section include anoxic limestone drains, aerobic wetland treatment systems and passive anaerobic treatment systems. Variations on these basic passive treatment methods such as open limestone channels, passive *in situ* treatment techniques, successive alkaline producing systems (SAPS), biosorbents and hybrid active/passive treatment technologies are not discussed.

Contaminant reductions in nature can occur passively through a variety of abiotic and biologically mediated processes, including oxidation and reduction, biological alkalinity production, metals re-mineralization as hydroxides and sulphides, plant uptake, and filtering and sedimentation. Whether these natural reactions will occur depends on the site-specific conditions, such as topography, oxidation state (aerobic or anaerobic), and water chemistry.

Natural treatment processes can be imitated in man-made treatment systems, such as constructed wetlands, passive anaerobic treatment systems, and anoxic limestone drains. The principal goal of a passive treatment system is the long term, sustainable neutralization of acid and immobilization of metals at low cost and with relatively minor labour, raw material, or energy inputs. The challenge facing the mining industry is to design passive treatment systems capable of consistently reducing contaminant concentrations in a time frame measured in hours or days, rather than centuries, (Hedin and Watzlaf, 1994). Hedin *et al.,* (1994), propose a selection scheme for choosing a passive treatment system for AMD based on water chemistry and flow rate, Figure 3.5.

Anoxic Limestone Drains (ALDs)

ALDs consist of limestone rock filters designed and constructed to gradually release alkalinity through dissolution of the limestone as acidic water flows through the drain. ALDs are truly passive treatment methods because the AMD flows through the limestone by gravity. Further, the rate of dissolution is controlled only by the flow rate through the drain and the size and quality of the limestone used. The maximum alkalinity achievable in ALD effluent is reported to be approximately 300 mg/L as $CaCO_3$ and cannot be increased significantly beyond this level by increasing the hydraulic retention time. ALDs are designed to exclude oxygen, as indicated by the term "anoxic" in their name. Excluding oxygen prevents iron oxidation and subsequent precipitation of ferric hydroxides within the drain. Also, the anoxic character of ALDs allows high CO_2 partial pressures to develop resulting in alkalinity additions greater than those possible in systems open to the atmosphere. Hence, anoxic conditions are critical to achieving effective treatment through the use of ALDs.

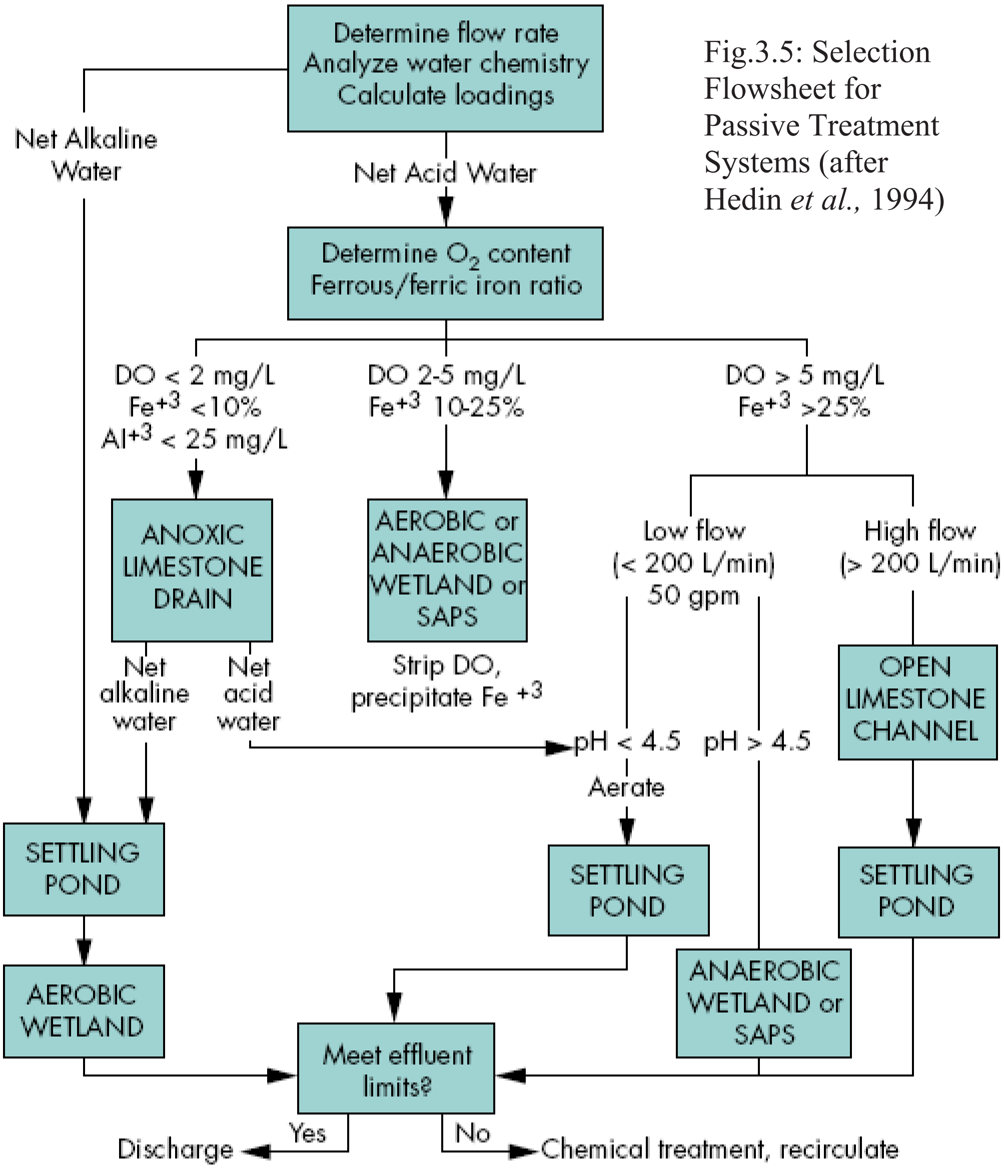

Fig.3.5: Selection Flowsheet for Passive Treatment Systems (after Hedin *et al.*, 1994)

Effective ALDs are reportedly capable of neutralizing acidity resulting in the subsequent removal of metals, including Al, Fe, and Mn, (Eger & Wagner, 1995). Metal removal occurs in an aerobic pond or wetland downstream of the ALD rather than within the ALD. Therefore, oxidative ponds or wetlands are typically installed in conjunction with and downstream of ALDs.

Woods and Noller (1995) report that in tropical climates, year round operation of wetlands can provide better efficiency than in temperate cold climates, particularly for near neutral drainage. However, dry periods can temporarily reduce biological activity and increase aqueous salinity due to evaporation. During the dry periods, diversion of mine water into the wetlands is critical to maintenance, (Noller *et al.,* 1994).

Eger *et al.,* (1994) examined the removal processes that operate in wetlands. Although metal removal levels in the vegetation increased by factors of 3 to 14, the vegetation actually accounted for less than 1% of metal removal. Instead, the researchers found out that the peat supporting the vegetation accounted for 99% of metal removal, primarily through organic complexing. If wetlands act simply as sorption media and filters, then they can eventually reach full capacity and cease filtering. This is not the primary concept of wetland treatment, where continual growth of vegetation would provide an ongoing source of metal removal. Sheoran (2006) argues that the primary and long term objective function of wetlands is to absorb and bind heavy metals and make them slowly concentrated in the sedimentary deposits to become part of the geological cycle.

Aerobic Wetland Treatment Systems

Aerobic wetlands are capable of facilitating a wide variety of abiotic chemical reactions and biologically mediated treatment processes for removing metal contaminants from aquatic environments. The key to successful treatment of AMD in constructed, aerobic wetland systems involves providing the proper combination of environments in the correct sequence required to facilitate the appropriate, site-specific removal processes. Price and Errington (1998) cite the unreliability of passive treatment systems for consistently achieving compliance with low metals discharge limits in Canada due to the high influent metals concentrations, low temperatures during Canadian winters, and high metal loadings during the spring freshet. The researchers indicate that aerobic wetlands may only be applicable for mitigating small, marginally contaminated drainages or for use in polishing effluent from active treatment plants.

The chemical and physical processes occurring in aerobic wetlands include oxidation, hydrolysis, chelation, adsorption, complexation, sedimentation and filtration, (Sobolewski 1997; Skousen *et al.,* 1996, Woulds and Ngwenya, 2004). Wildeman *et al.,* (1991) describe the abiotic removal processes occurring in passive wetland treatment systems. These processes include the exchange of metals onto naturally occurring organic matter, oxidation and oxy-hydroxide precipitation, coprecipitation, and adsorption. Fe, Al and Mn can form insoluble compounds through hydrolysis and/or oxidation depending on pH, redox potential and the presence of various anions.

Aerobic wetlands are frequently constructed to act as sedimentation basins aided by various plant-mediated filtering mechanisms. Concentrations of metals such as aluminum, copper, and iron can be significantly decreased through abiotic processes as AMD flows through an aerobic wetland. Further, oxy-hydroxide precipitates of ferric iron and aluminium are capable of scavenging other metal ions and removing them from solution by adsorption and coprecipitation reactions. For example, arsenic is readily removed from solution by coprecipitation with ferric hydroxide.

Oxidation of iron from ferrous (Fe^{2+}) to ferric (Fe^{3+}) is dominated by abiotic processes at pH greater than about 4.5. The subsequent hydrolysis reactions leading to precipitation occur abiotically in the presence of oxygen, i.e. the reactions are not catalyzed by microorganisms (Hedin *et a*l*.,* 1994). However, the rate of iron oxidation is highly pH dependent. Ackman and Kleinmann (1984) indicate that the relationship between pH and the time required to oxidize 97% of the ferrous iron in Pennsylvania coal mine drainage under oxygen saturation conditions was exponential. At a pH of 7, oxidation occurred in less than an hour, whereas at a pH of 6.0, 35 hours were required. At a pH of 5.5, more than 350 hours are required to oxidize 97% of the ferrous iron.
Ferric iron hydrolysis and precipitation reactions tend to proceed rapidly at pH greater than 3, but occur very slowly at pH less than 2.5. Provided oxygen and pH are not limiting and given the appropriate retention time, iron oxidation, hydrolysis, and precipitation occurs passively in oxidized portions of wetland environments. Oxidizing conditions needed to facilitate iron removal can be promoted in constructed wetlands in the following ways:

- By maintaining a shallow water depth, thereby by providing a large surface area for diffusion of atmospheric oxygen into the water;
- By planting aquatic plant species that oxygenate their root zones; and
- By providing mechanical aeration through construction of artificial riffles, such as small man-made cascades or drop structures.

Aerobic wetlands facilitate a wide variety of biologically-mediated chemical reactions and treatment processes capable of removing metal contaminants from aquatic environments. Biologically-mediated processes occurring in aerobic wetland systems include biological oxidation and plant uptake. Constructed aerobic wetlands are typically designed to mimic conditions in natural wetlands. Hence, an understanding of the biological processes occurring in aerobic wetlands is key to designing effective passive treatment systems. Metals are mainly removed by precipitation and exchange reactions while plant uptake and other processes are responsible for removal of a portion of the dissolved metals. Plants, especially the plant rhizosphere, provide large surface areas for oxygen exchange and also act as hydraulic baffles, thereby increasing the mass transfer of oxygen into the AMD. Plant growth and decay provide a constant supply of degradable organic matter. The organic matter provides sorption (adsorption and absorption) sites and stimulates bacterial activity.

Figure 3.6 illustrates a schematic view of the common passive treatment systems including: (a) aerobic wetlands; (b) anaerobic wetlands; (c) SAPS; (d) ALD; (e) settling pond; and (f) open limestone channel. The design selected will depend on site characteristics and other specific criteria, (Skousen, 1995).

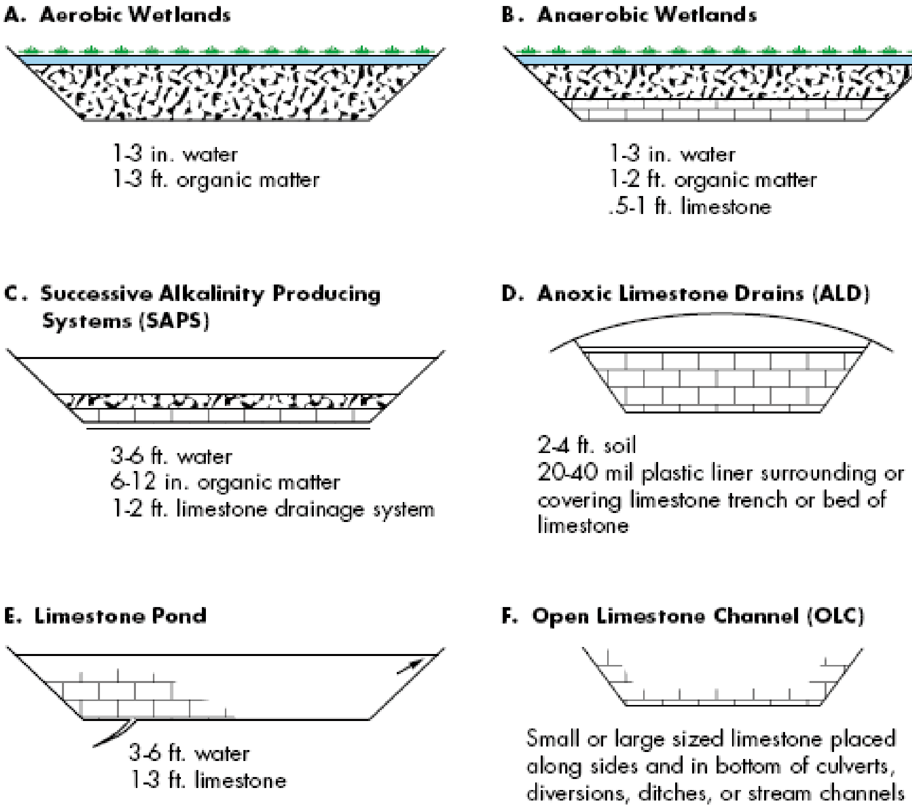

Fig.3.6 Common Passive Treatment Systems, Skousen (1995)

Anaerobic Wetland Treatment Systems

Passive anaerobic treatment systems are engineered ecological systems similar to wetlands in some respects, but are designed to optimize the natural microbially-catalyzed chemical processes resulting in AMD treatment. Whereas aerobic systems may be adequate for removing iron, aluminum, and manganese from sources of net alkaline AMD, anaerobic systems are needed to remove the heavy metals and acidity typical of metal mining sites. In an anaerobic system designed to treat AMD, microbiological and chemical processes are responsible for most of the neutralization and heavy metal removal. Metals removal and acid neutralization are achieved by the activity of sulphate reducing bacteria (SRB). Typically, degradable low-cost agricultural wastes are used as the organic substrate for a consortium of bacteria to generate free sugars and other metabolites. Anaerobic microorganisms utilize these free sugars to produce short chain organic acids that are further utilized as the carbon source for SRB. SRB derive energy by reducing sulphate ions to sulphide according to reaction 3.31.

$$2CH_2O + SO_4{}^{2-} \Rightarrow H_2S + 2HCO_3{}^{-} \tag{3.31}$$

This bacterial sulphate reduction reaction produces bicarbonate alkalinity and hydrogen sulphide (H_2S). The H_2S reacts with metals to form insoluble metal sulphides, (reaction 3.32) and the bicarbonate alkalinity neutralizes the AMD.

$$Zn^{2+} + H_2S \Rightarrow ZnS + 2H^{+} \tag{3.32}$$

The SRB consortium mineralizes degradable organic matter (CH_2O) in the process of reducing sulphate. The bicarbonate produced as a by-product of this reaction acts to buffer the pH at about 6.5, while dissolved zinc remineralises to form sphalerite as a result of sulphide precipitation. Conditions needed to promote biological alkalinity generation and sulphide precipitation include a highly reduced environment characterized by a low oxidation reduction potential (ORP) in the range of –100 to –300 millivolts (mV) and an abundance of degradable organic carbon, (Wildeman *et al.,* 1991). The organic carbon source is designed to be site-specific and waste-specific to provide a long-term food source for heterotrophic bacteria. The organic carbon source also exerts the biochemical oxygen demand (BOD) needed to create the highly reduced conditions.

Due to the absence of dissolved oxygen, iron oxidation and precipitation reactions that would normally occur rapidly at neutral pH are prevented from occurring in passive anaerobic treatment systems. Hence, ferric hydroxide precipitation is not a significant threat to system performance under normal operating conditions.

3.7 Chapter summary

Physical, chemical and biological processes all play important roles in the production, release, mobility and attenuation of contaminants in acid mine waters. The specific processes that have been reviewed and found to contribute to the overall phenomenon of AMD geochemistry are summarised in Table 3.3:

Table 3.3: Summary of Processes contributing to AMD Geochemistry

Physical	**Chemical**	**Biological**
▪ Geology ▪ Mineralogy ▪ Hydrology: water budget, porosity, permeability, flow direction, flow rate, dispersion, mixing, surface transport ▪ Climatic variations: diel, storm events, seasonal ▪ Mining method ▪ Mineral Processing methods	▪ Pyrite Oxidation ▪ Oxidation of other sulphides ▪ Oxidation & hydrolysis of iron & other elements ▪ Neutralising capacity of gangue minerals ▪ Oxygen transport ▪ Fluid transport of water & water vapour ▪ Evaporation, efflorescence & re-dissolution ▪ Temperature ▪ Mineral precipitation & dissolution during transport	▪ Microbial catalysis of reaction rates ▪ Microbial sorption & uptake of metals ▪ Organic complexing

The geochemistry of acid mine waters is a complex subject that draws upon many technical disciplines. There will always be insufficient data to understand such a complex natural phenomenon and although considerable research has been accomplished on this subject, the need for new challenges will continue to appear.

CHAPTER 4

CHARACTERISATION OF ACID MINE DRAINAGE AT SULPHIDE METAL MINES IN THE MAZOWE RIVER SUBCATCHMENT

4.1 Selection and Location of Study Sites

The general objectives in this chapter are to assess the environmental condition at metal mining sites in the Mazowe River watershed and characterise drainage from the mine sites with respect to metal leaching. Although there are several thousand claims, prospects and small mines in the selected mining district, the approach in this investigation was to identify the larger examples of active sulphide metal mines for observation, sampling and geochemical testing. The three metal mines selected as case studies lie in the Mazowe – Bindura area in North East Zimbabwe and are located on the same watershed presenting a good case for impact study from neighbouring mines on a catchment basis.

The scope of work for the assessment of AMD in semi arid Zimbabwe called for the selection of mine sites which deliberately or unwillingly discharge untreated or treated effluent to natural surface streams draining from their environs. To the extent possible, the study sites were selected on the basis that the mine site (1) processes sulphide bearing metal minerals on a large scale as described in Chapter 2. (2) perennially discharges effluent from mine dumps and (3) was willing to share their own historical data and allow access to the study of their mine components. The project sites selected for the case study are Trojan Nickel Mine, Mazowe Gold Mine and Iron Duke Pyrites. All the three mines are located north east of Zimbabwe in the Mazowe Valley sub-catchment, (Figure 4.1).

The mines are situated within the Harare – Bindura – Shamva greenstone belt of the Zimbabwean Archaean craton, west of the Chinhamora batholith, and they all process sulphide ores with varying amounts of pyrite, pyrhotite and arsenopyrite. Their relative proximity to the Mazowe River and its tributaries present the best case for a study of cumulative impacts and other geochemical investigations on acid mine drainage in Zimbabwe. Large commercial farms, small scale farms, urban councils & rural communities of Bindura, Goromonzi, Marondera and Mount Darwin draw water from the Mazowe River, a trans-boundary water system flowing into the Zambezi in Mozambique. Zimbabwe is signatory to the SADC Protocol on Shared Water and is committed to reducing and controlling pollution of the Zambezi River (SADC, 2000).

Trojan Nickel Mine is located 9km south west of Bindura town and extracts nickel sulphide ore that exists at the Cardiff and Trojan hills in north east Zimbabwe, 90km north of Harare. Trojan Nickel is part of Bindura Nickel Corporation (BNC), a subsidiary of Mwana Africa Pvt. (Ltd). Trojan mine is the largest base metal operation in Zimbabwe, producing Ni, Cu and Co.

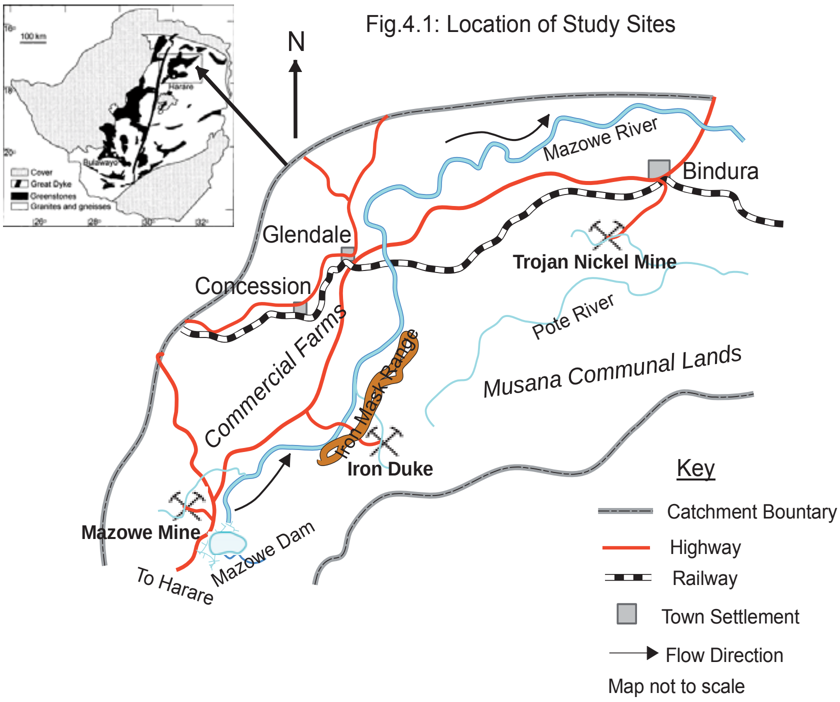

Fig.4.1: Location of Study Sites

The Mazowe group of mines consists of several shafts, (Jumbo, Bernheim, Ogilvy, Connaught, Nucleus, Vesivius and Stori's Golden Shaft); all located about 50km north of Harare, in an intensively cultivated commercial farmland producing citrus, maize and wheat. The shafts are situated within a 7km radius from the mine office and share a common gold treatment facility at Jumbo.

Iron Duke Mine is located approximately 65km north of Harare, at the southern end of a gorge in the SW – NE trending Iron Mask mountain range. Yellow Jacket River passes through the mine site, and receives drainage seeps from mine water, before the confluence with Mazowe River, approximately 2km downstream from mine site.

The mine draws processing water from Yellow Jacket River. Other major water users in the vicinity are a small scale gold mine, a horticultural flower project and commercial irrigation. Iron Duke is the only pyrite and most acidic mine in the country.

4.2 Basic Geology, Mineral Processing and Environmental Setting

4.2.1 Trojan Nickel Mine – Site 1

The nickel bearing minerals at Trojan are pentlantite ($(Fe,Ni)_9S_8$) and polydymite (Ni_3S_4), hosted in serpentinised ultramafic lavas, with a variety of iron, iron-nickel, copper-nickel sulphides and magnesium basalts, (Chimimba and Ncube, 1986). Pyrite, pyrrhotite and chalcopyrite exist in the ore in minor quantities. Ore production is exclusively by underground mining methods and about 90 000 tons per month of ore are crushed, milled and concentrated by flotation according to the flowsheet in Appendix B, Figure B1, to produce nickel concentrates grading an average 9.2% Ni, along with copper, cobalt and small quantities of precious and platinum group metals as by products.

Trojan Nickel mine is the largest base metal producer in Zimbabwe. The mine produces about 11,000 tonnes of refined nickel per annum of which about 7,000 tonnes are own production and the balance is toll material from Botswana and South Africa. Under current production rates, operations are expected to continue for at least another ten years. The Trojan shaft is currently being deepened by some 600 metres to access new reserves and it is expected that these will extend the life of the mine considerably, (Smith, 2003).

The mining activities at Trojan Nickel mine have directly created 28 million tons of sulphide bearing tailings situated in 10 tailings impoundments covering a combined area of 182 ha, approximately 5 million tons of permanent waste rock and overburden covering an additional area of 22.8 ha. On such a large scale operation, concerns for AMD during and after mine operation are very high on the mine’s rehabilitation program.

4.2.2 Mazowe Gold Mine – Site 2

The geology of the Mazowe group of mines has been discussed in detail by Bleknisop, *et al.,* (2000). Gold minerals in the form of quartz reefs are intimately associated with sulphide mineralization hosted within shear zones. The shear zones are basically situated in two different rock types: granodiorite in the west and feldsparporphyre in the east. In the granodiorite, the principal sulphide mineral is pyrite, which occurs in white to grey quartz. Minor sulphides which also occur include pyrrhotite, chalcopyrite, arsenopyrite and scheelite. In the porphyries, pyrrhotite is more abundant than pyrite and quartz.

Gold mining at Mazowe started in 1880. Ore from the different shafts is transported to the coarse ore bin and conveyed to the crushing plant where size reduction takes place in three crushing stages until the ore is 100% passing 12mm. The fine ore averaging about 12g/tAu is fed to the milling circuit consisting of two ball mills in closed circuit with two sets of hydrocyclones. The mill discharge enters a gravity circuit consisting of two superbowl concentrating units and a James Table for re-concentration. The gravity circuit recovers 70 – 75% of the gold, and the remainder is recovered by cyanidation in a Carbon In Leach configuration (CIL). Finely ground tailings are discharged at the rate of 10 tons per hour and stored in slimes dams. The production flowsheet is shown in Appendix B, Figure B2.

There is an excess of water within the plant and a dedicated return water dam to capture fugitive spills from the mill, underground mine water and run-off from tailings dams was constructed to recycle water to the plant for various purposes when need arises. Over the years, this dam has filled up and a perennial overflow of poor quality water is discharged to Murowodzi River, a tributary of the Mazowe River, presenting a significant risk of water pollution and environmental damage.

4.2.3 Iron Duke Pyrites – Site 3

The geology of the area around Iron Duke has been described by Ferguson and Wilson (1964), and Bleknisop, *et al.,* (2000). The Iron Mask mountain range occurs in the Zimbabwe Archean craton and is characterised by stratiform Fe mineralization, metasediments and metavolcanics. These rocks are locally succeeded by Archean greenstones of the Acturas Formation and metagreywackes of the Shamvain Group to the north east. The main orebody at Iron Duke comprises massive pyrite, with minor pyrrhotite, chalcopyrite, and scheelite. Traces of gold, arsenopyrite and other sulphides also occur. The gangue minerals comprise mainly chert (silica and manganese).

The mine started in 1914 as an open cast gold operation, (Smythe, 1996). Pyrites mining of the sulphide facies started in 1940. The mine targets to extract 12 500 tons per month of Run of Mine (ROM) ore with a minimum grade of 30%S using underground stopping method. The ore is mined with little waste that is stock piled on the surface. Wet drilling is used, and approximately 180m^3/day of water is drawn from nearby Yellow Jacket River for this purpose and to suppress dust and fumes during the blasting operations. The treatment flowsheet is shown in Appendix B, Figure B3. The ROM ore is stage crushed from <300mm to +/-12mm. A small gravity separation plant utilising two Velco jigs in parallel circuit (5ton/hr each), is used to upgrade the minus 12mm fraction of the pyrites from 30 to 36%S for the export market in Zambia, South Africa and Europe for applications in metallurgical fluid bed roasters and Foundry Industries. The bulk of the product output around 30%S is used in the production of phosphate based fertilisers at Zimbabwe Phosphate Industries (ZIMPHOS) in Masasa, Harare.

Introduction of water to the drilling faces with sulphudic rock chips in the drill holes forms sludge with the perfect mixture for acid mine drainage formation. Another source of acid drainage underground is associated with seepage of ground waters into old workings. The oozing takes place in stopped out areas. The reticulation is such that the acid water (pH ~2) gravitates to the bottom of the mine, 9th level (270m below ground level), collected in sumps and pumped in two stages to the surface, Figure 4.2. Special precautions are needed for equipment which includes stainless steel pumps, acid resistant paints, extra greasing and PVC piping. Due to intermittent drilling and blasting, the acidic mine water is pumped to a holding tank in the neutralisation plant in a batch wise operation, and treated with lime before discharge to evaporation ponds.

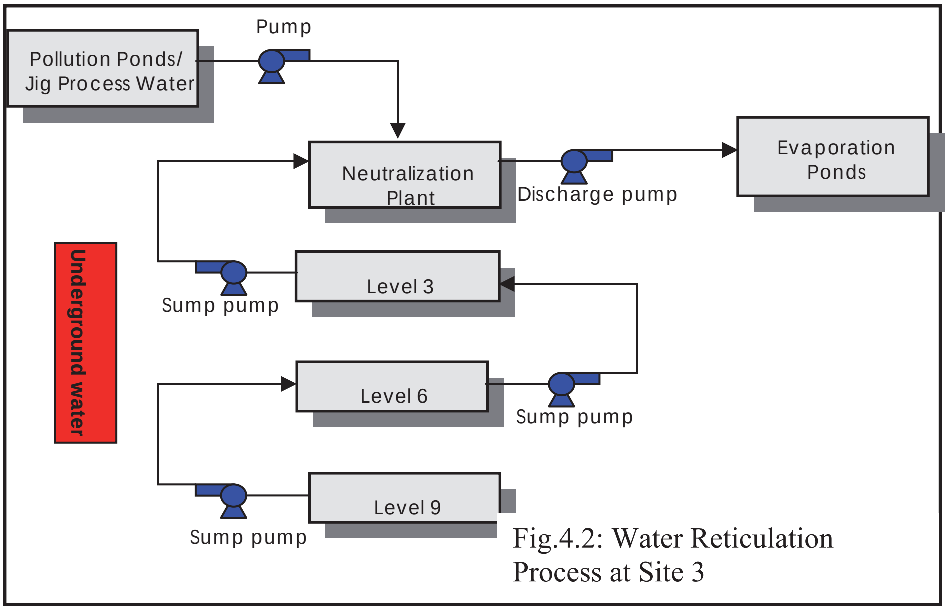

Fig.4.2: Water Reticulation Process at Site 3

4.3 Previous Work in the Study Area

Published previous work on mining and the environment in Zimbabwe has largely focussed on environmental problems caused by small scale mining, legal issues, and management of tailings dams with regards to geotechnical stability. At big mines, studies on environment are considered sensitive, access to the mine area is strictly prohibited unless by prior arrangement with mine management. Where permission to investigate environmental problems at a mine site has been given, publication of the results of such work is restricted to confidential reports for internal circulation only. The University of Zimbabwe's departments of Mining, Metallurgy, Geology and Institute of Mining Research, and some consulting firms have undertaken, to a limited extend, studies on environment work at mines in Zimbabwe in the form of consultancy reports and student thesis.

Maponga & Mutemererwa (1995), Svotwa (1996), Endahl & Hedenvind (1998), Thixtorn (1999) have documented evidence of the negative environmental effects of mercury and other chemicals used by small scale gold miners along the Mazowe and Ruenya rivers in north east Zimbabwe. Magadza & Masendu (1986) and Gratwicke (1999) studied the effects of seasonal changes on biota along the Yellow Jacket River. A study of the gold mineralization in the Mazowe area was done by Blenkinsop *et al.,* (2000). The study looked at tectonic controls on mineralization by considering the Harare – Bindura – Shamva greenstone belt. Lupankwa *et al.,* (2004) showed that drainage from the waste rock dump at Trojan nickel mine contains sulphate concentrations over100ppm and there is presence of metals such as lead, zinc and nickel, raising concerns of acid mine drainage. Williams & Smith (2000) and more recently Ravengai *et al.,* (2005) described the effects of Iron Duke mine water effluent to aquatic life biodiversity along Yellow Jacket River. As part of this study, several geochemical investigations to characterise the area have been undertaken, (Magombedze & Sandvik, 2006; Magombedze *et al.,* 2006; and a number of BSc and Master Thesis.

4.4 Field Work Program

4.4.1 Objectives

a) To determine the extent of possible environmental impacts associated with sulphide metal mining and establish geochemical baseline levels for acid mine drainage related pollution by characterising drainage at the selected mine sites.

b) To quickly assess the potential of metals and acid release from tailings and waste rock dumps at the three sites, and thereby establish potential to degrade water quality.

4.4.2 Water Sampling and Field Measurements

A field reconnaissance and drainage monitoring of sulphide metal mines in the Mazowe area was conducted once every month, from May 2004 to April 2005. The selected sites comprise a nickel mine, a gold mine and a pyrite mine operation.

Surface water samples were collected from nearby rivers, streams, ponds, seeps, mine water and drainage locations in proximity to tailings and waste rock piles. Ground water samples were collected from monitoring boreholes and domestic boreholes. The monitoring boreholes were flushed out by removing 20litres of water and given 30minutes to recharge before collecting the water sample. Photographs of contaminated locations within sites were taken for recording observations of colour, texture and physical appearance, where possible. Figures B4, B5 and B6 in Appendix B show the sampling and monitoring locations at each site used throughout the study.

Temperature, pH, ORP, EC, and TDS were measured in the field using the Myron ultra meter Model 6P. The quick analysis is done by just filling the cell cup, rinse three times with sample, pushing a parameter key and taking the reading. Dissolved oxygen was determined by means of a membrane based oxygen meter, after calibration and allowing for temperature correction. The performance of the probes in the reading cell was confirmed using the pH 4 and pH 7 buffer standards, and also calibrated using the standards for TDS and EC. All water samples collected for trace metal analysis were filtered at the site using a 0.45µm membrane filter. The filtered solution (1litre) was stored in polyethylene containers which were used exclusively throughout the sampling campaign. The sample containers were first rinsed with an aliquote of the filtered sample, then filled to the brim to exclude oxygen and acidified with 65% nitric acid solution to pH<2. Samples for major anion analysis were also filtered through 0.45 µm membrane filter but were not acidified. Samples were kept in a cool place until returned to the Department of Metallurgical Engineering, UZ, where they were analysed within 7days. Concentrations of Ca, Cu, Fe, K, Mg, Mn, Na, Ni and Zn were determined by atomic absorption spectrometry. Cl^-, CN^-, NO_3^- and SO_4^{2-} were determined by titration and gravimetric analysis.

4.4.3 Grid Composite Solids Sampling

To understand the complex chemistry taking place in a waste rock pile or a tailings disposal area, it is important that good sampling techniques and analysis are applied. Because of the differences in the physical and chemical nature of waste rock and tailings, the sampling procedures may differ slightly but are basically the same. A sample is defined as a small quantity of material relative to the geological mass it represents, collected according to a systematic procedure, of measurable reliability, from which the acid mine drainage potential of the mass which it represents may be estimated, based upon appropriate protocols, (Vallee, 1999). Poor sampling techniques and inadequate sample selection can contribute to excessive variance, difficulties in interpretation and incorrect assessment of AMD characteristics at mine sites, resulting in serious consequences and costs.

A detailed description of the sampling theory used in this study is given in Smith *et al.,* (2002). The primary goal in the use of this sampling technique is to determine the average properties and average geochemical behaviour so as to provide a rapid classification of weathered mine waste materials regarding AMD potential. The top surface of each mine dump was demarcated into a block of 50m by 50m. A grid pattern was marked at 5m intervals on both sides of the square, making 100 cells of 5m by 5m. Multiple surfical (top 5cm) samples were collected from at least 30 cells systematically chosen to cover the grid evenly. The samples from each cell were taken using a stainless steel trowel, were of roughly equal mass and were placed in a plastic bucket, and mixed to create a mine dump composite sample weighing at least 3kg. The sample was sun dried, thoroughly mixed, and then dry sieved to <2mm and subjected to diagnostic leaching as described below.

4.4.4 Diagnostic Bottle Role Leach Tests

The potential for leaching of soluble constituents from tailings and waste rock dumps was assessed for weathered materials by conducting simple bottle role leach tests. The leach test method developed by Hageman and Briggs (2000) was used with slight modification as briefly described below. The leach procedure is an effective indicator of mine waste geochemistry and is used to determine the mobility of inorganic analytes present in soils, waste and waste waters. The method assumes that the most chemically reactive material in weathered mine waste consists of relatively soluble components in the fine fraction, <2mm, (Price and Kwong, 1997).

About 200g of the dry solid weathered tailing sample (<2mm) from each site were riffle split from the bulk (~3kg) and pulverised for chemical analyses while 50g were prepared for leaching. Organic free, deionised water was acidified with a mixture of sulphuric acid and nitric acid (60/40 weight percent) to a pH = 4.20. Using a ratio of 20:1 water to sample, one litre of the acidified deionised water at 25°C was added to 50g of the sample in a rinsed polypropylene bottle. The mixture was rotated at 35 rpm for 18 hours. One blank sample using the acidified deionised water was included in the batch of samples leached to act as a control on solution compositional analysis. After rotation, measurements of pH, EC, TDS, ORP and temperature were made. Instead of filtering the entire 1litre leachate through a stainless steel positive filtration unit, only 400ml were filtered using disposable 0.45µm filters. The filtrate was immediately acidified with 65% nitric acid to pH<2 and saved for trace metal analysis.

4.5 Physical Data Analysis

4.5.1 Climate and Hydrology

The chemical composition of surface and groundwater draining from mine sites is controlled by many factors that include rainfall patterns, mineralogy of the watershed and mine waste materials, climate and topography. These factors combine to produce diverse water types that change spatially and temporally, (Guller and Thyne, 2004). Surface and groundwater flows originate from rainfall. Zimbabwe has an estimated area of 390 757 km^2 of which over 60% is underlain by Archean granite and greenstone belts that have a considerable influence on relief, (Mazvimavi, 2003). Altitude varies from 162 to 2592 m above sea level. On the basis of relief, Table 4.1, the country can be divided into four physiographic regions, Figure 4.2. Most of the rivers only flow during the rainy season.

Table 4.1: Physiographic Regions of Zimbabwe

Region	**Altitude (m)**	**Min and Max Temperatures (°C)**	**Mean Annual Rainfall (mm/yr)**
Lowveld	162 – 600	9.4 – 33.7	344 – 600
Middleveld	601 – 1200	5.5 – 30.7	601 – 700
Highveld	1201 – 1800	5.0 – 27.5	701 – 1200
Eastern Highlands	1801 - 2592	5.0 – 22.0	1201 – 2000
Seasons:	Duration:		
Rainy Season	November to March		
Cool Dry Season	April to August		
Hot Dry season	September to October		

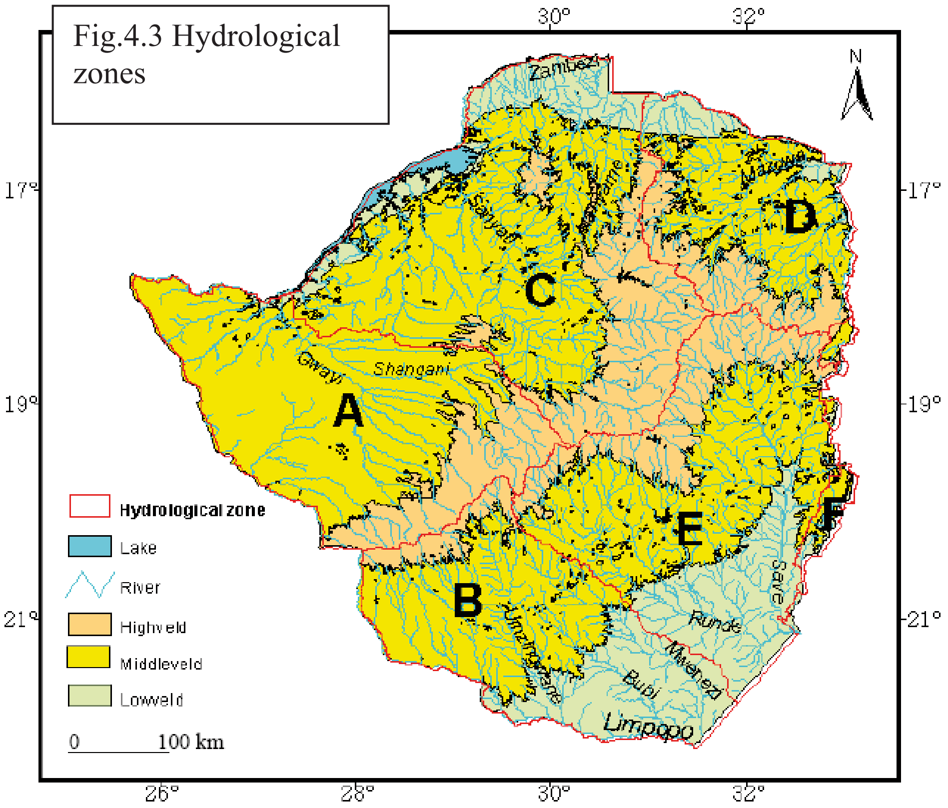
Fig.4.3 Hydrological zones

Zones: A - rivers draining into the Gwayi River and then into Zambezi River; B – rivers draining into the Limpopo River bordering South Africa; C – catchment of the Manyame and Sanyati Rivers draining into the Zambezi River; D – basin of Mazowe River which drains into the Zambezi River; E – basin drained by Save and Runde Rivers; F – rivers draining from the Eastern Highlands into Mozambique.

To quantify rainfall amounts and seasonal variability, historic daily rainfall data for each site was obtained from mine records. From these data, monthly rainfall, average annual rainfall amounts and extreme storm events were calculated for the period January 2000 to December 2005. Temperature data were also considered in the same way. Figure 4.4 shows the seasonal variation of rainfall at the three sites. The rainfall pattern at all three sites is almost similar as these mines fall within the same physiographic region and also located within 45km distance from each other. The mean annual rainfall is about 800mm, and most of it is recorded from November to March. A long dry spell is experienced from April to October.

Fig.4.4 Mean Monthly Rainfall 2000 - 2005

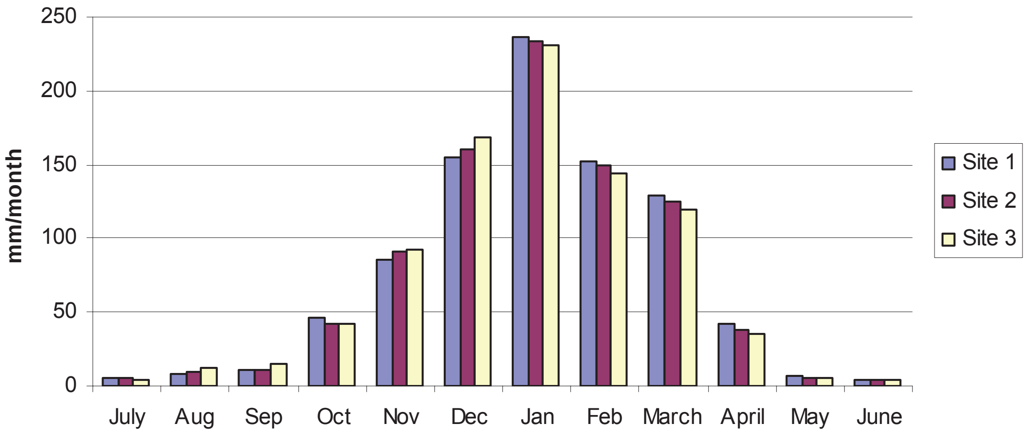

Stream flow measurements were done using flumes and weirs at Site 1 and Site 2, Figure 4.5(a) – (c), while river flow data was obtained from records at gauging stations of ZINWA for Yellow Jacket and Mazowe rivers.

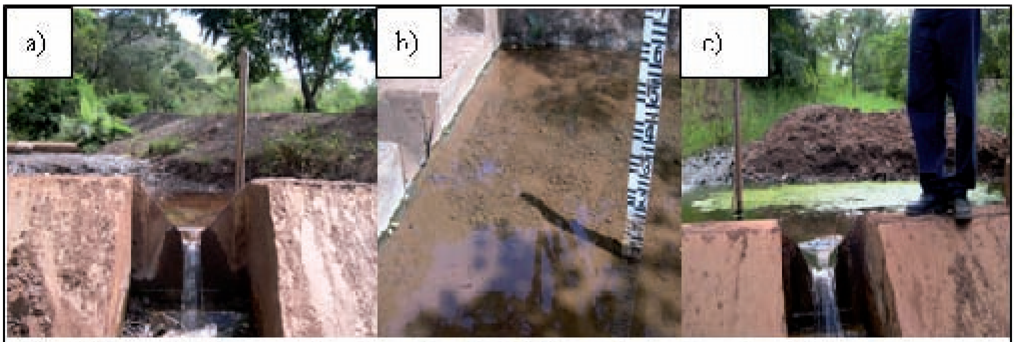

Fig 4.5(a) – (c) V – notch weir at sites 1 & 2 showing calibration & flow measurement

Figure 4.6 shows the hydrograph of mean monthly stream flows draining from the study sites and into the nearby Mazowe River. Runoff is highly variable and ranges from 60 to 80 mm/year in the catchment. Potential evaporation rates exceed rainfall except during the rainy season. There is a huge variation seen in the Mazowe River monthly flows due to abstraction by farmers in the area during the dry season and recharge from feeder streams attributable to a bigger catchment contributing to higher flows during the wet season. These changes are expected to impact on metal loadings and other pollutants draining from the mine sites.

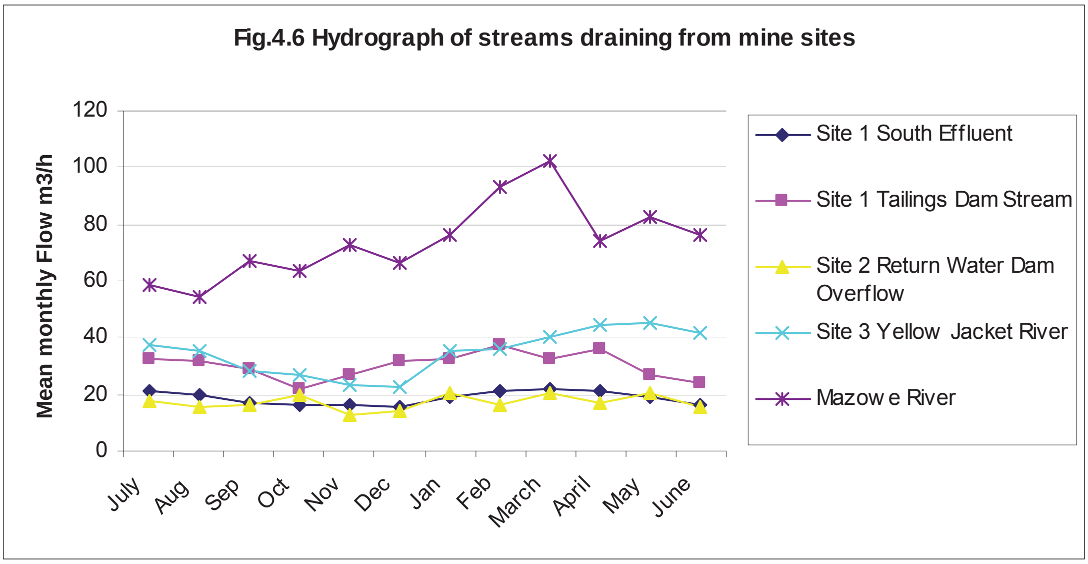

4.5.2 Sources of AMD Pollutants and Release Mechanisms

Pollutant sources, release mechanisms, pathways and receptors were identified at the three mine sites and summarised in Table 4.2. The potential and observations of acid generation are significant at Site 2, but due to the addition of lime and cyanide used in the gold processing plant, observed pH levels around the site are alkaline except for drainage from the old Bucks tailings dam where pH ~ 4.5. AMD is severe at Site 3, while no clear evidence of AMD could be seen from Site 1 during the field assessment.

All the three mine site facilities considered in this study are adjacent to freshwater systems in remote areas away from other industrial and urban developments. Drainage from the sites is discharged into small, headwater streams where the effluent dominates the flow of the system. Pollution control systems are complicated by diffuse drainage from waste rock piles and tailings areas. Under normal circumstances, the surface water streams have an elevated background level of contamination from the mineralized areas but effluents and runoff associated with the mining facilities add to increased pollutant levels. Unlike most other industries, mines still continue to contribute contaminants to local surface waters even when they have been closed and abandoned, implying that the potential for long term water quality impacts can not be ignored.

Table 4.2 Sources of AMD Pollution at mine sites

Category	**Site 1**	**Site 2**	**Site 3**
Constituents of Concern	Ni, Cu, Pb, Residual Flotation reagents& AMD	AMD, high pH, As & Cyanide	Low pH, AMD, Fe, Mn, TDS & SO_4
Primary Sources	Waste rock; Slag Dump; Tailings & Mine water	Mine water; Sulphide mineralogy in tailings;	Mine water; Old Waste rock dump; Jig Plant tailings
Secondary Sources	Process water & Plant Spills	Plant spills Hydrolysis of secondary salts	Evaporation ponds seepage; Soluble secondary salts Jig plant spills.
Primary Release Mechanisms	Chemical Dissolution; Metal Leaching; Water and wind erosion; Surface run off; Infiltration to groundwater	Sulphide oxidation; Cyanide dissolution of metal constituents; Percolation of dissolved metals to vadose zone & groundwater; Water Erosion; Wind erosion	Pyrite oxidation in the presence of drilling water; Chemical instability of neutral sludge; Iron hydrolysis
Pathways & Transport Mechanisms	Fine grained sediments scavenging metals in wetland. Surface run off	Surface run off; Infiltration of leachate & process spills to soil column; Sediment erosion	Infiltration of pond seepage to aquifer & recharge to Yellow Jacket River. Alluvial sediments provide sink for metals
Receptors & Exposure Routes	Pote River; Dermal contact & Consumption of contaminated fish and animals drinking from Pote & Mazowe Rivers	Return water dam; Sediments in wetland Domestic water dam	Ground water; Yellow Jacket River; Dermal contact with surface water.

The major constituents of concern at Site 2 are acidic drainage from the old tailings dump and the presence of cyanide and arsenic in plant solutions. While low pH is not an immediate problem at the site, it will be a matter of time before the alkalinity is used up in the fresh dumps and the drainage becoming net acidic as at old Bucks dam.

The primary sources of AMD at Site 3 are mine water used in the drilling and blasting operations which comes into contact with oxidising pyrite, fugitive drainage from the rehabilitated old waste rock dump and seepage from the jig plant tailings. Treated sludge is disposed in evaporation ponds but acidic seepage occurs on a grant scale leading to contamination of a shallow aquifer below the evaporation ponds and the Yellow Jacket River.

4.6 Analysis of Hydro-geochemical Data and Pollution Impacts

The Zimbabwe National Water Authority has developed and issued water quality guidelines to regulate the discharge of waste water from industry and mine facilities, (ZINWA, 1998). The guidelines define water quality as composing of the physical, chemical and biological characteristics of water and the biotic and abiotic interrelationships. The foregoing discussion focuses on AMD derived pollutants. Biological characteristics are not considered.

The major parameters summarising the main constituents of concern monitored at the three sites are summerised in Table 4.3, which gives the mean annual concentrations of pollutants for streams which drain out of the mine sites and mix with natural surface and ground waters. The values are compared to the regional background levels from Mazowe River at a sampling point upstream of all mining sites and also to ZINWA Regulations limits for effluent discharge to surface water streams. The full results of the monitoring program from which the foregoing discussions are based are given in Appendix C. The results are interpreted in the context of site conditions and where possible, an attempt is made to draw comparison with findings of other researchers under different environmental conditions.

4.6.1 Streamflow and Pollutant Loadings

There are more leachate streams at each mine site than finally presented in Table 4.3. However, most of these streams mix and co-mingle before exiting from the mine sites, so the loadings are presented for the composite streams discharging from each site, less unknown plumes to ground water. Streamflow is an important component to determine for surface water quality studies because it gives insight to hydrologic processes that influence geochemical reactions and is necessary to quantify the transport of constituent loads through the watershed.

Of the 21 variables measured and analysed in this study, 14 variables exceed regional background and regulation limits for effluent discharge at one or more sites. These variables are the major constituents of concern to human health and the environment as a direct or indirect consequence of acid mine drainage and related mining activities, and include pH, acidity, TDS, EC, sulphate, nitrate, chloride, As, Fe, Mn, Al, Cu, Ni and Zn. Based on the mean annual streamflows deduced from Figure 4.6 and the average pollutant concentrations given in Table 4.3, the pollutant loadings transported to surface water streams from each site are shown in Figure 4.7 for SO_4^{2-}, Fe, Mn, Al, As, Ni & Zn. The mean annual concentrations of the major pollutants exceed both the ZINWA limits for effluent discharge and background levels at one or more sites. The transported pollutants end up in the Mazowe River, representing a potential water quality problem to the Zambezi River Basin.

Figure 4.7: Pollutant Loadings transported to Mazowe River from each site

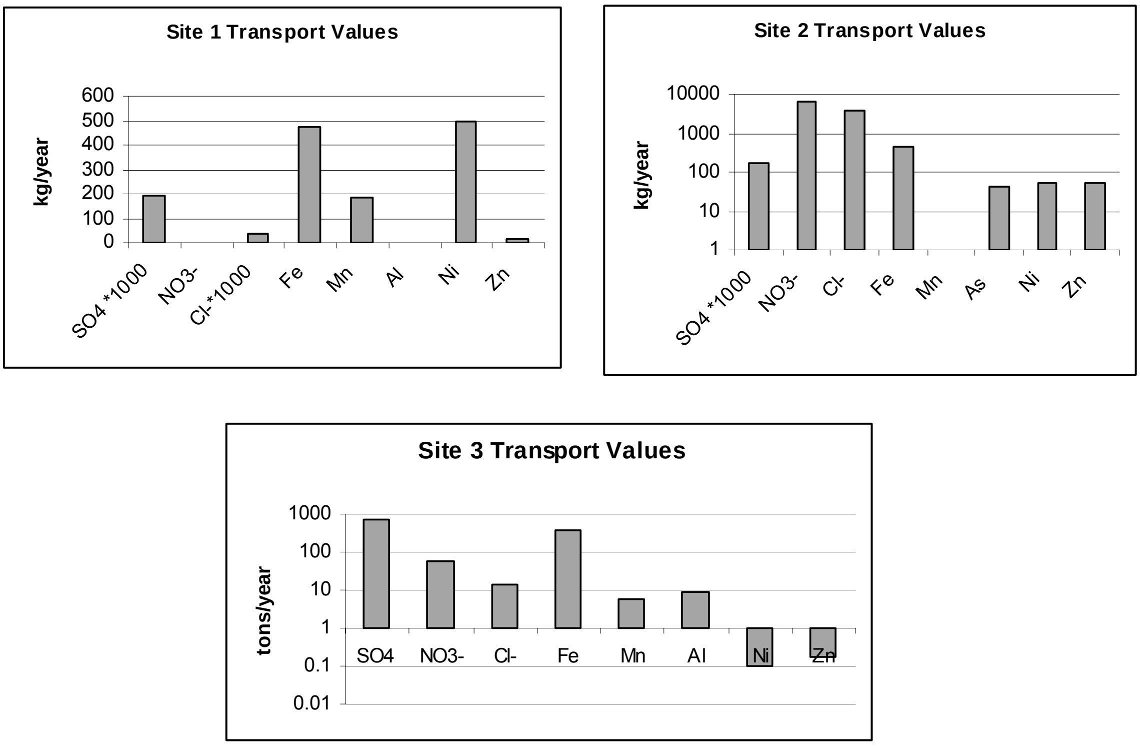

All three sites discharge in excess of 400tons per year of constituents of concern as total dissolved solids. Sulphate and chloride exceed the regulation limit at all sites. Arsenic is a problem at Site 2 where it is carried over to natural surface water via an overflow stream from the return water dam. At Site 3, iron, manganese and aluminium are discharged to surface water at the rate of 363ton/year, 6tons/year and 8tons/year, respectively, while these metals are discharged at rates below 1ton/year at the other 2 sites. Copper, nickel and zinc are discharged at rates below 1ton per year at all three sites.

Table 4.3 Mean Annual Pollutant Concentrations (mg/l unless otherwise stated)

	Site 1		Site 2		Site 3		Mazowe River	ZINWA
	Tailings Dam Stream	Waste rock South Effluent	Return Water Dam Overflow	Mine Water	Yellow Jacket River Seepage Point D	Ground Water Shallow Aquifer	Regional Background Levels	Limits *Normal*
Parameter								
Flow m3/h	30.23	18.77	17.18	7.49	34.75	4.46m_{Depth}	75.42	
Temp. ^{o}C	21.54	21.68	21.73	23.13	22.45	22.95	22.52	≤ 25
pH	7.97	8.06	7.88	2.40	3.86	2.86	8.15	5.50-9.00
Eh mV	292.08	302.00	293.75	49.25	222.17	235.48	236.00	*
Acidity	0.00	0.00	0.00	17563.83	209.28	1179.43	0.00	*
Alkalinity	226.47	120.43	82.32	0.00	7.13	0.00	154.29	≤ 500
DO	5.57	5.39	5.59	3.82	4.68	4.67	6.98	≥ 6.00
TDS	1065.57	992.83	1648.38	16149.55	907.51	5076.62	362.87	≤ 500
EC uS/cm	1304.14	1265.97	2116.92	19403.36	1279.21	6764.56	522.40	<2000
SO_4^{2-}	527.29	301.05	1189.40	10685.66	749.35	1737.06	96.97	≤ 250
NO_3^-	0.00	0.00	43.49	852.46	6.00	56.28	2.14	≤ 10
Cl^-	68.57	97.13	26.21	202.82	80.49	221.00	18.43	≤ 0.10
CN-	0.00	0.00	0.03	0.00	0.00	0.00	0.00	<0.05
As	<0.001	0.00	0.28	0.00	<0.001	<0.001	0.00	<0.05
Fe	0.86	1.52	3.04	5542.72	2.79	368.67	0.77	≤ 1.00
Mn	0.28	0.66	0.00	92.26	56.17	185.11	2.92	≤ 0.01
Al	0.00	0.00	0.00	133.73	10.91	1.57	0.06	< 5.00
Ni	0.57	2.09	0.37	1.50	0.89	1.58	0.02	≤ 0.30
Cu	0.04	0.06	0.04	0.31	0.07	0.41	0.01	≤ 0.50
Zn	0.02	0.05	0.33	2.68	1.01	1.40	0.02	≤ 0.50
Ca	79.03	58.41	296.96	1.65	156.32	236.97	40.77	*
Mg	153.02	105.15	107.88	215.64	77.06	27.30	20.58	*
K	2.97	2.59	22.26	12.01	5.46	6.33	3.73	*
Na	53.04	37.59	87.28	44.34	33.92	26.22	13.92	≤ 200

It should be appreciated that the above figures represent the dissolved fraction of the metals concerned. In acidic conditions ($pH<6$) prevalent at Site 3, it can be safely assumed that more than 80% of the metal is transported in dissolved form and less than 20% as colloidal form. Gundersen and Steinnes (2001) proposed a general relation between the dissolved fraction of a metal species (e.g. Cu), pH and total organic carbon (TOC) in stream waters in Norway.

$$\%\text{Dissolved fraction of Cu} = (61.894 - 6.482\text{pH} - 0.644\text{TOC}) \ln(\text{pH})^2 \qquad (4.1)$$

At $pH > 6$, the authors report that 55 to 81% of the metal can be in dissolved form depending on TOC concentration, (more TOC, less dissolved metal). The metal loadings to fresh water recipients in the cases considered in this study would therefore be expected to be much higher than those shown in Figure 4.7 when the colloidal fraction is also considered. Most of the pollution load will eventually end up in the Mazowe River, representing significant risk to downstream water users in the catchment.

4.6.2 pH, Alkalinity and Acidity

Undoubtedly the most frequently used water chemistry test is pH. Practically every phase of water chemistry, including acid-base neutralization, metal ion solubility, wastewater treatment and corrosivity is pH or acidity dependent. The acidity and alkalinity of mine effluent and receiving water bodies are measured to identify potential environmental effects and to plan appropriate treatment methods to remove metals and produce near neutral pH effluents.

The results of mine waters that drain from the three sites are summarised in Figure 4.8 (sites 1 & 3). The sum of cations includes the concentrations of Fe, Al, Mn, Cu, Ni, Zn, Ca, Mg, Na and K in miliequivalents per litre. Drainage leaving Site 1 is characterised by near neutral to alkaline pH with less than 50meq/l sum of cations. Occasional releases of high metal concentrations, above the regulation limit, especially iron and nickel, are however observed in South Effluent drainage from the waste rock pile and plant spillage. This might suggest an underlying problem with acid mine drainage at its early stages. The presence of magnesium and calcium carbonate in the tailings and waste rock could be buffering the effects of pyrite and pyrrhotite weathering. As the buffering capacity is used up, the acid problem may become more pronounced with time.

Alkalinity refers to the capability of water to neutralize acid. It is important to aquatic life and indicates water's ability to resist changes in pH if mixed with acidic water or waste. Alkalinity thus buffers against rapid pH change, and is often related to hardness - the concentration of divalent cations (e.g., Ca^{2+}, Mg^{2+}). Water-quality criteria for some metals are hardness-dependent as mobilisation of Ca^{2+}, Mg^{2+}, K^{+} and Na^{+} ions takes place from the weathering of a variety of minerals trying to buffer acid.

Fig.4.8 Comparison of drainage characteristics at sites 1 & 3

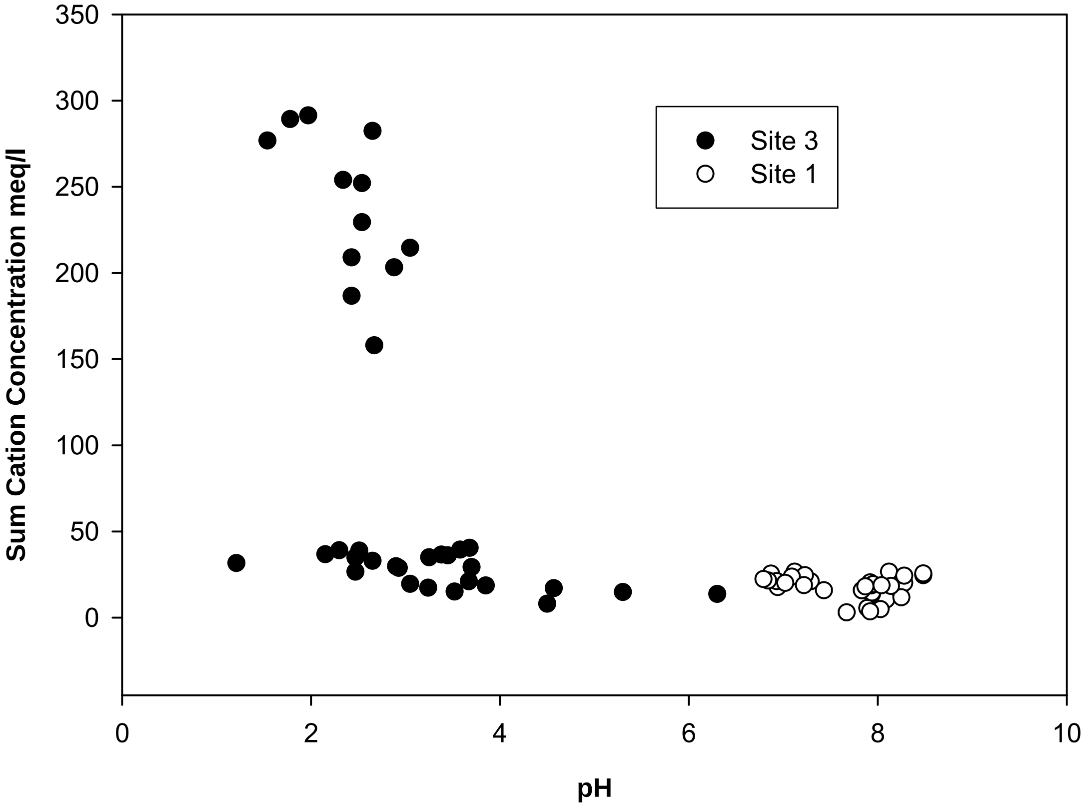

Stumm and Morgan (1996) define alkalinity as the ‘equivalent sum of the bases that are titratable with strong acid’. Based on electroneutality (charge balance), Drever, (1997) proposed that alkalinity can be computed as follows, for pH end point 4.5:

$$Alkalinity = \left[HCO_3^-\right] + 2\left[CO_3^{2-}\right] + \left[OH^-\right] - \left[H^+\right] \qquad (4.2)$$

There were a few cases where bicarbonate (HCO_3^-) data was not reported in the analysis and such missing values could be calculated from alkalinity and pH values. Inverting the problem, unreported pH values could be calculated from equation 4.3 if CO_3^{2-} and HCO_3^- values were given.

$$K_2 = \frac{[CO_3{}^{2-}]10^{-pH}}{[HCO_3{}^{-}]} \qquad (4.3)$$

where, $-\log K_2 = 10.33$.

Acidity in mine drainage is defined based on aqueous speciation at the sample pH and on the capacity of these species to undergo hydrolysis to pH 8.3, (Kirsby & Cravotta, 2005). Based on pH and concentrations of dissolved Fe(II), Fe(III), Mn and Al in mg/l, acidity can be computed in mg/l as $CaCO_3$, pH end point 8.3:

$$Acidity = 50\{10^{3-pH} + \frac{(2Fe^{2+} + 3Fe^{3+})}{56} + \frac{2Mn}{55} + \frac{3Al}{27}\} \quad \text{Hedin, } \textit{et al.}, \text{ (1994)} \quad (4.4)$$

Acidity levels up to 20 000 mg/l were measured in mine water from Site 3 and this can be supported by the high concentrations of Fe(5542.72 mg/l), Mn(92.26 mg/l) and Al(133.73 mg/l). In general, the trend of increasing soluble metal content with decreasing pH is strongly reflected in mine drainage from Site 3. The geologic and mineralogical characteristics of this site reveal a massive pyrite formation with about 5% pyrrhotite. These two and other sulphide minerals, coupled with lesser amounts of acid buffering minerals, have extreme acid generating capacity. As a result drainage from this site is highly acidic with extreme concentrations of iron, manganese, aluminium and sulphate. Mine water from Site 3 has a typical mean pH < 2.50, and is treated by lime neutralisation before discharge in evaporation ponds. However, as a result of seasonal wetting and drying, formation of secondary minerals such as jarosite promotes storage for sulphate, acidity (H^+) and iron, as in equation 4.5, (Bowell *et al.*, 2000):

$$3FeS_2 + \frac{9}{2}O_2 + \frac{15}{2}H_2O + 3K^+ \Leftrightarrow KFe_3(SO_4)_2(OH)_6 + 4SO_4{}^{2-} + 9H^+ \qquad (4.5)$$

Secondary minerals are highly soluble and they can be mobilised during periods of rainfall, potentially releasing sulphate, iron and acidity to the water environment as in equation 4.6.

$$KFe_3(SO4)_2(OH)_6 + \frac{3}{2}O_2 \Leftrightarrow 3FeO.OH + K^+ + 2SO_4{}^{2-} + 3H^+ + \frac{3}{2}H_2O \qquad (4.6)$$

Consequently, the potential for primary and secondary AMD generation, metal release and migration is considered very significant at Site 3. The immediate environmental impact of low pH is acidification of fresh water recipients.

4.6.3 Acidification of Recipient Waters

Since acidity is the capacity of a system to neutralize base, the more acidic a solution is, the more base that must be added to raise the pH to an acceptable level. By monitoring acidity in mine waste drainage, runoff, and receiving waters, it can be determined whether or not and when acid is being produced. The range of pH suitable for most life in freshwater environments is between about 5 and 8.5. Values below 6 suggest some input of acidic substances. Many different measures would have to be taken at a site to prevent the production of acidic waters or treat waters that are acidic. The overall reaction taking place during pyrite oxidation is given in equation 4.7:

$$4FeS_2 + 15O_2 + 14H_2O \Rightarrow 4Fe(OH)_3 + 16H^+ + 8SO_4{}^{2-} \qquad (4.7)$$

Similar reactions may be written for other sulphides. The sulphuric acid generated by the above reaction lowers the pH of recipient waters consequently dissolving other metals in the mineral assemblage into solution. Once dissolved, the heavy metals can be transported over long distances along the flow path, severely degrading water quality. The acidification of the water has immediate deleterious effects on aquatic ecosystems. Firstly, a direct effect is the conversion below pH 4.2 of all carbonate and bicarbonate into carbonic acid, which dissociates into carbon dioxide and water. This destroys the bicarbonate buffer system in the water, which acts as a control on acidity.

Secondly, since many photosynthetic organisms use bicarbonate as their inorganic carbon source, their ability to photosynthesize is limited or destroyed altogether as bicarbonate decomposes and becomes less available (Kelly, 1988). This probably explains the absence of any life forms over a distance of about 650 m downstream of the seepage point D along Yellow Jacket River at Site 3. Ravengai *et al.,* (2005), report that a marked reduction in the number of aquatic micro invertebrate was recorded during a nine month study of aquatic life in the Yellow Jacket River, downstream of mine site. This was just 30% of the number being recorded each month at a reference site on the Mazowe River. Thirdly, decomposition (and hence nutrient cycling) will be reduced and eventually cease, in water bodies severely affected by acid inflow (Dallas & Day, 1993). Fourthly, acid waters kill some organisms, by destroying ionic balances, or damaging cell components or carbonate exoskeletons (Kelly, 1988).

The method chosen to process the ore at Site 2 involves cyanide. The highly toxic hydrogen cyanide is formed below a pH of 9.5, and therefore a protective alkalinity (pH~10) for optimal gold dissolution is maintained by adding lime in the CIP circuit. This naturally buffers any acid generated by sulphide weathering and delays onset and discharge of acidic drainage from fresh tailings. While mine water and drainage from the fresh tailings indicate neutral to alkaline pH ranges, Figure 4.9, drainage analysed during the sampling campaigns from the weathered tailings at Old Bucks dump show evidence of AMD with very low pH~3, and high metal concentrations including arsenic, above the regulation limit. This drainage is directed to a natural wetland within the mine site, where dilution and metal deposition in sediments take place.

Fig. 4.9 Site 2 Drainage Characteristics

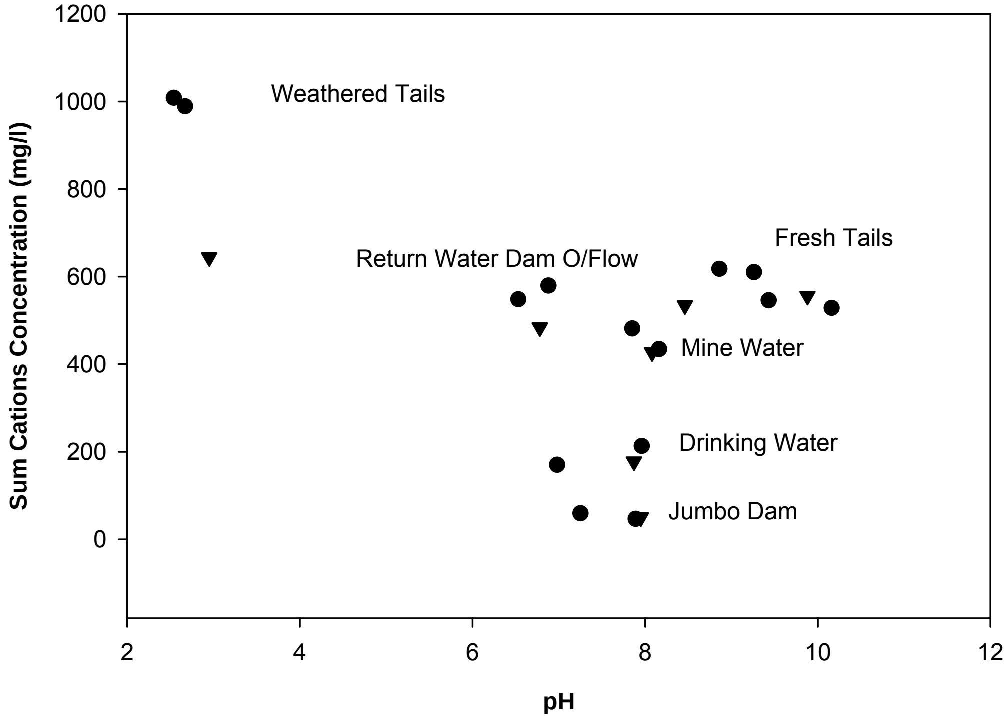

The wetland is however overflowing all year round and the situation is aggravated by rainfall and plant spills. Overflow from the wetland is captured in the return water dam, but this also overflows all the time, leading to a contaminant stream with near neutral pH but high concentrations of dissolved metals and other pollutants leaving the mine site. The sum of cations which can be as high as 700mg/l in the return water dam overflow might be attributed to the complex chemistry of cyanide since pH values are mostly alkaline($6.8 < pH > 8$) and not expected to dominate metal dissolution in this range. The behaviour of cyanide in mine site drainage is of particular concern due to its toxicity. Cyanide, a highly toxic substance, is indispensable in the extraction of gold. Cyanide is typically used in the milling of precious metal ores to simultaneously solubilise gold and stabilize it in solution as a gold-cyanide complex (Marsden & House, 1993). However, due to its complexing abilities, cyanide also mobilises other metals like iron, asernic, copper and zinc. Cyanide also forms cyanate (CNO^-) when oxidised and thiocyanate (SCN^-) when in contact with sulphide and other reduced sulphur species, (Smith, 1994).

At the Old Bucks tailings dam prevalent $pH < 4$, cyanide toxicity is naturally reduced by mechanisms such as volatilisation of HCN into the atmosphere; formation of strong aqueous metal complexes with copper and zinc; precipitation of relatively insoluble metal-cyanide compounds; biodegradation and adsorption to mineral and soil surfaces.

4.6.4 Dissolved Oxygen, Sulphate, TDS and Electro-conductivity

Oxygen plays an important role in any aerobic natural ecosystem because as an electron acceptor it is at the origin of all biological life in aqueous media and also plays a major role in redox reactions where iron is involved. The saturation concentration of dissolved oxygen in water is a function of temperature, partial pressure of oxygen in the surrounding air, and concentration of solutes in the water. In this study, dissolved oxygen was measured by means of a membrane probe and the result compared to the maximum saturation value given by equation 4.8, (Stumm and Morgan, 1996).

$$[O_2]_{mg/l} = 14.552 - 0.3735T + 0.005016T^2 \qquad (4.8)$$

The measured values are then reported as percent of saturation in some cases. As expected oxygen solubility decreases with increasing cation content of drainage at all sites. Drainage from Site 3 contains the highest amount of dissolved solutes (sum cations = 300meq/l) and DO as low as 34.8% of saturation value at the seepage point D along Yellow Jacket River. Other processes influencing the oxygen balance in surface water streams are physical diffusion through the air – water boundary layer and photosynthesis and biological respiration reactions in the water.

Figure 4.10 compares sulphate, TDS and electrical conductivity in selected streams draining from each of the three mine sites to the permissible levels from ZINWA guidelines. Although sulphate is a naturally occurring ion and may be present in waters over a wide range of concentration, acidic drainage does contribute large amounts of sulphate from oxidation of pyrite and other sulphide minerals at all three sites. Increased levels of sulphate are usually the first indication of acid generation. The average sulphate values for the three sampling campaigns indicate that permissible levels are exceeded in one or more streams leaving each site. The main limitation of sulphate contamination lies in accounting for the source of the sulphate ion. At site 1, spillage from the smelter and refinery contains sulphuric acid and some times this is washed away during rainfall events and mixed with the tailings dam stream effluent leaving the mine site. Copper sulphate is also used in the flotation plant as an activator and spillages occasionally find their way into the south effluent draining from the waste rock. This stream also shows sulphate levels sometimes as high as 301.5 mg/l compared to the regulated discharge limit of 250 mg/l.

Fig.4.10 Pollutants of Concern compared to ZINWA limits

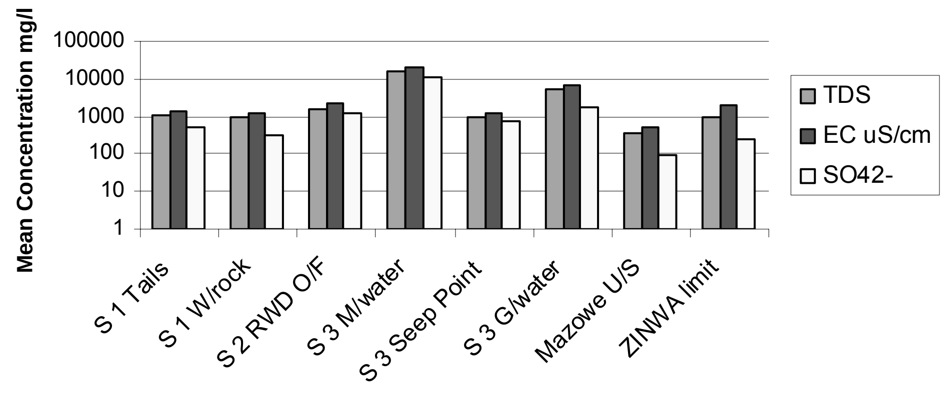

At Site 3, sulphate levels in excess of 11000mg/l are prevalent in mine water with ground water values around 2300mg/l. However, sulphate can be incorrectly attributed to acidic drainage, when in fact it may be from solubilisation of salts such as gypsum formed during neutralisation at the lime treatment plant. The gypsum releases sulphate but does not produce acid mine drainage. The release of sulphates and other sulphide breakdown products leads to increased suspended solids and dissolved solids, and thus to salinization. This is enhanced by the dissolving effect of acidic waters on country rock along the flowpaths. Dallas & Day, (1993), report that while acidic drainage leads to a reduction in dissolved oxygen concentration in the water system, precipitation of iron hydroxides and other sulphate species on aquatic plant leaves may also inhibit photosynthesis (Dallas & Day, 1993).

Fig.4.11 SO4 correlation to TDS at Site 3

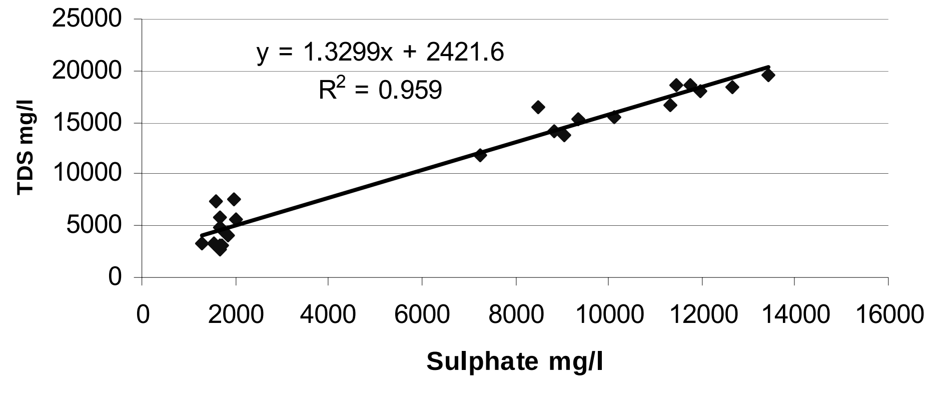

Total dissolved solids (TDS), (also referred to as filterable residue) represents the portion of the sample that passes through a filter of a particular size. Usually 0.45 µm is considered to be adequate to differentiate between microscopic particulate and dissolved material. The final result, after evaporation and drying to constant weight at 180°C, represents the total dissolved solids. The correlations depicted in Figures 4.11 and 4.12 can be used to calibrate TDS to sulphate and electrical conductivity to TDS, respectively, allowing reduction in frequency of analysis of either parameter. Total dissolved solids results are limited to providing a measure of the total water soluble fraction and do not reveal the quantity or type of individual contaminants in the sample (MEND, 2001).

Fig.4.12 Correlation of EC to TDS at Site 3

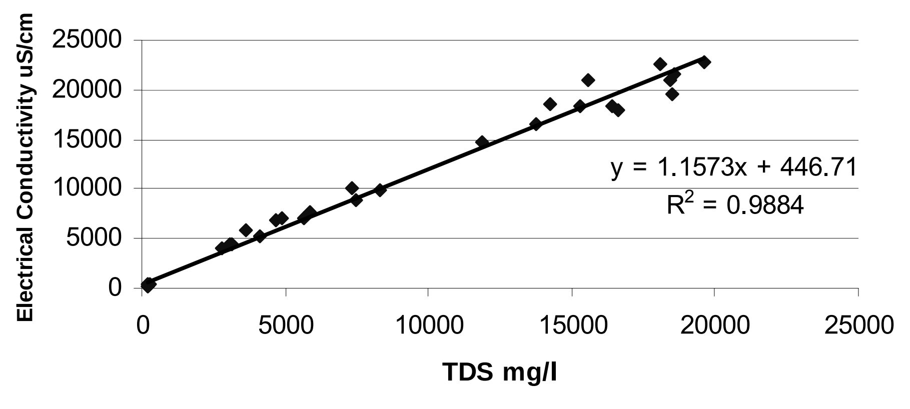

4.6.5 Effect of pH on metal solubility

The solubility and mobility of metals are generally increased by acidification of water, (Adriano, 1992). This is probably the result of the combination of washout processes in waste rocks and tailings at mine sites, enhancing the mobility of metals along flow paths. Figure 4.13 shows Fe, Mn and Al variation with pH for Site 3 mine water.

The dissolution of feldspars and clay minerals in the pyrite and chert becomes enhanced in acidic solution, and this results in the release of Fe, Mn and Al into the water. There is a trend where the concentrations of these metals increase in the drier months of the year (May to October) due to reduced percolation of ground and surface water. In the wetter months (November to April), dilution is an important factor in reducing metal concentrations.

Similar trends are observed for Cu, Zn and As at Mazowe mine. However, at Site 1 the waste material contains buffering minerals and the low pH promotes hydrolysis of carbonates and silicates, thus releasing base cations to the water according to reactions 4.9 and 4.10.

$$CaCO_3 + H^+ \Rightarrow Ca^{2+} + HCO_3^- \qquad (4.9)$$

$$2NaAlSi_3O_8 + 2H^+ + H_2O \Rightarrow 2Na^+ + Al_2Si2O_5(OH)_4 + 4SiO_2 \qquad (4.10)$$

Fig.4.13 Variation of dissolved metal concentration with pH

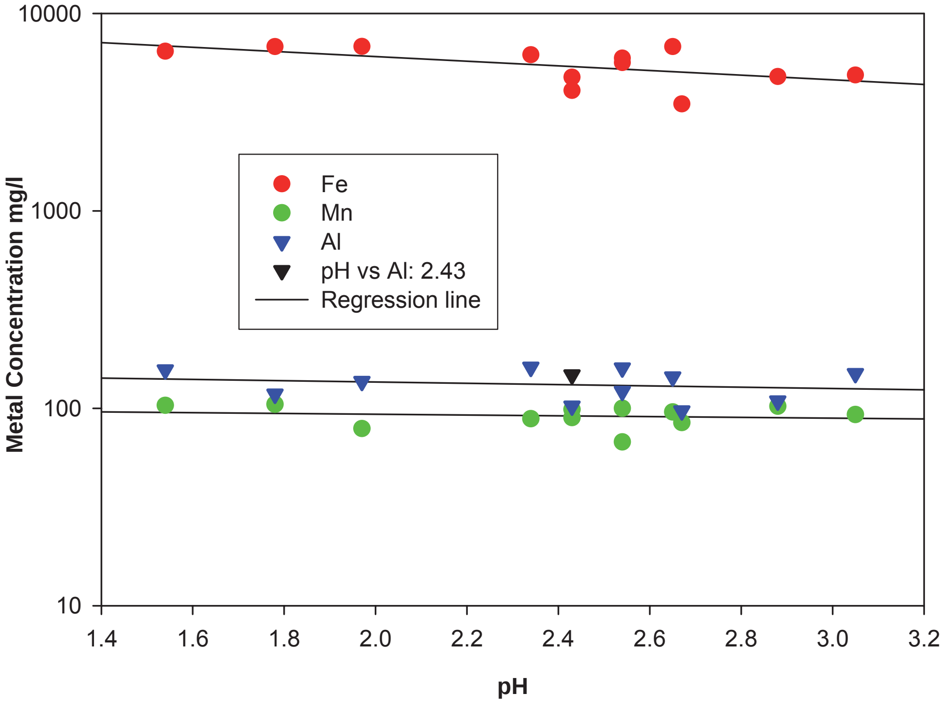

The rates of carbonate and silicate dissolution increase with increasing acidic conditions, however, calcite reacts several orders of magnitude faster than silicate, (Plumer *et a.l,* 1978). Copper, cobalt, manganese, nickel and zinc also become more soluble in acidic solution (Dallas & Day, 1993; Edmunds & Smedley, 1996; Aström, 1998).

At Site 3 the waste rock and jig tailings contain insufficient neutralising minerals, and a dry cover system was implemented to minimise water and oxygen access to the sulphide minerals. However, the system is failing, and oxidation 'pipes' or 'holes' can be seen on top of the caped waste dump, resulting in very concentrated acidic drainage when rain falls, Figure 4.14(a) & (b). When the acidic mine waters on the surface evaporate, they leave behind metal-bearing salts, such as chalcanthite, a complex hydrated copper sulphate, Figure 4.14 ©. As the next pulse of water passes through the area, these salts re-dissolve, releasing acid and metals into solution, leading to sharp seasonal peaks in metal content in the nearby Yellow Jacket River.

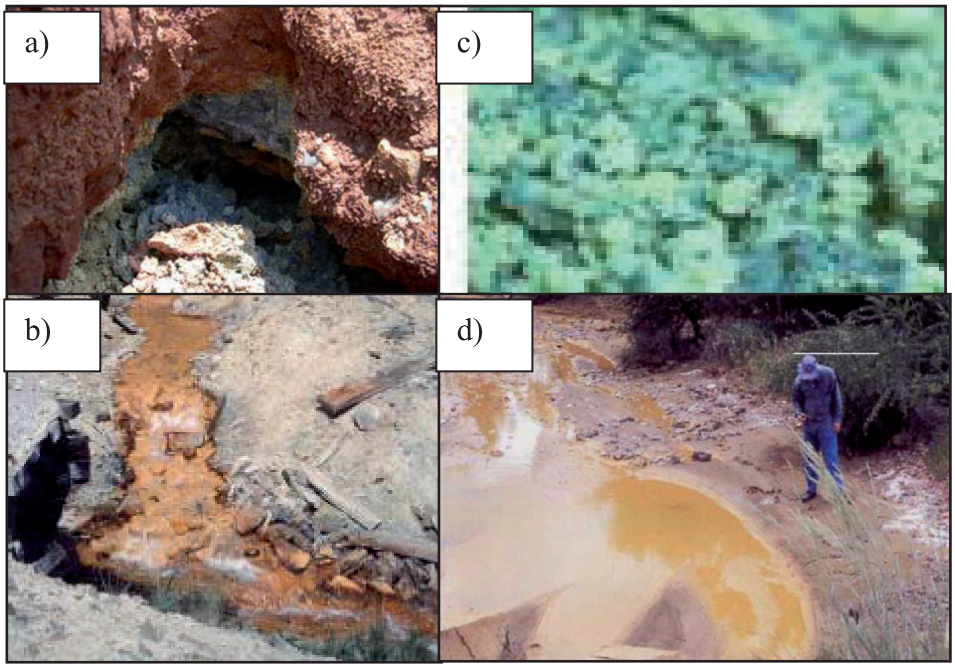

Fig.4.14(a) – (d): Sulphide Oxidation Products at Site 3

Associated with acid mine drainage is the precipitation of iron (III) hydroxide and oxyhydroxide complexes, which give the water an orange colour. These are referred to frequently as "ochres" or "yellow boy", Figure 4.14(d). The hydroxides and sulphides are precipitated at moderately low pH (5-6), but once the pH drops below 4.3 they are soluble. This often means that iron (III) stays in solution near the source of contamination, but precipitates downstream, where the pH has been neutralized somewhat, and has risen above 4.3. These hydroxides form flocs, which can block light penetration, clog the bottom of the river and have abrasive affects on biota. Dissolved metals may re-precipitate when the iron (III) hydroxide flocs form at slightly raised pH (Kelly, 1988).

4.7 Weathered Tailings Potential for Metal Leaching

Metal leaching into the environment is the principal concern of acidic drainage. The potential for metal leaching and release to receiving waters was evaluated using the bottle role leach test procedure on the minus 2 mm fraction of the weathered waste materials from the three sites. The sample from Site 2 was taken from the Old Bucks dam to deliberately avoid the influence of cyanide present in fresh and some aged samples. Table 4.4 shows that the paste pH for sites 2 & 3 were acidic, while Site 1 was alkaline, with an alkalinity of 32.18mg/l HCO_3^-. Electrical conductivity and sulphate concentrations are significant in all leachates.

Table 4.4 Leachate Quality of weathered mine waste materials

	Site 1	**Site 2**	**Site 3**
	Flotation Tailings *Composite Dams 1- 9*	Cyanidation Tailings *Old Bucks Dam*	Jig Plant Tails *New Dump Site*
Top size (mm)	<0.20	<0.20	<8.00
Paste pH	7.83	5.97	3.05
Eh (mV)	274	306	271
DO (mg/l)	4.54	6.84	4.22
Alkalinity (mg/l HCO_3^-)	32.18	0	0
TDS (mg/l)	878.5	1615.9	1873.8
E.C. (uS/cm)	1126.8	2287.2	2431.5
SO_4^{2-}	246.83	304.71	673.82

Metal analysis in leachate samples after 18 hours of bottle rolling was used in assessing the weathering characteristics of the mine wastes and predicting the quality of water that will contact mine waste. The results are plotted in Figure 4.15. Fe, Cu, Mn and Ni are fairly solubilised at all sites. Zn is not mobile at Site 1 but Ca and Mg are almost 100µg/l, possibly due to dissolution of the carbonate minerals trying to buffer acid.

However, at Site 3, Ca and Mg are depleted suggesting that these minerals could have been already used up in the field prior to sample collection. Al is quite mobile at Site 3, with a concentration nearly 200 µg/l in the leachate. From these simple tests it is possible to estimate that the potential for metal release, mobility and likely impact on the water quality of runoff, receiving surface water, and groundwater after it has contacted mine waste is quite high at Site 3, significant at Site 2 and not significant at Site 1.

Fig.4.15 Trace metal concentrations in weathered materials

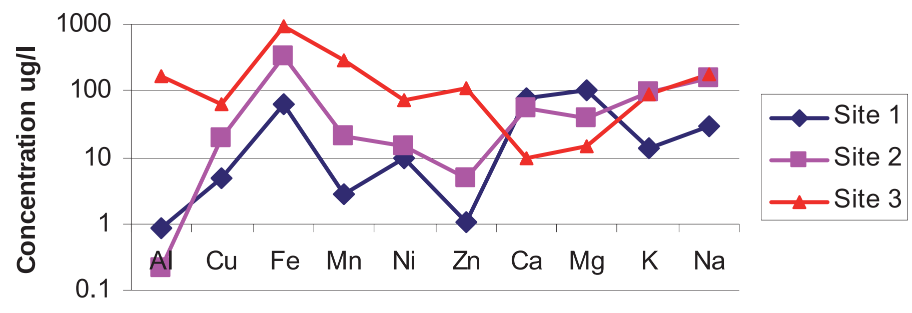

Presumably other most important effects of acidification of water by AMD are the changes that result in the speciation of metals which can have a strong influence on mobility and bio-availiability. Bio-availability is the proportion of total metals that are available for incorporation into biota (bioaccumulation). Total metal concentrations do not necessarily correspond with metal bioavailability and hence the associated environmental effects may be low, (Davies *et al.*, 1994). At very low pH levels, aluminium is present as the toxic species Al^{3+}. Al^{3+} is complexed by SO_4^{2-} anions and since these are a major component of water subject to acid mine drainage, the effect on aluminium may be reduced somewhat by this process (Driscoll & Schecher, 1990).

4.8 Concluding Remarks

This characterisation study demonstrates that drainage compositions from mine dumps are the main factors controlling water chemistry in the vicinity of mine operations located in the Mazowe River sub-catchment. The most possible pathway of pollution from all three sites is surface streams passing through the mine sites and discharging into Mazowe River. Groundwater levels are too deep (>60 m) to be impacted by the pollution.

Strong buffering from silicates and metal scavenging in the natural wetland seems to be the main mechanisms controlling alkaline pH levels and trace metal concentrations at Trojan and Mazowe mines. Lime addition during the cynidation process and containment of process solutions at Mazowe Mine are helping to keep the pollution within the mine site, but for a limited time frame. A dilution process from Yellow Jacket River mainly accounts for the distinct decrease in concentrations of Fe, Mn, Al, Zn, Ni, acidity and sulphate that are released well above regulation limits at Iron Duke.

The behaviour of AMD pollutants in the streams draining the mine sites is complex. There are several simultaneously acting mechanisms including precipitation and adsorption reactions which lead to fluctuating pollutant concentrations and possibly attenuation. A more detailed study to quantify the reactivity of the waste materials, ascertain potential for AMD generation and predict the drainage chemistry changes with time and impact on watercourses is necessary. These issues are investigated in Chapter 5.

CHAPTER 5

LABORATORY GEOCHEMICAL PREDICTION TESTS

5.1 Introduction

In order to design and implement effective mitigation systems for reducing the potentially adverse effects of AMD, it is important to predict the release, solubility, mobility and retardation of contaminants from the waste materials under different physical, geochemical and climatic conditions. Prediction refers to a suite of integrated approaches used to determine in advance the geochemical behaviour of mineral waste for new, operating or closed mines, (Mills, 1998). The objective is often to determine whether wastes are potentially acid generating and what impacts may be expected as a result of metal leaching, so that problematic wastes can be managed to prevent acid generation.

Several methods have been developed to predict the acid forming characteristics of mine waste materials. In general, testing programs utilise a two step approach of Acid Base Account (ABA) originally developed by Sobek *et al.,* (1978), in which *Static tests* on numerous samples are used to identify potentially acid generating geologic units and to characterise the variability that occurs within them. *Kinetic tests* are then performed on samples deemed likely to generate acid. Static procedures are so referred because each involves a single measurement in time and provide no information on the speed or kinetic rate of the reaction producing or consuming acid. Kinetic test procedures involve a number of measurements over time, and are used to assess a range of AMD issues including sulphide reactivity, oxidation kinetics, metal solubility and the leaching behaviour of test materials.

Waste rock and metallurgical tailings from the three mine sites selected as case studies were tested to determine the acid generation and metal leaching potential, and hence provide information required to predict the downstream effects on water quality in the Mazowe River sub-catchment. This concern has developed because there is a lag period between waste placement and observation of an acid drainage problem. This lag period is variable from site to site and calls for site specific investigations, (Miller *et al.,* 2003). Drainage quality and progression of weathering reactions were assessed on laboratory scale in order to estimate rates for sulphide mineral oxidation under field conditions.

5.1.1 Objectives

a) To evaluate the acid generating and acid neutralising potential of mine waste materials at the selected case study sites
b) To determine the lag period between waste placement and observation of an acid problem, and
c) To estimate field weathering rates under semi arid conditions

5.1.2 Collection and Preparation of non grid solid samples

During the fieldwork and characterisation programs described in Chapter 4, solid samples were collected from the three case study mines and returned to the laboratory for confirmatory testing. Sampling concentrated on obtaining representative samples with respect to the physical and chemical characteristics of the waste material. Characterisation of waste rock dumps and tailings is quite challenging because the structure, physical nature, mineralogical and chemical characteristics in a dump always tend to be heterogeneous. The variation in such properties is caused by factors such as geology, construction technique, weathering rates, climate, and others (Williams *et al.*, 2003).

Non grid composite samples were collected by walking over the entire waste pile collecting at least 30 increments in a random manner. Tailing samples were collected by first removing the vegetation at the sample location by scrapping away with a stainless steel trowel. A 10cm diameter hand auger was advanced to a depth of at least 50cm and the sample extruded directly into sampling containers. Large samples of 5-10kg were collected and returned to the laboratory for geochemical tests and analysis. Static and kinetic tests were performed on the samples as received.

Waste rock piles exhibited a wide variability in particle size, making them very difficult to sample using the method for tailings described above. In such cases grab sampling was done around and on top of the dump to try as much as possible to collect a representative composite sample. In the laboratory, waste rock samples were coarse crushed to 100% passing 5mm, coned and quartered, and then split with a Jones Riffle to obtain about 1kg head sample. From each head sample, approximately 200g were riffled out to determine the mineralogy by hand specimen examination and petrographic microscopic analysis, and also determine elemental chemical analysis. The bulk of the sample was saved for geochemical static and kinetic tests.

5.2 The Test Program

The test program follows an industry standard consisting of staged static and kinetic testing of sample materials. Minor modifications were done to try and simulate local onsite conditions where possible. Static tests are designed to measure the quality and quantity of different mineral constituents in a sample at one point in time, (Price, 1997). Such tests include analyses of elemental sulphur, sulphur species, neutralisation potential, pH measurements, particle size and mineralogical analysis. Kinetic tests provide a measure of the dynamic performance or reactivity of a sample and include laboratory procedures such as column tests, humidity cell tests and field studies such as rock pile tests. Table 5.1 lists the number of tests conducted on waste rock and tailings in this case study. A brief description of each test is included in the preceding sections.

Table 5.1 Static and Kinetic Testing of Tailings and Waste rock samples from the three case study sites

Test Description	Tailings	Waste Rock
Petrographic analysis (thin section)	3	1
Acid Base Accounting (ABA) Tests		
Paste & Rinse pH	49	7
Total Sulphur	49	7
Total Carbon	49	7
Sobek Acid Neutralising Capacity (ANC)	49	7
Net Acid Generation (NAG)	49	6
Acid Base Characteristic Curve	0	1
Humidity cells	6	1
Metal analysis (AAS)	16	2

5.2.1 Acid Base Accounting (ABA) Procedure

Static Tests

The ABA procedure was formerly developed by Sobek *et al.*, (1978), as a laboratory protocol for determining the acid production potential of mine overburden containing sulphide mineralisation. It is based on the premise that the likely hood for a site to produce acid mine drainage can be predicted by quantitatively determining the amount of acidity (termed maximum potential acidity – MPA) and the alkalinity (termed acid neutralising capacity – ANC) of the sample material. The relative acid forming potential of a sample was categorised using some basic screening tests as follows:

- Paste $pH_{1:2}$ and Electrical Conductivity ($EC_{1:2}$) test
- Total Sulphur Determination
- Fizz rate and Acid Neutralising Capacity (ANC) test (Sobek *et al.*, 1978)
- Net Acid Producing Potential (NAPP) calculation (based on %sulphur and ANC)
- Single addition Net Acid Generation (NAG) test (Miller *et al.*, 2003)

Each method used alone has its own limitations as to how reliably it can predict acid forming potential. The modification and approach used in this study was to apply these test methods in combination, so as to get a better definition of the acid forming potential of mine waste materials and highlight samples that may require AMD management.

i) Paste and rinse pH

The $pH_{1:2}$ also known as the *paste and rinse pH*, and electrical conductivity ($EC_{1:2}$) were determined by equilibrating 10-gram samples ≤ 2mm material in deionised water for 12 - 16 hours (or overnight), at a solid to liquid ratio of 1:2 (w/w). Waste rock samples from Site 1 had to be pulverised first.

ii) Total Sulphur Determination and Maximum Potential Acidity (MPA)

Total sulphur and carbon were determined by the LECO combustion analytical technique at Iron Duke Pyrites. By this technique, a pulverised sample 0.5 to 5g was combusted in a stream of oxygen at approximately 1350°C in an induction furnace, forming a mixture of SO_2/SO_3 and CO_2 gasses. Sulphur dioxide released from the sample was measured by an Infra Radiation detection system and the percent sulphur and percent carbon were analysed and graphically plotted on a digital display as the combustion progressed.

The ABA procedure uses the percent sulphur to predict the maximum potential acidity that a sample can produce if all the sulphur reacts. The calculation assumes that the measured sulphur content occurs as pyrite and that pyrite reacts under oxidising conditions to generate sulphuric acid according to the reaction 3.1. MPA = wt %S X 31.25 in kg H_2SO_4/ton of material. Sulphate sulphur or HCl-leachable sulphate was determined by heating 0.5g of sample with 10 ml dilute hydrochloric acid (0.1M) for 30 minutes. Silica and any acid insoluble materials were removed by filtration and ferric iron was reduced to ferrous by the addition of hydroxylamine hydrochloride. The sulphate in the resulting filtrate was then precipitated with barium chloride in a dilute hydrochloric acid medium. The barium sulphate was filtered, ignited, weighed and calculated as %S in the original sample. Sulphide Sulphur was determined by subtracting the sulphate sulphur obtained from the HCl Leach from the total sulphur obtained from the LECO analyser.

iii) Fizz Rate and ANC

Before performing the analysis for determination of the acid neutralisation capacity, the sample must be rated as to its carbonate content in order to determine the volume and normality of hydrochloric acid to be used in the analysis. The ANC result is somewhat dependent on the fizz test results, which in turn are a matter of human judgement, (Evans and Skousen, 1995; Skousen *et al.,* 1996).

The fizz test was performed by adding a few drops of 25%HCl to 2g of pulverised sample on a watch glass and observing the degree of reaction. The observed degree of reaction was assigned a fizz rating according to a four tiered system where the reaction is judged to be 'none - (1), slight - (2), moderate - (3) or strong - (4)' as indicated in Table 5.2.

Table 5.2: Volume of HCl added for various Fizz ratings in the Modified ABA Procedure for ANC determination.

FIZZ RATING	**HCl**	
	(mL)	**(Normality)**
(1)	20	0.1
(2)	40	0.1
(3)	40	0.5
(4)	80	0.5

About 2g of pulverised sample were weighed into a 250ml volumetric flask and as a first approximation, the volume and normality of HCl indicated by the fizz rate in Table 5.2 added. The contents were agitated by means of a magnetic stirrer for 24 hours. After approximately 6 hours of the reaction, the agitation was stopped and checked for pulp pH. In cases where the pH was above 2, a known volume of HCl was added and the agitation continued for the remaining 18 hours. The end pH target range was 2.0 – 2.5. In cases where the final pulp pH was below 2.0 or above 2.5, the amount of acid was judged to be insufficient and too high respectively, in which case the test was repeated with the next higher or lower volume or strength of HCl as appropriate. The contents of the flask were then titrated to pH 8.3 with NaOH of the same normality as HCl used during the agitation. The ANC in kg $CaCO_3$/ton of the sample were then calculated as follows:

$$ANC = \frac{50a\left(x - \frac{b}{a}.y\right)}{c} \tag{5.1}$$

where a is the normality of HCl; b is the normality of NaOH; c is the sample mass in grams; x is the volume of HCl added (ml); and y is the volume of NaOH added (ml) to pH 8.3.

iv) Single Addition NAG Test

The NAG test (after Miller, 2003) is used to determine the net acid remaining, if any, after complete oxidation of the materials with hydrogen peroxide and allowing complete reaction of the acid formed with the neutralising components of the material. The NAG test provides a direct assessment of the potential for a material to produce acid after a period of exposure and weathering and is used to refine the results of ABA predictions.

In the NAG test, 250ml of 15% H_2O_2 was added to 2.5g of pulverised sample. Tailings were tested as received. The slurry was allowed to react until boiling or effervescing ceased, and then heated gently for a minimum of 2 hours. The amount of acid generated by NAG reaction was determined by titration with standardised sodium hydroxide. Titration to pH 4.5 (NAG_{pH}) measures acidity due to free acid (H^+), Fe^{3+} and Al^{3+}, and titration to pH 7 measures acidity due to other dissolved metals such as Zn and Cu. The net acid generation NAG in kg H_2SO_4/ton was calculated as follows:

$$NAG = \frac{49xy}{c} \tag{5.2}$$

where x is the volume of NaOH titrated (ml); y is the molarity of NaOH; and c is mass of sample in grams.

5.2.2 Kinetic Tests

Kinetic tests are procedures in which the mine waste samples are subjected to dissolution with the objective of determining rates of mineral oxidation & dissolution and empirically estimating the potential quality of drainage from the mine waste, (White & Lappako, 2000). These tests are distinguished from static tests in that they try to simulate mineral weathering rates in the field. There is no standard in dimensions of humidity cells, or mass of sample to use or duration for which the cells should be operated before they can be discontinued. The Humidity cell test as conducted by Sobek (1978) leaches a 200g sample crushed to minus 2.38mm in a closed plastic container. The industry standard for the humidity cell is a cell 200 mm in height by 100 mm diameter for material crushed to 100% passing 6.3 mm (crushed ore or waste rock or coarse tailings), (Scott *et al.,* 2000). A cell 102 mm in height and 203 mm in diameter is specified for material passing 150µm.

Modified Humidity Cell Tests

Three different types of kinetic tests were conducted under different conditions: standard humidity cells, non – aerated cells and simulated rainfall cells. The tests were run on 1 waste rock sample from Site 1 and 2 tailing samples collected from sites 2 & 3. All sample materials had been exposed to weathering for at least one month, estimated from the waste disposal cycles and practice on each site. The humidity cell used in this study is essentially a cylindrical reactor of PVC material with same dimensions as the industry standard. A perforated support base with three layers of stainless steel screen of aperture size 38 µm was used to support the sample previously crushed and screened through 6mm for waste rock and used in 'as received' state for tailings.

An array of 7 identical cells, such as the one shown in Figure 5.1, were used with a sample mass of 1kg carefully loaded into each cell taking care to minimise sample stratification and consequent fluid channelling in the cells. The tests were run for twenty eight weeks following a seven day cycle. For all samples, the initial leach (week 0) consisted of a 600ml flooding with deionised water, soaking the sample for a day before draining to remove residual reaction products generated prior to sample collection and storage. The recovered volume was weighed and preserved for analysis of cation and anion loads. Subsequently, the weekly cycles consisted of passing dry air through the cells for three days, moist air for three days, and washing with water on the seventh day. The airflow through each cell was maintained at about 1litre per minute and the temperature between 23 and 30^{o}C.

During the wash, 500ml of deionised water was drip trickled into the cell over a period of one hour, and the leachate collected after one day. Cells were weighed after the dry air cycle, the moist air cycle and after the wash to determine gain or loss in interstitial water.

Fig. 5.1: Humidity Cell Set up

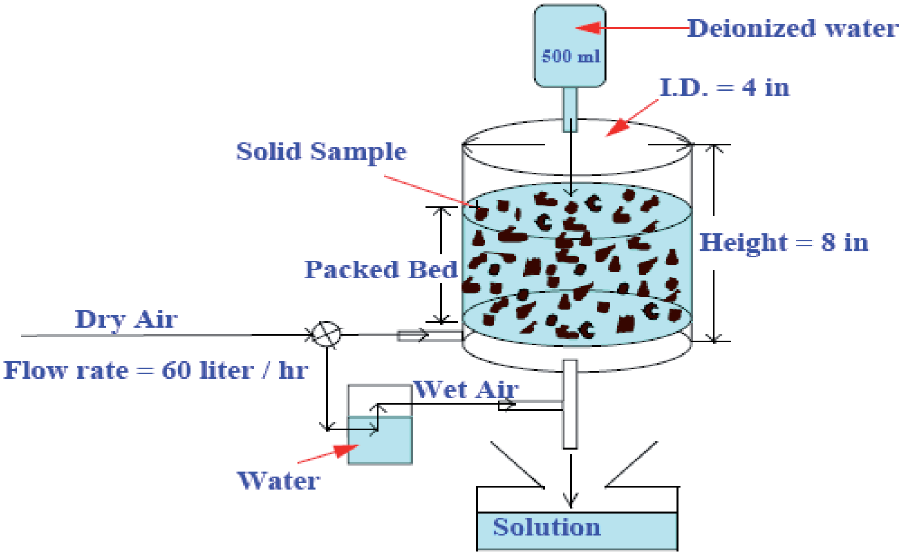

The typical sequence of subsequent weekly cycles is summarised in Figure 5.2. Leachate samples were analysed for pH, EC, alkalinity, acidity & sulphate. Fe, Mn, Cu, Ni & Zn concentrations were analysed in leachate from the initial rinse and the last five weeks.

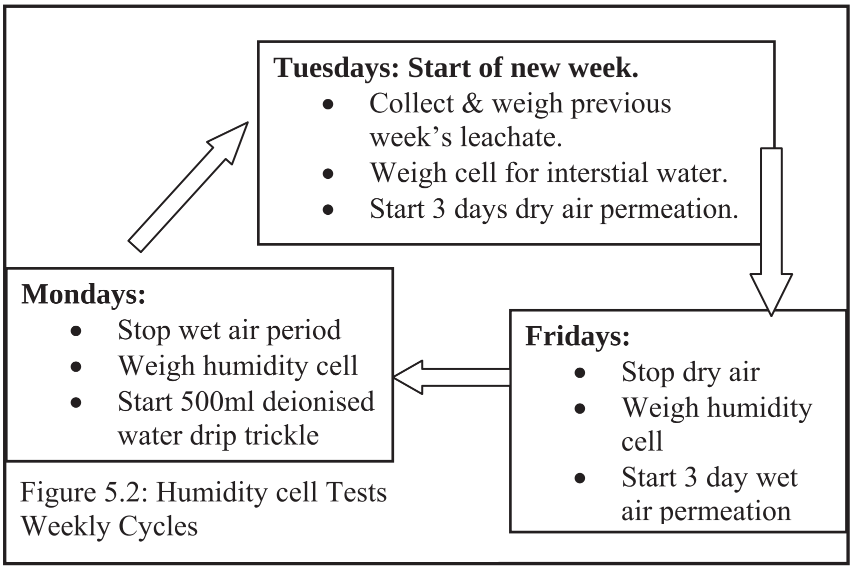

Tuesdays: Start of new week.

- Collect & weigh previous week's leachate.
- Weigh cell for interstial water.
- Start 3 days dry air permeation.

Fridays:

- Stop dry air
- Weigh humidity cell
- Start 3 day wet air permeation

Mondays:

- Stop wet air period
- Weigh humidity cell
- Start 500ml deionised water drip trickle

Figure 5.2: Humidity cell Tests Weekly Cycles

Non aerated cells were not subjected to weekly cycles of dry air and wet air, but were drip trickled with 500ml distilled water (after the first flooding and draining) over a period of one hour per week. The cells were not actively aerated but remained open at the top and bottom allowing unrestricted air access. Simulated rainfall cells were treated in the same way as standard cells for the first 14 weeks, after which the rinse water volume was changed to 150ml for the remaining duration of the test.

5.3 Waste Rock and Tailings Bulk Mineralogical Analysis

The comparative bulk sulphide mineralogy obtained from analysis of the relatively unaltered portion of the tailings is summarised in Table 5.3. It must be recognised that tailings deposits are not completely homogeneous and minor changes in the composition of the deposited solids occur due to variations in the ore being processed. Other causes of heterogeneity in tailings include changes in the extractive metallurgy process and physical segregation during deposition due to density and particle size differences. Large variations in composition are caused by oxidative weathering reactions which occur on tailings surfaces after deposition and on exposure to air and water. The distinctive mineralogical features of the three mine sites are as follows:

Sites 2 & 3 contain significant quantities of pyrite, pyrrhotite and charlcopyrite whereas Site 1 waste rock and tailings show minor to trace amounts of these minerals which are the parent minerals for of the heavy metals such as Fe, Mn, Cu, Ni and Zn. These elements are easily mobilised during weathering in acidic environments posing great danger to human health and aquatic life. Pyrrhotite is present in tailings from all sites in minor quantities but oxidises more rapidly than pyrite. However, one mole of pyrrhotite produces only one mole of acidity whereas one mole of pyrite has the ability to produce two moles of acidity when oxidised in a wet environment. Carbonate and silicate minerals are important in acid generating tailings because of their buffering capacity. Carbonate content at all sites is less than 2% implying potentially low values of carbonate neutralisation capacity.

Table 5.3: Tailings & Waste rock Bulk Mineralogy

System Characteristics		**Site 1**	**Site 2**	**Site 3**
Mineral Mined		**Ni**	**Au**	**FeS_2**
	Historical	1969 - current	1880 - current	1940 - current
	Grade	0.67% Ni	12.2g/tAu	30%FeS_2
	Beneficiation	Flotation	Shaking Tables	Jigging
	Recovery	65 – 80%	70-75%	90-96%
	Trace Metals	Co, Cu, Fe, Pb	Fe, Cu, Zn & Ni	Fe, Mn, & Al
Tailings	MillionTons	28.50	0.71	0.25
	Pyrite	Minor	Minor	Major
	Pyrrhotite	Major	Minor	Major
	Sphalerite	Trace	Minor	Trace
	Chalcopyrite	Minor	Minor	Trace
	Galena	Minor	Trace	Trace
	Pentlandite	Major	Trace	Trace
	Arsenopyrite	Trace	Minor	Trace
	Calcite	Trace	Minor	Trace
	Dolomite	Minor	Trace	Trace
	Quartz	Minor	Major	Minor
	Chrorite	Minor	Minor	Minor
Waste Rock		Metabasalt, dolerite & quarts	Granodiorite + felsparporphrye	Chert + pyrrhotite
Tailings Management		Revegetation	Cyanide Detoxification	Lime Treatment

Components: major > 10%; minor <10% and >1%; Trace < 1%.

Figure 5.3 shows mineral abundance in the samples from petrographic analysis of thin sections using optical microscopy and modal analysis. The samples from the three sites were analysed at Trojan Mine Chemistry laboratory. The waste rock and tailings samples of Site 1 are closely similar. They consist of strongly altered igneous rock of intermediate felsic composition, with only traces of pyrite and pyrrhotite present, so these samples lack potential to generate significant acid mine drainage.

Tailings from Site 2 are composed predominantly of plagioclase feldspar and accessory mafics with some quarts. Pyrite and arsenopyrite are present in significant quantities (2-5%, and 1- 3%) respectively. Though minor carbonates (<2%) are present, these are insufficient to provide long term buffering, therefore Site 2 tailings constitutes a high potential to generate AMD under conditions of active atmospheric oxidation.

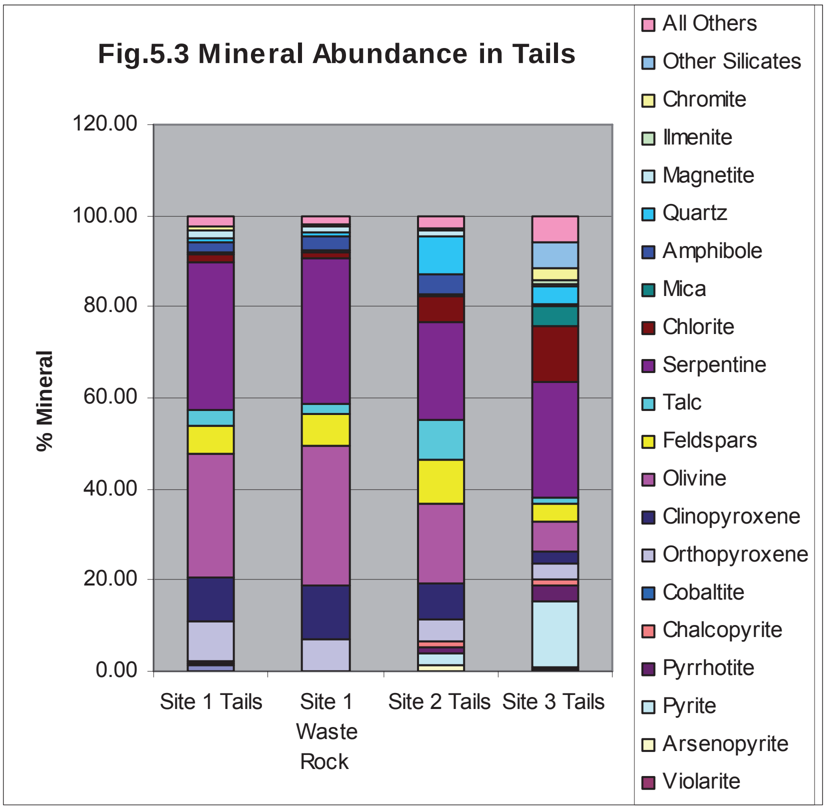

The principal constituents of Site 3 tailings are chlorite, seperntine, massive pyrite estimated at >14% and pyrrhotite (~ 4%) mainly as liberated grains. Trace amounts of carbonates, <1%, are present but this is not enough to offset acid generation in the event of exposure to atmospheric oxidation.

Physical properties such as grain size and permeability affect the quantity and quality of seepage from waste rock piles and tailings impoundments. Mineralogical characteristics, chemical and biochemical interactions between solutions and solids during the weathering process result in precipitation, dissolution and other processes such as sorption and ion exchange occurring. These reactions further affect the physical properties such as permeability, the most notable being secondary minerals or salts.

5.4 Discussion of ABA Results

5.4.1 Paste pH, Sulphur Species and Acid Potentials

Figure 5.4 shows the combined measurements of paste pH against sulphur content for samples from the three study sites. As provided by Sobek *et al.*, (1978), the paste pH indicates whether the sample was acidic, near neutral or alkaline at the time of measurement. The figure clearly shows that all samples from Site 1 were alkaline, while all samples from Site 3 had an acidic paste pH. For Site 2, there is a wide variation of paste pH suggesting that with acidic samples, the neutralisation potential had been completely used up or was not reactive at the time of measurement, while for near neutral to alkaline samples, acid producing and acid neutralisation reactions could be still in progress. There is no clear correlation between paste pH and sulphur content although 61% of samples with more than 3%S indicated an acidic paste pH.

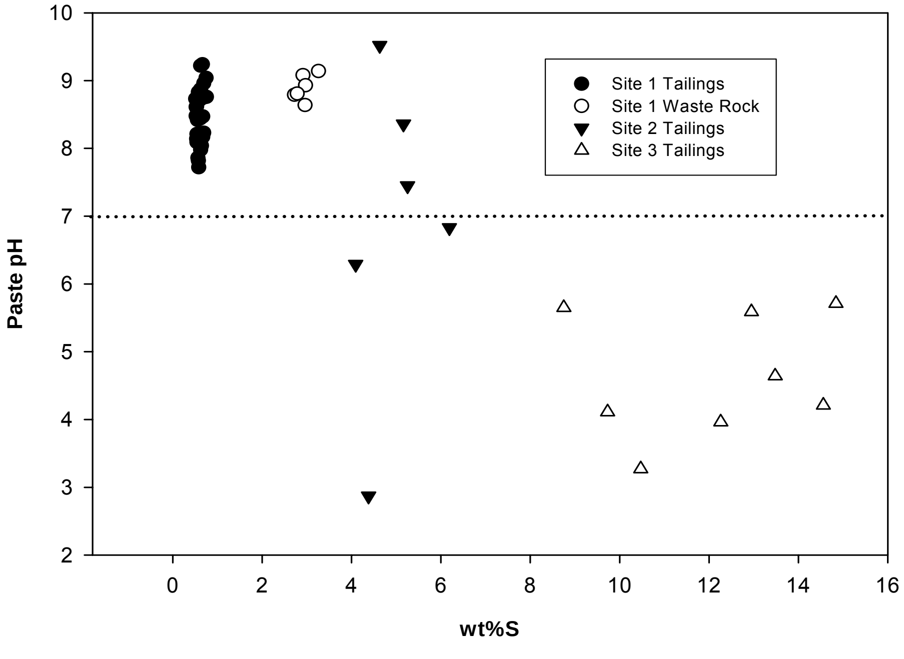

Fig. 5.4 Paste pH vs %S

The paste pH gives an indication of the inherent acidity of the waste material when initially exposed in a waste emplacement area. Sobek *et al*., (1978) defined materials that have a paste pH of less than 4.0 as being acid - toxic. Its limitation is that acid generating minerals are often located preferentially on the outside of particles and pulverising could expose acid neutralising minerals that would not be exposed in the field. To combat this, a rinse pH procedure was developed where the unpulverised sample was mixed with deionised water. However, distilled water typically has a pH of about 5.5 – 6.5 and therefore might still not reflect the pH of rain water or react in the way run off water would. Thus a material categorised as non acid forming (NAF) may still have existing acidity and salinity risks that make it unsuitable for surface or uncontrolled placement due to potential effects on drainage and vegetation.

ABA identifies the capacity of a sample to generate acidity based on total sulphur analysis. The result is converted to maximum potential acidity (MPA) by multiplying with a conversion factor of 31.25 derived from the stoichiometric ‘standard’ equation for pyrite oxidation (equation 3.1), and that one mole of acid is neutralised by one mole of $CaCO_3$. Other assumptions in using this factor are that the measured sulphur occurs in the solid phase only as disulphide (pyrite), and it oxidises completely to sulphate; oxygen and water are the only oxidants; iron from pyrite oxidises to the ferric state and all iron precipitates as $Fe(OH)_3$ and that all of the neutralising capacity is carbonate neutralising capacity, the carbonate is available to react and the acid consuming reactions are instantaneous and run to completion.

These assumptions are not always appropriate and alternative equations would apply. For example, ferric iron can oxidise pyrite in the absence of oxygen. If the ferric iron is originally derived from pyrite, the conversion factor from sulphur to acid potential is 15.63 rather than 31.25. Alternatively, the conversion factor could be 125.0 if the ferric iron is derived from ferric iron minerals. Also, sulphide minerals other than pyrite are associated with other conversion factors including zero.

Furthermore, the use of sulphide sulphur instead of total sulphur also helps to reduce the uncertainty in calculated MPA. The determination of sulphide sulphur involves measurements of total sulphur, leachable sulphate, and other forms of sulphur such as organic sulphur and barite ($BaSO_4$). The appropriate mass balance equation is:

$$\%S_{(total)} = \%S_{(sulphide)} + \%S_{(leachable\ sulphate)} + \%S_{(other)} + \Delta\%S \qquad (5.4)$$

$\Delta\%S$ represents any imbalance such as analytical error.

The sulphide acid potential would then be calculated as %$S_{(sulphide)}$ * 31.25. At the three mine sites considered in this study, it was found out that the dominant form of sulphur is the sulphide form as shown in Figure 5.5, and thus sulphide acid potential and maximum potential acidity are equivalent. The advantage in this situation is that analytical efforts and costs are reduced by analysing for total sulphur only.

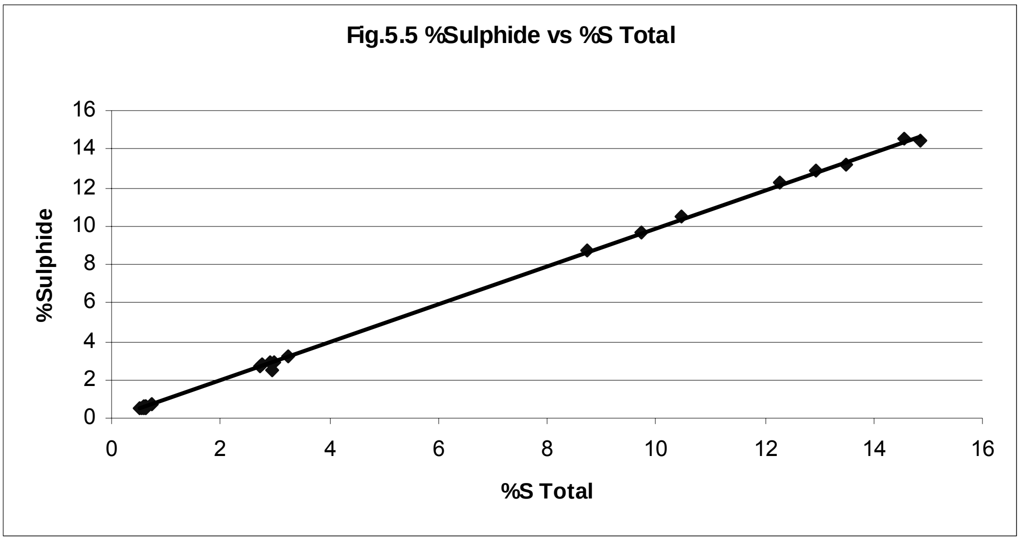
Fig.5.5 %Sulphide vs %S Total

5.4.2 Geochemical Classification of Samples

Table 5.4 shows the ABA criteria for classifying samples with regard to AMD generation potential. To account for the uncertainty in AMD predictions using ABA test results, the criteria for acid generation and neutralisation include a broad range of NAPP and ANC/MPA values that are classified as non acid forming (NAF), potentially acid forming (PAF), acid generating (AG) and uncertain. Used in combination with the NAG test results, ABA prediction and geochemical classification of samples results in reduced uncertainty in AMD prediction since the tests are independent. The statistical summary of ABA data is presented in Table 5.5.

Table 5.4: Criteria for acid generating potential

Criteria	**NAPP kgH_2SO_4**	**ANC/MPA (SRK, 1992)**	**ANC/MPA (Price, 1997)**	**NAG_{pH} (Miller, 1998)**	**NAG kgH_2SO_4/t**
Non Acid Forming	<20	> 3	> 2	>4.5	< 0
Potentially acid Forming	≥20	< 1	< 1	≤ 4.5	≥ 5
Acid Generating	>20	< 1	< 1	<4.5	> 5
Uncertain	>-20 and <20	< 3 and > 1	1 to 2	(< 4.5 & NAPP < 0)	< 5 & NAG_{pH}<4.5

Site 1 tailings meet all criteria for the samples to be classified as NAF. This is due to a combination of low sulphide sulphur (average 0.60%S) and the presence of neutralising minerals. Though analysis shows a rather low carbonate neutralisation capacity of 4.50kg $CaCO_3$/t, the total ANC averages 54.90kg $CaCO_3$/t suggesting that the majority of this buffering capacity should be a contribution from the silicates which are abundant in the form of serpentine and olivine as previously seen in Figure 5.3.

Table 5.5: Summary Statistics of ABA data from tailings and waste rock samples

Sample	**Paste pH**	**Total S wt%**	**MPA kgH$_2$SO$_4$/t**	**ANC kgCaCO$_3$/t**	**NAPP kgH$_2$SO$_4$/t**	**ANC/MPA**	**NAG$_{pH}$=$_7$ kgH$_2$SO$_4$/t**	**ARD Class**
Site 1 Tailings								
Max^m	9.24	0.75	23.44	67.22	-22.88	4.08	7.38	
Min^m	7.72	0.51	15.94	41.32	-49.01	2.12	0.00	
Mean	8.50	0.60	18.90	54.90	-36.01	2.94	1.49	
Std. dev	0.4	0.07	2.07	7.09	7.38	0.51	2.49	
Median	8.50	0.59	18.44	56.51	-35.67	2.83	0.00	
Count	30	30	30	30	30	30	30	**NAF**
Site 1 Waste Rock								
Max^m	9.14	3.26	101.86	119.27	5.22	1.37	7.32	
Min^m	8.64	2.72	85.00	87.64	4.04	0.91	0	
Mean	8.90	2.93	91.67	100.14	4.84	1.10	2.86	
Std. dev	0.19	0.19	5.90	12.74	0.46	0.18	3.29	
Median	8.87	2.94	91.72	95.55	5.04	1.07	2.05	
Count	6	6	6	6	6	6	6	**PAF**
Site 2 Cyanidation Tailings								
Max^m	9.53	5.25	164.06	139.04	34.10	1.09	22.18	
Min^m	2.87	4.09	127.81	125.64	-11.23	0.79	0.00	
Mean	6.90	4.70	146.94	130.29	16.65	0.90	16.01	
Std. dev	2.55	0.50	15.57	5.25	18.96	0.12	9.28	
Median	7.45	4.63	144.69	128.84	19.05	0.87	19.84	
Count	5	5	5	5	5	5	5	**AG**
W/Rock	6.83	6.19	193.44	137.92	55.52	0.71	24.56	**AG**
Site 3 Jig Plant Tailings								
Max^m	5.97	14.84	463.75	32.81	432.86	0.11	287.41	
Min^m	3.19	8.75	273.44	22.86	247.25	0.05	174.92	
Mean	4.87	12.13	379.06	28.46	350.61	0.08	221.08	
Std. dev	0.93	2.26	70.57	3.50	71.56	0.02	36.46	
Median	4.82	12.61	393.91	28.75	364.50	0.07	217.02	
Count	8	8	8	8	8	8	8	**AG**

Site 1 waste rock has relatively high sulphur content, average 2.93%S representing an acid potential of 91.67kg/t H_2SO_4. NAPP and ANC/MPA data indicate the waste rock could be a potentially acid forming low capacity sample, and a significant lag before development of full acid conditions can be expected. The lag period could be due to silicate buffering. Straight forward predictions of silicate buffering are difficult due to the variable composition of silicate minerals and complex kinetics of silicate dissolution, (Nicholson, 2003). However, Kleiv *et al.,* (2001) showed that silicate minerals can buffer acid and adsorb heavy metals on silica tetrahedral. The silicate dissolution is essentially an exchange of protons for counter ions from silicate structure as depicted in equation 5.5 for magnesium rich olivine.

$$Mg_2SiO_4 + 4H^+ = 2Mg^{2+} + H_4SiO_{4(aq)} \tag{5.5}$$

This reaction shows that the counter ion Mg^{2+} in the silicate structure goes into solution and H^+ binds to the silicate ion as it dissolves. The lower the Si/O ratio in the silicate structures, the higher the charge on the silicate tetrahedral. This greater charge is counter balanced by counter ions, which in turn are replaced by more protons. This implies that in general, the lower the Si/O ratio of a mineral, the greater the potential to neutralise acid. Figure 5.6 illustrates the neutralisation potential as a function of paste pH for all three sites.

Fig. 5.6 Paste pH vs ANC

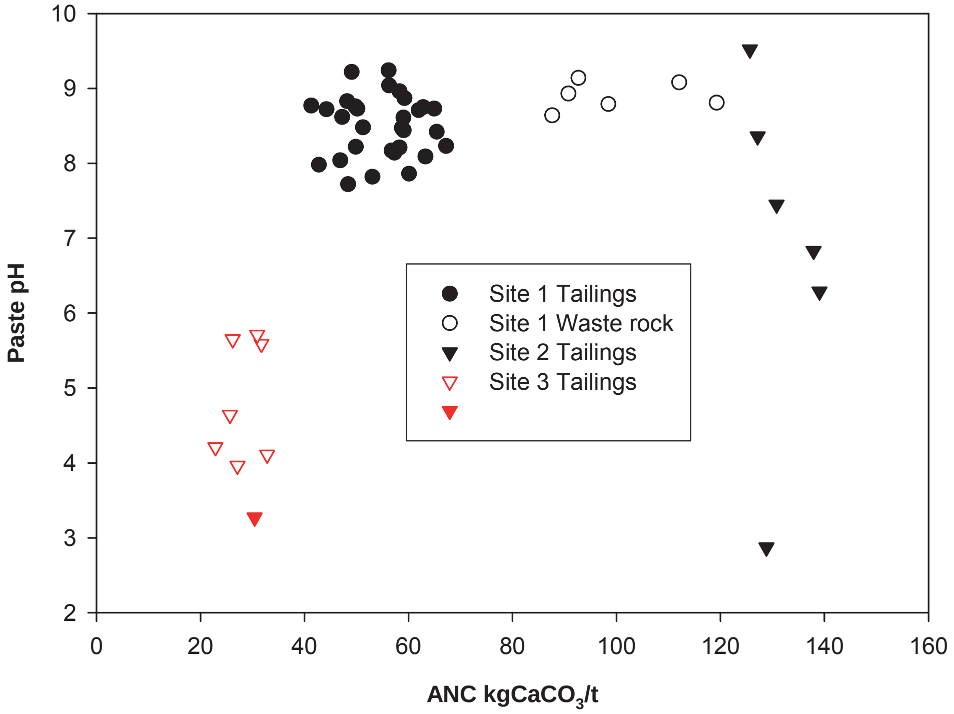

The range of ANC for the acid generating samples of Site 3 is between 22.86 and 32.81kg H_2SO_4/t, which is well out weighed by the MPA averaging 379.06 kg H_2SO_4/t. Hence these samples are classified as having a very high potential for acid generation when exposed to oxidising conditions. Though Site 3 samples also contain substantial amounts of silicates, it appears the neutralising capacity is very low compared to samples from Site 1, suggesting that the silicate buffering in Site 3 samples is not as effective. A possible explanation for this is that Site 3 samples contain significant amounts of aluminium and iron, (2.46% & 24.85% respectively). These elements tend to hydrolyse in solution, producing acid, (equation 3.18). Malmstrom and Barnwart (1997) showed that minerals with Al and Fe in octahedral sites will have lower buffering capacities than similar minerals with no Al and Fe.

There is a lot of uncertainty behind determination of ANC by any of the methods found in litrature, mainly due to lack of a fundamental definition of ANC. Based on analytical procedures, a single sample may have ANC's spanning an order of magnitude (Morrin and Hutt, 1997). Other shortcomings of the ABA methods include:

- Minerals with slow rates of dissolution, such as silicates and aluminosilicates, are not included in the 24 hr ANC determination.
- It is not possible to assess the effect of secondary minerals precipitating at the pH of these tests, e.g. $Fe(OH)_3$ formation generates more acid that is not covered by these tests.
- Many potential neutralising minerals might have no significant solubility at the pH found in acid mine drainage, so these minerals do not effectively contribute to neutralising capacity, a factor not considered in ANC tests. Thus it is common for ANC to overestimate neutralisation capacity in the field (Miller *et al.,* 2003).

In recognition of the difficulties in the determination of ANC & MPA, another approach, based on mineralogical composition was proposed by Paktunc (1999), where bulk values for the MPA and ANC of a sample in kgH_2SO_4/t can be calculated as follows:

$$MPA = \sum_{s=1}^{m} \frac{n_s x 98 x X_s x 10}{W_s} \qquad (5.6)$$

$$ANC = \sum_{i=1}^{k} \frac{n_s x 98 x X_i x 10 x c_i}{n_i x W_i} \qquad (5.7)$$

where: n_s = the number of moles of H_2SO_4 formed by the oxidation of 1 mole of sulphide minerals;
98 = the molecular weight of H_2SO_4;
X_s or X_i = weight % of sulphide mineral s or neutralising mineral i;
10 = the conversion factor for kg/t units
W_s or W_i = the molecular weight of sulphide mineral s or neutralising mineral i, in g/mole;
m& k = the number of sulphide minerals in the sample;
n_i = stoichiometric number of moles of neutralising mineral;
ci = stoichiometric number of moles of H_2SO_4

The advantage in these formulae is that they take into account the presence of more than one type of sulphide or neutralising mineral, thus a bulk acid potential or bulk neutralisation potential is calculated. The problem is that equation 5.7 is bound to overestimate the neutralising capacity of samples as some of the calculated ANC may not actually be available in the field.

5.4.3 Acid Base Characteristic Curve

From Figure 5.6, Site 2 samples exhibit high ANC, giving a NAPP value of average 16.65kg H_2SO_4/t, which would be classified as NAF. However, combining NAPP with

Fig. 5.7 ANC vs MPA

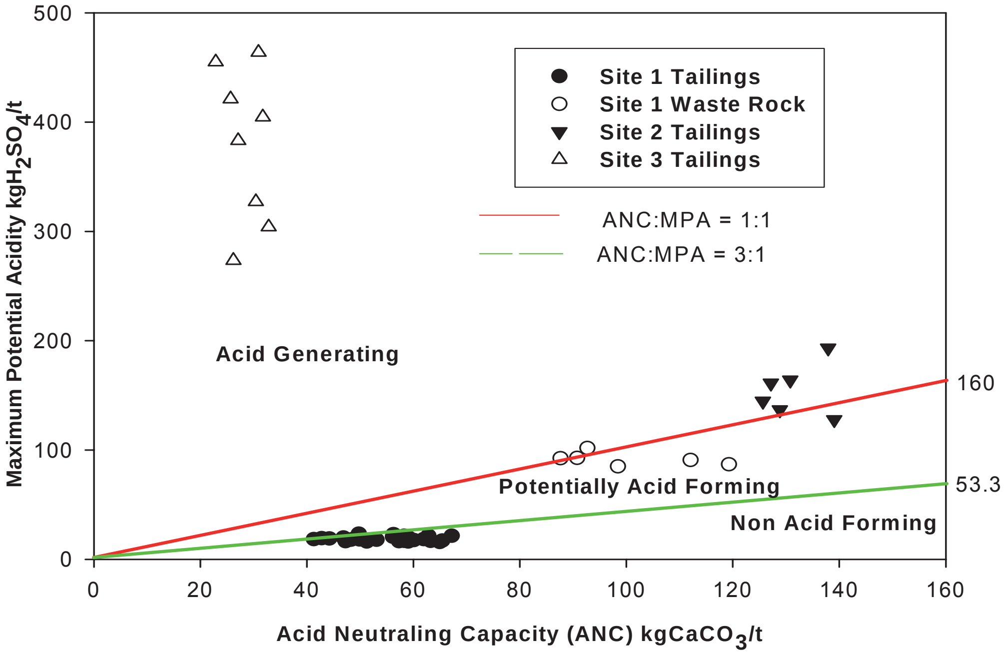

other criteria (ANC/MPA ratio) and NAG results in Figure 5.7, and it becomes evident that these samples would be categorised as PAF to AG. Due to the low ANC/MPA ratios of Site 1 waste rock, they fall in the PAF category according to Figure 5.7 classification, raising concerns of acid generation. An acid buffering characteristic curve (ABCC) test was conducted on Site 1 waste rock and the results presented in Figure 5.8. The ANC of the material was determined to be 89.47kg H_2SO_4/t.

The results of the ABCC test indicate relative strong buffering, up to the equivalent of about 15kg H_2SO_4/t, after which the pH then dropped moderately with further acid addition. However, the buffering capacity of the waste rock sample is way below when compared to that of calcite, limestone or dolomite calculated from mineralogical composition, (Panktunc, 1999). The approximate lag period by which this buffering can delay onset of acid generation can only be estimated from kinetic tests. If buffering rate reactions occur faster than acid producing reactions, then as long as fresh waste rock continues to be mined, acid neutralisation will continue to take place delaying the net acid effect. From the kinetic tests in section 5.2.2, the lag period before acid conditions develop in the field could not be estimated for this sample. Once the ANC is used up, an 'acid breakthrough' condition may then begin to be observed at this site, possibly long after mining has stopped.

Fig. 5.8 ABCC for Site 1 Waste Rock compared to carbonates

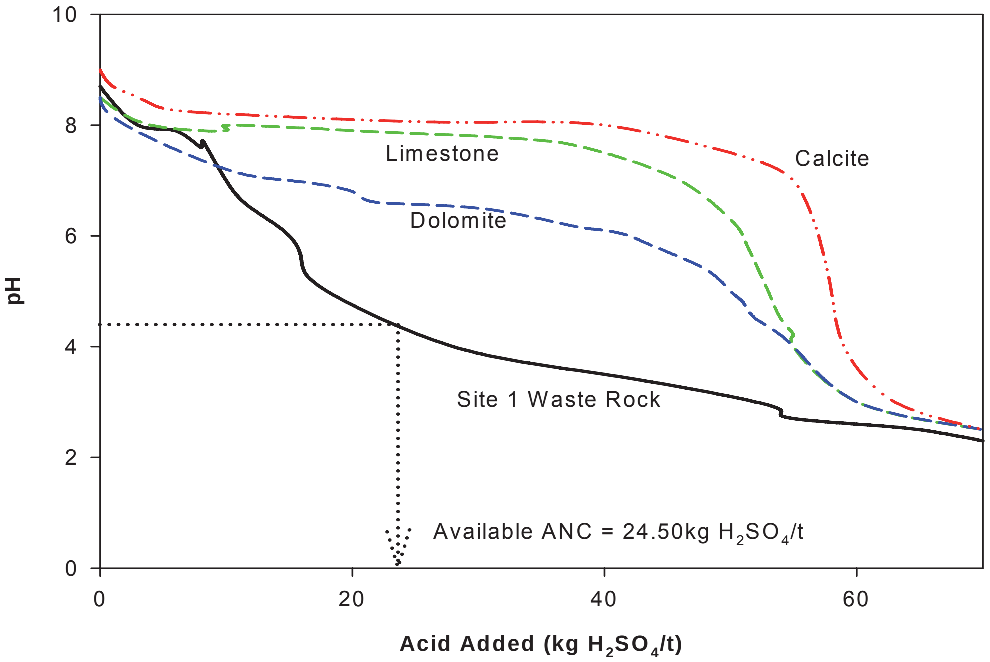

5.5 Effects of Kinetic Test Conditions on Weathering Rates

5.5.1 Sulphate Production Rates

Following the ABCC test on Site 1 waste rock, a kinetic test using the standard Sobek protocol only was performed to determine if ever the sample would go acid and if so, after how long? For sites 2 and 3, kinetic test conditions used included the standard Sobek, non – aerated cells and simulated rainfall cells. Variations in kinetic test conditions were done to compare the effects on sulphate production rate, drainage chemistry and estimated time to acidity. Difficulties were encountered in maintaining equal and uniform airflow through the Standard Sobek and the Simulated Rainfall cells.

The moisture content of the non – aerated cells remained relatively steady at about 14.27% & 12.86% for Site 2 samples, and 11.54% & 12.08% for Site 3 on a week to week basis. The moisture content of the standard cells and simulated rainfall cells fluctuated throughout the testing. Visual observation revealed that all the cells dried up slightly on the top after the 5th day. The sulphate production profile for Site 1 waste rock is shown in Figures 5.9.

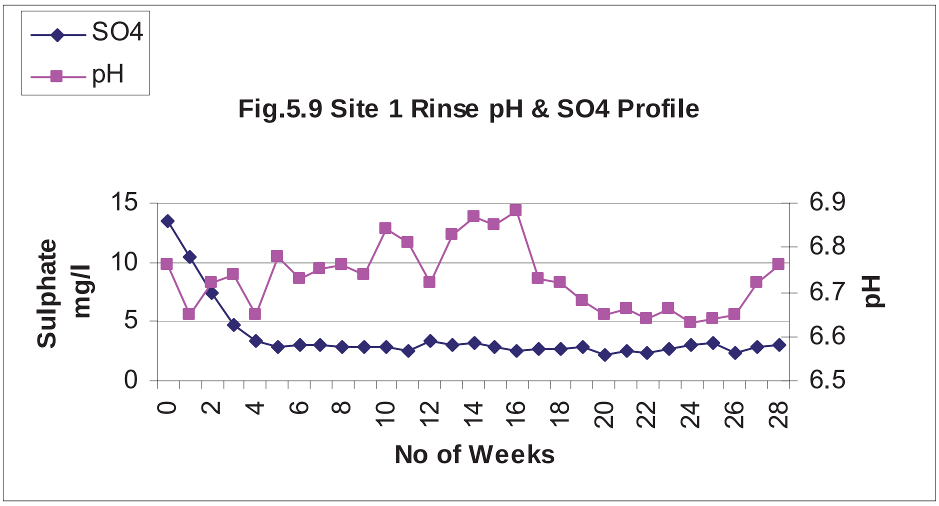

Site 1 waste rock maintained a leachate pH above 6.5 for the duration of the test. The average rate of sulphate production, based on the last five weeks, is 2.89 mg/kg/week. The pattern of sulphate production shows that there was some accumulated sulphate in the sample before the kinetic test started possibly due to sulphide weathering in the field. Since the samples were taken prior to the rain season, oxidation products were not being flushed out but accumulated, a trend shown in samples from all the three sites.

Going by the average rate of sulphate production in the last five weeks of the test, extrapolation indicates that the sample could become acid after several years.

The sulphate production profiles shown in Figures 5.10 & 5.11 show that the non - aerated cells exhibit relatively smooth patterns and approached stabilisation early in comparison to standard and simulated rainfall cells. This can be attributed to the relatively consistent moisture content in the non – aerated cells. Consistent moisture content creates an operating condition similar to what the sample could attain under field conditions. There is a somewhat erratic pattern in sulphate production for the standard Sobek cells and also simulated rainfall cells for Site 2. The distortion in trends of sulphate production with time can be attributed to the weekly wetting and drying cycles which create an unnatural environment that can potentially affect the acid generation process.

Fig. 5.10 Site 2 SO_4 Production Rates

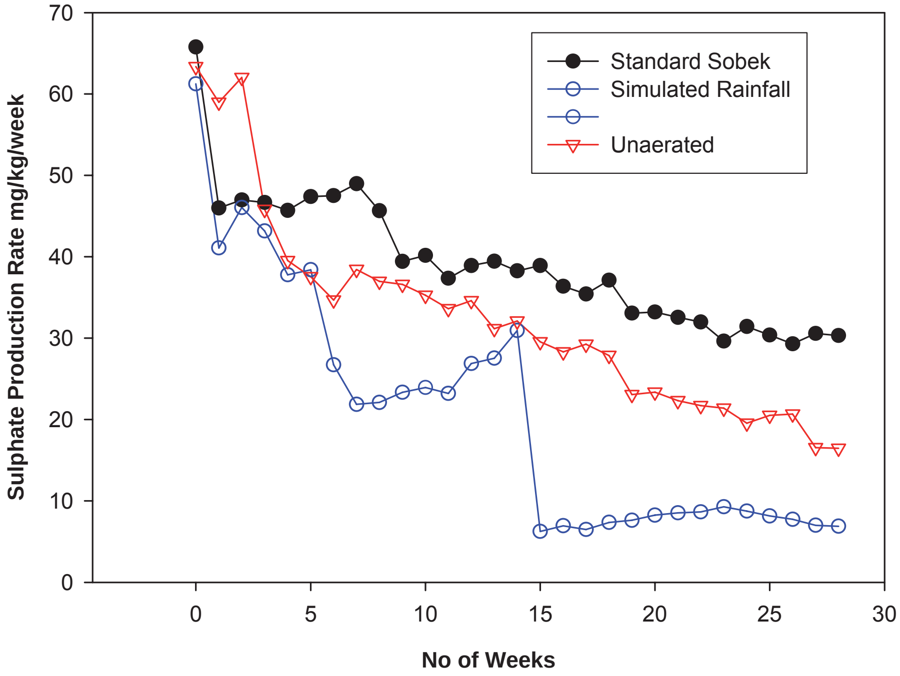

However, non – aeration seems to limit oxygen diffusion rates resulting in lower levels of sulphate production compared to standard Sobek cells. Eliminating the dry and wet air cycles mimics the natural environment at mine sites and presumably gives repeatable and representative reaction rates. The oxidation rates are relatively high up to week 16 for Site 2 samples, then decrease gradually reaching steady state from week 22.

Fig. 5.11 Site 3 SO_4 Production Rates

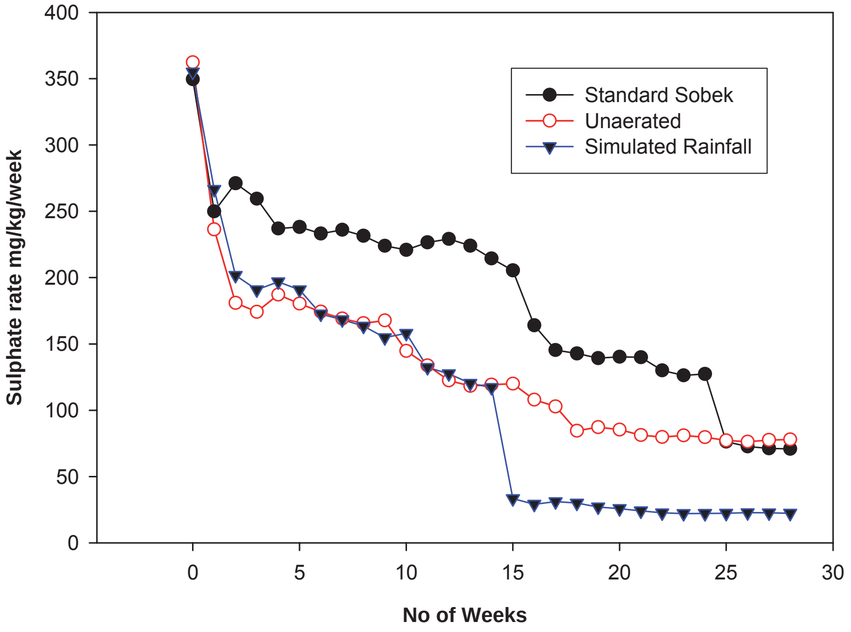

Simulated cells started with a high volume of flush water (500ml) for the first 14 weeks, which was then reduced to 150ml for the remainder of the test. This caused the sulphate release rate to drop sharply at first but then increased slightly before stabilising. The sharp decrease in sulphate release can be attributed to the influence of rinse water volume on pore water concentrations. The lower volume of rinse water led to less dilution of the pore water but left more sulphate in the cells thus disrupting pore water chemistry and the established oxidising environment. Consequently, the sulphate release rate is much lower than for standard Sobek and non – aerated cells. These results support other studies by Frostad *et al.,* (2002) who showed that changing the leach volume or frequency affects the kinetics of precipitate formation in humidity cells and that could decrease the oxidation rate by removing ferric iron, a potential oxidant, from solution.

5.5.2 Estimated Time to Acidity

Table 5.6 gives the estimated times for 'acid breakthrough' ($pH < 6$) along with cumulative sulphate production up to the point of acidity. The results show that conditions which increase the time to acidity permit high levels of sulphate release possibly suggesting higher rates of neutralisation. Figure 5.12 shows the pH profiles for the different test conditions and for the two sites. It can be seen that the standard Sobek cells reached the 'acid breakthrough point' first while the simulated rainfall cells took the longest time. For Site 2, the standard Sobek cell became acidic after 9 weeks but it took 21 weeks for the simulated rainfall cell to become acidic. A similar trend is also observed for Site 3 samples although the time interval to cells becoming acid is shorter and within two weeks of each other.

Table 5.6: Estimated Times for Acid Breakthrough

Kinetic Test	**Time to pH<6 Weeks**	**Average SO_4 Rate (last 5 wks) mg/kg/week**	**Cumulative SO_4 Released mg/kg**	**Sulphur Depleted % of original**
Site 2 Standard	9	30.40	454.39	0.32
Site 2 Non aerated	17	18.75	672.32	0.48
Site 2 Simulated	21	7.70	484.40	0.34
Site 3 Standard	4	83.63	1255.62	0.35
Site 3 Non aerated	6	77.72	1133.31	0.31
Site 3 Simulated	7	22.43	1387.57	0.38

A possible explanation for this is that conditions that promote reaction products to remain and build up on the exposed surfaces of neutralising minerals decrease their rate of dissolution. This should be the case in simulated rainfall cells with reduced amount of rinse water and also in non - aerated cells. Apart from supplying oxygen saturated atmosphere during the dry air and wet cycles, aeration helps to shake and detach reaction products from reacting mineral surfaces which then remain exposed for further reaction. As soon as sufficient reaction product, e.g. iron oxide, has precipitated to limit neutralisation, the leachate can become acidic. A high sulphide oxidation rate may enhance acidification from the precipitated secondary mineral products, and thereby shorten the time to acidity. This is supported by the profiles of Site 3 which has pyrite content averaging 12.13%S compared to that of Site 2 with 4.7%S.

Fig. 5.12 Predicted Time to acidity

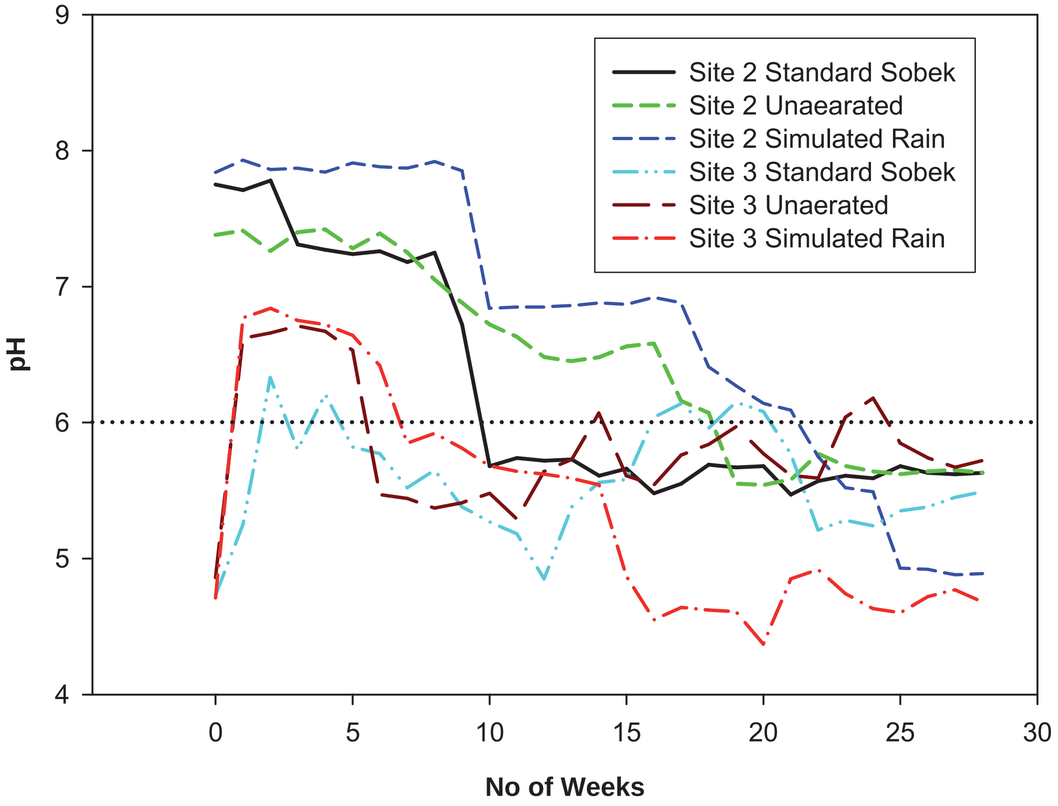

Site 2 samples exhibited significant buffering during the first 8 weeks. This is possibly due to the effect of residual lime added to the cyanidation plant in order to achieve protective alkalinity required for optimal gold dissolution. Very little initial buffering is seen in profiles of Site 3 samples. The pH profiles seem to stabilise after reaching acidification, presumably a sign of equilibrium between acid producing reactions and late stage neutralising silicates.

5.6 Correction of Laboratory Data to Estimate Field Weathering Rates

5.6.1 Specific Surface Area

The surface area of exposed sulphide minerals has been reported to be directly proportional to the oxidation rate (Lappako, 1994a; Lappako, 1994b). The approximate specific surface area of granular material per unit mass can be calculated from knowledge of the particle size distribution by the summation equation proposed by Hillel, (1982):

$$a_m = \left({}^{6}\!/_{\rho} \right) \sum \left({}^{c_i}\!/_{d_i} \right) \qquad (5.6)$$

where a_m is the total surface area per unit mass, ρ is the particle density, c_i is the mass fraction of particles of average diameter d_i. Using the grain size distributions of the samples from sites 2 & 3 shown in Figure 5.13 and the formula in equation 5.6, a spreadsheet was used to calculate the grain specific surface area of the samples. Table 5.6 shows the sulphate production rate on a surface area basis calculated from sulphate production on a mass basis (Table 5.5) and specific surface area.

Fig.5.13 Particle size distributions of sites 2 & 3 Tailings

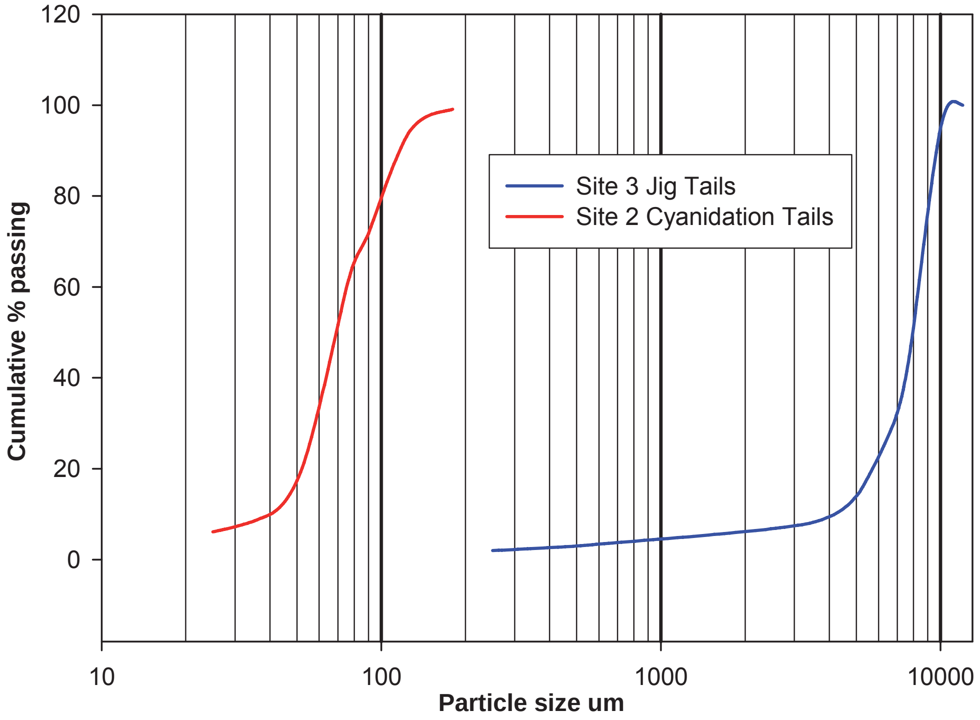

Table 5.6: Sulphate production rates on surface area basis

	Particle Characteristics			**Sulphate Production Rate on a surface area basis (mg/m^2/wk)**		
Sample ID	Specific Surface Area m^2/kg	100% passing size (mm)	Specific gravity	Standard Sobek	Non-aerated	Simulated Rainfall
Site 2 Tails	39.18	0.25	2.67	0.76 T = 28°C	0.48 T = 29°C	0.20 T = 27°C
Site 3 Jig Tails	0.57	6.00	4.19	146.72 T = 31°C	136.35 T = 33°C	39.35 T = 33°C

5.6.2 Temperature Effect on Weathering Rates

The rate of most chemical reactions are observed to increase with increasing temperature, and the reaction rate constant can be related to temperature through the Arrhenius expression, equation 5.7, for temperatures T_1 & T_2 in Kelvin:

$$\log\frac{k_1}{k_2} = \frac{E_a}{2.303R}\left[\frac{1}{T_2} - \frac{1}{T_1}\right] \qquad (5.7)$$

where k_1 and k_2 are the rate constants at these temperatures, E_a is the activation energy (kcal/mol), and R is the gas constant, 8.31 kcal/mol/K.

The laboratory weathering rates are corrected using the Arrhenius equation 5.7, pH specific activation energy values and temperature measurements from the sites. At Site 2, the activation energy used for pyrite at pH 7.8 is 88 000 kcal/mol, and pyrrhotite 100 000 kcal/mol, (Nicholson & Scharer, 1994). These values are averaged together for an E_a of 94 000 kcal/mol, since the tailings at Site 2 contain approximately, pyrite:pyrrhotite = 1:1. Drainage from Site 3 jig tailings average pH = 3.5 and the ratio of pyrite to pyrrhotite is 4:1. At this pH, the E_a for pyrite is 52 000 kcal/mol, (McKibben and Barnes, 1986) and for pyrrhotite its 46 000 kcal/mol, (Nicholson & Scharer, 1994), giving a weighted average in activation energy of 50 800 kcal/mol.

During the fieldwork period, the estimated internal average temperatures in Site 2 tailings and Site 3 jig tailings were 34°C and 41°C, respectively. Table 5.7 gives the estimated field weathering rates, K_2 in mg-SO4/m^2/week, corrected for field temperatures, $T_2(^oC)$, where T_1 and K_1 are the laboratory conditions given in Table 5.6.

Table 5.7: Estimated Field Sulphate Production Rates

	Standard Sobek				**Non Aerated**				**Simulated**			
	T_1	T_2	K_1	K_2	T_1	T_2	K_1	K_2	T_1	T_2	K_1	K_2
Site 2	28	34	0.76	1.40	29	34	0.48	0.81	27	34	0.20	0.42
Site 3	31	41	146.72	253.67	33	41	136.35	210.73	33	41	39.35	60.82

The rates of sulphate release in the field are estimated much higher than laboratory rates mainly due to higher temperatures experienced in the waste piles due to overburden, sulphide oxidation and the tropical heat. An often quoted rule of thump is that the rates of reactions roughly double for every 10°C increase in temperature. This data shows a similar trend.

5.7 Concluding Remarks

The geochemical prediction tests performed in this chapter provide critical classifying information concerning the acid generation potential of the tailings and waste rock piles at the three sites. At Trojan Nickel (Site 1), the tailings are non acid forming due to low sulphide sulphur content and buffering from silicates. Results from the Acid Base Characteristic Curve tests show that the waste rock pile at this site is potentially acid generating and current buffering is being provided from freshly mined rock containing acid neutralising minerals. Drainage from this pile could become acidic within a few years after mining stops. Kinetic tests show that the tailings at Mazowe Mine (Site 2) are net acid generating with a lag period estimated at 2 years due to buffering from lime added during gold cyanidation.

By simulating the hydrological regime on site in the humidity cell tests, sulphate production rates were much lower by a factor of 4, and the predicted time to acidity longer by 3 weeks than for the standard Sobek cells in the case of Iron Duke (Site 3) samples. Sample leachates from this site typically have high sulphate, zero alkalinity, and high metal concentrations although these decline with time.

The laboratory prediction tests provide key parameters to the understanding of geochemical behaviour of the waste materials under different environmental conditions, but extrapolation or correction of the data to field conditions is very difficult. Therefore, to improve the understanding on the geochemical controls on leachate behaviour at the worst affected mine, it was necessary to implement a full plant and field scale geochemical investigation at Iron Duke, as discussed in Chapter 6.

CHAPTER 6

GEOCHEMICAL CONTROLS ON THE NEUTRALISATION AND ENVIRONMENTAL BEHAVIOUR OF AMD AT IRON DUKE MINE

6.1 Overview of the Acid Problem

Mining and processing of pyrite ore at Iron Duke Mine generates large quantities of acidic mine water as a result of the oxidation of iron sulphides on exposure to air and water. The main flows of water into the underground workings include cooling water used in the drilling & blasting operations and groundwater percolating through fissures. These streams are mixed, gravitate to the lowest level and pumped to the surface where they combine with spillage from the jig processing plant and collected drainage from the jig plant tailings. The combined acid stream of about $180m^3$/day and an annual average acidity level of 17563.84 mg/l $CaCO_3$ is neutralised with lime before discharge in evaporation ponds.

The acid mine drainage contains elevated levels of dissolved Fe, Al, Mn & sulphate and has characteristic pH values ranging from about 0.50 to 3.00. Handling and disposal of such a drainage places significant impacts on the economics of the mining operation due to the corrosive nature of the drainage on infrastructure, the limitations placed on water reuse and discharge to the environment under a new law governing effluent discharge. Treated sludge at Iron Duke is chemically unstable, changing pH from ~7 to ~3 within four days after deposition in the evaporation ponds. The effluent does not meet the permitted discharge level of neutral pH, 250 mg/l sulphate and less than 500 mg/l total dissolved solids. Excessive acid seepage from the evaporation ponds has resulted in contamination of the ground water below the ponds area which shows high mean annual levels of iron (368.67mg/l), sulphate (1702.89mg/l) and low pH (2.86) in addition to other pollutants. This poor quality seepage infiltrates into the nearby Yellow Jacket River, contaminating the public water source. Furthermore, a deterioration of the land area and vegetation adjacent to the tailings dump is also observed.

Understanding the controls on the neutralisation of acidic drainage and long term sludge stability after placement in evaporation ponds is essential to minimise costs of closure requirements and for the protection of environment and human health. The objectives of this chapter are to evaluate the processes controlling the behaviour of major and trace components in acidic drainage and to use chemical equilibrium analysis methods to interpret the chemical evolution of AMD.

6.2 Materials and Methods

6.2.1 The Neutralisation Plant Process

Figure 6.1 shows the process flow diagram for neutralisation treatment of the acidic mine effluent at Iron Duke. The neutralisation plant consists of 6 tanks fitted with agitators, each with a volume of 32.5m^3. The first two are used as lime mixing and storage units. The lime is simply added into water with continuous stirring to produce a paste. The lime paste from the dosing tank gravitates at a controlled rate to the buffer tank or first neutralising stage where it's continuously mixed with raw mine effluent, pH ~2.5, at predetermined rates. It is then allowed to overflow into the second stage tanks which provide for residence time. When pH reaches the desired range (6.5 – 7) the second stage tanks are drained through a pump and the neutralised discharge is stored in holding ponds. The ponds are designed so as to allow for solids settlement in the receiving compartment with the clean overflow collecting and draining into a separate pond where it is expected to evaporate.

The chemical instability of the neutralised sludge is a cause for concern and a study was carried out to determine through laboratory and full scale experience the geochemical parameters controlling the acid neutralisation treatment, and hence the most suitable effluent treatment configuration that can give a chemically stable sludge.

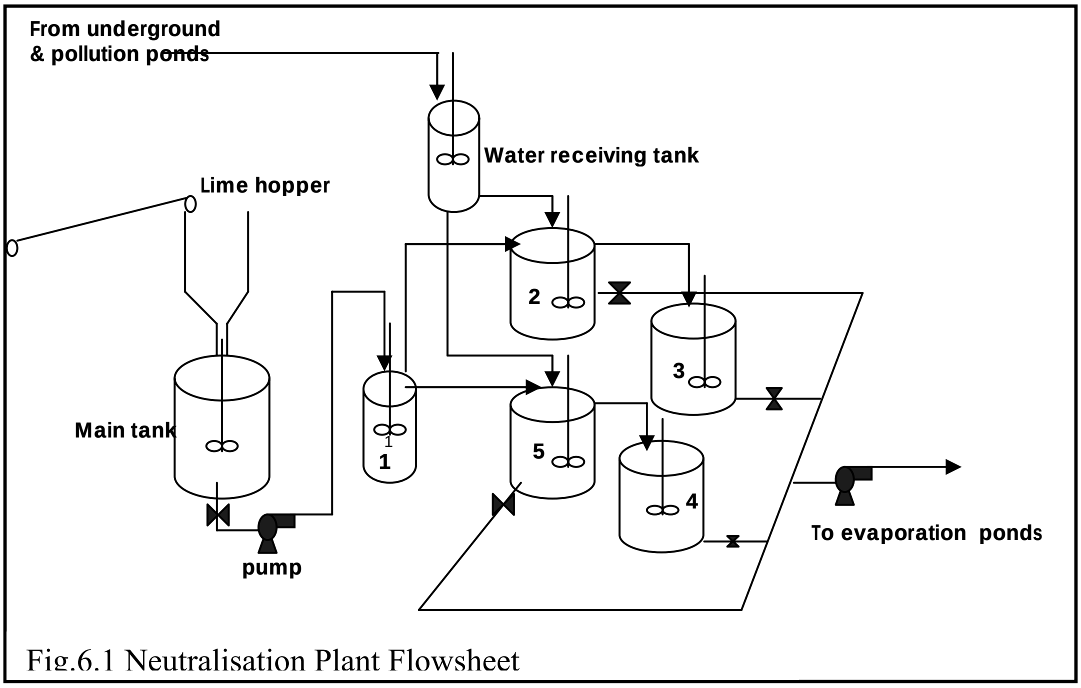

Fig.6.1 Neutralisation Plant Flowsheet

6.2.2 Sampling and Analysis of Water & Sediments

Treatment of water samples

A field reconnaissance and drainage monitoring at Iron Duke was carried out once every month, from May 2004 to April 2005. Surface water samples were collected from the nearby Mazowe and Yellow Jacket rivers, evaporation ponds, seeps, mine water and drainage locations in proximity to tailings and waste rock piles. The water samples were treated as described in Chapter 4 section 4.4.2.

Treatment of Solid Samples

i) Stream Sediments

Stream sediments were collected from upstream and downstream of the mining site to provide information about baseline conditions for drainage streams proximal and distal to the mine area, and to investigate their role in the removal of metals and other contaminants from surface water.

Stream sediment samples were composited by collecting sediment increments from several places at the sample site, generally along a 100 m stretch of the stream. Attempts were made to collect 20 to 30 increments in order to improve sample representativeness. About 1 kg of sediment sample sieved on site through a 2mm stainless steel screen was collected in plastic sample bags and then air dried. Sediment samples were predominantly stream alluvium but a few were collected from ponds and others from runoff gullies below the jig tailings dump and old waste rock pile. In the laboratory, samples were oven dried at 50^{o}C to prevent baking and sieved through 180 μm. The coarse fraction was discarded and the finer fraction was random sampled in 30 small increments and pulverised in preparation for chemical analysis.

ii) Precipitate Samples

Secondary minerals collected were resulting from the weathering of waste rock and metallurgical tailings, evaporation salts, and from precipitation due to mixing, dilution and neutralisation. Secondary minerals and precipitate samples of flocs precipitating out of acidic metaliferous waters were collected by the grab sampling technique. The samples were composited from wet areas such as ponds and tailings drainage gullies and placed in sealed plastic bags. The samples were bagged in plastic sample carriers and retained to the laboratory where they were oven dried at 40^{o}C, riffle split, pulverised without sieving and then prepared for chemical analysis by XRF.

6.3 Results and Discussion

6.3.1 Controls on Mine Drainage Composition

a) Variation in heavy metals composition with drainage pH

Figures 6.2 shows the sum of base metal cations concentration in mili-equivalents per litre as a function of pH for mine waters that drain from the different mineral deposit types in the Mazowe area in NE Zimbabwe, compared to that of Iron Duke. In general, metal content increases with decreasing pH reflecting greater amounts of pyrite and other sulphide minerals coupled with lesser amounts of acid buffering minerals. The massive pyrite ore body at Iron Duke has extreme acid generating capacity, (up to 463.75 kgH_2SO_4/t) a feature common to all massive pyrite orebodies. As a result, the acidic drainage mine water contains extreme concentrations of Fe, Mn, and Al, moderate amounts of Cu, Ni and Zn. In contrast, carbonate containing tailings deposits and olivine rich waste rock piles most commonly generate drainage with near neutral pH values and associated moderate quantities of Ni (as high as 7.52 mg/l) and lesser copper (maximum 1.06 mg/l).

The importance of geologic controls can be illustrated in other mine waste components of environmental concern such as tailings drainage, cyanide processing solutions, waste rock, etc. It can be seen that environmental signature of mine site drainage is a predictable function of mineral deposit geology, deposit size, host rocks, ore and gangue mineralogy.

The scale of environmental effects generally increases with increasing deposit size. Host rock influences factors such as mineral textures, trace element geochemistry and the rate at which minerals weather and oxidise. As weathering and erosion of mineral deposits and waste piles take place, secondary mineralogy in the form of new, more chemically stable mineral suites develop and exert a predominant controlling effect on the environmental behaviour of acid mine drainage.

Fig.6.2: Variations in trace metal concentrations in streams draining from different rock typ

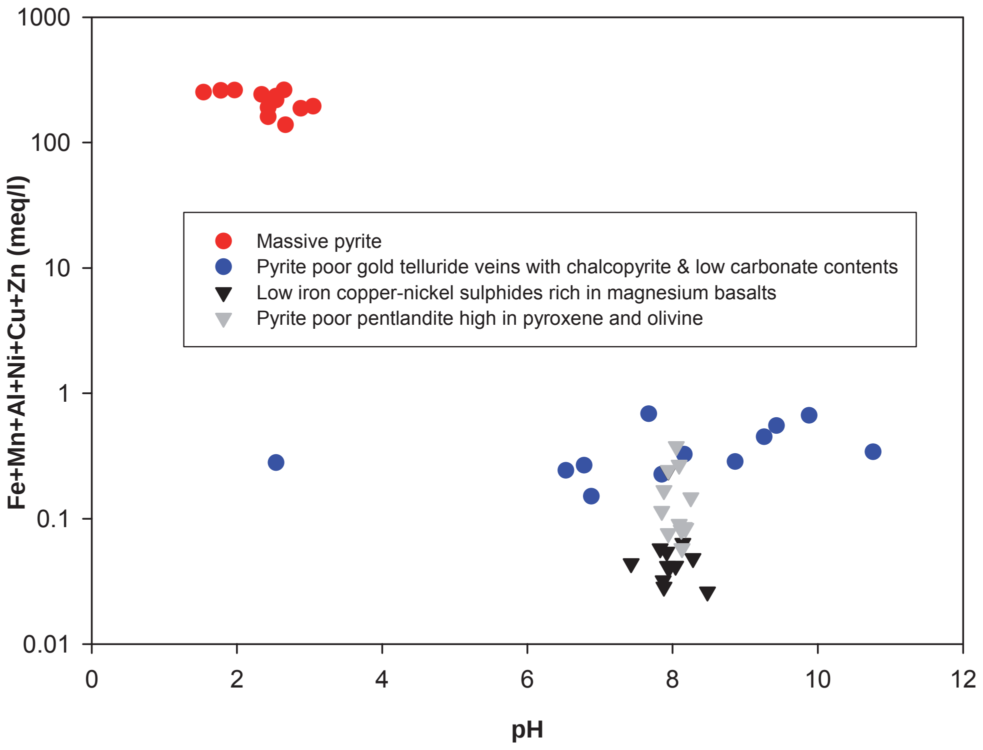

b) Climatic Controls on Drainage Chemistry

Amounts of rainfall and prevailing temperatures influence the amount of water available as surface runoff, the level of the water table, rates of reaction, amounts of organic material, and other parameters that affect the oxidation of sulphide minerals. Water tables are shallow in wet climates and deep in semi arid climates. However, depth to the water table can be highly variable across short distances within a mine site as observed at Iron Duke where water tables vary from 2.25m to 60m. Drinking water borehole levels are in excess of 45m, whereas a shallow aquifer with water levels from 2.25m to 9m exists on the down gradient of the evaporation ponds.

Table 6.1 compares the summary statistics (maximum, minimum, mean, geometric mean, standard deviation, skewness and kurtosis) of hydro-geochemical parameters of mine water during the dry and wet seasons. The statistics for elemental concentrations including sulphate are based on 12 measurements and 24 measurements for the field parameters like flow, pH, temperature, redox (Eh), TDS and EC. Skewness describes the symmetry of the data distribution around the mean, and kurtosis is a measure of whether the data is peaked or flat relative to a normal distribution. Most of the data shown is skewed to the left and slightly more flat around the mean. The rest of the monitoring data supporting the fore going discussions is presented as Figures, in Appendix D.

Acidity, metal concentration and levels of other pollutants generally tend to increase in the dry season with lower values observed in the wetter months from December to March due to increased percolation of ground water to the mining level. The increased volume of mine water has ramifications in terms of water handling procedures for the mine in that it means more pumping and treatment costs. Although there seems to be small differences between the dry and wet season pollutant concentrations in Table 6.1, a clear pattern is shown by plotting the full data in Figure 6.3. In this figure, the effect of seasonal variation on water chemistry is clearly illustrated where the pH of surface water in Yellow Jacket River upstream of the seepage point D is seen to vary about a mean throughout the year. However, the moving average for the seepage point shows a trend where pH decreases significantly to as low as 2.5 in the drier months, June to October, and steadily increases to above 5.0 at the peak of the rain season between January and March. This implies that pollution by AMD has a significant impact on water quality during the dry period. This is further evidenced in Figure 6.4 by the seasonal variations in TDS, sulphate, iron and manganese concentrations.

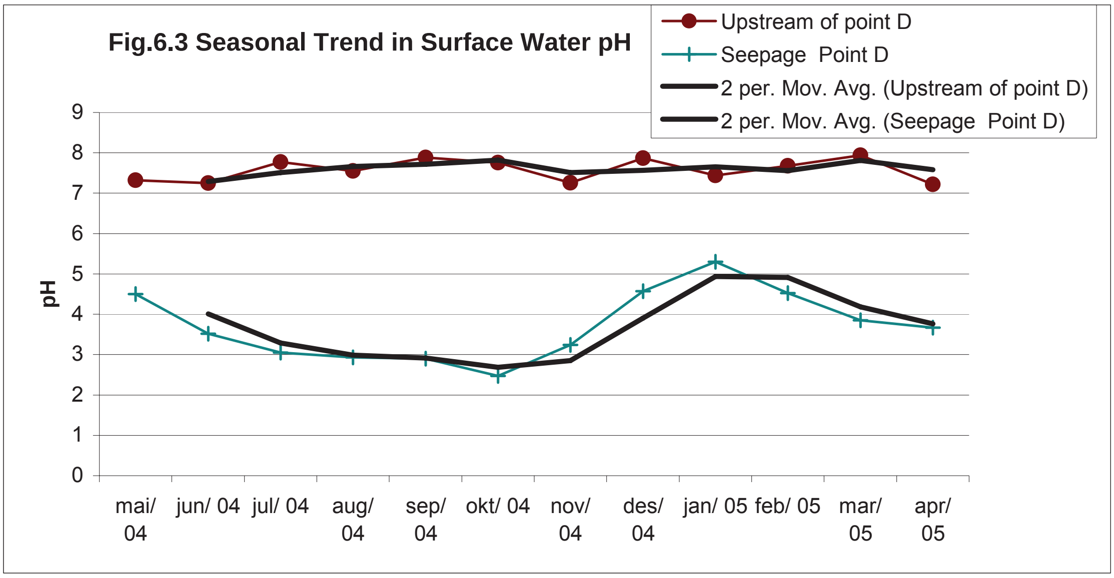

N.B. When the data set for an individual parameter was partially censored, (i.e. some measurements below the detection limit), the parameter means, standard deviations, skewness & kurtosis are calculated using half the value of the lower detection limit.

Table 6.1 Statistics of Hydrochemical Parameters in Dry & Wet Season

		DRY SEASON							WET SEASON						
Parameter		Max	Min	Mean	Geomean	Stand. Dev	Skewnes	Kurtosis	Max	Min	Mean	Geomean	Stand. Dev	Skewnes	Kurtosis
Flow	m^3/h	7.74	7.21	7.46	7.46	0.18	0.30	0.60	38.86	12.22	27.52	27.52	0.23	0.09	-0.40
Temp.	^oC	25.20	15.80	21.07	20.72	4.06	-0.51	-1.87	26.20	23.20	25.03	25.01	1.10	-0.87	2.37
pH		2.88	1.54	2.30	2.26	0.48	-0.64	-0.11	4.05	1.78	2.50	2.47	0.41	0.78	1.26
Eh	mV	96.40	27.40	67.13	61.15	27.53	-0.77	-1.36	112.80	85.60	97.30	96.95	9.22	0.56	-0.93
Acidity	mg/lCaCO3	21498.90	16842.49	18812.04	18752.46	1658.67	0.70	0.27	19265.42	14231.43	16315.63	16222.17	1934.61	0.01	0.88
TDS	mg/l	18603.30	13771.60	17118.97	17007.54	2065.49	-1.17	-0.52	19642.90	11843.70	15713.47	15529.67	2603.79	-0.01	0.40
EC	uS/cm	22645.20	16489.60	19953.73	19842.10	2273.62	-0.51	-0.69	20843.10	12690.20	18852.98	18678.27	2786.84	0.64	-0.13
SO42-	mg/l	12647.87	9067.84	11046.56	10960.29	1476.81	-0.67	-1.66	13414.29	7256.18	9909.75	9710.73	2213.35	0.70	-0.33
Cl	mg/l	1237.04	548.77	867.53	838.07	246.86	0.33	-0.51	1107.82	653.28	837.39	823.75	169.01	0.77	0.06
NO_3^-	mg/l	287.26	107.59	207.09	196.85	67.76	-0.19	-0.77	265.88	148.66	198.56	195.02	41.98	-0.33	0.26
Fe	mg/l	6805.76	4065.87	5841.77	5738.28	1143.32	-0.96	-0.94	6784.92	3478.45	5243.67	5133.10	1139.68	-1.26	1.32
Mn	mg/l	103.46	78.98	93.14	92.74	9.33	-0.38	-0.71	104.77	67.54	91.38	90.45	13.55	-0.40	-1.24
Al	mg/l	161.43	102.76	135.07	133.14	24.36	-0.48	-1.76	160.25	96.98	132.38	130.48	23.99	-0.33	0.08
Ni	mg/l	2.41	0.76	1.37	1.26	0.64	1.04	-0.23	2.31	0.84	1.63	1.55	0.51	-0.42	-1.73
Cu	mg/l	0.46	0.08	0.27	0.23	0.13	-0.02	-0.23	0.45	0.26	0.36	0.35	0.08	0.07	-2.65
Zn	mg/l	3.89	1.78	2.79	2.65	0.97	-0.02	-2.82	3.23	1.87	2.57	2.51	0.61	-1.09	2.78
Ca	mg/l	2.54	0.33	1.30	1.04	0.87	0.50	-1.42	2.56	1.18	1.99	1.94	0.45	0.77	2.36

Fig.6.4: Box plots of Pollutants Concentration in stream water for Dry & Wet Season

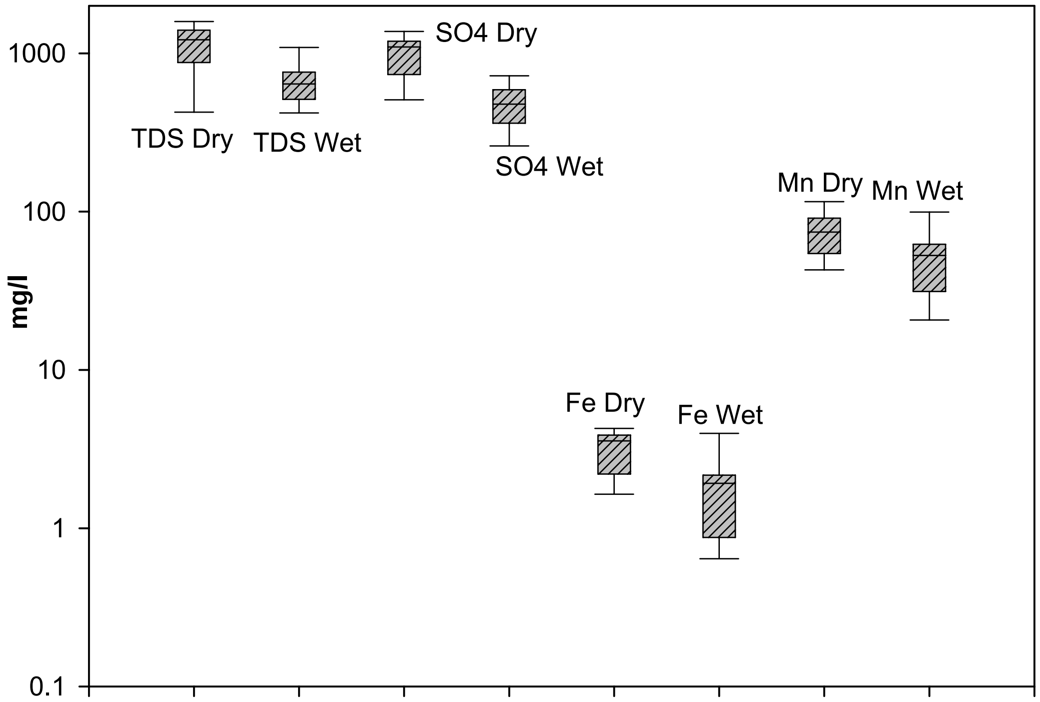

6.3.2 Effects of Dry and Wet Cycles on the Evolution of AMD

a) pH and Trace metal Fluctuations

The range of pH fluctuation throughout the year for various drainage waters at Iron Duke is best illustrated by the box plot in Figure 6.5. As expected, neutral treated sludge and surface water along Yellow Jacket River, upstream of mine site, have the least range (difference between minimum & maximum pH) throughout the year. In contrast, the pH in the evaporation ponds after sludge disposal shows a wide range, with minimum non outlier pH values around 3.0 observed in the drier months of the year. The same applies to ground water from the contaminated shallow aquifer, which shows an outlier minimum pH of 1.1 recorded in October (the hottest and driest month just before the rain season starts in November). Drainage from the jig tails dump is most acidic as well during the drier months, but the flow is only a trickle, greatly reducing pollution impacts. Surface water at the seepage point is greatly influenced by recharge along the Yellow Jacket River and mixing with fresh streams due to rainfall in the wet season resulting in a wide range between the 25 & 75% quartiles. Non outlier maximum pH is also high at 5.5 in the wet season, compared to 2.7 in the drier months.

Fig.6.5: Summary Statistics of Drainage pH

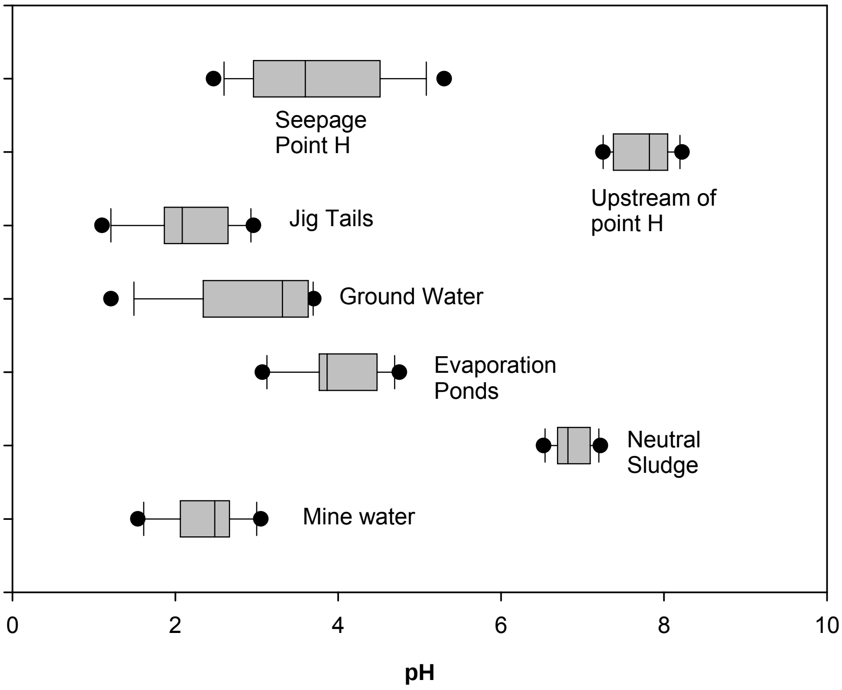

b) Contaminant Fluxes and Flushing Model

The release of acidity from the jig plant tailings is controlled to varying degrees by the dry and wet cycle changes throughout the year. It has been observed that:

i) During the dry spells, base flow conditions develop, a small proportion of the reactive surfaces are leached which allows oxidation products to build up in some sections of the dump. During this period, drainage flow decreases markedly, sometimes even drying up completely. However, intermediate oxidation products (sulphate and hydroxysulphate minerals) accumulate in the dump as oxidation proceeds. Based on the mineralogy, the intermediate products may include melanterite – $Fe^{II}SO_4.7H_2O$; jarosite – $NaFe_3(SO_4)_2.(OH)_6$ or $KFe_3(SO_4)_2.(OH)_6$; Coquimbite – $Fe^{III}_2(SO_4)_3.9H_2O$; alunite – $KAl_3(SO_4)_2.(OH)_6$ and Jurbanite – $AlSO_4OH.5H_2O$.

ii) When rainfall first comes, infiltration into the dump occurs, resulting in leaching and rinsing of more reactive surface areas. The accumulated secondary products are dissolved and mobilised, resulting in a highly potent 'first flush' of concentrated contaminant load in the jig tailings drainage water, equation (6.1).

$$KAl_3(SO_4)_2(OH)_6 + 3H_2O \Leftrightarrow K^+ + Al^{3+} + 2SO_4{}^{2-} + 6OH^- + 3H_2O \Leftrightarrow 3Al(OH)_3 + K^+ + 2SO_4{}^{2-} + 3H^+ \tag{6.1}$$

iii) As wet conditions persist, the high initial acidity and metal concentrations of the first flush decay, leading to reduced pollutant loadings and diluted drainage flow. The most abundant dissolved components in mine water and tailings drainage at Iron Duke are sulphate and iron. Figure 6.6 shows the decay of iron concentrations in the jig tailings drainage following a series of rainfall events between November 2004 and February 2005. The dotted line is the predicted non – linear exponential decay for the iron concentration (contaminant load, Y) in mg/l and is given by:

$$Y = [Fe] = 1906.5e^{-0.0708t} \tag{6.2}$$

and t = x is the time taken for exponential decay flushing in days.

Fig.6.6: Contaminant loading in jig tails drainage following rainfall events

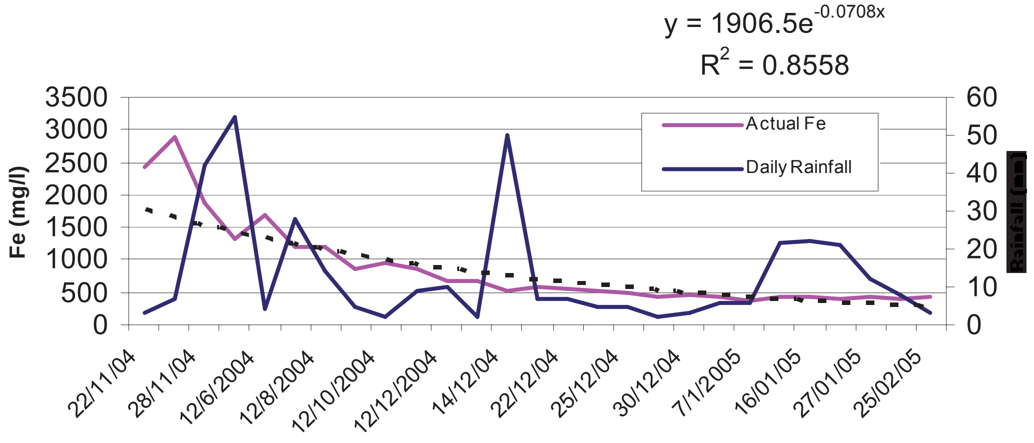

iv) When dry conditions are re-established, contaminant loads are generally lower than wet conditions due to reduced flow. However, Fe concentrations begin to increase again, but with trickle flow, reaching a steady peak around 1100mg/l during the cool and hot dry months from May to October, Figure 6.7. There is a sudden jump in concentration when rainfall starts again in November, and the rise in Fe concentration reaches a level around 1800mg/l, somewhat lower than the level witnessed at the onset of rainfall in the previous season. With increased rainfall, concentration falls exponentially, and the cycle is repeated.

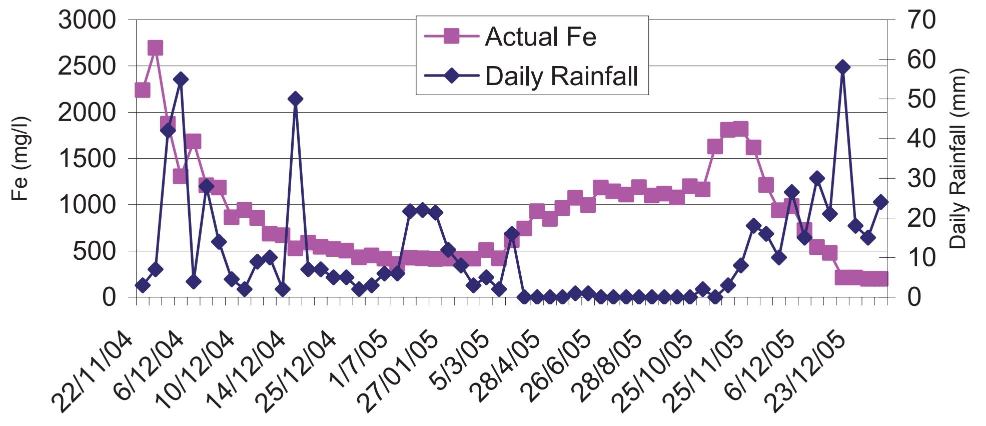
Fig.6.7 Seasonal variation in Iron Concentration

v) The cycle in Fe concentration fluxes is indicative of the flushing out of accumulated oxidation products from the tailings dump with rainfall water. The steady state trend observed from May to October possibly reflects ongoing acidity production due to pyrite oxidation. Some comparisons can be drawn between this scenario and that found out by other researchers. Younger *et al.,* (2002) studied the evolution of contaminant loading from Wheal Jane tin mine in Cornwall, UK, following its overflow in 1992. They found that acidity seemed to follow a quasi exponential decay curve and the flushing time can be related to the time taken for the mine to fill with mine water following cessation of pumping. This means that the rate of decay is related to the floodable mine volume.

vi) Each time it rains, drainage flow increases proportionally. Although surface runoff is influenced by rainfall, Fe concentrations in the drainage water are proportional to the flush volume which depends on porosity and permeability of the tailings among other factors like held up oxidation products. For unconsolidated materials, porosity and permeability depend on packing of grains, grain shape and the variation in grain size. Porosity is a measure of the water bearing capacity and is part of the tailings capability to hold water. It depends primarily on the degree of compaction, the state of solution and existence of channelling in the dump. Permeability is the ease with which fluids pass through a porous media and is reflected by the hydraulic conductivity, K, given by Darcy's Law (equation 6.3):

$$q = \frac{Q}{A} = -K\frac{\Delta h}{\Delta l} = -\left(k\frac{\rho g}{\mu}\right)\frac{\Delta h}{\Delta l} \qquad (6.3)$$

Q is the rate of fluid discharge through an area A, and q is the flux proportional to the hydraulic gradient ($\Delta h/\Delta l$), k is the permeability, ρ is fluid density, μ is fluid viscosity and g gravitational force factor.

Based on contaminant loading data from Wheal Jane tin mine, following its overflow in 1992, Younger *et al.*, (2002), found out that rising mine water levels dissolved and mobilised accumulated secondary products and acidic pore waters resulting in a highly potent 'first flush' of concentrated mine water. With time, the high initial acidity and metal concentrations of the first flush are expected to decay exponentially towards a steady state contaminant loading that reflects ongoing pyrite weathering.

vii) The flushing model is characterised by an abrupt increase in concentration of contaminants near the zone of pollution input between Points C and E, then continuous and smoothly decreases downstream.

6.4 Mechanisms of Metal Attenuation

The principal objectives in treating AMD at Iron Duke are to neutralize free acidity and reduce the concentrations of Fe, Al, Mn and sulphate to very low levels so that the effluent quality is acceptable for recycle or release. The active chemical treatment of acidic drainage is typically accomplished using lime to raise the pH of the acidic stream and remove dissolved metals through precipitation and co-precipitation. These processes result in the formation of a gypsum/metal and/or hydroxide/carbonate sludge which requires disposal in evaporation ponds.

Concentrations of metals in mine site drainage are typically created by the dissolution of minerals into that drainage. According to principles of geochemistry, there are two endpoint controls on aqueous concentrations in waters draining from mine sites, namely kinetic and equilibrium processes. Kinetic controlled concentrations fluctuate with time and are dependent on physical factors such as flow rates and dilution. If the drainage remains in contact with minerals long enough such as happens with stagnant drainage, equilibrium may eventually be reached. In contrast, equilibrium controlled concentrations are often more stable and do not change with time. Aqueous concentrations are independent of the amount of water and mineral, and if drainage moves into contact with other minerals, equilibrium will change, resulting in either new equilibrium or kinetic conditions.

The overall picture for the mobilisation, dispersion and attenuation of AMD pollutants at Iron Duke can be summarised as in Figure 6.8. About 3t/day of acid are neutralised and deposited as sludge in the evaporation ponds. Acid and metal fluxes have been monitored through the flow pattern and the attenuation takes place through four major stages as depicted in the diagram. The mechanisms of metal attenuation are discussed in the sections that follow.

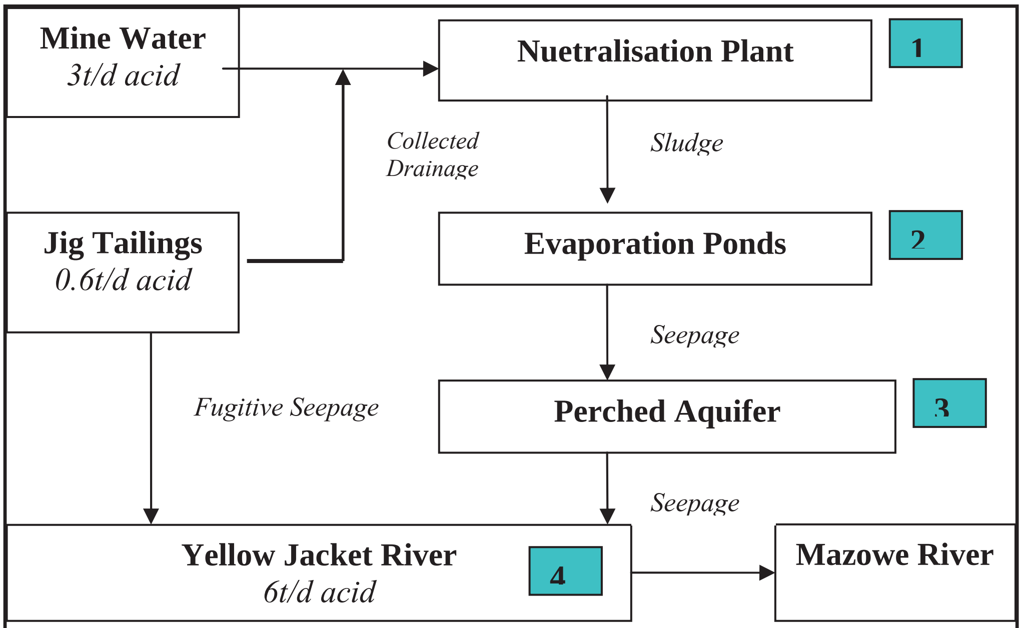

Fig.6.8: Schematic overview of drainage flow pattern at Iron Duke

6.4.1 Stage 1: Equilibrium Controls on Acid Neutralisation with Lime

The most common by – product of lime neutralisation is gypsum, which is precipitated when the acid mine water comes into contact with the added lime according to equation 6.4.

$$Ca(OH)_2 + H_2SO_4 \Rightarrow CaSO_4.2H_2O = Ca^{2+} + SO_4{}^{2-} + 2H_2O \qquad (6.4)$$

This reaction is responsible for scale formation and excessively large volumes of sludge observed in the treatment plant. It is presumed that the large amount of sulphate in the feed water (~9700 mg/l) most likely pushes the solubility product well above saturation. The approximate concentrations of Ca and SO_4^{2-} that may be expected upon gypsum saturation can be estimated from the Law of Mass action and hydrochemical data tables (Appelo and Postma, 1996), for reaction 6.5, where K_{eq} is $10^{-4.58}$ at 25°C.

$$K_{eq} = \frac{(Ca^{2+}).(SO_4{}^{2-}).(H_2O)^2}{(CaSO_4.2H_2O)} = (Ca^{2+}).(SO_4{}^{2-}) = 10^{-4.58} \frac{mol^2}{dm^6} \qquad (6.5)$$

Thus, as (Ca^{2+}) = ($SO_4{}^{2-}$), the activity of both Ca and sulphate must be $10^{-2.29}$ mol/dm^3 for dissolution of gypsum at 25°C. Assuming that the activities of Ca and sulphate approximate to concentrations, and that Ca weighs 40 080 mg/mol & sulphate weighs 96064 mg/mol, gives Ca = 206 mg/l and sulphate = 493 mg/l upon gypsum saturation. Hence a sulphate concentration above 9700 mg/l in the feed water to the neutralisation plant will precipitate a lot of gypsum. The Saturation Index, (SI) is defined as the logarithm to base 10 of the ratio of the product of the activities of the relevant ions to the K_{eq}.

$$SI = \log\left(\frac{(Ca^{2+}).(SO_4{}^{2-})}{K_{eq}}\right) \qquad (6.6)$$

If SI = 0, equilibrium exists; SI < 0, the solution is under saturated with respect to gypsum and gypsum will dissolve; and when SI > 0, the solution is oversaturated and gypsum will precipitate. The major components in mine water before and after treatment by the normal plant configuration are presented in Table 6.2. The SI of gypsum for treated water is 1.66, suggesting that it will tend to precipitate even after deposition. However, this is not the case as explained below.

Table 6.2: Chemical composition of mine water before and after lime treatment

Parameter	Feed ± Standard Deviation	Treated	Treatment Efficiency (%)	Target
pH	2.84 ± 0.48	6.75	$100_{\text{temporary}}$	6.5 – 7.0
Eh (mV)	67.13 ± 27.53	207	-	-
Acidity (mg/l $CaCO_3$)	17 538.42 ± 658.67	370.16	$97.89_{\text{temporary}}$	< 50
Sulphate (mg/l)	9705.77 ± 1476.81	3108.53	67.97	< 500
Iron (mg/l)	5379.18 ± 1143.32	3564.96	33.73	< 10
Aluminium (mg/l	146.03 ± 24.36	33.08	77.35	< 5
Manganese (mg/l)	96.52 ± 9.33	74.18	23.15	< 5
Calcium (mg/l)	1.30 ± 0.87	1486.75	-	-

Although titrated acidity is greatly reduced (97.89%) by neutralisation, it has been observed that the pH of treated sludge shifts markedly from within the target range of 6.5 – 7.0 to less than 3.0 in the evaporation ponds just after 2 days deposition. Except for aluminium, the removal of iron and manganese is not efficient and way off target. One possible explanation for this is that while the influent to the evaporation ponds is a weak acid semi neutral sludge, what evaporates is pure water. This means that acid and metal concentrations rise as a function of time. The ponds have reached supersaturation with respect to jarosite and other iron hydroxides which form a thick yellowish to brown red sludge at the bottom of the pond. The pH of the ponds has dropped to around 3.0 and acid is seeping to the ground water down gradient of the ponds area.

6.4.2 Stage 2: pH - E_h Controls on Metal Precipitation and Hydrolysis in the Evaporation Ponds

Precipitation and Co-Precipitation of Hydroxides and Oxy-hdroxides of Fe, Al and Mn

When the mine water is pumped to the neutralisation plant, increased access to oxygen and increase in pH on mixing with lime causes oxidation, hydrolysis and precipitation of metal oxy-hydroxides. Ferrous iron oxidises and precipitates as an orange ferric oxy-hydroxide (ochre) as depicted in equations 6.7 and 6.8.

$$4Fe^{2+}+O_2+4H^+ \Leftrightarrow 4Fe^{3+}+2H_2O \qquad (6.7)$$

$$Fe^{3+}+3H_2O \Leftrightarrow 3H^+ + Fe(OH)_3 \qquad (6.8)$$

The overall ochre precipitation reaction is proton generating and this may further explain why the evaporation ponds have become ‘acid generators’, and hence pH of neutral sludge does not remain stable after deposition. However, the reaction may become potentially self limiting in that generation of protons may lower the pH to a point where ferric ions no longer precipitate as hydroxide unless adequate neutralization capacity (alkalinity) is present in the pond.

More than a dozen compounds fit within the designations of iron oxides, hydroxides, and oxyhydroxides (Schwertmann and Cornell, 1991). Some of the most common are ferrihydrite [$Fe_5O_7(OH)_nH_2O$], goethite (α-FeOOH), lepidocrocite (γ-FeOOH), hematite (α-Fe_2O_3), and amorphous ferric hydroxide $Fe(OH)_3$. The bottom of the ponds is characterised by reddish brown and brownish yellow (orange) sediments (precipitates) suggesting domination of the composition by ferrihydrite and schwertmannite, respectively. This is supported by the evidence of other researchers (Webster *et al.,* 1998; Carlson *et al.,* 2002; Kim & Chon, 2002) who performed XRD analysis on precipitates from similar samples and found out that the two minerals commonly precipitate from acid sulphate rich waters. A chemical analysis by XRF was performed on the ponds sediments to check the composition of major oxides. Table 6.3 shows that the reddish brown precipitate consists approximately of 68 – 77% Fe, and 7.8 – 9.5% CaO, with small amounts of 0.8 – 1.7% MnO_2, 2.5 – 3.6% Al_2O_3, and 0.9 – 1.4% SiO_2. The balance (LOI – Loss on Ignition) is probably mostly chemisorbed water. The brownish yellow precipitate exhibited Fe:S ratios from 4.72 – 6.31 (deduced from sulphate content by the barium chloride precipitation and gravimetric method). Although Fe:S ratio for the ideal schwertmannite [$Fe_8O_8(OH)_6SO_4$] is 8, the lower values are usually found and are attributed to adsorption of excess sulphate on the schweertmannite surface, (Ghiorse and Ehrlich, 1992; Schwertmann *et al.,* 1995).

Additional minerals form when the sludge comes into contact with acidic/sulphate water in the evaporation ponds. Bigham *et al.,* (1994), reported that such minerals may include jarosites [$(H,K,Na)Fe_3(OH)_6(SO_4)_2$], melanterite [$Fe(SO_4)7H_2O$] and ferric sulfate [$Fe_2(SO_4)_3$]. These minerals differ in important characteristics, including degree of crystallinity, solubility, and thermodynamic stability. Amorphous ferric hydroxide exhibits no long range order (and thus no X-ray diffraction pattern with conventional methods), and appears to be the most common initial solid formed when iron(III) precipitates. With time and loss of water, amorphous solids tend to convert to the crystalline forms of goethite and/or to hematite (Schwertmann and Cornell, 1991). These minerals are important because of their common occurrence in mine waste environments and demonstrated ability to adsorb or form co-precipitates with organic compounds and ions of a wide variety of elements (Jambor, 1994; Jambor and Dutrizac, 1998).

Table 6.3: Chemical Composition of Evaporation Ponds Precipitates by XRF

Sample ID	**Fe_2O_3**	**CaO**	**Al_2O_3**	**MnO_2**	**SiO_2**	**P_2O_5**	**LOI**
RB - 1	67.84	7.81	3.58	0.76	0.88	0.06	17.14
RB - 2	75.53	9.47	2.50	1.24	1.37	0.08	15.82
RB - 3	76.92	8.05	3.27	1.65	1.04	0.11	16.07
BY - 1	48.26	9.37	4.06	1.14	0.82	0.31	28.11
BY - 2	58.19	12.18	3.25	0.96	1.26	0.18	33.29
BY - 3	52.06	10.94	2.93	1.42	1.19	0.07	27.95
RB – reddish brown (ferrihydrite); BY – brown yellowish (schwertmannite)							

Iron(III) usually has an ionic radius of 0.063 nm in octahedral coordination. Because both Al(III) and Mn(III) are of similar size (0.053 and 0.065 nm, respectively), they may substitute for Fe(III) with little to moderate distortion. Mn(II) on the other hand, has an ionic radius of 0.082 nm (Schwertmann and Cornell, 1991). The authors suggested that Al for Fe substitution should introduce considerable strain into the lattice structure due to shorter bond lengths with oxygen and result in the inclusion of additional hydroxyl ions.

Since the efficiency of technology would be limited by the effective solubility of iron as solution moves through the treatment system, an understanding of iron solubility fundamentals is important. Ferric iron is quite insoluble compared to ferrous iron. The K_{sp} for ferrous hydroxide is 4.87×10^{-17}, while the K_{sp} for ferrihydrite is 2.64×10^{-39} (CRC Handbook of Chemistry and Physics, 71st Edition) and the K_{sp} for amorphous ferric hydroxide is often taken to be 10^{-38}. While there is some dispute among researchers as to the precise K_{sp} for each of the oxy-hydroxide forms of Fe(III), there is no disagreement that ferric oxy-hydroxides are extremely insoluble, with minerals of increasing crystallinity being more insoluble.

The hydrolysis of ferric iron in the presence of sulphate is strongly influenced by pH. Figure 6.12 shows how pH controls the solubility of ferric aluminium hydroxide species in water. Appelo and Postma (1996) suggest a value for $K_{eq} = 10^4 = [Fe^{3+}]/[H^+]$. Thus for systems in equilibrium with $Fe(OH)_3$:

$$\mathrm{Log}[Fe^{3+}] = 4 + 3\log[H^+] \qquad (6.9)$$

$$\mathrm{Log}[Fe^{3+}] = 4 - 3pH \qquad (6.10)$$

Equation 6.10 approximates to the line marked Fe^{3+} in Figure 6.9. At pH = 6, $[Fe^{3+}] = 10^{-14}$ mol/dm^3, when pH = 2, $[Fe^{3+}] = 10^{-2}$ mol/dm^3, which explains the very low solubility of ferric iron at high pH and appreciable solubility at very low pH. At pH values more than 8, the solubility increases as a result of complexation with the OH ligand. In a similar way dissolved aluminium precipitates as a white to yellowish hydroxide commonly observed along the seepage zone C to E along Yellow Jacket River.

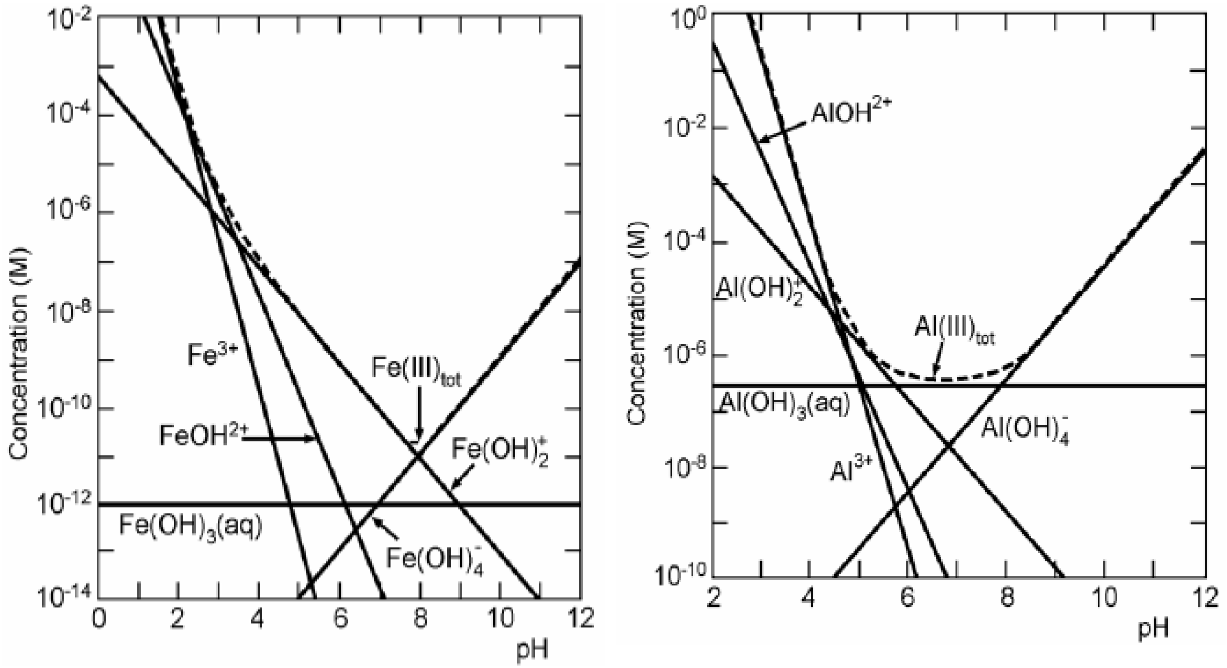

Fig. 6.9: pH dependence of ferric & aluminium hydroxide species in water. Dashed lines represent total element solubility (after Stumm & Morgan, 1996, and Younger *et al.,* 2002)

Redox and Stability of Iron Phases

The redox potential describes the reduction – oxidation state of a solution and controls the oxidation state of elements that can exist in several oxidation states, hence element mobility. Some metals are more mobile in one oxidation state than the other. The lower the value, the more reducing the solution, and the higher the value, the more oxidizing the solution. The Eh for the mine water before treatment is very low averaging 67.13 mV but rising to 207 mV after lime treatment. The stable phases for a combination of Fe – S – C – H_2O species in solution under a variety of Eh – pH values at temperature 25°C, is shown in Figure 6.10, together with that of manganese superimposed (modified after Appelo and Postma, 1996).

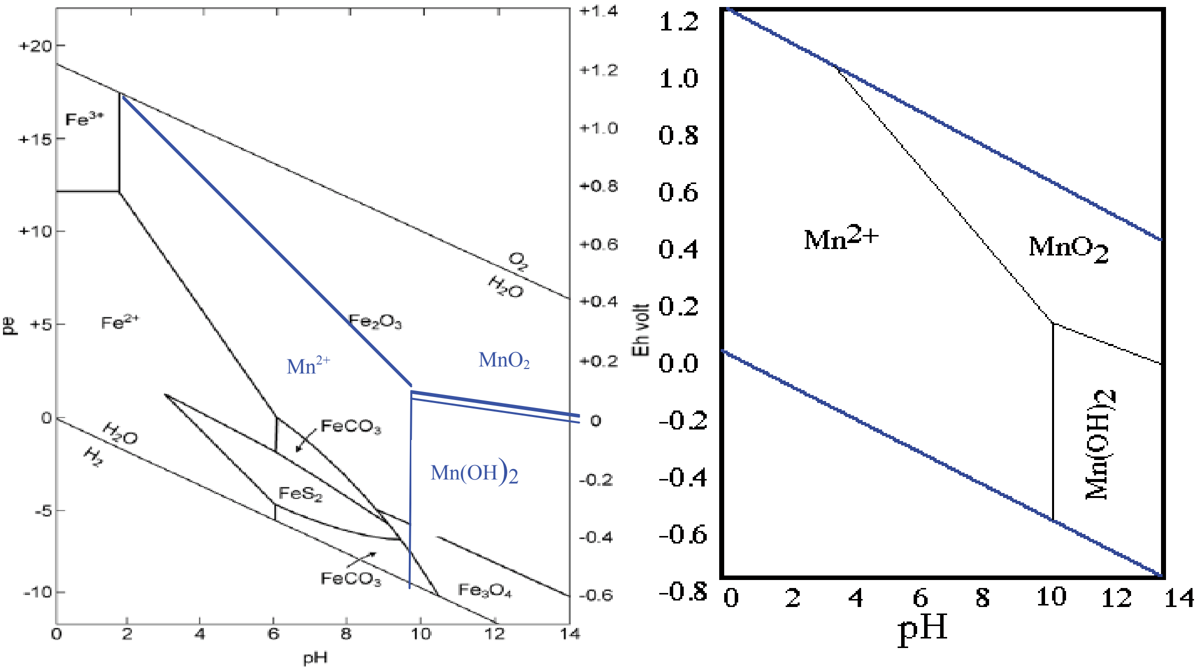

Fig. 6.10 Eh – pH diagram for iron and manganese systems

The figure shows the following:

- That pyrite is stable in circum – neutral, reducing conditions, i.e. the subsurface of the geosphere.
- By increasing Eh and thus moving vertically from the pyrite field, we see that pyrite becomes unstable and gives way to siderite or ferric oxyhdroxide domains. As a result, in acidic mildly reducing conditions in the untreated mine water ferrous ions are the most stable, while ferric ions become more stable in strongly acidic and oxidizing conditions in the evaporation ponds.
- $Mn(OH)_2$ is precipitated at very high pH >9.5 under reducing conditions and this explains the very low removal efficiency (23.15%) observed for manganese during treatment.

The implications of these deductions on the technology of AMD control at Iron Duke are as follows:

i) Aeration – Oxidation

Ferrous hydroxides (Fe^{2+}) precipitate at a much higher pH, and are not as stable as ferric hydroxides when the sludge is exposed to acidic waters. This implies more lime consumption and higher operating costs. As a result, aeration should be applied to oxidize the iron to the stable form according to equation 6.11.

$$Fe(OH)_2 + \frac{1}{2}H_2O + \frac{1}{4}O_2 \Rightarrow Fe(OH)_3 \qquad (6.11)$$

Other observed problems with ferrous hydroxides are that they do not settle as well as ferric hydroxides and they can create a highly viscous sludge. There are three major advantages for proper oxidation of iron, namely: sludge stability, better treatment efficiency and sludge viscosity. Therefore, it appears that the inclusion of an aeration step in the lime neutralization circuit will be advantageous.

ii) Formation of calcite (Calcium Carbonate)

Calcium carbonate is also a common by product of lime neutralization, reaction 6.12.

$$Ca^{2+} + CO_3^{\ 2-} \Rightarrow CaCO_3 \qquad (6.12)$$

The inorganic carbon for this reaction comes from the AMD itself or the carbon dioxide in air, which is dissolved during agitation. This carbon dioxide converts to bicarbonate and then partially to carbonate at high pH (Figure 6.11), and the carbonate fraction will precipitate with the high calcium content of the slurry to form calcite. This calcite can play an important role in the stability of the final sludge product as it provides neutralizing potential to the sludge when deposited in the evaporation ponds.

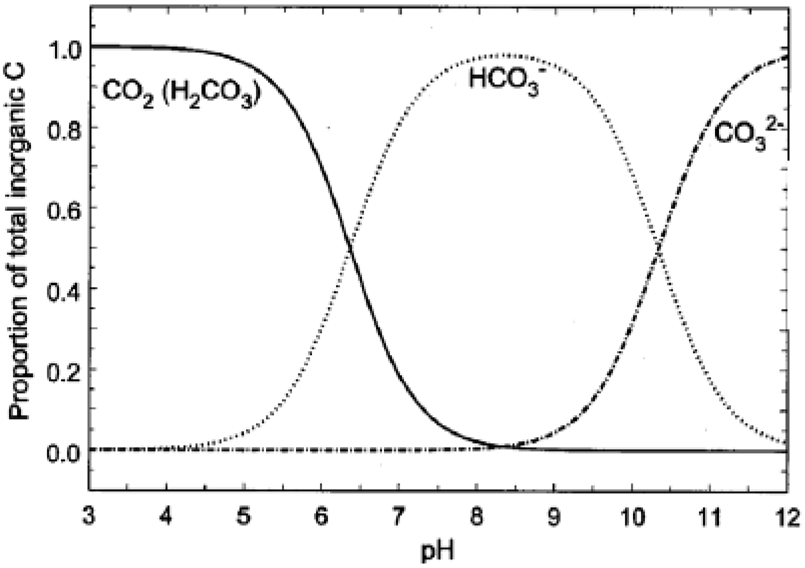

Fig.6.11: Inorganic Carbon Equilibrium (after Langmuir, 1997)

As shown in Figure 6.11, the carbonate species (CO_3^{2-}) is only prevalent at pH values more than approximately 10.3 and is practically non existent at pH values less than 8.5. Therefore, calcite precipitation at pH values below 8.5 is not expected unless the total inorganic carbon concentration is very high. The implication is that the treatment pH target range of 6.5 – 7.0 is too low for the low density sludge process and at least 8.5 should be the target if also manganese and aluminium are to be precipitated.

6.4.3 Stage 3: Adsorption and Ion Exchange in the Shallow Aquifer

The water chemistry of the shallow aquifer located on the down gradient of the evaporation ponds was monitored on a monthly basis from May 2004 to April 2005, and the summary statistics are presented in Table 6.4. The ground water is heavily impacted by acidic seepage from the ponds and show low pH (1.21 – 3.70), high levels of iron (265.11 - 406.71) mg/l, Mn (149.23 – 245.03) mg/l, Al (0.46 – 3.56) mg/l, sulphate 1301.30 – 2007.74 mg/l and considerable amounts of Ni, Zn and Cu. Iron values are negatively skewed, while Ni values are positively skewed, suggesting poor distribution around the mean for these elements.

Table 6.4: Summary Statistics of Ground Water Composition in the polluted aquifer

Count = 12		Max	Min	Mean	Median	Geomean	Sta.Dev	Skewness	Kurtosis
Well Depth	m	6.56	2.25	4.47	4.47	4.23	1.46	-0.05	-0.83
Temperature	^{o}C	24.10	22.30	22.95	22.65	22.94	0.65	0.62	-1.28
pH		3.70	1.21	2.86	2.95	2.74	0.77	-0.77	0.11
Eh	mV	243.00	221.00	235.48	236.90	235.41	6.14	-1.16	1.58
Acidity	mg/lCaCO3	4324.06	603.45	1179.43	820.47	983.62	1026.32	3.07	9.90
Alkalinity	mg/lHCO3	0.00	0.00	0.00	0.00	#NUM!	0.00	#DIV/0!	#DIV/0!
DO	mg/l	5.74	3.82	4.67	4.68	4.64	0.56	0.35	-0.20
TDS	mg/l	8338.00	2765.20	5076.62	4761.15	4765.55	1878.39	0.49	-1.03
EC	uS/cm	10043.20	4128.60	6764.56	6862.10	6471.99	2079.78	0.33	-1.10
SO_4^{2-}	mg/l	2007.74	1301.30	1702.89	1689.69	1693.56	182.50	-0.39	1.56
NO_3^-	mg/l	98.33	42.04	56.28	48.87	54.43	16.80	1.80	2.85
Cl^-	mg/l	308.42	122.89	218.50	216.81	205.69	75.78	-0.06	-1.95
Fe	mg/l	406.71	265.11	368.67	381.84	366.08	42.66	-1.80	2.62
Mn	mg/l	245.03	149.23	193.44	193.37	191.18	31.03	0.24	-1.19
Al	mg/l	3.56	0.46	1.57	1.19	1.35	0.90	0.96	0.58
Ni	mg/l	3.41	0.87	1.58	1.16	1.41	0.87	1.53	1.19
Cu	mg/l	0.53	0.31	0.41	0.41	0.41	0.06	0.38	-0.15
Zn	mg/l	2.04	1.06	1.40	1.23	1.36	0.35	0.74	-1.01
Ca	mg/l	268.44	178.93	236.97	248.63	235.00	30.51	-1.12	0.07
Mg	mg/l	42.65	14.04	27.30	26.27	26.22	8.02	0.56	0.30
K	mg/l	8.76	3.05	6.33	6.40	6.13	1.51	-0.61	0.93
Na	mg/l	35.21	16.18	26.22	27.94	25.64	5.42	-0.58	0.08

The migration of contaminants through the aquifer (vadose zone) takes place through advection, mechanical dispersion and molecular diffusion. These mechanisms take place on the dissolved and suspended contaminants in response to gravity flow, pressure and density difference, and chemical kinetic activity over a concentration gradient as the water containing contaminants flows around the solids in the aquifer media. The fate of contaminants in the vadose zone is such that their transport or mobility may be retarded and attenuation may take place yielding lower concentrations in the liquid/mobile phase. This is due to processes such as adsorption and ion exchange, where ions are transferred from water to the soil. Heavy metals are adsorbed to the soil particles by either cation exchange or chemisorption. Saether, *et al.,* (1997) reported that dispersion of contaminants into soil and groundwater at a former industrial site in Norway was mostly controlled by strong bonding between the contaminants and the aquifer soil matrix. Patrick and Verloo (1998) reported that heavy metals are adsorbed to the clay and organic matter by electrostatic attraction and will remain attached as metal atoms. Their speciation may change as aquifer geochemical conditions such as pH & Eh change, (Groudev *et al.,* 1999; Weibner *et al.,* 2005).

Clay mineralogy influences attenuation capacity as the mass of metal which can be electrostatically bound to a unit mass of clay increases with specific surface area, (Young *et al.,* 1996). Additional compositional control on attenuation of metals in the aquifer is exerted by secondary minerals such as metal oxides and hydroxides. Both Mn and Fe oxides, hydroxides and oxy-hydroxides are well known to precipitate from mine drainage waters and to have high levels of substitution of heavy metal cations for other metal ions within their respective crystal lattices, (Gong and Donahoe, 1997; Lin and Herbert, 1997). The ‘contaminant front’ has reached breakthrough point, and leakage of metal laden seepage into the Yellow Jacket River is testimony that the sorption capacity of the shallow aquifer is now exceeded with respect to some of the contaminants.

6.4.4 Stage 4: Dilution and Immobilisation in the Yellow Jacket River

The Yellow Jacket River is the principal pathway of AMD related pollutants at Iron Duke. The river receives direct seepage from the contaminated perched aquifer and also fugitive seepage from the jig tailings dump. River waters at the seepage point exhibit elevated levels of several contaminants and trace metals (Al, Cu, Ni, Mn, and Zn) in comparison with background values, Table 6.5.

Table 6.5: Surface water concentrations (mg/l) of dissolved and particulate trace metals for the dry (August 2004) and wet season (February 2005) along Yellow Jacket River

	***Background**		**Dry Season**		**Wet Season**	
	Total	Dissolved	Total	Dissolved	Total	Dissolved
Al	0.12	0.07	12.85	12.34	10.82	9.30
Mn	4.36	2.89	127.06	115.67	164.17	124.08
Fe	1.05	0.67	5.16	2.66	7.42	3.97
Cu	0.02	0.01	0.22	0.13	0.35	0.23
Ni	0.18	0.06	1.58	1.44	0.95	0.43
Zn	0.03	0.02	3.17	1.03	1.83	0.34

* Upstream of mining influence on the Mazowe River

In the dry season, Al, Mn, Cu and Ni were primarily present as dissolved species (< 45 µm), while Fe and Zn were largely hosted in particulate phases. Increased river flow caused by rainfall in the wet season results in erosion of weathered minerals around the mine site leading to increased concentrations of both particulate and dissolved metals in the river. This explains the high levels of Mn (164.17 mg/l) and Fe (7.42 mg/l) observed during the wet season, and it results in greater loadings of metals to the Mazowe River sub-catchment. The high particulate Fe concentrations during the wet season suggest that trace metal associations with Fe oxy-hydroxides may be significant.

Rapid attenuation of acidic drainage input is demonstrated by the changing aqueous concentrations of metals and sulphate along a 110 m stretch starting 25 m before the seepage zone continuing downstream as shown in Figure 6.12. In general all metal concentrations rise above background values as the river passes through the mine site, reaching a peak and then decrease rapidly after the seepage zone. Concentrations decrease more or less to background levels just before the confluence with Mazowe River mostly due to dilution. The pattern of changing concentrations of dissolved sulphate parallels that of the metals and can be explained by the formation of Al, Fe, or Mn oxy-hydroxides and scavenging of sulphate and trace metals from water to these minerals. Alternatively, sulphate can also be removed through the formation of Fe & Al hydroxyl-sulphate precipitates, (Ali and Dzombak, 1996; Munk *et al.,* 2002).

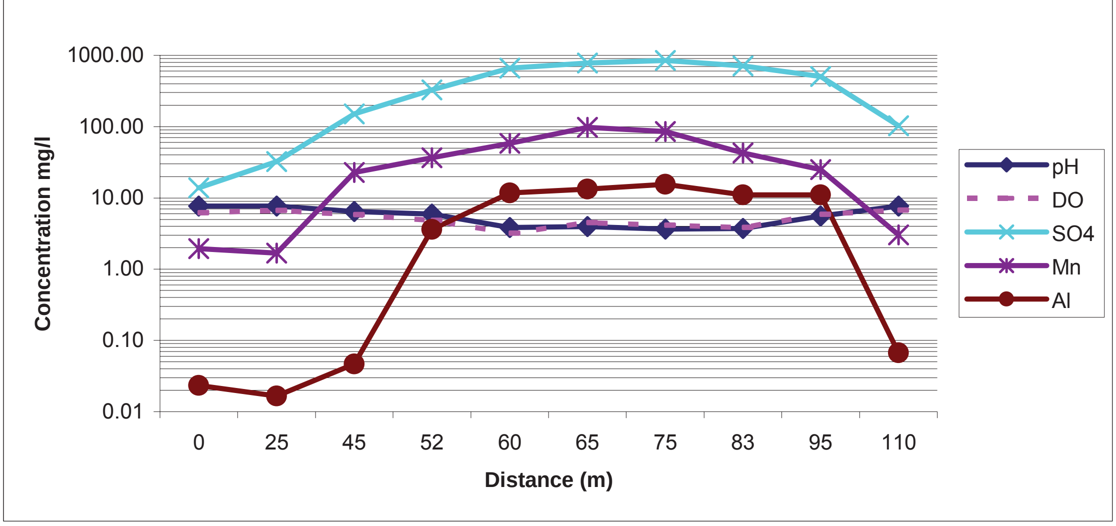

Fig.6.12 Pollutant Profile along Yellow Jacket River

Sorption is possibly the most important mechanism that can explain the observed changes in metal concentration along Yellow Jacket River. Sorption is a chemical reaction in which metals are transferred between stream water and the surfaces of streambed materials, such as sediments, rocks and aquatic plants. During desorption, metals are detached from streambed materials and added to stream water, thereby increasing dissolved metal concentrations in stream water. During adsorption, metals are transferred from stream water to streambed material, thereby decreasing metal concentrations.

Sorption of a specific metal is affected by its charge, temperature and pH of stream water. Water temperature and pH commonly increase in streams during the day and decrease during the night in response to the daily cycles of daylight and darkness. Negatively charged ions may desorb while positively charged ions are adsorbed under the same conditions of temperature and pH, (Nimick *et al.,* 2003). These changes are key factors in determining the amount of each metal that is adsorbed or desorbed.

Adsorption mechanisms are generally categorized as either physical adsorption, chemisorption, or electrostatic adsorption. Weak molecular forces, such as Van der Waals forces, provide the driving force for physical adsorption, while a chemical reaction forms a chemical bond between the compound and the surface of the solid in chemisorption. Electrostatic adsorption involves the adsorption of ions through coulombic forces, and is normally referred to as ion exchange.

6.4.5 Dispersion of Heavy Metals in Stream Sediments

The concentrations of Fe, Mn, Al, Cu, Ni and Zn in the stream sediments of Yellow Jacket River exhibit high enrichment along 110 m downstream of the seepage point in comparison to background values. This means that the sediments are serving as a diffusive sink for the dissolved metals. These metals are most likely fixed as authigenic sulphide minerals as evidenced by the smell of rotten eggs characteristic of hydrogen sulphide. Figure 6.13 shows that Fe, Mn and Zn exhibit maximum concentrations further away from the contamination point. Conversely, Cu, Ni and Al show higher levels near the contamination point. The contrasting behaviour of these elements suggests that their distributions may be governed by different controls.

A number of physical, chemical and biological controls may explain the patterns observed in Figure 6.13. These mechanisms include sorption of metals to the surfaces of streambed material; formation and dissolution of minerals containing metals; preferential uptake of metals by growing aquatic plants; changes in the input of metals from perched aquifer seepage/recharge or upstream source; changes of geochemical conditions within the streambed and variation of streamflow.

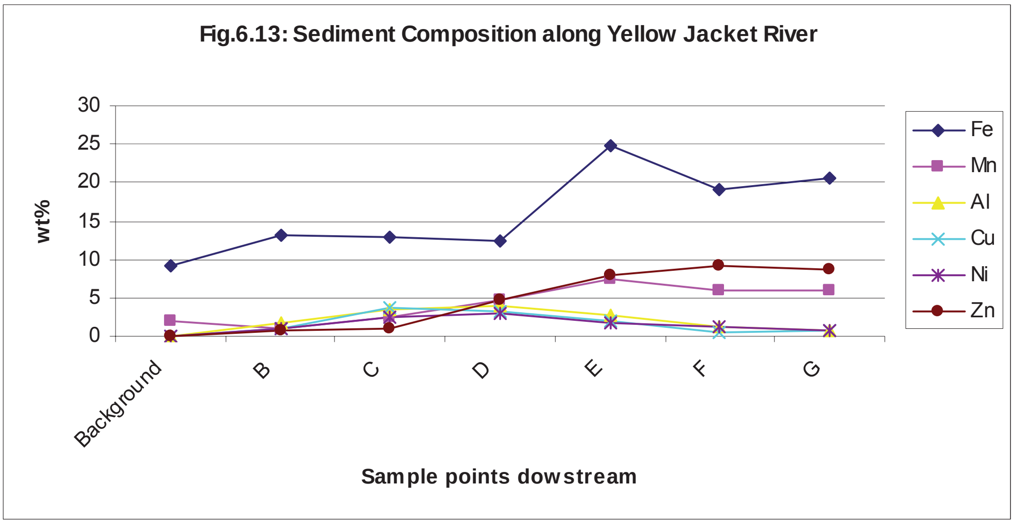

6.5 Chapter Summary

The hydro-geochemical study at Iron Duke shows that the major pathways for contaminant transport and attenuation at the site are through the Yellow Jacket River and shallow aquifer down gradient of the evaporation ponds. The concentration of contaminants in the Yellow Jacket River is controlled primarily by dilution and the amount of seepage released from evaporation ponds and old waste rock dump. The rate of pollution release from these sources is a function of climatic conditions, hydrologic factors, dissolution/precipitation and adsorption/desorption mechanisms.

pH and redox potential are the master variables that control the solubility and oxidation state of pollutant metal ions, the mobile phases of these elements, and also control much of the hydrochemistry of AMD, the mineralogical reactions which the acidic water can undergo and therefore its character and signature. In Chapter 7, an attempt is made to model some of these processes and assess the effects on natural attenuation as a remedial option at Iron Duke.

CHAPTER 7

GEOCHEMICAL MODELLING OF PROCESSES CONTRIBUTING TO NATURAL ATTENUATION OF AMD AT IRON DUKE MINE

7.1 Modelling Objectives

As leachate flows away from the reaction site, the drainage reacts with the rock and soil with which it comes into contact, changing the pH and metal composition of the drainage. In the case for Iron Duke, the dissolved constituents are reflective of the geochemical processes taking place underground, in the waste rock pile and other controls on secondary mineral reactions between the evaporation ponds, aquifer and Yellow Jacket River. The seepage waters mix with surface flows and groundwater and undergo further changes in constituent concentrations along the flow path. Geochemical models are required to estimate the nature of such interactions and the associated environmental implications over time, (Salmon and Malmstrom, 2003).

This chapter presents a modelling approach for predicting changes in solution composition after AMD – mineral - water reactions based on the geochemical code PHREEQC (Parkhurst & Appelo, 1999). First, the theoretical basis for modelling is presented, and secondly the simulations. Emphasis is placed on the application of Phreeqc in assessing and quantifying the geochemical processes responsible for the dispersion, reaction, and fate of environmentally significant contaminants (e.g., Al, Fe, Mn, sulphate & Zn) originating from mine water treatment problems at Iron Duke. Based on the model, an attempt is made to predict future contaminant loads to the Mazowe River sub-catchment and assess the effectiveness of injecting uncontaminated streamwater into the polluted aquifer as a remediation option.

The goals for geochemical modelling can be summed up as follows:

a) To assess the solubilities and speciation of chemical components in mine water, background water, seepage from evaporation ponds, ground water in shallow aquifer and downstream water
b) To evaluate the benefit of oxidising the AMD solution (mine water) in achieving chemical stability of neutral sludge
c) To predict changes in solution composition after mineral water reactions in the aquifer and Yellow Jacket River
d) To model the remedial effects of injecting uncontaminated stream water into the polluted aquifer

7.2 Principles of Aqueous Geochemical Equilibria

The influence of chemical equilibrium and kinetics on the progress of chemical reactions often determines the abundance, distribution, and fate of substances in the environment (Langmuir, 1997). Therefore, an understanding of the basic concepts of chemical equilibrium and chemical kinetics may help us to explain and predict the environmental concentrations of contaminant species in aqueous systems, whether these species are present naturally or anthropogenically. The direction of spontaneous change of chemical reactions and the conditions for chemical equilibrium in any system can be computed without having to measure them.

The basic principles which apply in aqueous geochemistry are the same as in other fields of science. The conservation of mass is the basis for mass balance and mass flow calculations on inputs and outputs in a natural system, while energy conservation permits the calculation of energy balances and flows for specified processes. The unidirectional redistribution of mass and energy principle provides the basis for calculating that portion of the total energy available for useful work and chemical reaction, i.e. for calculating what processes are energetically possible.

The dominant processes that control metal behaviour in soil and water media, and thus effect a distribution of the elements in the environment can be described by considering multiphase equilibria as summarised in Figure 7.1.

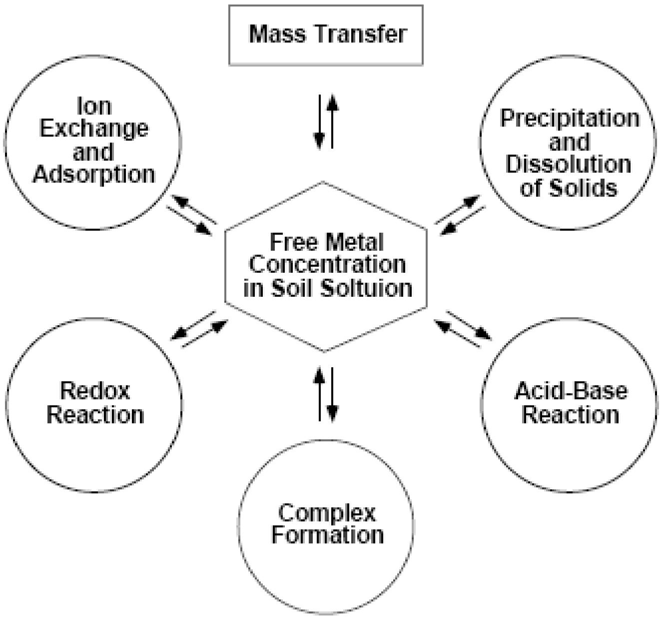

Fig.7.1: Principal Controls on trace metal concentrations in soil – solution, after Mattigod *et al.,* (1981)

The relative behaviour of the element shown as free metal in Figure 7.1 is critically dependent on two fundamental parameters of the element: namely size (ionic radius) and charge. The ratio of ionic radius to charge is the *ionic potential*, the basis on which behaviour in solution can be assessed, viz: solubility, precipitation or complexation. The activity (a_i) of a species is a measure of its effective concentration, and is usually smaller than concentration. Activity is related to concentration through the expression: $a_i = \gamma m_i$, where γ is the activity coefficient and m_i is the concentration of the ith species. This difference between activity and concentration arises because in a solution, each ion is surrounded by a shell of oppositely charged ions, which decreases the ability of the central ion to enter into chemical reactions.

The distribution of dissolved species and complexes in water is governed by the law of mass action. For a reaction of the form $aA + bB = cC + dD$, a mass action equation that describes the distribution of species can be expressed as:

$$K = \frac{\gamma_C [C]^c \gamma_D [D]^d}{\gamma_A [A]^a \gamma_B [B]^b} \qquad (7.1)$$

where the bracketed terms represent the molal concentrations, the gammas are the activity coefficients, the lower case letters are stoichiometric coefficients, and K is the equilibrium constant.

In pure water, all solute ions or molecules contact only water molecules, and the activity coefficients of all solutes equal to unity. As salt concentrations increase, individual aqueous species move closer together and ionic interaction between adjacent ions becomes more pronounced. This interaction due to Coulombic forces is proportional to the charge of the ions involved and is embodied in the definition of *ionic strength* (I), in mol per litre, which may be calculated from analytical molal concentrations (m_i) and the charge on the species (z_i):

$$I = \frac{1}{2} \sum m_i z_i^{\,2} \qquad (7.2)$$

The ionic strength is a parameter used to describe concentration of charge. To calculate the activity coefficient of ions, virtually all geochemical modelling programs in use today use either a variation of the Debye-Huckel equation or the Pitzer equation, (Zhu and Anderson, 2002). Two variations of the Debye-Huckel equation in common use are the Davies equation and the extended Debye – Huckel equation, Perkins *et al*., (1995). Based on I, the activity coefficients of ionic species can be calculated using the Davies equation (Davies, 1962):

$$\log \gamma_i = \frac{-Az_i^{\,2}\sqrt{I}}{1+\sqrt{I}} + 0.3Az_i^{\,2}I\,, \tag{7.3}$$

A is a constant which varies slightly with temperature, but equal to 0.512 for most practical purposes. The 0.3 in the final term, is entirely empirical and sometimes changed to 0.2. The ionic strength *I* can be estimated from field measurements from the following approximations, Zhu and Anderson (2002):

$$I \approx 0.25\text{x}10^{-4}.\text{TDS (mg/l)}, \tag{7.4}$$
$$I \approx 1.6\text{x}10^{-4}.\text{Conductivity } (\mu\text{mho}) \tag{7.5}$$

The tendency towards dissolution or precipitation is expressed as the saturation index (*SI*), and can be evaluated by comparison of the reaction quotient with the ion activity product (IAP: calculated using measured concentration):

$$SI = \log\left(\frac{IAP}{K_{sp}}\right) \tag{7.6}$$

where K_{sp} is the solubility product. If SI<0, solution is under saturated and dissolution should occur. At SI=0, the solution is in equilibrium, and when SI>0, the solution is said to be oversaturated with respect to the solid and precipitation should occur. In practice, kinetic effects may delay actual dissolution or precipitation. The SI or Pitzer method (Pitzer, 1995), permits activity calculations to very high ionic strengths but the range of components is more limited than with ion association (IA) method.

The ion association (IA) theory explicitly defines electrostatic interactions between ions of opposite charge by equilibrium constants for ion pair or complex formation. In acid mine waters, most divalent and trivalent metal cations (Fe^{2+}, Cu^{2+}, Zn^{2+}, Ni^{2+}, Fe^{3+}, Al^{3+}) are attracted to SO_4^{2-} to form ion pairs such as $AlSO_4^{+}$. If the thermodynamic stability constants for the formation of these ion pairs are known, then they can be entered into a numerical algorithm to solve simultaneously the speciation among several competing species. Water analysis can be used as input data along with the thermodynamic properties of ion pair formation (equilibrium constants, free energy, enthalpies, entropies, and heat capacities) to solve mass balance equations for every component.

7.3 Overview of Geochemical Modelling

Detailed descriptions of geochemical models have been extensively reviewed in the literature, (Appelo and Postma, 2005; Plumer *et al,* 1992, and others). Geochemical models are used to predict the concentrations of species present in a system. From this data, they can be used to deduce and quantify the chemical and biologic processes that affect the fate and transport of pollutants in soils and aquifers. They can be used to deduce what minerals dissolve or precipitate, how many moles of mineral enter or leave a flow path at each step, and to make priori predictions of water chemistry based on assumed geochemical processes. Geochemical models are essentially of two types:

a) Speciation models that calculate activities (chemically reactive concentration) and species distribution for elements in the database and other related parameters such as pH, pe, saturation indices, and ion ratios. The usual input is a chemical analysis of water sample or a solution with user specified chemistry.

b) Reaction Path models use speciation calculation as starting point and then make forward predictions of changes in water and rock (dissolution/precipitation) along reaction path, specifying change in temperature, pressure, pH, new reactants and their concentrations.

Models work by converting the chemical concentrations, usually reported in mg/kg or mg/L to moles, and then solving a series of simultaneous non – linear algebraic equations (chemical reaction, charge balance and mass balance equations) to determine the activity concentration relationship for all the chemical species in the specified system. The models usually require electrical balance and will force charge balance with one of the components (can be designated), as they solve a matrix of non – linear equations. A common simplification of the geochemistry within coupled reactive transport models is the use of the Local Equilibrium Assumption (LEA). All reactions are assumed to attain geochemical equilibrium and occur instantaneously; chemical kinetic limitations are assumed to be insignificant.

7.4 The Governing Equations

7.4.1 Debye – Huckel Model of Ionic Interactions

For dilute solutions, (ionic strengths up to about 0.1 molar) the activity coefficients may be obtained with sufficient accuracy with the use of the Debye-Huckel (Robinson & Stokes, 1970) theory of ionic interactions:

$$-\log\gamma_i = \frac{Az_i\sqrt{I}}{1+\mathring{a}_i B\sqrt{I}} \qquad (7.7)$$

A = $1.82\text{x}10^6(\epsilon T)^{-3/2}$ and B = $50.3(\epsilon T)^{-1/2}$ are pressure and temperature-dependent empirical constants specific to the solvent, and $\mathring{a}_i$ is an adjustable parameter corresponding to the effective size of the ion. Other equations, such as the Guntelberg equation or Davies equation have been developed for higher ionic strengths up to 0.5 molar. Truesdell and Jones, (1973); and subsequently Parkhurst & Plumer (1993), fitted a modified version of the Debye - Huckel equation to activity coefficient data for chloride solutions and proposed the extended Debye – Huckel equation (7.8):

$$\log\gamma_i = -Az_i^{\,2}\frac{\sqrt{I}}{1+B\mathring{a}_i\sqrt{I}} + b_i I \qquad (7.8)$$

where b_i is an empirical parameter designed to reproduce the activity coefficients of NaCl bearing solutions.

The partial derivatives of these activity coefficient equations with respect to ionic strength are:

$$\frac{\partial}{\partial I}\ln\gamma_i = -\ln(10)\left[Az_i^{\,2}\left(\frac{1}{2\sqrt{I}(\sqrt{I}+1)^2} - 0.3\right)\right] \qquad (7.9)$$

for the Davies equation, and

$$\frac{\partial}{\partial I}\ln\gamma_i = -\ln(10)\left[\left(\frac{Az_i^{\,2}}{2\sqrt{I}(B\mathring{a}_i\sqrt{I}+1)^2} + b_i\right)\right] \qquad (7.10)$$

for the extended Debye Huckel equation. A plot of these derivatives is shown in Figure 7.2, (after Garrels and Christ, 1965).

Fig. 7.2: Activity coeffcients vs ionic strength (Garrels & Christ, 1965)

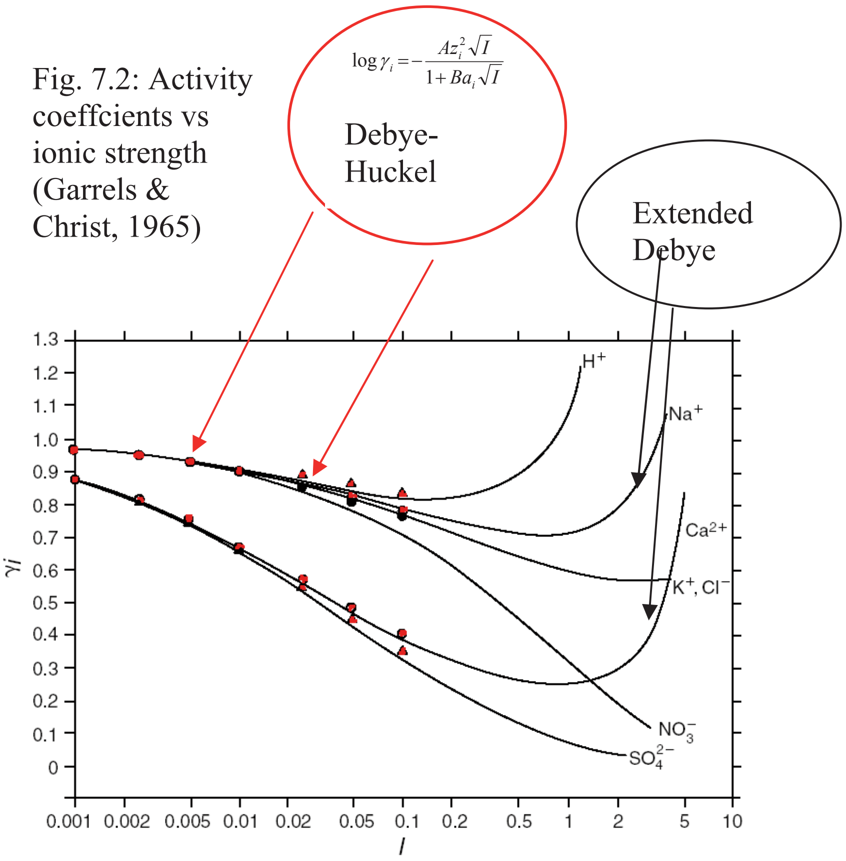

The symbols in Figure 7.2 depict activity coefficients of various ions as a function of ionic strength as calculated with the Debye – Huckel equation, (7.7). Activity coefficients are seen to decrease with I, strongest for the divalent ions. At an ionic strength of 0.1, γ is about 0.8 for monovalent ions and 0.4 for divalent ions. The lines in Figure 7.2 correspond to the Truesdell and Jones equation (7.8). At low ionic strength, they agree well with the values obtained with the Debye – Huckel equation (7.7). At high ionic strengths, the activity coefficients of cations are seen to increase by the action of the term ($b_i.I$). Equation 7.8 is a reasonable approximation up to I values of about 2 in dominantly chloride solutions, (Parkhurst & Plumer, 1993). Another model intended specifically for activity coefficients for brines and solutions with higher ionic strengths such as occurs in AMD is the Pitzer model (Pitzer, 1995). This model requires a large number of experimentally determined parameters, of which there is currently insufficient for AMD solutions.

Differences between model results, even when based on the same conceptual model, are due to differences between the constants and chosen method of calculation for the thermodynamic properties, and/or the accuracy of the numerical method of the solution of equations.

7.4.2 Sorption and the K_d Model

Sorption describes the processes by which a contaminant migrating through porous media partitions between the solid and aqueous phases. It includes all surface related reactions, (illustrated in Figure 7. 3) such as adsorption, absorption, surface complexation, surface precipitation and ion exchange.

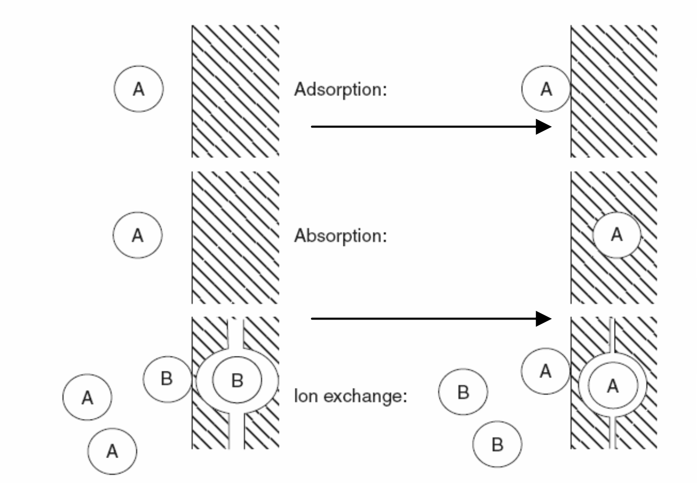

Oxy-hydroxides

Humic Substance

Clay Minerals

Figure 7.3: Sorption Processes

Sorption of dissolved ionic contaminants can occur as a result of:

- Adsorption – This is the attachment of a contaminant to a solid surface caused by the action of van der Waals forces, hydrogen bonding, ligand exchange, surface complexation, dipole forces and hydrophobic forces.
- Absorption caused by the diffusion of a contaminant into the structure of a porous particle.
- Electrostatic forces leading to cation exchange – the replacement of a previously sorbed cation such as Na^+ or Ca^{2+}, by another positively charged ionic species.

The effect of sorption is to slow or retard the rate of migration of the contaminant relative to the average water flow velocity. It may have three distinct implications for attenuation processes:

a) Removal of contaminants from the dissolved phase. This reduces the contaminant mass in solution although the total mass in the system is conserved, and has the apparent effect of decreasing the transport velocity of the contaminant. The decreased transport velocity resulting from sorption will lower the overall contaminant flux to the receptor.

b) The contaminant remains sorbed to the solid material in the aquifer until desorption occurs. Desorption occurs due to reversed concentration gradients and/or displacement by substances with a higher affinity for the occupied sorption sites. Desorption rates are typically limited by chemical equilibrium reactions in the case of charged ionic species.

c) Limitations on bio-availability. Contaminants normally have to be in aqueous solution to cross the microbial cell membrane into cells, where they are subject to biodegradation reactions. Therefore sorption may render contaminants unavailable for degradation unless and until desorption into the aqueous phase takes place.

Sorption processes are grouped, assessed and quantified by a single sorption parameter called the partition coefficient, K_d. This is defined as the ratio of the quantity of metal adsorbed (adsorbate) per unit mass of solid to the quantity of the adsorbate remaining in solution at equilibrium. For the reaction,

$$A \quad + \quad C_i \quad = \quad A_i \qquad (7.9)$$

the mass action expression for K_d in L/kg derived from Henry's Law (Appelo and Postma, 2005) is:

$$K_d = \frac{A_i}{C_i} \qquad (7.10)$$

where, A = free or unoccupied surface adsorption sites; C_i = total dissolved adsorbate remaining in solution at equilibrium (mg/l) and A_i = adsorbate on the solid at equilibrium. Equation 7.10 describes a linear isotherm because it applies at a single temperature, and often varies with temperature. The Langmuir isotherm, Appelo and Postma, (2005), assumes that there are a finite number (β) of surface sites that have identical sorption characteristics. It is commonly expressed as:

$$A_i = \beta \frac{\alpha C_i}{1 + \alpha C_i} \qquad (7.11)$$

where, α = the partition coefficient (L/mg); β = the maximum amount of solute that can be sorbed by the solid (mg/kg). Taken to the limit of a continuous Gaussian distribution of α and β in order to represent a heterogeneous exchanger, Lungmuir isotherms may be integrated to give the Freundlich isotherm, in equation 7.12.

$$A_i = KC_i^{\,N} \qquad (7.12)$$

where K and N are constants, with N constrained to lie between 0 and 1. Figure 7.4 compares the characteristic shapes of the linear, Langmuir and Freundlich isotherms. Both Freundlich and Langmuir isotherms are essentially linear at low concentrations, as may the case in a dilute contaminant plume. However, near contaminant sources, dissolved concentrations may be sufficiently high that isotherm non – linearity may be important. Non linear isotherms are therefore generally more appropriate at high concentrations when the sorption capacity of the solids is approached. Furthermore, physical adsorption to heterogeneous sorption sites is a process best described by the concentration dependent Freundlich isotherm model, (Sposito, 1984). Hence it is important to consider the use of non linear isotherms to interpret the results of sorption experiments and for K_d to be measured at concentrations relevant to those encountered in the field.

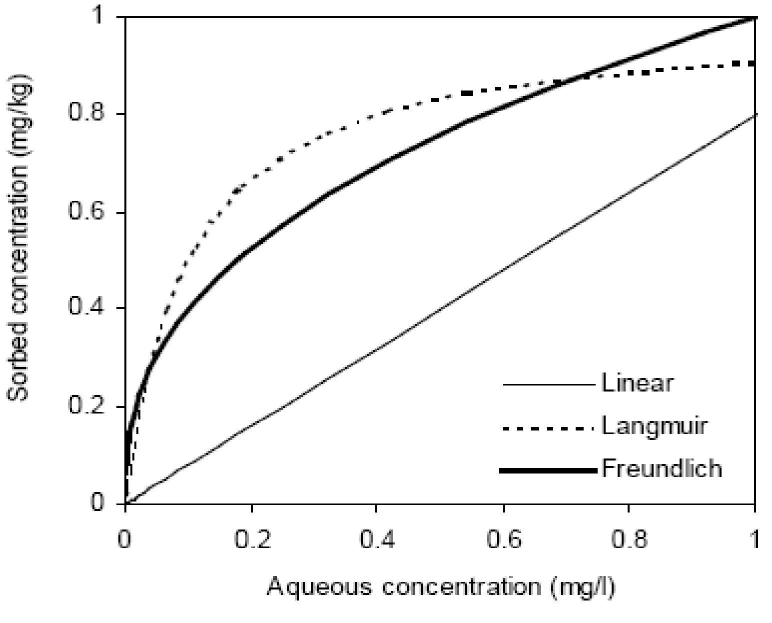

Fig.7.4: Comparison of Linear, Langmuir & Freundlich isotherms

An important limitation of the constant K_d model is that it does not address sensitivity to changing conditions. If the groundwater properties (e.g. pH, solution ionic strength) change, a different K_d value should be used in the model. Thornton *et al.,* (2000), used column experiments to estimate contaminant retardation factors and then calculated values of the linear partition coefficient K_d using equation 7.13,

$$R = 1 + K_d \frac{\rho_B}{n} \qquad (7.13)$$

Where, R = retardation factor (ratio of solute velocities); ρ_B = porous media bulk density in (kg/m^3); n = the effective porosity of the media at saturation.

Various adsorption models have been incorporated into a small number of chemical reaction codes to calculate the mass of a dissolved component adsorbing on a user specified mineral phase, such as iron hydroxide that coat mineral grains in soil. The adsorption modelling capabilities in these codes have been briefly reviewed by other researchers. Adsorption models incorporated into chemical reaction codes include non-electrostatic, empirical models as well as the more mechanistic and data intensive, electrostatic, surface complexation models such as the diffuse double layer model (DDL), illustrated in Figure 7.5, the triple layer model and the constant capacitance layer model.

The DDL model considers that a bulk solution in which the number of cations and anions are equal has zero electric potential. A negatively charged surface has a negative potential that attracts positively charged ions and repels negative ones. However, diffusion will smear out concentration steps, and cause the transitions to become more gradual. The net effect is a gradual change in concentrations in the so called Gouy – Chapman diffuse double layer which surrounds the charged surfaces in a solution. The electric potential, ψ, will not change abruptly at the solid solution interface, but gradually lessen as the distance from the interface increases.

Fig. 7.5: Gouy Chapman Model

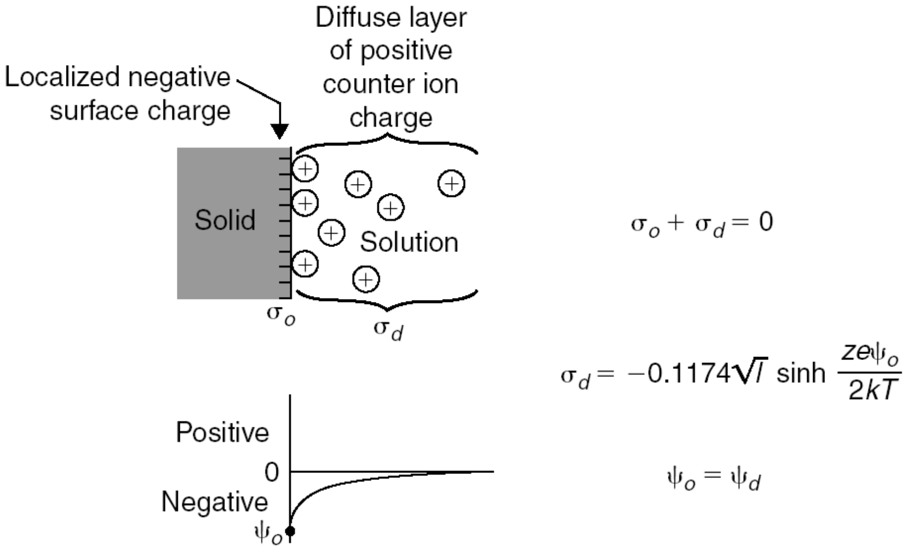

7.4.3 Transport and Retardation of Contaminants in Groundwater

In order to predict the spreading of acid mine drainage in groundwater and the breakthrough of acidity and heavy metals from the aquifer at Iron Duke, it is necessary to quantify the hydrological conditions and geochemical processes that act to retard and transform the transported solutes. In groundwater solutes are transported by advection, mechanical dispersion and molecular diffusion. Advection is the bulk motion of flowing groundwater (Freeze & Cherry, 1979). Mechanical dispersion is the process by which solutes are moved at velocities different from that of the bulk motion and is caused by drag along pore surfaces, differing velocities in the pore spaces and the tortuous nature of intergranular flow (Freeze and Cherry, 1979). Molecular diffusion causes net motion that is proportional to concentration gradient. At Iron Duke, velocities are large and molecular diffusion is assumed negligible relative to advection and mechanical dispersion. For 1 – dimensional advection – dispersion flow with chemical retardation, the conservation of mass for a chemical that is transported as in Figure 7.6 yields the transport equation 7.14, (Appelo and Postma, 2005).

$$\frac{\partial C_i}{\partial t} = D_L \frac{\partial^2 C_i}{\partial x^2} - v\frac{\partial C_i}{\partial x} - \frac{\partial q_i}{\partial t} \qquad (7.14)$$

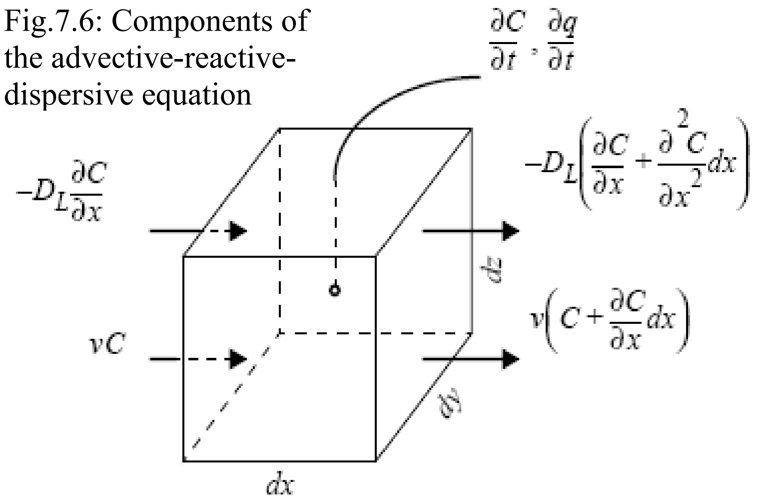
Fig.7.6: Components of the advective-reactive-dispersive equation

where C_i is solute concentration (mol/l), t is time (s), D_L is the hydrodynamic dispersion coefficient [(m^2/s), $D_L = D_e + \alpha_L \upsilon$, with D_e the diffusion coefficient, and α_L the dispersivity (m)], x is the distance (m), υ is the pore water flow velocity (m/s), and q_i is the sorbed concentration (retardation factor) expressed in mol/l of pore water. The term $-\upsilon(\partial C_i/\partial x)$ represents advective transport, $(\partial q_i/\partial t)$ is reaction with the solid and $D_L(\partial^2 C_i/\partial x^2)$ gives dispersive transport. The usual assumption is that υ and D_L are equal for all solute species so that C_i can be the total concentration for a component, including all redox species.

The relative strength with which cations bond to the charged mineral surface is determined by selectivity coefficients, which are a function of both surface properties and the species in solution, (Dzombak and Morel, 1990). In a solution containing multiple species, some will sorb more strongly than others. For most sediments and soils, divalent ions sorb more strongly than monovalent ions and for cations with the same charge, those with smaller hydration shells sorb more strongly. Domenico and Schartz, (1998), proposed a series of relative selectivity in order of decreasing affinity to ion exchange sites:

$$Al^{3+} > Ca^{2+} > Mg^{2+} > NH_4^{+} > K^{+} > H^{+} > Na^{+}$$

Furthermore, it has also been noted that an abundance of one cation may cause preferential sorption over another cation that is much less abundant, but has greater selectivity coefficient.

The cation exchange capacity (CEC) of a material expressed in milli-equivalents of charge per 100g of dry matter (meq/100g) is a measure of the quantity of sites on solid surfaces that can retain cations by electrostatic forces. Cations retained electrostatically are easily exchanged with other cations in the aquifer and are thus readily available for reactions with other ions in solution. Exchange sites are found primarily on clays and organic matter surfaces, and also on some metal oxides such as MnO_2 and $Fe(OH)_3$. CEC is pH dependent, since at low pH, hydrogen ions may compete with other ions for exchange sites, and exchange sites may therefore become positively charged at low pH.

7.5 Characteristics of Popular Geochemical Modelling Codes

The following key components are essential to perform geochemical modelling:

- A computer code.
- A thermodynamic, kinetic and surface property database for the specific chemical system.
- Conceptualisation of what chemical reactions are occurring and what chemical reactions are important to answer the questions being asked.
- Chemical and Physical measurements of the natural system of concern.

A computer modelling code or program is a set of computer commands that include algorithms to solve a set of mathematical equations describing chemical equilibria, chemical mass balance, various kinds of bookkeeping, and input and output controls.

The code is designed in a general way, and only deals with the mathematical framework and computation tasks, with no reference to any particular chemical system. As a result the mathematical framework for all such codes is similar, although the mass balance accounting and computational techniques for solving the mathematical equations may vary in each code. The mathematical formulation of geochemical models and the numerical methods to solve the algebraic equations have been described by Salmon and Malmstrom (2003), and other researchers. A few that are most popular are summarised in Table 7.1. All the programs have an associated database which contains the information on species properties and equilibrium constants required by the program. Each program uses the data in the database, which may or may not be the best available at the present time.

Table 7.1 Characteristics of Popular Geochemical Computer Codes

Model Code	Reference	Application	Characteristics Model type	Strengths	Weaknesses
PHREEQC	Parkhurst & Appelo, 1999. USGS	Low temperature aqueous geochemical calculations	Performs speciation & solubility, reaction path, inverse mass balance modelling, & 1D advective-dispersive-reactive transport calculations.	Accounts for analytical uncertainties. Widely used & tested on AMD. Input preparation program available.	Not suitable at higher ionic strengths. Lack of internal consistency in the data in databases.
MINTQA2	Allison et al., 1991. Frind & Molson, 1994. Cited in Woolery 1992. USEPA.	Most flexible for surface reactions, AMD model.	Primary purpose is speciation modelling, including redox, ion-exchange, surface complexation.	Extensive database of reliable thermodynamic data.	Requires another program to create input file.
EQ3/6	Wolery, 1992. Daveler and Wolery, 1992. Delaney et al., 1986.	General aqueous and ARD model.	Speciation & reaction path	Comprehensive database, source of thermodynamic data documented by Dr. James Johnson. Kinetics option,	Complex to use. No dissolution or precipitation, coprecipitation or wet dry cycles.

				solid solution available.	
NETPATH	Plumer et al., 1991 & 1992. Cited in Perkins et al., 1995. USGS	For calculating NET reactions & radiocarbon dating along a flow path.	Inverse Mass Balance code.	Includes evaporation, dilution & isotopes.	No thermodynamics.
GEOCHEMIST'S WORKBENCH	Bethke, 1994, 1996.	For solving problems in aqueous geochemistry, environmental protection and remediation, the oil industry, and economic geology.	Manipulating chemical reactions, calculating stability diagrams & equilibrium states of natural waters. Tracing reaction processes.	Plots results of calculations with graphical output. Capable of performing virtually all options.	Only lacks coupled reactive transport.

7.5.1 The PHREEQC Model

PHREEQC (Version 2) is a computer program for speciation, batch reaction, and one dimensional transport calculations, distributed free of charge by the U.S. Geological Survey (http://www.brr.cr.usgs.gov/projects/GWC_coupled/phreeqc/index.html). The acronym PHREEQC stands for PH (pH), RE (redox), EQ (equilibrium), C (program written in C). It is one of the most comprehensive geochemical models available (Zhu and Anderson, 2002). This program has been selected for simulating chemical reactions and transport processes in natural and polluted water at Iron Duke Mine because its cheap and has capabilities to meet the intended objectives.

7.5.2 Overview of Program Capabilities and how it works

PHREEQC is designed to perform a wide variety of low-temperature (less than 100°C) aqueous geochemical calculations. It is based on an ion-association aqueous model and has capabilities for (1) speciation and saturation-index calculations; (2) batch-reaction and one-dimensional (1D) transport calculations involving reversible reactions, which include aqueous, mineral, gas, solid-solution, equilibrium with surfaces (sorption reactions using the Dzombak and Morel (1990) double layer formulation), surface-complexation, and ion-exchange equilibria, and irreversible reactions, which include specified mole transfers of reactants, kinetically controlled reactions, mixing of solutions, and temperature changes; and (3) inverse modelling, which finds sets of mineral and gas mole transfers that account for differences in composition between waters, within specified compositional uncertainty limits.

PHREEQC can perform batch reaction simulations, which are mixing different waters or water and minerals or water and gases, etc., together in a beaker. The model uses three types of key words (commands) that are input using text files. The first type is the "manager" commands such as:
KNOBS, PRINT, TITLE, USE, END, SAVE, SELECTED_OUTPUT, SOLUTION_SPREAD, etc.
The second type is the commands used to specify the system:
SOLUTION_SPECIES; MASTER_SOLUTION_SPECIES; SURFACE_SPECIES; GAS PHASE; SOLID_SOLUTIONS; RATES; etc.
The third type is the batch-action or transport that performs an action:
SOLUTION; REACTION; INCREMENTAL_REACTIONS; MIX; SURFACE; ADVECTION; INVERSE_MODELING; EXCHANGE; EQUILIBRIUM_PHASES; KINETICS; etc.

Command blocks may be strung together in an input deck to simulate complex situations. For instance, batch reactions are implicitly defined whenever a solution or mixture that is defined in the simulation and any one of the keyword data blocks, EXCHANGE, EQUILIBRIUM_PHASES, GAS_PHASE, KINETICS, REACTION, REACTION_TEMPERATURE, SOLID_SOLUTIONS, or SURFACE, is also defined in the same simulation). Spreadsheet data may be imported directly and selected output values can be written to a text file for import into spreadsheet programs like MS Excel for plotting graphs. The version of the program used in this study has a simple window interface that facilitates use, multiple databases and x-y graph plotting capability.

7.5.3 Phreeqc Input and Output Files for the Simulations

To describe and model the geochemical processes responsible for the observed trends in pH and metal concentrations in drainage several hypothesis were considered, that:

a) Aeration or oxidation of the AMD solution will lead to better lime neutralisation treatment and a more stable sludge
b) Mixing background water with drainage water changed its chemistry
c) The drainage is neutralised along the Yellow Jacket River as a result of dilution, dissolving limestone and silicate minerals in the bed rock
d) Sorption mechanisms will prevent the movement of metals to ground water unless the retention capacity of the soil is overloaded
e) A breakthrough point will be reached when the sorption capacity of the soil beneath the evaporation ponds will be exceeded resulting in a massive pollution flux into Yellow Jacket River and subsequently into the Mazowe River

Input Files

Input files were constructed by defining solution compositions with the keyword SOLUTION. Solutions could be mixed and equilibrated with mineral phases or gases by keywords MIX and EQUILIBRIUM_PHASES. Chemicals were added by REACTION and kinetic calculations were specified using the keyword KINETICS and formulations specified in the database. Four solution samples were used for modelling. Sample Solution 1 - AMD is the untreated **a**cid **m**ine **d**rainage at Iron Duke. Sample Solution 2 - BGSW is the **b**ackground **s**urface **w**ater **u**pstream of the mine site along Yellow Jacket River. Sample Solution 3 - GWA is the contaminated **g**round**w**ater from the shallow **a**quifer beneath the evaporation ponds. Sample Solution 4 - SPD is from the **s**eepage **p**oint **D** along Yellow Jacket River. All the input files created for the simulations are appended in Appendix E.

Output Files

When the files are run, the program reports ‘Done’, and if enter is pressed the output tab appears where the results of the calculations are recorded. The solution composition is listed as molality (moles per kg of water), the default units in Phreeqc and as number of moles of each element specified in the input file. These two are equal since by default Phreeqc assumes that the solution consist of 1kg of water unless defined otherwise in the input file. Then follows the ‘Description of solution’ which gives default values for pH, pe and temperature, and calculated values for ionic strength, alkalinity, electrical balance, carbon, CO_2, and charge balance error. Next follows the distribution of species in alphabetical order, and finally the saturation indices. All this information is extracted and slightly modified for presentation purposes in this report. Sometimes units of molality are converted to mg/l for easy of comparison with units used in the input files.

7.6 Discussion of Modelling Results

7.6.1 Speciation and Solubility Analysis of Drainage Solutions

Metal concentrations determined by Atomic Absorption Spectrophotometers (AAS) and similar techniques are total concentrations in the solution. The methods can not distinguish metal speciation or oxidation state. Free metal, complexed metal ion concentration and concentrations of metals in different oxidation states can be determined using ion selective electrodes, polarography, calorimetric procedures, gas chromatography and high performance liquid chromatography. However, these methods are not routinely performed in most laboratories.

Solutions 1 to 4 were speciated using Phreeqc. Aqueous speciation refers to the distribution of aqueous species between free ions such as Ca^{2+}, Mg^{2+}, and Al^{3+}, and ion pairs, complexes, and natural species such as $CaSO_4^0$, $MgOH^+$, and $AlSO_4^+$. The type and degree of speciation in the solutions is necessary for many purposes including interpretation of toxicity, bioavailability, mineral stabilities, sorption reactions, redox reactions, gas reactions and rate mechanisms, Alpers and Nordstrom (1999). In general, the free metal ion is the most bio-available and toxic form of the metal.

Speciation and solubility analysis was performed in order to evaluate the concentrations and activities of ionic and molecular species in the aqueous solutions, and also to determine the saturation states with respect to various minerals in the system, and hence the directions of reactions that might occur towards achieving equilibrium.

The stable species distribution on surfaces or ion-exchangers that is in equilibrium with the aqueous solution was also determined. Modified input (all solutions) and output files (solution 1) for speciation analysis and calculation of saturation indices are presented in Table 7.2. Saturation indices and the distribution of species are shown in Appendix E for solutions 2, 3 & 4.

The data shown in Table 7.2 as measured represents the analysis (mg/l) from field samples taken during the sampling campaign described in Chapter 6. The elemental concentrations are converted to molality. The program performs a data quality check on the analytical composition by calculating the activity of water (default is 1), ionic strength, electrical balance and %charge balance error. If the measured solution composition is not electrically neutral and charge balance error exceeds 10%, the program reports errors and does not speciate the solution. As seen in Table 7.2, the saturation indices are negative indicating under saturation with respect to all mineral phases predicted by the model for Solution 1, at pH 2.34. Thus the mine water is strongly reducing (pe 4.6) and corrosive such that even quartz will dissolve (Saturation index SI = -0.67). This is a sharp contrast to the background surface water with a pH of 7.32 (Solution 2 in Appendix E1) where most of the mineral phases such as $Fe(OH)_{3\ (a)}$ (ferrihydrite), gibbsite, goethite, jarosite – K, and a number of clay minerals are oversaturated and precipitate. Due to these differences between Solution 1 and Solution 2, equilibrium shifts can be expected when untreated mine water mixes with stream water. The effects of such mixing are explored in one of the model simulation experiments, section 7.6.3

Table 7.2: Modified Phreeqc Input and Output File for Solubility and Speciation Analysis of mine site drainage solutions

Title # Speciation and Solubility Analysis								
SOLUTION	**1**	**1**	**2**	**2**	**3**	**3**	**4**	**4**
	Measured		Measured		Measured		Measured	
	mg/l	**Molality**	**mg/l**	**Molality**	**mg/l**	**Molality**	**mg/l**	**Molality**
pH	2.34		7.32		2.3		2.47	
pe	4.6		12.63		12.27		13.35	
temp	21.4		20.4		23.3		24.9	
Al	161.43	6.10E-03	0.05	1.85E-06	3.56	1.32E-04	9.11	3.38E-04
Ca	2.13	5.42E-05	28.06	7.00E-04	243.12	6.09E-03	320.43	8.01E-03
Cl	1237.04	3.56E-02	12.34	3.48E-04	201.45	5.70E-03	75.72	2.14E-03
Cu	0.34	5.46E-06	0.02	3.15E-07	0.31	4.89E-06	0.04	6.31E-07
Fe	6172.45	1.13E-01	0.87	1.56E-05	401.22	7.21E-03	3.87	6.94E-05
K	14.32	3.74E-04	5.03	1.29E-04	5.76	1.48E-04	5.12	1.31E-04
Mg	98.67	4.14E-03	29.04	1.20E-03	24.64	1.02E-03	78.9	3.25E-03
Mn	88.45	1.64E-03	1.87	3.41E-05	231.35	4.23E-03	45.42	8.28E-04
N(5)	287.26	2.09E-02	1.34	9.57E-05	78.54	5.63E-03	3.54	2.53E-04
Na	67.24	2.98E-03	12.66	5.51E-04	35.21	1.54E-03	26.86	1.17E-03
S(6)	11754.22	1.25E-01	139.45	1.45E-03	2007.74	2.10E-02	1242.32	1.30E-02
Si	1.12	1.90E-05	0.44	7.33E-06	0.92	1.54E-05	1.06	1.77E-05
Zn	3.43	5.35E-05	0.61	9.34E-06	1.45	2.23E-05	0.54	8.28E-06
HCO_3^-	0	0.00E+00	108.25	1.78E-03	0	0.00E+00	0	0.00E+00
End								

Description of Solution	Calculated	Calculated	Calculated	Calculated
	1	**2**	**3**	**4**
Activity of water	0.996	1	0.999	1
Ionic Strength	2.99E-01	7.31E-03	5.29E-02	3.74E-02
Mass of water (kg)	1.00E+00	1.00E+00	1.00E+00	1.00E+00
Total alkalinity	-1.62E-02		-1.97E-02	-5.59E-03
Total Carbon	0.00E+00	1.93E-03	0.00E+00	0.00E+00
Total CO2	0.00E+00	1.93E-03	0.00E+00	0.00E+00
Electrical Balance (eq)	-3.10E-02	-5.44E-04	-6.53E-05	3.87E-03
% charge balance error	-9.15	-6.23	-0.1	9.19
Iterations	11	9	8	9
Total H	1.11E+02	1.11E+02	1.11E+02	1.11E+02
Total O	5.61E+01	5.55E+01	5.56E+01	5.56E+01

Table 7.2 continued: Saturation Indices							
SOLUTION 1 Mine Water							
	Phase	**SI**	**log IAP**	**log KT**			
	Al(OH)3(a)	-8.24	2.8	11.04	Al(OH)3		
	Albite	-16.42	-34.66	-18.23	NaAlSi3O8		
	Alunite	-4.94	-5.89	-0.95	KAl3(SO4)2(OH)6		
	Anhydrite	-2.54	-6.88	-4.35	CaSO4		
	Anorthite	-30.42	-50.24	-19.82	CaAl2Si2O8		
	Ca-Montmorillonite	-18.88	-64.43	-45.55	Ca0.165Al2.33Si3.67O10(OH)2		
	Chalcedony	-1.09	-4.69	-3.59	SiO2		
	Chlorite(14A)	-70.67	-0.93	69.74	Mg5Al2Si3O10(OH)8		
	Chrysotile	-37.51	-4.86	32.65	Mg3Si2O5(OH)4		
	Fe(OH)3(a)	-8.1	-3.21	4.89	Fe(OH)3		
	Gibbsite	-5.51	2.8	8.31	Al(OH)3		
	Goethite	-2.34	-3.21	-0.87	FeOOH		
	Gypsum	-2.31	-6.89	-4.58	CaSO4:2H2O		
	H2(g)	-13.83	29.76	43.6	H2		
	H2O(g)	-1.6	0	1.6	H2O		
	Halite	-5.89	-4.32	1.57	NaCl		
	Hausmannite	-44.68	17.25	61.93	Mn3O4		
	Hematite	-2.69	-6.42	-3.73	Fe2O3		
	Illite	-22.6	-63.36	-40.76	K0.6Mg0.25Al2.3Si3.5O10(OH)2		
	Jarosite-K	-14.99	-23.92	-8.93	KFe3(SO4)2(OH)6		
	K-feldspar	-14.75	-35.6	-20.85	KAlSi3O8		
	K-mica	-20.18	-6.95	13.23	KAl3Si3O10(OH)2		
	Kaolinite	-11.52	-3.77	7.75	Al2Si2O5(OH)4		
	Manganite	-17.28	8.06	25.34	MnOOH		
	Melanterite	-1.3	-3.55	-2.25	FeSO4:7H2O		
	O2(g)	-56.67	-59.53	-2.87	O2		
	Pyrochroite	-14.08	1.12	15.2	Mn(OH)2		
	Pyrolusite	-26.96	15	41.96	MnO2:H2O		
	Quartz	-0.67	-4.69	-4.01	SiO2		
	Sepiolite	-26.91	-11.06	15.86	Mg2Si3O7.5OH:3H2O		
	Sepiolite(d)	-29.72	-11.06	18.66	Mg2Si3O7.5OH:3H2O		
	SiO2(a)	-1.95	-4.69	-2.74	SiO2		
	Talc	-36.05	-14.23	21.81	Mg3Si4O10(OH)2		
	Willemite	-21.37	-5.74	15.63	Zn2SiO4		
	Zn(OH)2(e)	-12.03	-0.53	11.5	Zn(OH)2		

Complexation lowers the activity of the free ion in water, thereby increasing the solubility of minerals and also the mobility of trace metals. The distribution of species shown in Appendix E1 for all solutions, shows that metals exist in solution as either free (uncomplexed) metal ions (e.g., Cu^{2+}, Zn^{2+}, Cr^{3+}), or in various soluble complexes with inorganic or organic ligands, (e.g., $Al(SO_4)_2^-$, $ZnCl^+$). Metals may also associate with mobile inorganic and organic colloidal materials. Colloidal size particles are particles with a diameter ranging from 0.01 and 10um, (Sposito, 1984), and include iron oxy-hydroxides (jarosite) and manganese (pyrolusite) oxides, clay minerals such as Ca -

montmorillonite and other phases shown in Appendix E1, in addition to organic matter. These surfaces have a high capacity for metal sorption, and greatly enhance transport of contaminants as suspended load in the Yellow Jacket River. For example, the total amount of Al in Solution 1 is given by a mass balance equation comprising the various complexes of Al^{3+} given in molal units in Appendix E1:

$$\sum Al = m_{AlSO_4}{}^{+} + m_{Al(SO_4)^{2-}} + m_{Al^{3+}} + m_{Al\,HSO4^{2+}} + m_{AlOH^{2+}} + m_{Al(OH)_2{}^{+}} + m_{Al(OH)_3} + m_{Al(OH)_4{}^{-}}$$

= 3.78E-03 + 1.77E-03 + 5.49E-04 + 3.74E-06 + 3.57E-07 + 1.76E-10 +
2.95E-15 + 1.69E-18
= 6.10E-03 M

The predominant species can be easily seen. Phreeqc considers corrections for activity and complexing of these ions as long as the log K values are in the database.

7.6.2 Simulation Experiment 1: Oxidation of the AMD Solution

A plant study of the lime neutralisation plant considered in chapter 6 concluded that aeration of the AMD solution would result in a more chemically stable sludge. A geochemical modelling experiment involving oxidation of mine water by aeration in steps 1 to 11 and subsequent reaction with calcite was performed using the following kinetic relations programmed in Phreeqc. The Phreeqc in put file is given in Appendix E2 – Simulation Experiment 1: The specific rate for calcite dissolution and precipitation is given by Plumer *et al.,* (1978):

$$r_{cc} = k1\left[H^{+}\right] + k_2\left[CO_2\right] + k_3\left[H_2O\right] - k_4\left[Ca^{2+}\right]\left[HCO_3^{-}\right] \qquad (7.15)$$

where the square brackets indicate activity for the ions and $k_{1..3}$ are temperature dependent constants given by Plumer *et al.,* (1978). The value of k_4 is variable but it must be such that the reaction rate becomes zero at equilibrium. It has been approximated in Phreeqc as follows. If the specific rate equation is arranged in part r_f, for dissolution, and a part r_b, for precipitation, then:

$$r_{cc} = r_f - r_b \qquad (7.16)$$

In a pure water and calcite system the precipitation rate becomes

$$r_b = k_4\left[Ca^{2+}\right]\left[HCO_3^{-}\right] \approx 2k_4\left[Ca^{2+}\right]^2 \qquad (7.17)$$

At equilibrium $[Ca^{2+}]$ is the activity at saturation, $[Ca^{2+}{}_s]$ and also the net reaction rate $r_{cc} = 0$, and therefore:

$$r_{cc} = r_f \left\{ 1 - \left(\frac{[Ca^{2+}]}{[Ca^{2+}{}_s]} \right)^2 \right\} \tag{7.18}$$

In a pure Ca-CO_2 system at constant CO_2 pressure, the ion activity product IAP is

$$IAP_{calcite} = \frac{[Ca^{2+}][HCO_3{}^-]^2}{P_{CO_2}} \approx 4\frac{[Ca^{2+}]^3}{P_{CO_2}} \tag{7.19}$$

The rate for calcite dissolution and precipitation used in the model was thus approximated by:

$$r_{calcite} \cong r_f \left(1 - \frac{IAP}{K_{calcite}} \right)^{2/3} \tag{7.20}$$

The precipitation and dissolution of minerals are simulated through the use of mass action equations that include the solid phase, which by convention is assigned an activity of 1. The equation describing equilibrium with calcite is:

$$K_{sp} = \frac{\gamma_{Ca^{2+}}[Ca^{2+}]\gamma_{CO_3^{2-}}[CO_3{}^{2-}]}{\{CaCO_3\}_s} \tag{7.21}$$

The addition of oxygen to mine water through aeration (Reaction steps 1 to 11) increases the pe value drastically from 4.6 to a maximum of 18 as shown in Figure 7.7. A low pe value indicates a high concentration of electrons and this suggests that the mine water is strongly reducing. This is supported by the concentration of iron which is present predominantly (~100%) as Fe^{2+}. However, this is rapidly oxidised to Fe^{3+} whose concentration peaks to 0.11M (6143.17 mg/l) and is maintained throughout the aeration steps. Calcite dissolution starts in Reaction Step 12. This is marked by a sudden drop in Fe^{3+} concentration to almost zero due to precipitation of ferrihydrite, goethite and other phases such as gypsum caused by the increase in pH. It is reported by several researchers that ferrihydrite is an amorphous ferric hydroxide with good surface adsorption properties and will partition many metals from solution. Ferrihydrite is gradually converted by dehydration to limonite, goethite, and finally hematite. A slight decrease in pe is also observed after calcite starts to dissolve. This can be a result of several competing reactions (mixed potential) that are not in equilibrium with each other.

Fig.7.7: Effect of AMD Oxidation on pe & Fe speciation

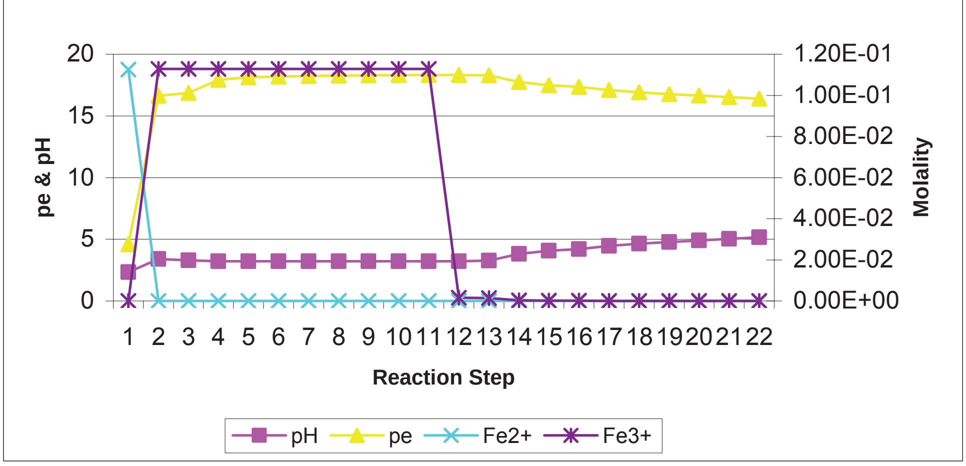

The saturation states of different mineral phases in the mine water at Iron Duke upon contact with the atmosphere are shown in Figure 7.8. Step 0 is the initial solution state underground, which shows that all the four phases considered here are under saturated (SI<0). Upon contact with the atmosphere, gypsum attains equilibrium, gibbsite & goethite become supersaturated while pyrolusite remains under saturated.

Fig.7.8:Precipitation of mineral phases without oxidation of AMD

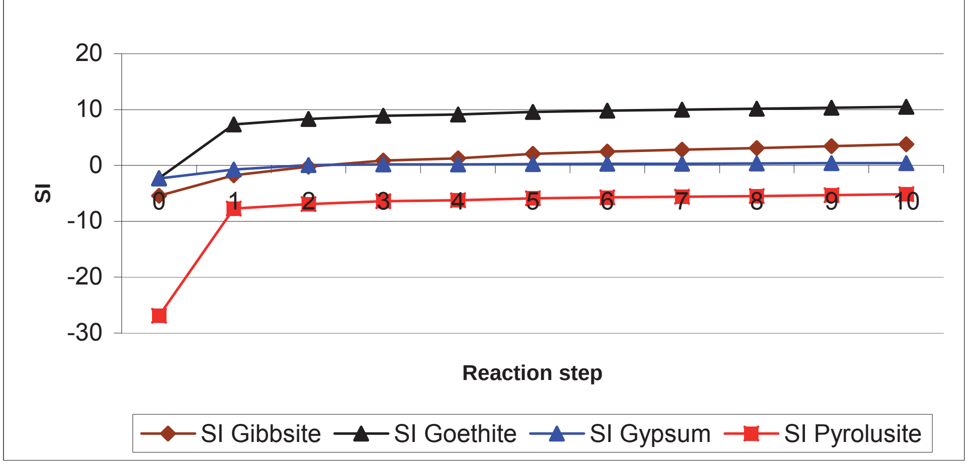

When the mine water is oxidised by "REACTION" with oxygen in the simulation, a noticeable difference in the saturation states is that pyrolusite becomes immediately super saturated and continues to do so on dissolution of calcite from Reaction Step 12 to 22, in Figure 7.9. In the mine water, Mn is in solution chiefly as Mn^{2+} (60%) and $MnSO_4^0$ (40%), based on Phreeqc speciation calculations.

Fig.7.9: Precipitation after oxidation of AMD

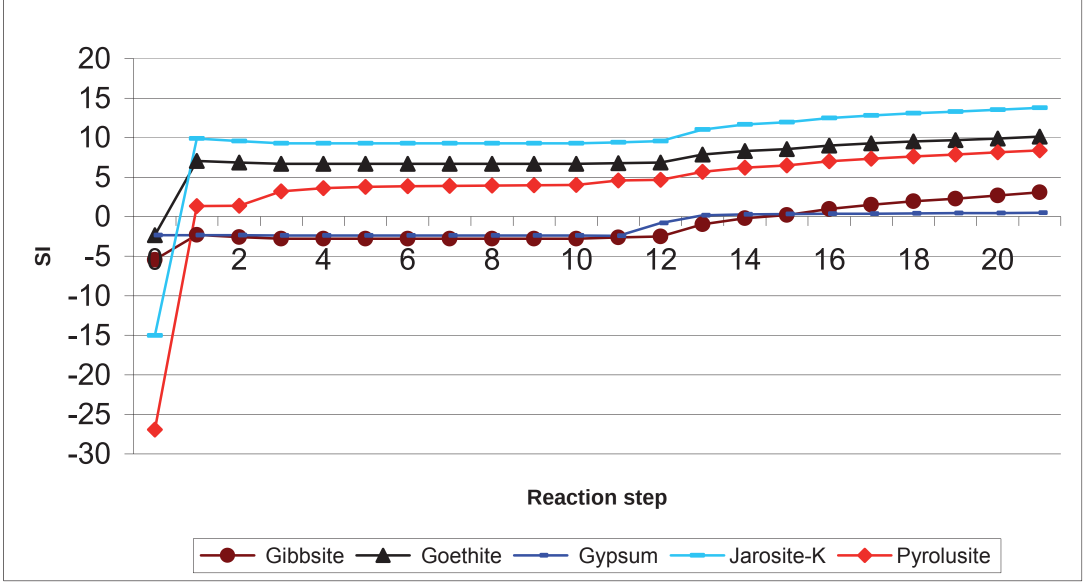

The correlation between saturation index of pyrolusite and pe is shown in Figure 7.10., and is strongly negative, correlation coefficient, $R^2 = 1$. This can possibly be explained by a redox reaction between Fe^{2+} and Mn^{4+} taking place in the reducing mine water.

Fig.7.10: SI of Pyrolusite vs pe

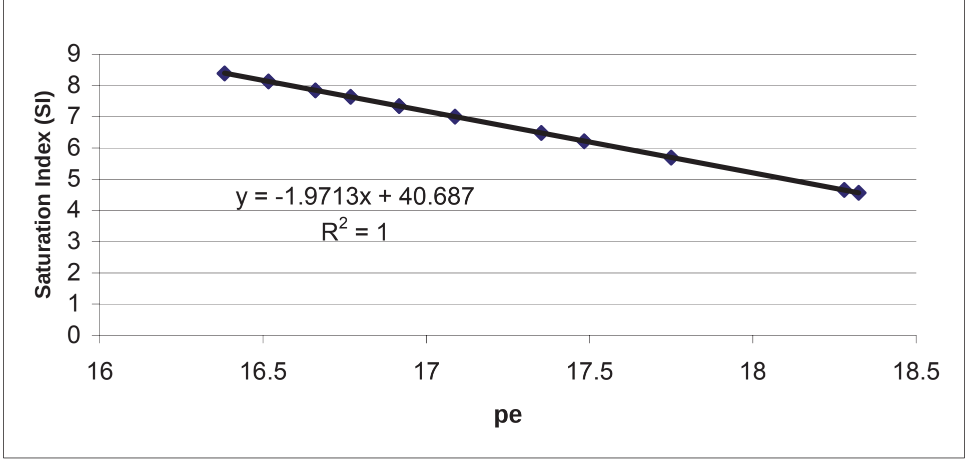

$$2Fe^{2+} + MnO_2 + 4H^+ \Leftrightarrow 2Fe^{3+} + Mn^{2+} + 2H_2O \qquad (7.22)$$

In reaction (7.22), two electrons are transferred from Fe(II) to reduce Mn(IV) in MnO_2. Ferrous iron acts as the reductant that reduces Mn(IV), while MnO_2 is the oxidant for Fe(II). This means that the precipitation of pyrolusite is not only equilibrium dependent but also redox controlled, and this may have a significant pH effect as expected from the Nernst equation, 7.23.

$$E = E^{o} + \frac{RT}{2F} \ln \frac{\left[Fe^{3+}\right]^{2}\left[Mn^{2+}\right]}{\left[Fe^{2+}\right]^{2}\left[H^{+}\right]^{4}} \qquad (7.23)$$

7.6.3 Simulation Experiment 2: Effect on Downstream water chemistry when AMD mixes with Uncontaminated Stream Water

Direct discharge of mine water used to take place before commissioning of the neutralisation plant, from 1980 to 1996, (Magombedze & Sandvik, 2006). The resultant effect of mixing untreated mine water with uncontaminated stream water on downstream water chemistry of the Yellow Jacket River was investigated by means of Phreeqc. The situation was modelled for a dry season, wet season and under heavy storm (flood) conditions by changing the ratio of stream water to mine water as the two solutions mix and equilibrate. The pH was modelled by simulating the dissolution and precipitation of calcite, ferrihydrite, gypsum, gibbsite, pyrolusite and other phases suggested by the speciation analysis in section 7.4.1, at $P(CO_2)$ and $P(O_2)$ of $10^{-3.5}$ and $10^{-0.68}$ respectively. Equilibrium sorption by the ferrihydrite surface was also allowed. Eh (pe) was fixed for each modelled point to simplify the modelling of redox sensitive species. This ensured that the pe used in the model was equivalent to the value measured in the field. Phreeqc then calculates the chemical reactions and equilibria between a set of exchangers, mineral phases and the solution using a programmed Runge-Kutta procedure to integrate kinetic reactions during each time step.

Figure 7.11 shows the variation of pH with ratio of stream water to AMD. The predicted pH varies as the ratio of the mixture increases according to a natural logarithmic expression given by equation 7.24:

$$pH = 2.3772 \ln(x) + 1.925 \qquad (7.24)$$

where x is the number of parts of uncontaminated stream water to one part of mine water. Field measurements of pH along the Yellow Jacket River from the seepage point downstream were found to lie between 3.27 and 5.18 for the dry season, and between 4.08 and 5.84 during the wet months, which are in agreement with the model prediction.

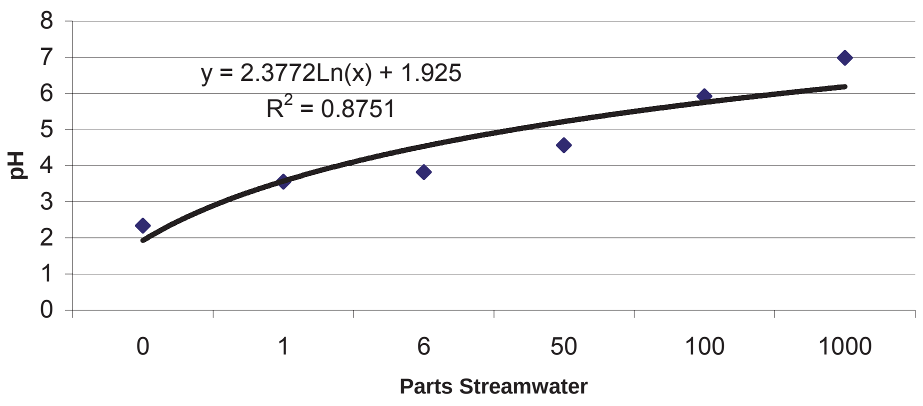
Fig.7.11: Variation of pH with AMD to Streamwater mixing ratio

Concentration profiles of pollutants in the downstream water are predicted as shown in Figure 7.12. From the hydrological data in Chapter 4, a dry season is depicted by a ratio from 1 to 6, while a normal wet season is from 6 to 50 and a very wet season or flood conditions exceed a ratio of 50 parts of stream water to 1 part mine water. It is clear from Figure 7.12 that for a normal year (ratio < 50), the concentrations of all five pollutants shown exceed regulated levels, (Appendix A). This means that large quantities of pollutant loadings were over the last 8 years discharged to Yellow Jacket River and subsequently to the Mazowe River supporting field data measured in Chapter 4. The seepage from polluted aquifer and old waste rock dump infiltrating into Yellow Jacket River has chemical composition similar to untreated mine water. It can be expected that the effect on contaminant concentrations will be similar to the profiles predicted by the model in Figure 7.12. This simulation shows that dilution is not a possible solution to meet regulated discharge levels in contaminant concentrations all year round. There is simply not enough fresh water in the Yellow Jacket River.

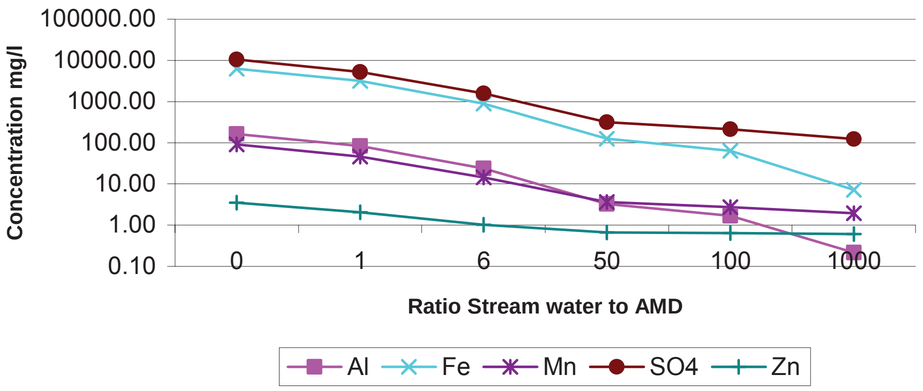
Fig.7.12: Effect of Mixing AMD & Stream water on pollutants composition

7.6.4 Simulation Experiment 3: Effects of Acidification and Buffering Processes in Contaminated Aquifer for the Past 8 years

The acid water that percolates from the evaporation ponds seeps into the soil down gradient and may be neutralised by reactions with minerals in the shallow aquifer matrix. The reacted seep emerges as a contaminant plume along Yellow Jacket River, 90 to 100 m from the evaporation ponds. The pollution seepage is diffused and dispersed along several points (C, D, & E, map Figure B3 in Appendix B) over a distance of about 50m along the river.

This simulation tries to predict the extend of acidification and buffering in the aquifer over the past 8 years. The modelling is performed from the time the acid front is perceived to have started contaminating the ground water, 2 years after commissioning the neutralisation plant in 1996, (Magombedze *et al.,* 2006). The shallow aquifer is assumed to be in equilibrium with gibbsite and an exchanger. Pre – contamination water quality is unknown and assumed to be similar to the groundwater in the deep zone. Phreeqc input files used to generate Figures 7.13 and 7.14 are shown in Appendix E, Simulation 3.

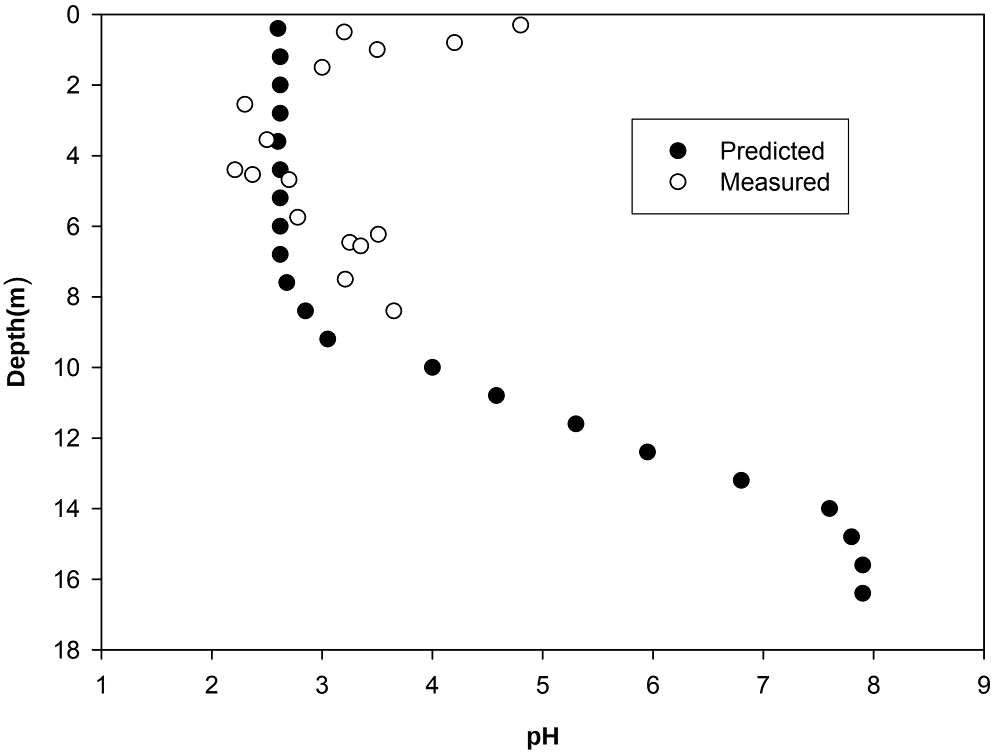

Fig.7.13: Acidification & Buffering in aquifer

The initial environmental conditions existing in the aquifer before acidification can be imagined as consisting of quartz, calcite ($CaCO_3$), goethite or any form of ferric hydroxide, $Fe(OH)_3$, and kaolinite ($Al_2Si_2O_5(OH)_4$), in contact with the acidic solution from evaporation ponds. As the acid reacts with the mineral assemblage, the pH stays relatively constant until calcite disappears. When calcite is gone, the pH drops to a new lower level, controlled by kaolinite. As the strength of the acid increases, eventually kaolinite also disappears, leaving only goethite, and the pH drops again to a level controlled by goethite. The dissolution of calcite raises the calcium content of the solution, causing gypsum to precipitate. Quartz is present throughout and is relatively unaffected.

The contaminant plume's preferred flow direction is not vertically downwards as with most cases, but rather inclined following the hydraulic gradient or head drop per unit distance between the evaporation ponds and infiltration depth into Yellow Jacket subsurface water. Higher pH levels were measured in the unsaturated zone. They are all acidic showing possible influence from strongly acidified and fluctuating groundwater levels. Figure 7.13 shows how the aquifer pH changes with depth from the surface. The blank circles from 0 to 1.5 m are pH measurements from pore water samples in the unsaturated zone. Groundwater field measurements are all below 2 m. Phreeqc predicts that the aquifer is currently acidified down to a depth of approximately 13 m where the pH is between 0 and 6.5. The model further predicts that there is a shift in pH from about 2.5 to 7.5 at a depth between 8 and 15 m. The measured pH data in the groundwater (saturated zone below 2 m) show a shifting trend from lower to higher pH values between depths of 2.5 to 9 m. Both measured and predicted pH profiles suggest that the most likely flowpath for the contaminant plume from evaporation ponds flows between 2.5 and 8 m depths towards Yellow Jacket River.

Field measurements could not be performed below 9 m due to technical problems encountered during drilling of monitoring boreholes. From these pH profiles, it can be expected that other pollutants such as Al, Fe, Mn, Ni, Zn and sulphate have also build up in the unsaturated zone over time since a strong correlation between pH and dissolved pollutant concentrations was verified in Chapter 4. Generally speaking, groundwaters that are low in alkalinity are most vulnerable to acidification. Since the results show that the ground water is neutral to alkaline below 13 m, it can be concluded that buffering processes are neutralising the acid at these depths or that the groundwater below this depth has not been acidified yet. According to Sverdrup (1990), the presence of minerals such as pyroxene, hornblende or biotite, even in small amounts would suffice to prevent acidification when the acid load is less than 0.5 keq/ha/yr.

The natural groundwater level in the area is below 45 m (or at least much lower than the Yellow Jacket River). Pollution to this depth may not be expected for many years due to the inherent buffering and sorptive capacity with depth exhibited by the aquifer. Furthermore, this gradient that exits between the evaporation ponds and Yellow Jacket River promotes preferential flow (suction effect) of pollutants in the forward direction than downwards. This suction potential could have a strong influence in the way the pollutants are distributed in the lateral direction from the evaporation ponds to the banks of Yellow Jacket.

Fig.7.14: Contaminant Transport in Aquifer

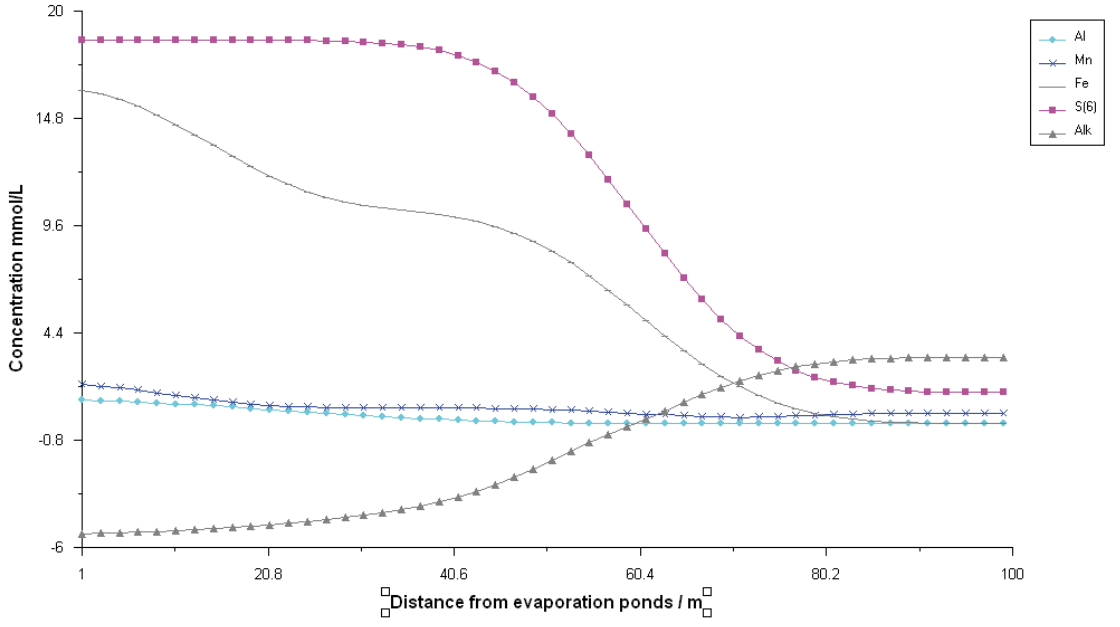

Figure 7.14 shows model predictions for pollutant concentrations in the forward direction from evaporation ponds towards the Yellow Jacket River. The results show that sulphate concentration in the groundwater has reached an equilibrium value of 18.7mmol/l (1795.2 mg/l) over a distance of about 40 m from the evaporation ponds towards the river which is located between 90 and 100 m from the ponds. That means the sub-soil of the land area lying between the ponds and the river is now saturated with sulphate between 2.5 and 8 m depths (preferred flowpath) over a lateral distance of 40m towards the river. The sulphate levels decrease sharply from 18.7 mmol/l (1795.2 mg/l) to 3.6 mmol/l (345.6 mg/l) between 40 and 70 m, after which the concentration remains constant as the case for all the other pollutants. Measured sulphate concentration from monitoring borehole No 2 which is 3.8 m deep, and located 55 m from the ponds has a dry season average of 1307.67 mg/l (13.62 mmol/l) which falls to 702.89 mg/l (7.32 mmol/l) during the wet season, with a standard deviation of 182.50 mg/l. The lower wet season levels are due to freshening of infiltrating groundwater caused by dilution from surface flows.

Iron shows initial levels of 16.1 mmol/l (899.14 mg/l) and the concentration gradually decreases towards the river reaching a constant value around 2.0 mmol/l (111.69 mg/l) at a distance 70 m from the ponds. The model predicts an iron concentration of 319.21 mg/l against a measured value of 368.67 mg/l (42.66 mg/l standard deviation) at borehole No 2. This discrepancy could be arising from the equilibrium phases such as ferrihydrite and goethite assumed in the model. It seems that there are geochemical reactions taking place involving iron such that it may take several decades to reach saturation under the current conditions. For example, the formation of siderite, through reaction between dissolved ferrous iron in the acidic seepage and calcite initially present in the groundwater is a thermodynamically favoured reaction.

$$CaCO_{3(s)} + Fe^{2+} + SO_4^{\ 2-} + 2H_2O \Leftrightarrow FeCO_{3(s)} + CaSO_4.2H_2O_{(s)} \quad (7.25)$$

This reaction may be responsible for reducing Fe concentrations in the groundwater and prolonging the breakthrough point. The groundwater contains measured Zn^{2+} up to 2.04mg/l. Speciation calculations show that, of the Zn^{2+} containing minerals rated by Nordstrom and Alpers, (1999) as likely to control metal concentrations in AMD-environments, smithsonite ($ZnCO_3$) may become oversaturated in the AMD plume. Thus the potential precipitation of this phase slows the breakthrough of zinc. Aluminium and manganese show slight changes in concentration from the ponds to the river suggesting that the aquifer is near saturation with respect to these elements and will not retain much of them anymore. This implies that Al and Mn seeping from the evaporation ponds have nearly reached their breakthrough points and may no longer be sorbed in the aquifer. Hence, they are discharged into the Yellow Jacket River at concentration levels more or less similar to their initial values. This point is confirmed by field monitoring data at borehole No 4, 2.7m deep and 65 m from the ponds, which shows that ground water composition in the aquifer is almost the same as seepage from the evaporation ponds as seen in Figures AP6.5 & AP6.6 in Appendix D.

Alkalinity is completely depleted in the aquifer and only shows some recovery after 75 m from the ponds, a location which in reality is 15 m from the edge of Yellow Jacket River. It has taken 6 years for the sulphate to saturate and reach breakthrough capacity over 40 m of the aquifer. This translates to a ‘saturation rate’ of 6.67 m per year towards the Yellow Jacket River. Therefore it will take approximately 7.5 more years for the ‘sulphate saturation front’ (1795.2 mg/l) to reach the banks of Yellow Jacket River, located 90 m from the contamination source. Since most of the metal cations are bound to sulphate as the dominant anion, the ‘arrival of sulphate’ at the banks of Yellow Jacket River can be expected to trigger a significant breakthrough of pollutants.

The breakthrough is a pollution time bomb. This suggests that an outbreak of AMD pollution in the Yellow Jacket and downstream water courses such as Mazowe River is likely to take place in 7.5 years time or less considering that alkalinity is now completely depleted in the aquifer. However, the suction potential and dilution effects from Yellow Jacket may also prolong the expected breakthrough of massive pollution.

7.6.5 Simulation Experiment 4: Modelling Pollutants Removal from Aquifer through Injection of Uncontaminated Stream Water

In-situ iron removal is a useful technique for reducing the iron concentration in groundwater pumped for consumption or industrial purposes, Van Beek, 1980; Rott and Lamberth, 1993). The technique involves periodic injection of a volume of aerated or oxygenated water in an aquifer, followed by pumping of the injected water and subsequently of the groundwater whose iron concentration is now lower than in native groundwater. By analogy, this principle can be 'borrowed' and adapted to remediate the contaminated aquifer at Iron Duke.

The proposed option seeks to make use of the natural flow conditions at the site as well as the natural attenuation mechanisms in soil and groundwater in the aquifer. A fraction of fresh stream water would be diverted from Yellow Jacket River into one of the evaporation ponds located up-gradient of the aquifer. The fresh water would be allowed to seep into the aquifer in the same way acidic water from the evaporation ponds is doing at the moment. After contacting the groundwater and subsurface soil matrix, desorption and dilution take place, and finally the 'wash water' exits the polluted aquifer through the same flow lines currently used by contaminated groundwater infiltrating into Yellow Jacket. No pumping would be necessary as the hydraulic gradient is expected to drive the 'injection' of fresh water through the aquifer. The situation is modelled with Phreeqc by considering a forward flow line of 90 m in length (average distance from pollution source to river), and a dispersivity of 1.

Sorption is modelled in this experiment as taking place on clay minerals illite and montmorilonite which carry a negative charge due to structural substitutions, and also on iron oxy-hydroxide. Sorption of cations is, in this case, a cation exchange reaction which does not affect the charge of the clay mineral but affects the speed with which the solutes travel through the aquifer.

The model predictions for contaminants removal are shown in Figure 7.15. When the aquifer is equilibrated with 100, 200 or 300 m^3 of unpolluted water, pollutant concentrations decrease very slightly, but then decrease fast and reach steady state with 500 m^3. This is considered as one pore volume of the aquifer. Chloride is reduced from 8.1 to 0.4 mmol/l (287.15 – 14.18 mg/l); sulphate from 15.1 to 2.1 mmol/l (1449.5 – 201.6 mg/l); manganese from 4.2 to 0.7 mmol/l (230.74 – 38.46 mg/l) and iron from 7 to 0.15 mmol/l (390.93 - 8.25 mg/l). ZINWA permissible levels for effluent discharge for these pollutants are: Cl – 250 mg/l; SO_4 – 250 mg/l; Fe – 1 mg/l & Mn – 1 mg/l. It is clear that chloride and sulphate concentrations can be reduced to meet permissible discharge levels while manganese would require further contact with more fresh water. Iron may not be removed further unless other geochemical conditions such as pH or redox potential change.

Fig.7.15: Pollutants Clean up by Injecting Stream Water

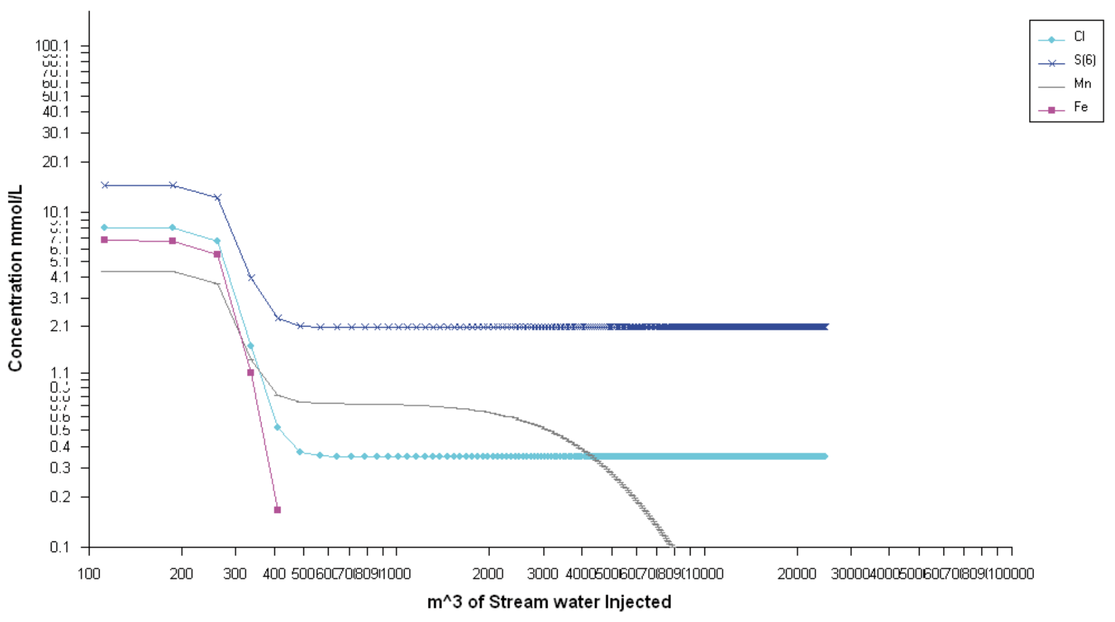

The total surface area extent of the aquifer is approximately 700 m^2. Considering that contamination has progressed downwards to a depth of 13 m as predicted in Figure 7.11, the total volume requiring clean up can be estimated at 700 x 13 = 91000 m^3. This means 91000/500 = 182 pore volumes are required to reduce pollution levels to those shown in Figure 7.15. The hydraulic conductivity of the aquifer was estimated by Ravengai *et al,* (2005) as 7.92 m/day. This means each batch of fresh water or pore volume takes 90/7.92 = 11.4 days to pass through the aquifer and infiltrate into Yellow Jacket subsurface water.

Assuming no fresh inputs of pollution loads to the aquifer, clean up to levels shown in Figure 7.15 may be achieved in 11.4 x 182 days = 2074.8 days, which is 5.7 years by this method. The only input cost is construction of the diversion canal for fresh surface water at the beginning of the installation and some costs for continuous monitoring.

While sulphate is attenuated through precipitation of gypsum, under the conditions at Iron Duke, this reaction could be limited by the rate of acidity supply from ferric iron, aluminium and manganese species which are dominant in the source AMD. The injection of fresh aerated water into the aquifer may slow down the breakthrough of pollutants by freshening sorption sites and increasing the retention time of pollutants.

7.7 Summary

Understanding and predicting the spreading of AMD in groundwater and breakthrough of acidity and heavy metals from the shallow aquifer at Iron Duke is important for assessing the risk of a ‘pollution time bomb’ to the Mazowe River sub-catchment. The fate of AMD pollutants (Al, Fe, Mn, Zn, acidity, sulphate and chloride) discharged from the mine was assessed by Phreeqc geochemical modelling in order to interpret the effects of over 6 years of acidic seepage infiltration from the evaporation ponds into the aquifer and subsequently into Yellow Jacket and Mazowe rivers.

The model predicts that oxidising the mine water through aeration before neutralisation with lime results in a more chemically stable neutral sludge. This will significantly reduce new inputs of acidic seepage into the polluted aquifer which is currently acidified to a depth of 13 m. Dilution and sorption processes in the aquifer and Yellow Jacket are responsible for attenuating most of the metals including Cu, Ni and Zn. A sulphate saturation front is progressing through the subsurface of the land lying down gradient of the evaporation ponds at the rate of 6.67 m per year towards the Yellow Jacket River. Considering that most of the metal pollutants are associated with sulphate as the dominant anion, a major pollution breakthrough can be expected to occur with the arrival of the sulphate front on the banks of Yellow Jacket River.

If the current geochemical conditions continue to prevail, Phreeqc predicts that the ‘pollution time bomb’ could explode within the next 7.5 years. However, the situation could be abated by diverting unpolluted stream water from Yellow Jacket into the evaporation ponds and ‘injecting’ or allowing it to seep through the aquifer. Assuming no new pollution inputs to the aquifer, using this method, it may be possible to significantly reduce pollutant concentrations in the groundwater to levels suitable for effluent disposal within a period of 6 years.

CHAPTER 8

CONCLUSIONS AND RECOMENDATIONS

8.1 Conclusions

This study shows that acid mine drainage problems are complex and multidisciplinary in nature. Solutions often require a comprehensive and integrated approach incorporating site assessment, prediction, control, treatment and monitoring as part of an overall AMD management plan. Effective control measures including statutory regulations can only be designed based on proper assessment of the key geochemical processes which impact the environmental system at the location in question.

Site assessment and characterisation studies show that at Trojan Nickel Mine (Site 1), drainage from the tailings dumps is essentially neutral to alkaline due to the low acid generating potential and magnesium silicates buffering capacity of the tailings. Acid Base Characteristic Curve tests show that the waste rock pile is potentially acid generating but the estimated time for the drainage to attain net acid conditions could not be established during the duration of the tests. Kinetic tests show that the tailings at Mazowe Mine (Site 2) are net acid generating with a lag period estimated at 2 years due to buffering from residual lime added during gold cyanide leaching. The behaviour of AMD contaminants is more complex at the most acidic mine, Iron Duke Pyrites (Site 3).

The variation in prediction data for different rainfall conditions further shows how difficult it is to design definitive experiments that can accurately reproduce the hydrologic, chemical complexity and geological time scales of natural systems. Onsite field studies should thus become increasingly more important for characterising acidic drainage and improve the understanding of mechanisms controlling the evolution and behaviour of AMD in semi arid climates. This greatly improves the identification, control and management of AMD under local conditions. Based on the results of this study, it can be concluded that the geochemistry of acid mine drainage in semi arid environments is strongly controlled by the following processes:

1. Conditions of aridity such as dryness and evaporation stop flow of leachate from waste dumps leading to accumulation and storage of oxidation products in the dumps. These effects are observed during the dry season from May to mid November, meaning that pollution loads to fresh water courses decay exponentially to a minimum.

2. During the wet season, mid November to March, accumulated oxidation products are flushed, leading to high contaminant fluxes in the drainage, and high potential for pollution of natural water courses in the mining areas. However, short spell duration, heavy thunderstorms result in erosion and dilution as the main mechanisms by which metal concentrations are reduced in surface water.
3. During transport of the dissolved phase, mixing occurs due to molecular diffusion of contaminants from higher to lower relative concentration, and also due to dispersion arising from the variation in flow velocities. These cause the contaminant plume to spread, thereby enlarging and developing a concentration gradient within the spatial area affected. Dilution of dissolved contamination by mixing with clean surface water, groundwater and/or infiltration water (recharge) results in significant reduction of the contaminants concentration and may be an important contributor to the overall attenuation effect.

4. Dissolution, precipitation and hydrolysis are the most important processes affecting contaminant interaction with surface water at all sites. These processes are more important at the pyrite mine operation, where chemical non-equilibrium exists due to point source nature of the pollution, extremely high contaminant concentrations, and because of high pH and redox potential gradients. Adsorption, desorption, complexation and cation exchange are the key processes controlling inorganic pollutant migration in the shallow aquifer at Iron Duke where continuous supply of contaminants result in equilibrium shifts.

The following conclusions can also be drawn based on Phreeqc geochemical modelling of the processes controlling the spreading and attenuation of AMD at Iron Duke Mine:

5. The model predicts that the resultant effect of over 6 years of acidic seepage infiltration from the evaporation ponds into the groundwater and subsequently into Yellow Jacket River is a ‘pollution time bomb’. A sulphate saturation front is progressing through the subsurface at an estimated rate of 6.67 m per year towards the banks of Yellow Jacket River and could trigger a massive pollution breakthrough in the Mazowe River sub-catchment within 7.5 years.
6. Assuming no new pollution inputs to the aquifer, Phreeqc predicts that injecting uncontaminated stream water into the aquifer and allowing it to seep by means of the hydraulic gradient existing between the evaporation ponds and Yellow Jacket River, it may be possible to significantly reduce pollutant concentrations in the groundwater to levels suitable for effluent disposal within a period of 6 years.

8.2 Recommendations

Since knowledge of how to combat pollution from sulphide mineral processing is not well distributed in Zimbabwe, the strongest recommendation from this study is the development of 'A National Framework or Guidelines for the Assessment and Management of AMD'. The guidelines can be developed in conjunction with the metal mining industry, government and scientific community with a primary purpose to provide advice on how to identify, evaluate and manage mine waste materials with potential to generate acidic drainage under local conditions. Studies similar to this present study could be extended to cover all catchments affected by metal mining operations in Zimbabwe and thus provide the 'basis characterisation data' for formulating such guidelines.

Mine water neutalisation at Iron Duke should incoorperate an aeration step and the flowsheet modified to the High Density Sludge Treatment process. The evaporation ponds should be cleaned of any previous slugde deposits and be lined with HDPE material to prevent any leaks into ground water. The ponds should be limed with coarsely crushed limestone prior to fresh sludge disposal. The natural wetlands existing at Trojan and Mazowe mines should be re-engineered to increase retention capacity and scavenging of heavy metals from discharge solutions. It is also recommended to use monitored natural attenuation as a management technique at all sites to control the migration and environmental impacts of AMD derived pollutants.

<u>Areas for further study</u>

- Sorption could be an important process controlling contaminant transport and attenuation in the vadose zone since groundwater levels in the country are generally very deep (> 45 m). However, the kinetics or rate mechanism of adsorption and desorption processes are too poorly understood to conclude that there is no threat from AMD pollution to groundwater, and therefore more research is required in this area.

- Geochemical modelling is a powerful tool for predicting the concentrations and fate of contaminants that leach from mine waste dumps and deciphering their transport in water and in the invisible subsoil. For it to be used to guide management decisions, it is recommended that detailed characterisation and study of several carefully selected field sites should be contacted in order to provide guidance on which parameters are more sensitive to local conditions.

REFERENCES

Ackman, T. E and Kleinmann, R.L.P., (1984). In-line aeration and treatment of acid mine drainage. In: D. H. Graves (ed). *Proc. Symp. Surface Mining Hydrology, Sedimentology, and Reclam.,* Univ. KY, Lexington, pp. 29-34.

Adriano, D.C., (ed), (1992). Biogeochemistry of trace metals. Lewis Publications, Boca Raton, Fla, pp. 514.

Ahonen, L and Tuovinen, O. H., (1994). Solid phase alteration and iron transformation in column bioleaching of a complex sulfide ore. In: Alpers C.N., and Blowes, D.W., (eds.), *Environmental Geochemistry of Sulfide Oxidation*: Washington, D.C. American Chemical Society Symposium Series ***550***, pp. 79-89.

Ali, M. A. and Dzombak, D. A., (1996). Interactions of Copper, Organic Acids, and Sulfate in Goethite Suspensions, *Geochimica et Cosmochimica Acta*, ***60(12)****:* pp 5045-5053.

Alpers, C. N. and Blowes, D. W. (eds), (1994). Environmental Geochemistry of Sulfide Oxidation, in *American Chemical Society Symposium Series* **550** (Washington, D.C.).

Appelo, C. A. J. and Postma, D., (2005). *Geochemistry, Groundwater and Pollution*, 2nd ed. A.A.Balkema, Rotterdam, pp. 635.

Arnesen, R.T., (1999). Loadings of Heavy Metals from Sulphide Ore Mines on Norwegian Freshwater Recipients. *Norwegian Pollution Control Authority, Report O-97175*, pp. 152.

Ashton, P.J., D. Love, H., Mahachi, R & Dirks, P.H.G.M., (2001). An Overview of the Impact of Mining and Mineral Processing Operations on Water Resources and Water Quality in the Zambezi, Limpopo and Olifants Catchments in Southern Africa. *Contract Report to the Mining, Minerals and Sustainable Development (SOUTHERN AFRICA) Project,* by CSIR Environmentek, Pretoria, South Africa and Geology Department, University of Zimbabwe, Harare, Zimbabwe.

Aström, M., (1998). Mobility of Al, Co, Cr, Cu, Fe, Mn, Ni and V in sulphide-bearing fine-grained sediments exposed to atmospheric O_2: an experimental study *Environmental Geology* ***36****,* pp. 219-226.

Atkins, R.J., Hay, D., and Robertson, J., (1997). Shallow water cover design methodology and field verification. In: Proceedings *of the 4th International Conference on Acid Rock Drainage,* Vancouver, B.C., vol. I, pp. 211–228.

Aubé B. and Zinck, J.M., (1999). "Comparison of AMD Treatment Processes and their Impact on Sludge Characteristics". *Proceedings for Sudbury '99, Mining and the Environment II.*

Aubé, B. (2004). "Successful Use of Design of Experiment to Improve Treatment of Zn in a Pond System" *Presented at the Ontario Mining Association Mines Rehabilitation Field Conference.* Thunder Bay, Ontario, September 13-16, 2004.

Banwart, S.A., and Malmström, M.E., (2001). Hydrochemical modelling for preliminary assessment of mine water pollution. *Journal of Geochemical Exploration* ***74***: pp. 73 - 97.

Banwart, S.A., Evans, K.A., and Croxford, S., (2002). Predicting mineral weathering rates at field scale for mine water risk assessment. In Younger, P.L., and Robins, N.S., (eds) *Mine Water Hydrogeology and Geochemistry*. Geological Society, London, Special Publications ***198*** pp. 137-157.

Baron, D. and Palmer, C.D., (1996). Solubility of jarosite at 4–35 °C. *Geochimica et Cosmochemica Acta****, 60,*** 185–195.

Batholomew, D.S., (1994). Gold deposits of Zimbabwe. *Mineral Resources series, Zim. Geol. Surv., **23***, pp 75.

Batty, L. C. and Younger, P. L., (2002). Critical role of macrophytes in achieving low iron concentrations in mine water treatment wetlands. *Environmental Science and Technology*, ***36***, pp. 3997-4002.

Bigham, J. M, Carlson, I and Murad, E., (1994). Schwertmannite, a new iron oxyhydroxysulphate from Pyhasalmi, Finland, and other localities. *Mineralogical Magazine* ***58,*** pp. 641–648.

Bigham, J.M. and Nordstrom, D.K., (2000). Iron and aluminum hydroxysulfates from acid sulfate waters. In: Alpers, C.N., Jambor, J.L., Nordstrom, D.K. (Eds.), *Sulfate Minerals, Reviews in Mineralogy and Geochemistry, **40,*** pp. 351–403.

Blenkinsop, T. G., Oberthur, T. and Mapeto, O., (2000). Gold mineralization in the Mazowe area, Harare – Bindura – Shamva greenstone belt, Zimbabwe: I. *Tectonic controls on mineralization. Mineralium Deposita (2000)* ***35***, pp. 126-137.

Bryner, L. C., Walker, R. B. and Palmer, R., (1967). Some factors influencing the biological oxidation of sulfide mineral. *Transactions of AIME*, **238**: pp. 56-62.

Burns, R. G. and Fisher, D. S., (1990). Journal of Geophysical Research, **95**, pp. 14169-14173.

Carlson, I. Bigham, J. M., Schwertmann, U., Kyek, A. and Wagner, F., (2002). Scavenging of As from acid mine drainage by schwertmannite and ferrihydrite: A comparison with synthetic analogues. *Environmental Science and Technology* ***36***, pp. 1712–1719.

Chen, M., Soulsby, C., and Younger, P.L., (1999). Modelling the evolution of minewater pollution at Polkemmet Colliery, Almond catchment, Scotland. *Quarterly Journal of Engineering Geology* ***32***: pp. 351 – 362.

Chimimba, L. R. and Ncube, S. M. N., (1986). Nickel sulphide mineralization at Trojan Mine, Zimbabwe; *in* Anhaeusser C R, Maske S, (Eds.), *Mineral Deposits of Southern Africa, Geol. Soc. South Africa, Johannesburg,* v1 pp. 249-253.

Coakley, G.T. and Mobbs, P.M., (2003). The Mineral industry of Zimbabwe.

Cornell, R.M. and Schwertmann, U., (1996). The Iron oxides: Structure, properties, reactions, ccurrence and uses. VCH, Weinheim, Germany.

Dallas, H. F. and Day, J. A ., (1993). The effect of water quality variables on riverine ecosystems: A review *Water Research Commission Report* TT61/93.

Davies, C.W., (1962). Iron Association. London. Butterworths.

Davis, A., Ruby, M. V. and Bergstrom, P. D., (1994). Factors controlling lead bioavailability in the Butte mining district, Montana, USA: *Environmental Geochemistry and Health*, *v.* ***3/4***, pp. 147-157.

DeVos, K.J., Pettit, C., Martin, J., Knapp, R.A. & Jansons, K.J., (1997). Whistle Mine waste rock study: Volume I. MEND Project 1.41.4.

Dold, B., (1999). Mineralogical and geochemical changes of copper flotation tailings in relation to their original composition and climatic settings - Implications for acid mine drainage and element mobility. *Terre & Envirnoment, Geneva*, ***18***, pp. 230.

Domenico, P.A. and Schwartz, F.W., (1998). Physical and Chemical Hydrogeology, (2nd edn.), Wiley and Sons, pp. 824.

Doyle, Fiona. M., (1986). Acid mine drainage from sulphide ore deposits. *CIM Bulletin,* ***vol.72, no.752,*** pp. 301 - 310.

Drever, J. I., (1997). The Geochemistry of Natural Waters, 3rd ed. Prentice-Hall, NJ.

Driscoll, C. T. and Schecher, E. D., (1990). The chemistry of aluminum in the environment. *Environmental Geochemistry and Health* ***12***, pp. 28-49.

Dzombak, D.A and Morel, F.M.M., (1990). Surface Complexation modeling: hydrous ferric oxide. Willey and Sons, New York, pp. 393.

Edmunds, W. M. and Smedley, P. L., (1996). Groundwater geochemistry and health, an overview: In Appleton, J. D, Fuge, R and McCall, G. J. H., Eds, *Environmental Geochemistry and Health, with special reference to developing countries, Geological Society Special Publication* ***113***, pp. 91-105.

Eger, P. and Wagner, J., (1995). Sulfate reduction for the treatment of acid mine drainage: Long term solution or short term fix? In: *Proceedings of Sudbury 95 - Mining and the Environment*. Sudbury, Ontario, Canada. Pp. 515-524.

Ehrlich, H. L., (1996). *Geomicrobiology,* Dekker, New York, ed. 3, pp. 330-332.

Engdahl, D. and Hedenvind, H., (1998). Environmental Impacts Caused by Small-Scale Alluvial Gold mining. *Environmental Engineering Department Royal Institute of Technology.* Stockholm, unpublished M.Sc Thesis.

Eriksson, N., and Destouni, G., (1997). Combined effects of dissolution kinetics, secondary mineral precipitation, and preferential flow on copper leaching from mining waste rock. *Water Resources Research* ***33****:* 471 - 483.

Erlich, H.L., (1996). Geomicrobiology: 3rd edition, Marcel Dekker Inc., New York, pp. 719.

Evangelou, V.P., (1995). Pyrite oxidation and its control: solution chemistry, surface chemistry, acid mine drainage. J. Willey & Sons: New York, pp. 293.

Evans, P. and Skousen, J., (1995). Effect of digestion method on neutralization potential of overburden samples containing siderite. In: *Proceedings 1995 National Meeting of the American Society for Surface Mining and Reclamation*, Gillette, Wyoming, pp. 696-707.

Faulkner, Ben B. and J.G. Skousen., (1994). Treatment of AMD by Passive Treatment Systems. In: *International Land Reclamation and Mine Drainage Conf.,* US BOM SP 06A, Pittsburgh, PA.

Fergusson, J. C. and Wilson, T. H., (1964). The geology of the country around the Jumbo Mine, Mazowe District. *Bulletin of the Geological Survey of Rhodesia, vol.* ***33***, pp. 137.

Fernando, Q., (1995). Metal speciation in environmental and biological systems. *Environmental Health Perspectives* ***103*** (Suppl. 1) 13-16.

Förstner, U and Wittmann, G. T. W., (1979). Metal Pollution in the Aquatic Environment, Springer-Verlag, Berlin, pp. 486.

Freeze, R.A and Cherry, J.A., (1979). Groundwater Prentice-Hall. Engelwood Cliffs, N.J.604.

Frostad, S., Klein, B. and Lawrence, R.W., (2002). Evaluation of Laboratory Kinetic Test Methods for Measuring Rates of Weathering. *Mine Water and the Environment* ***21*** pp:183-192

Garrels, R.M., and Christ, C.L., (1965). Solutions, minerals, and equilibria: New York, Harper and Row, pp. 450.

Ghiorse, W. C., and Ehrlich, H. L., (1992). Microbial biomineralization of iron and manganese. In Skinner, H. C. W., and Fitzpatrick, R. W. (Eds.), *Biomineralization: Processes of iron and manganese*, pp. 75–99, Catena Verlag, Cremlingen, Germany.

Ghiorse, W. C. (1984). "Biology of iron- and manganese-depositing bacteria," *Annual Review of Microbiology,* ***38****, pp. 515-530.*

Gong, C. and Donahoe, R. J., (1997). An experimental study of heavy metal attenuation and mobility in sandy loam soils. *Applied Geochemistry*, **12(3)**, pp. 243-254.

Gratwicke, B., (1999). The effect of season on a biotic water quality index: A case study of the Yellow Jacket and Mazowe Rivers, Zimbabwe. *South African Journal of Aquatic Sciences* ***24,*** pp. 24 – 35.

Groudev, S. N., Bratcova, S. G. and Komnitsas, K., (1999). Treatment of waters polluted with radioactive elements and heavy metals by means of a laboratory passive system*.* *Minerals Engineering* ***12***, pp 261-270.

Guller, C and Thyne, G D (2004). Hydrologic and geologic factors controlling surface and groundwater chemistry in Indian Wells-Owens Valley area, southeastern California, USA. *Journal of Hydrology 285*, 177–198.

Gundersen, P. and Steinnes, E., (2003). Influence of pH and TOC concentrations on Cu, Zn, Cd and Al speciation in rivers. *Elsevier Water Research* ***37***, pp. 307 – 318.

Hageman, P. L. and Briggs, P. H., (2000). A simple field leach test for rapid screening and qualitative characterization of mine waste dump material on abandoned mine lands. In *Proceedings from the Fifth International Conference on Acid Rock Drainage (ICARD2000)*, Denver, Colorado, Soc. Mining, Metallurgy, and Exploration, Inc., v.II, pp. 1463-1475.

Hedin R. S, Watzlaf, G. R. and Nairn, R. W., (1994). Passive treatment of acid mine drainage with limestone. *Journal of Environmental Quality* ***23,*** pp. 1338-1345.

Hedin, R.S., and Watzlaf, G.R., (1994). The effects of anoxic limestone drains on mine water chemistry: U.S. Bureau of Mines Special Publication SP 06A, pp. 185-194.

Hillel, D., (1982) *Introduction to Soil Physics.* Second edition. Academic Press, London.

Hollings, P., Hendry, M. J. and Kirkland, R. A., (2000). Quantification of oxygen consumption rates for gneissic waste rock piles, Key Lake Uranium Mine, Northern Saskatchewan, Canada: application of the kinetic cell technique. In *Proceedings Fifth International Conference on Acid Rock Drainage,* pp. 163-171.

Hornberger. R.J. and Brady, K.B.C., (1994). Kinetic (leaching) tests for the prediction of mine drainage quality. On-line manual for mine drainage in Penyslvannia. http://www.dep.state.pa.us/dep/deputate/minres/districts/cmdp/chap07.html

Hutt, N.M., and Morin, K., (2000). Observations and lessons from the International Static Database (ISD) on neutralizing capacity. pp. 603–611. *In* Proc. 5th Int. Conf. on Acid Rock Drainage, Denver, vol. 1. Soc. Mining Metall. Explor., Littleton, CO.

Hyman, D.M., and G.R. Watzlaf., (1995). Mine drainage characterization for the successful design and evaluation of passive treatment systems. In: *Proceedings, Seventeenth Annual Conference of the National Association of Abandoned Mine Lands,* French Lick, IN.

Jambor, J. L., (1994). Mineralogy of Sulfide-rich Tailings and Their Oxidation Products. *In Environmental Geochemistry of Sulfide Mine-wastes*, Mineralogical Association of Canada Short Course vol. **22**, pp. 59-102.

Jambor, J. L. and Blowes, D. W., (1998). Theory and Application of Mineralogy in Environmental Studies of Sulfide-Bearing Mine Wastes. In: *Modern Approaches to Ore and Environmental Mineralogy* (Cabri, L.J. and Vaughan, D.J., Eds.), Mineralogical Association of Canada Short Course, vol. **27**, pp. 367-402.

Jambor, J. L., and Blowes, D. W., (1994). The Environmental Geochemistry of Sulphide mine wastes, in *Mineralogical Association of Canada Short Course Handbook* (22): pp. 438.

Jambor, J. L and Dutrizac, J E (1998). Occurrence and constitution of natural and synthetic ferrihydrite, a widespread iron oxyhydroxide: Chemical Reviews, v 98, pp 2549-2585.

Jambor, J.L, Dutrizac, J.E, Raudsepp M and Groat L. A, (2002). Effect of Peroxide on Neutralization-Potential Values of Siderite and Other Carbonate Minerals, in Journal of Environmental Quality **32**:2373-2378.

Jambor, J.L., J.E. Dutrizac, L.A. Groat, and M. Raudsepp (2002). Static tests of neutralization potentials of silicate and aluminosilicate minerals. *Environ. Geol. (Berlin)* ***43***: pp.1–17.

Jaynes, D.B., Pionke, H.B., and Rogowski, A.S., (1984). Acid mine drainage from reclaimed coal strip mines--2. Simulation results of model: *Water Resources Research,* ***vol. 20 (2),*** p. 243- 250.

Jennings, S.R., D.J. Dollhopf, and Inskeep, W.P., (2000). Acid production from sulfide minerals using hydrogen peroxide weathering. *Appl. Geochem.* ***15***, pp. 35–243.

Jin, Y.L, Jeong, Y.C, Kang, K.L, Seok, Y.L and Min, H.L (2001). Staticastical Evaluation of Geochemical Parameters Distribution in a Grounwater System Contaminated with Petroleum Hydrocarbons. *In Journal of Environmental Quality,* ***35(5)***, pp. 1548 1563.

Kelly, M., (1988). Mining in the freshwater environment. Elsevier, Applied Science, Lon., U.K.

Kim, J. Y. and Chon, H. T., (2002). Pollution of a water course impacted by acid mine drainage in the Imgok creek of the Gangreung coal field, Korea. *App. Geochem.,* ***16***, pp 1387-1396.

Kimmel, W., (1983). The impact of acid mine drainage on the stream ecosystem. *In Pennsylvania Coal: Resources, Technology and Utilization, S. Majundar and W. Miller, (eds.).* pp. 142 – 146.

Kirsby, C. S. and Cravotta, C. A., (2005). Net Alkalinity and Net Acidity 1: Theoretical considerations. *Applied Geochemistry* ***20***, pp. 1920-1940.

Kleiv, R.A., Sandvik, K.L. & Thornhill, M.(2001): Pre-treatment of acid mine drainage using magnesium olivine. In: *Securing the Future - International Conference on Mining and the Environment,* Skellefteå, Sweden, vol. 1, pp. 336-342. The Swedish Mining Association.

Kwong, Y.T.J., (1993). Prediction and prevention of acid rock drainage from a geological and mineralogical perspective: *Canadian National Hydrology Research Centre Contribution CS-92054,* pp. 47.

Langmuir, D., (1997). Aqueous Environmental Geochemistry. Prentice Hall, Inc., New Jersey.

Lapakko, K.A., (1994a). Comparison of Duluth Complex Rock Dissolution in the Laboratory and Field. *Paper Presented at the International Land Reclamation and Acid Mine Drainage Conference and the Third International Conference on the Abatement of Acidic Drainage*, Pittsburgh, PA. April 24-29, 1994.

Lappako, K. A., (1994b). Evaluation of neutralization potential determinations for metal mine waste and a proposed alternative. In: *International Land Reclamation and Mine Drainage Conference and Third International Conference on the Abatement of Acidic Drainage*, U. S. Bureau of Mines Special Publication SP 06A-94, pp. 129-137.

Lappako, K., (2002). Metal Mine Rock and Waste Characterisation Tools: An Overview. MMSD Report No. **67**, pp 31.

Larson, B.R. and Guyette, W., (2002). Zimbabwe – A Crumbling Economy. In Economic Report on Africa 2002: Tracking Performances and Progress, pp. 109 – 135.

Lasaga, A.C., (1981). The sulfur cycle: University Park, Pennsylvania State University Earth and Mineral Sciences, vol**. 51(1)**, p. 1-11.

Lawrence, R.W., and Wang, Y., (1997). Determination of neutralization potential in the prediction of acid rock drainage. In: *Proc. 4th Int. Conf. on Acid Rock Drainage, Vancouver, BC, Canada.* Vol. 1, pp. 451–464.

Ledin, M. and Pedersen, K., (1996). The environmental impact of mine wastes—roles of microorganisms and their significance in treatment of mine wastes. *Earth-Sci. Rev.* ***41***, pp. 67–108.

Li, M.G., Aube, B., and St-Arnaud, L., (1997). Considerations in the use of shallow water covers for decommissioning reactive tailings. In: *Proceedings of the 4th International Conference on Acid Rock Drainage, Vancouver, BC, Canada.* Vol. 2, pp. 352–364.

Lin, Z. and Herbert, R. B. J., (1997). Heavy metal retention in secondary precipitates from a mine rock dump and underlying soil, Dalama, Sweden. *Environmental Geology*, ***33(1),*** pp. 1 -12.

Lupankwa, K., Love. D., Mapani, B., S and Museka, S., (2004). Impact of a base metal slimes dam on water systems, Madziwa Mine, Zimbabwe. *Physical Chemistry of the Earth* **29**, pp. 1145 – 1151.

Madigan M.T., Martinko J.M. and Parker J (2000). Brock Biology of Microorganisms, 9th edition. Prentice Hall, New Jersey.

Magadza, C. H. D. and Masendu, H., (1986). Some observations in the Yellow Jacket Stream, Zimbabwe. *Zimbabwe Science News 20*, pp 11 – 15.

Magombedze, C. and Sandvik, K.L., (2006). Profile of the Zimbabwe Metal Mining Industry and its Impact on the Environment. In *African Journal of Environmental Impact Assessment and Management*, vol. 11, pp. 64 - 86.

Magombedze, C., Sandvik, K.L., Dube, N., & Mutevhe, C., (2006). Geochemical Mass Balance of Pollutants Draining from a Nickel Mine Site. In *Proceedings of Metallurgical Plant*

Design and Operating Strategies (MetPlant 2006), Perth, Australia, 18 – 19 September 2006.

Magombedze, C., Sandvik, K.L., Manda, B. & Musiwa, K., (2006). Geochemical Controls on Acid Mine Drainage Neutralization Treatment at Iron Duke Mine. In *Proceedings of Metallurgical Plant Design and Operating Strategies (MetPlant 2006),* Perth, Australia, 18 – 19 September 2006.

Magombedze, C. and Brattli, B., (2003). The Role of Acid Mine Drainage in Heavy Metal Dispersion. *In Proceedings of the 6th International Conference on Acid Rock Drainage, pp. 1079 – 1085.*

Malmström, M., and Banwart, S., (1997). Biotite Dissolution at 25 °C: The pH Dependence of Dissolution Rate and Stoichiometry. *Geochim. Cosmochim. Acta, :**61**(14), pp.* 2779-2799.

Malmström, M., Destouni, G., Banwart, S.A., and Strömberg, B., (2000). Resolving the scale dependence of mineral weathering rates. *Environmental Science and Technology **34***: pp. 1375 - 1377.

Maponga, O. and Mutemererwa, A.., (1995). Management of Natural Resources and the Environment in Zimbabwe: The Case for Gold. *United Nations Conference on Trade and Development, 18 – 20 October, 1995,* Harare, Zimbabwe.

Marsden, J. and House, I., (1993). The chemistry of gold extraction. Ed. Ellis Horwood.

Mazvimavi, D., (2003). Estimation of Flow Characteristics of Ungauged Catchments, *PhD Thesis, 2003.*

Mckibben, M.A. and Barnes, H.L., (1986). Oxidation of Pyrite in Low Temperature Acidic Solutions: Rate Laws and Surface Textures. *Geochim. Cosmochim. Acta* **50,** pp. 1509 – 1520.

MEND (2000). MEND Manual, Volume 3 – Prediction (Eds: Trembay, G.A. and Hogan, C.M.). MEND project **5.4.2c.** MEND (Mine Environment Neutral Drainage) Programme, Natural Resources Canada, Ottawa, Ontario.

MEND (2001). Mine Environment Neutral Drainage (MEND) technical reports.

Miller, S. D., J. J. Jeffery, and J.W.C. Wong, (1991). Use and misuse of the acid base account for "AMD" prediction. In: *Proceedings Second International Conference on the Abatement of Acidic Drainage, Vol. 3,.* CANMET, Ottowa, Ontario, pp. 489-506.

Miller. S., Smar. R., Andrina. J., Neale, A. and Richards, A., (2003). Evaluation of Limestone Covers and Blends for Long-Term Acid Rock Drainage Control at the Grasberg Mine, Papua Province, Indonesia. *In Proceedings of the 6th International Conference on Acid Rock Drainage, pp. 132 – 142.*

Mills, C., (1998). Kinetic testwork procedures. http://www.enviromine.com/ard.index.html

Mok, W.M. and Wai, C.M., (1994). Mobilisation of Arsenic in river waters. In Journal of arsenic in the Environment (ed. O. Nrigau). Part 1: Cycling and Characterisation. Willey, New York, pp. 99 – 118.

Morin, K.A. and Hutt, N.M., (1997). Environmental Geochemistry of Minesite Drainage: Practical Theory and Case Studies. MDAG Publishing, Vancouver, Canada.

Morrison, J.L., Scheetz, B.E., Strickler, D.W., Williams, E.G., Rose, A.W., Davis, A., and Parizek, R.R., (1990). Predicting the occurrence of acid mine drainage in the Alleghenian coal-bearing strata of western Pennsylvania; an assessment by simulated weathering (leaching) experiments and overburden characterization. In Chyi, L.L., and Chou, C.L., (editors), *Recent advances in coal geochemistry. Geological Society of America, Special Paper* ***248***. pp. 87 - 99.

Moses, C. O, and Herman, J S (1991). Pyrite oxidation at circumneutral pH. *Geochimica et Cosmochimica Acta* ***55***, pp. 471-482.

Moses, C.O., Nordstrom, D.K., Herman, J.S. and Mills, A. L., (1987). Aqueous pyrite oxidation by dissolved oxygen and by ferric iron. *Geochim. Cosmochim. Acta,* ***51***, pp. 1561-71.

Moyo, N.A.G., (1999). Impact on the Zimbabwean Lake Waters by Industrial, Agricultural and Other Pollution Sources. Workshop on Sustainable Management of the Lakes of Zimbabwe by the International Lake Environment Conservation, Harare, Zimbabwe.

Mukasa, S.B., Wilson, A.H. & Carlson, R.W., (1998). A multielement geochronological study of the Great Dyke, Zimbabwe: significance of the robust and reset ages. *Earth and Planetary Science Letters,* ***164****,* pp. 353-369.

Munk, L., Faure, G., Pride, D. E. and Bigham, J. M., (2002). Sorption of trace metals to an aluminum precipitate in a stream receiving acid rock-drainage; Snake River, Summit County, Colorado. *Applied. Geochemistry* ***17***, pp. 421–30.

Murdock, D. J., Fox, J. R. W. and Bensley, J. G., (1994). Treatment of acid mine drainage by the high density sludge process. *International Land Reclamation and Mine Drainage Conference and the Third International Conference of the Abatement of Acidic Drainage*, April 24-29, Pittsburgh, PA.

Newman, L.L., Herasymuik, G.M., Barbour, S.L., Fredlund, D.G., and Smith, T., (1997). The hydrogeology of waste rock dumps and a mechanism for unsaturated preferential flow. In *Proceedings of the Fourth International Conference on Acid Rock Drainage,*Vancouver, Canada, May 31 - June 6, Volume III, pp. 551 - 565.

Nicholson, R.V and Scharer J.M., (1994). Iron-sulphide oxidation mechanisms: Laboratory studies. In*: Environmental Geochemistry of Sulphide Mine-Wastes.* J.L. Jambor and D.W. Blowes (Editors), Short course handbook, vol.22, Mineralogical Association of Canada, pp.163-183.

Nimick, D. A., Gammons, C. H., Cleasby, T. E., Madison, J. P., Skaar, D. and Brick, C.M.,(2003). Diel cycles in dissolved metal concentrations in streams - Occurrence and possible causes. *Water Resources Research,* ***39*****:** pp. 1247-1264.

Noller, B.N., P.H. Woods, and B.J. Ross., (1994). Case studies of wetland filtration of mine waste water in constructed and naturally occurring systems in Northern Australia. *Water Sci. Tech.* ***29*****:** pp. 257-266.

Nordstrom, D. K. and Alpers, C. N., (1999). Geochemistry of acid mine waters, In *The Environmental Geochemistry of Mineral Deposits* (eds: Plumlee, G S and Logsdon, M J), Part A. Processes, methods, and health issues: Reviews in Economic Geology, (6) pp. 27.

Nordstrom, D. K., (1977). Thermochemical redox equlibria of ZoBell's solution, in *Geochim. Cosmochim., Acta* ***(52):*** pp. 1077 – 1085.

Nordstrom, D. K., (1982). The effect of sulphate on aluminium concentrations in natural waters: some stability relations in the system Al_2O_3-SO_3-H_2O at 298 K, in *Geochim. Cosmochim., Acta* ***(46)***: pp. 681 - 92.

Nordstrom, D. K., (2000). Advances in the hydrochemistry and microbiology of acid mine waters, in *International Geology Review* ***(42):*** 499–515.

Nordstrom, D. K, Alpers, C.N., Ptacek, C.J., and Blowes, D.J., (2000). Negative pH and extremely acidic mine waters from the Iron mountain, California, *in Environmental Science Technology* ***(34)***: pp 254 – 258.

Nordstrom, D.K., Jenne, E.A and Ball, J.W., (1979). Redox equilibria of iron in acid mine waters. *In Chemical Modeling in Aqueous Systems.* Jenne, E A (ed). American Chemistry Society Symposium Series 93, pp 51- 80.

Paktunc, A.D., (1999). Characterization of mine wastes for prediction of acid mine drainage. pp. 19–40. *In* J.M. Azcue (ed.) *Environmental impacts of mining activities.* Springer-Verlag, New York.

Parkhurst, D.L., and Appelo, C.A.J., (1999). User's guide to PHREEQC (Version 2) - a computer program for speciation, batch-reaction, one-dimensional transport, and inverse geochemical calculations. US Geological Survey, Denver (CO), *Water-Resources Investigations Report 99-4259.* pp. 312.

Parkhurst, D.L., and Plummer, L.N., (1993). Geochemical models, in Alley, W.M., ed., Regional ground-water quality: New York, Van Nostrand Reinhold, chap. 9, p. 199-225.

Parliament of Zimbabwe, (2003). Environmental Management Act [Chapter 20:27], Zimbabwe Government Publications, Harare, Zimbabwe, 2003.

Patrick Jr, W.H. and Verloo, M., (1998). Distribution of soluble heavy metals between ionic and complexed forms in saturated sediments as affected by pH and redox conditions, in *Water Science and Technology* ***37 (6 – 7),*** pp. 165 – 172.

Perkins, E.H., Nesbitt, H.W., Gunter, W.D., St-Arnaud, L.C. and Mycroft, J.R., (1995). Critical Review of Geochemical Processes and Geochemical Models Adaptable for Prediction of Acidic Drainage from Waste Rock. MEND Project report 1.42.1.

Pitzer, K.S., (1995). Activity Coefficients in Electrolyte Solutions. 3rd ed, Boca Raton, CRC Press.

Plumlee, G.S., Smith, K.S., Montour, M.R., Ficklin, W.H., and Mosier, E.L. (1999). Geologic controls on the composition of natural waters and mine waters draining diverse mineral-deposit types, pp. 373-432 In: Filipek, L.H., and Plumlee, G.S. (eds.), *The Environmental Geochemistry of Mineral Deposits, Part B.* Society of Economic Geologists, Reviews in Economic Geology, v. 6B.

Plummer, L. N., Parkhurst, D. L., Fleming, G. W. and Dunkle, S. A.: *A computer program incorporating Pitzer's equations for calculation of geochemical reactions in brines,* U.S. Geological Survey Water-Resources Investigations Report 92-4153 (1992), 310 p

Plummer, N., Wigley, T. M. L., and Parkhurst, D L., (1978). "The Kinetics of Calcite Dissolution In $C0_2$-Water Systems 5^0C to 60^0C And 0.0 To 1.0 Atm CO_2" *In American Journal Of Science*, ***vol. 278,*** pp 179-216.

Price, W. A. and Kwong, Y. T. J., (1997). Waste Rock Weathering, Sampling and Analysis: Observations from the British Columbia Ministry of Employment and Investment Database, *Proceedings 4th International Conference on Acid Rock Drainage, Vancouver*, pp. 31-45.

Price, W.A.. (1997). Draft: Guidelines and Recommended Methods for the Prediction of Metal Leaching and Acid Rock Drainage at Minesites in British Columbia. British Columbia Mine Reclamation Section (MRS). British Columbia Ministry of Employment and Investment, Energy and Minerals Division

Price, W.A., and Errington, J.C., (1998). Guidelines for metal leaching and acid rock drainage at minesites in British Columbia: British Columbia Ministry of Energy and Mines, pp. 86.

Ravengai, S., Love, D., Love, I., Gratwicke, B., Mandingaisa, O., and Owen, O.R.J., (2005). Impact of Iron Duke Pyrite Mine on water chemistry and aquatic life – Mazowe Valley, Zimbabwe, in *Water SA,* pp. 219 – 228.

Rimstidt, J.D., and Newcomb, W.D., (1993). Measurement and analysis of rate data - The rate of reaction of ferric iron with pyrite: *Geochimica et Cosmochimica Acta,* ***57***, pp. 1919-1934.

Rimstidt, J.D., and Vaughan, D.J., (2003). Pyrite oxidation: a state-of-the-art assessment of the reaction mechanism. *Geochimica et Cosmochimica Acta,* ***67***: pp. 873 - 880.

Ritchey, G. M., (1989). *Tailings Management: Problems and Solutions in the mining industry*, pp. 69 – 345 (Elsevier, Amsterdam).

Ritchie, A.I.M., (1994). The waste-rock environment. pp. 133–161. *In* J.L. Jambor and D.W. Blowes (ed.) *The environmental geochemistry of sulfide mine-wastes*. Mineral. Assoc. Canada Short-Course Vol. 22. Mineral. Assoc. Canada, Nepean, ON.

Robertson, W.D., D.W. Blowes and C.J. Hanton-Fong, (1997). Sulfide oxidation related to water table depth at two Sudbury, Ontario tailings impoundments of differing physiography. In: *Proceedings of the Fourth International Conference on Acid Rock Drainage*, Vancouver, British Columbia, pp. 621-629.

Robinson, R.A., and Stokes, R.H., (1970). Electrolyte Solutions, second edition. Butterworth, London. pp. 571.

Rose, A. W. and Cravotta, C. A., (1998). Geochemistry of Coalmine Drainage, *in Coal Mine Drainage Prediction and Pollution Prevention in Pennsylvania* (Eds: Brady, K B C, Smith, M.W. and Schueck, J), pp 1.1–1.22.

Rott, U., and B. Lamberth (1993). Groundwater cleanup by in situ treatment of nitrate, iron and manganese. *Water Supply* 11, 143-156.

SADC (2000). Revised protocol on Shared Watercourses in the Southern African Development Community. Southern African Development Community, Gaborone, Botswana.

Saether, O.M., Storroe, G., Segar, D. and Krog, R., (1997). Contamination of Soil and groundwater at a former industrial site in Trondeim, Norway. In: *Applied Geochemistry,* ***vol. 12,*** pp. 327 – 332.

Salmon, S.U. and Malmström, M.E., (2003). Biogeochemical processes in mill tailings impoundments: Modelling of groundwater composition and remediation effects. *Appllied. Geochemistry,* ***vol.*** **19**: pp. 1-17.

Salomons, (1995). Environmental Impact of metals derived from mining activities: Processes, prediction, prevention. *Journal of Geochemical Exploration,* ***52,*** pp. 5 – 23.

Sandvik, K.L and Esse, R., (2002). Private Communication.

Sato, M., (1960). Oxidation of sulfide ore bodies - Ll: Oxidation mechanism of sulfide minerals at 25°C. In: *Economic Geology*, ***55:*** pp. 1202-1231.

Schneider, W. & Schwyn B., (1987). The hydrolysis of iron in synthetic, biological and aquatic media. In: *Aquatic surface chemistry:Chemical processes at the particle-water interface.* Ed: W. Stumm. J. Wiley & Sons, New York, 1987; Ch. 7, pp. 167–196.

Schwartz, F.W., and Crowe, A.S., (1985). Simulation of changes in ground-water levels associated with strip mining. *Geological Society of America Bulletin,* ***9*****:** pp. 253 - 262.

Schwertmann, U. and Cornell, R.M., (1991). Iron oxides in the laboratory: Preparation and characterization. VCH, Weinheim, Germany.

Schwertmann, U., Murad, E., Bigham, J. M., and Carlson, L., (1995). Mineralogical characteristics of poorly crystallized precipitates formed by oxidation of Fe^{2+} in acid sulfate waters. In E*nvironmental Geochemistry of Sulfide Oxidation* (eds. Alpers, C.N., and Blowes, D B,): *American Chemical Society Symposium Series (****550****)* pp. 190-200.

Sheoran, A.S. and Sheoran, V., (2006). Heavy metal removal mechanism of acid mine drainage in wetlands: A critical review. In: *Minerals Engineering,* ***19(2),*** pp. 105-116.

Sherlock, E. J., Lawrence, R. W. and Poulin, R., (1995). On the neutralization of acid rock drainage by carbonate and silicate minerals. *Environmental Geology*, ***25,*** pp. 43-54.

Singer, P. C. and Stumm, W., (1970). Acidic mine drainage: The rate-determining step. In *Science*, **(167),** pp. 1121-1123.

Skousen, J., Politan, K., Hilton, T., Meek, A., (1995). Acid mine drainage treatment systems: chemicals and costs. In: Skousen, J.G., Ziemkiewicz, P.F., (Compilers), Acid Mine Drainage—Control and treatment. West Virginia University and the National Mine Land Reclamation Center, Morgantown, WV, pp. 121-129.

Smith, A., (1994). The geochemistry of cyanide in mill tailings. In: *Environmental geochemistry of sulphide mine wastes* (D.W. Bowles & J.L. Jambor, Eds). Mineralogical Association of Canadá, Ontario, pp. 293-332.

Smith, K. S., Plumlee, G. S. and Ficklin, W. H., (2002). Predicting water contamination from metal mines and mining wastes. *USGS open file report 2002-264.*

Smith, K.S., and Huyck, H.L.O., (1999). An overview of the abundance, relative mobility, bioavailability, and human toxicity of metals. In: *The Environmental Geochemistry of Mineral Deposits.* Part A: Vol. 6A, Chapter 2. Plumlee, G., Logsdon, M. (eds.). Reviews in Economic Geology. Society of Economic Geologists, Inc., Chelsea, MI.p p. 29-70.

Smith, V.W., (2003). Experience in mine closure planning and implementation in Bindura Nickel Corporation, Zimbabwe. *Bullion Conference on Mine Closure, Johannesburg, S.A.*

Smythe, G. R., (1995). Iron Duke Acid mine drainage. In: *Proceedings of Mining and Environment in Zimbabwe*, 1995. The Institute of Mining and Metallurgy in Zimbabwe, pp. 92 – 98.

Sobek, A. A., Schuller, W.A., Freeman, J.R., Smith, R.M., (1978). Field and laboratory methods applicable to overburdens and mine soils. EPA-600/2-78-054. Ohio: U.S. Environmental Protection Agency, Cincinnati.

Sobolewski, A., (1997). The Capacity of Natural Wetlands to Ameliorate Water Quality: A Review of Case Studies. In: *Proceeding from 4th International Conference on Acid Rock Drainage,* ***Vol. 4***, pp. 1551–63.

Sposito, G., (1984). The surface chemistry of soils. Oxford Univ. Press, Oxford, England.

Strömberg, B. and Banwart, S.A., (1994). Kinetic modelling of geochemical processes at the Aitik mining waste rock site in northern Sweden. *Applied Geochemistry,* ***9***: pp. 583 - 595.

Stumm, W. and Morgan, J.J., (1996). Aquatic Chemistry (3^{rd} Edition). J. Wiley and Sons, New York.

Sverdrup, H., (1990), The Kinetics of base cation release due to chemical weathering, Lund University Press, pp. 245.

Svotwa, R. S., (1999). Assessment of the impacts of mining in Zimbabwe with a focus on small scale and artisanal mining. *Mining and the Environment in Zimbabwe, 1999,* pp. 11 – 29.

Thixton, D.H., (1999). Managing Mercury in Mining. *Zimbabwe Chamber of mines Journal,* ***21 (5),*** pp. 19 – 35.

Thornton, S.F., Tellam, J.H. and Lerner, D.N., (2000). Attenuation of landfill leachate by UK Triassic Sandstone aquifer materials: 1. Fate of inorganic pollutants in laboratory columns. *Journal of Contaminant Hydrology.,* ***43****,* pp. 327–354.

Truesdell, A.H. and Jones, B.F., (1973). Wateq, a computer program for calculating chemical equilibria of natural waters. US Geological Survey, NTIS PB 220 464, pp. 73.

Vallee, M., (1999). Sampling Quality Control, Exploration and Mining Geology, **7** (1 & 2).

Van Beek, C.G.E.M., (1980). A model for the induced removal of iron and manganese from groundwater in the aquifer. In *Proc. 3rd Water-Rock Interaction Symp.,* Edmonton, Canada, 29-31.

Walder, I. and Schuster, P., (1998). Acid Rock Drainage. In: *SARB Consulting, Inc. Environmental geochemistry of ore deposits and mining activities*. Short course Notes, Albuquerque, New Mexico.

Watzlaf, R.R., Schroeder, K.T., Kairies, C.L., (2000). Long-term performance of anoxic limestone drains. *Mine Water Environ.* ***19****,* pp. 98–110.

Weatherell, C.S, Feasby, D.G., and Trembley, G.A., (1997). A decade of technology improvement to the challenge of acid mine drainage – A Canadian Perspective. In *Proceedings of the Fourth International Conference on Acid Rock Drainage,* pp 1-10.

Webster, J. G., Swedlund, P. J. and Webster, K. S., (1998). Trace metal adsorption onto an acid mine drainage iron(III) oxyhydroxy sulphate. *Environmental Science and Technology,* ***32****,* pp 1361 – 1368.

White, W.W. III., and Lapakko, K.A., (2000). Preliminary Indications of Repeatability and Reproducibility of the ASTM 5744-96 Kinetic Test for Drainage pH and Sulfate Release Rate. In: *Proceedings from the Fifth International Conference on Acid Mine Drainage.* SME, Littleton CO, pp. 795 – 818.

White, W.W. III., Lapakko, K.A. and Cox, R.L., (1999). Static-test methods most commonly used to predict acid-mine drainage: Practical guidelines for use and interpretation. *In* G.S. Plumlee and M.J. Logsdon (ed.) The environmental geochemistry of mineral deposits. Rev. Econ. Geol. 6A, pp. 325–338.

WHO (2003). World Health Organisation. Guidelines on Drinking Water Quality, http://www.who.int/water_sanitation_health/dwq/guidelines/en/

Wiebner, A., Kappelmeyer, U., Kuschk, P., Kastner, M., (2005). Influence of the redox condition dynamics on the removal efficiency of a laboratory scale constructed wetland, in *Water Research* ***(29)***, pp. 248 – 256.

Wildeman, T., J., Gusek, J., Dietz, B. and Morea, S., (1991). Handbook for Constructed Wetlands receiving Acid Mine Drainage. US EPA, Cincinnati, OH.

Williams, T. M., and Smith, B., (2000). Hydrochemical characterisation of acute acid mine drainage at Iron Duke Mine, Mazowe, Zimbabwe. *Environmental Geol.* ***39***, pp. 272 – 278.

Winland, R.L., Traina, S.J., and Bigham, J.M., (1991). Chemical composition of ochre-ous precipitates from Ohio coal mine drainage. *Journal of Env. Quality,* ***20,*** pp. 452–460.

Wood, S.C., Younger, P.L., and Robins, N.S., (1999). Long-term changes in the quality of polluted minewater discharges from abandoned underground coal workings in Scotland. *Quarterly Journal of Engineering Geology,* ***32***: 69 – 79.

Woods, P.H. and B.N. Noller, (1995). Medium-term performance of wetlands improving water quality of near-neutral mine drainage in the Northern Territory. In: *National conference on Wetlands for water quality control.* James Cook University, Townsville, Australia. 25-29 September, 1995.

Woulds, C. and Ngwenya B.T., (2004). Geochemical processes governing the performance of a constructed wetland treating acid mine drainage, Central Scotland. In: *Applied Geochemistry*, ***19 (11)***, pp. 1773-1783.

Young, G. K., Stein, S., Cole, P., Kammer, T., Graziano, F. and Bank, F., (1996). Evaluation and Management of Highway Runoff Water Quality. FHWA-PD-96-032. Federal Highway Administration, Office of Environment and Planning.

Younger, P. L, Banwart, S. A. and Hedin, R. S., (2002). Mine water hydrology, pollution, remediation. Kluwer Academic Publ., Boston.

Younger, P.L., (1995). Hydrogeochemistry of minewaters flowing from abandoned coal workings in the Durham Coalfield. *Quarterly Journal of Eng. Geology,* ***28:*** S101 - S113.

Younger, P.L., (1998). Coalfield abandonment: geochemical processes and hydrochemical products. In: Nicholson, K., (ed), *Energy and the Environment - Geochemistry of Fossil, Nuclear and Renewable Resources.* Society for Environmental Geochemistry and Health. McGregor Science, Aberdeen. pp. 1 - 29.

Yu, J.Y., Heo, B., Choi, I., Cho, J., Chang, H., (1999). Apparent solubilities of schwertmannite and ferrihydrite in natural stream waters polluted by mine drainage. *Geochim. Cosmochim. Acta* ***63,*** pp. 3407–3416.

Zelmanowitz, S., W.C. Boyle, D.E. Armstrong, and J.K. Park., (1995). Ability of subsoils to buffer extremely acidic simulated coal-pile leachates. *Journal of Env. Eng.* ***121****:pp.816–823.*

Zhang, C.S. and Selinus, O., (1998). Statistics and GIS in environmental geochemistry -- some problems and solutions. *Journal of Geochemical Exploration,* ***64(1-3)***: pp. 339-354.

Zhu, C. and Anderson, G. M., (2002). Environmental Applications of Geochemical Modeling. Cambridge University Press, London, pp. 304.

Ziemkiewicz, P.F., Skousen, J.G., Brant, D.L., Sterner, P.L., Lovett, R.J., (1997). Acid mine drainage treatment with armored limestone in open limestone channels. *Journal of Environmental Quality*, ***26***, pp. 1017–1024.

Zimba, O.L., (1999). Water Pollution Law, Institution and Administration for the Management of Fresh water Resources in Zimbabwe. Study Report for the Lake Environment Conservation in Developing countries, Harare, Zimbabwe, pp. 155.

Zinck, J.M., (2004). Lime Sludge Management – An Update on Technologies. Presented at Sludge Management and Treatment of Weak Acid or Neutral pH Drainage. In: *Proceedings of the 2004 Ontario MEND Workshop, MEND report W.017*, Sudbury Ontario.

ZINWA (1998). Zimbabwe National Water Authority, Water Act No. 31, *Waste Discharge and Disposal (Water Pollution), Chapter 20: 24 – 25*. Harare, Government of Zimbabwe Publications.

APPENDICES

APPENDIX A: Water Quality Guidelines

Table A1: ZINWA Water quality guidelines for Effluent Discharge (1998)

CONSTITUENT	**MAXIMUM PERMISSIBLE CONCENTRATION (mg/l)**			
	ZONE 1	***ZONE 2***	***SAZ, 1997 (7-9$_{Drinking}$)***	***WHO (Drinking H_2O)***
Temperature ^{o}C	25	35	< 20	< 15
pH	6.0 – 7.5	6.0 – 9.0	6.5 – 8.5	6.5 – 8.5
Dissolved Oxygen (DO)	60%	75%		
Total Suspended Solids (TSS)	10	25		
Total Dissolved Solids (TDS)	100	500	< 500	< 500
Chemical Oxygen Demand (COD)	30	60		
Biological Oxygen Demand (BOD)	5	10		
Soap, oil & grease	0	2.5		
Free Ammonia (N)	0.5	0.5		
Arsenic (As)	0.05	0.05	0.005	0.01
Barium (Ba)	0.1	0.5		0.7
Boron (Bo)	0.5	0.5		0.5
Cadmium (Cd)	0.01	0.01	0.01	0.003
Chlorides (Cl)	50	100	< 200	<200
Chlorine residual	0	0.1		
Chromium (Cr)	0.05	0.05		0.05
Copper (Cu)	0.02	0.05	0.1	2.0
Cyanides & related compounds (CN)	0.2	0.2	0.1	0.07
Detergents (as manoxo 100T)	0.2	0.1		
Fluoride (F)	1.0	1.0	<1.0	1.50
Iron (Fe)	0.3	0.3	<0.3	<0.5
Lead (Pb)	0.05	0.05	0.05	0.01
Manganese (Mn)	0.1	0.1	0.1	0.5
Mercury (Hg)	0.5	0.5	0.001	0.001
Nickel (Ni)	0.3	0.3		0.02
Nitrogen (Total N)	10.0	10.0	10.0	3.0
Phenolic compounds (as Phenol)	0.01	1.0	0.005	
Phosphate (Total P)	1.0	1.0		
Sulphate (SO_4)	50	200	<200	<250
Sulphides (S)	0.05	0.2		
Zinc (Zn)	0.3	1.0	<1.0	<5.0
Total Heavy Metals	1.0	2.0		
Herbicides, pesticides & insecticides	Not to be found in concentrations injurious to health of humans, animals, vegetable or aquatic life.			

Table A2: ZINWA Classification Standards for Effluent Disposal*

Parameter	**Blue**		**Green**	**Yellow**	**Red**
	Sensitive	**Normal**			
Temperature ^{o}C	≤25	≤35	≤40	≤40	≤40
pH	6.0-7.5	5.5– 9.0	5.5 – 9.0	5.5 – 9.0	5.5 – 9.0
BOD	≤15	≤30	≤50	≤100	>100
COD	≤30	≤60	≤90	≤150	>150
TSS	≤10	≤25	≤50	≤100	>100
TDS	≤100	≤500	≤1000	≤1500	>1500
DO	≥7	≥6	≥5	≥4	>4
Free Ammonia	≤0.5	≤0.5	≤1.0	≤1.5	>1.5
Chloride (Cl)	≤200	≤250	≤300	≤400	>400
Chloride residual	Nil	≤0.1	≤0.2	≤0.3	>0.3
Sulphate	≤100	≤250	≤300	≤400	>400
Sulphide	≤0.05	≤0.2	≤0.3	≤0.4	>0.4
CN	≤0.05	≤0.05	≤0.1	≤0.15	>0.2
Detergents	≤0.2	≤1	≤2	≤3	>3
Grease & Oil	Nil	≤2.5	≤5	≤7.5	>7.5
As	≤0.05	≤0.05	≤0.1	≤0.15	>0.15
Fe	≤0.3	≤1	≤2	≤5	>5
Ba	≤0.1	≤0.5	≤1	≤1.5	>1.5
Bo	≤0.5	≤0.5	≤1	≤1.5	>1.5
Cu	≤0.02	≤0.5	≤1.5	≤3	>3
F	≤1	≤1	≤2	≤4	>4
Ni	≤0.3	≤0.3	≤0.6	≤0.9	>0.9
Total N	≤10	≤10	≤20	≤30	>30
Total P	≤0.5	≤0.5	≤1.5	≤3	>3
Cd	≤0.01	≤0.01	≤0.5	≤0.1	>0.1
Cr (IV)	≤0.05	≤0.05	≤0.1	≤0.2	>0.2
Hg	≤0.01	≤0.01	≤0.02	≤0.03	>0.03
Pb	≤0.05	≤0.05	≤0.1	≤0.2	>0.2
Total Heavy Metals	≤1.0	≤2.0	≤4	≤10	>10
Feacal coliforms (No. per 100ml)	≤1000	≤1000			

*Measurements are in mg/l unless otherwise stated.

The classification is based on the quality of effluent and the potential environmental risk as submitted by the permit applicant and as assessed by the Water Pollution Control Section.

APPENDIX B: Plant Flowsheets and Sampling Locations

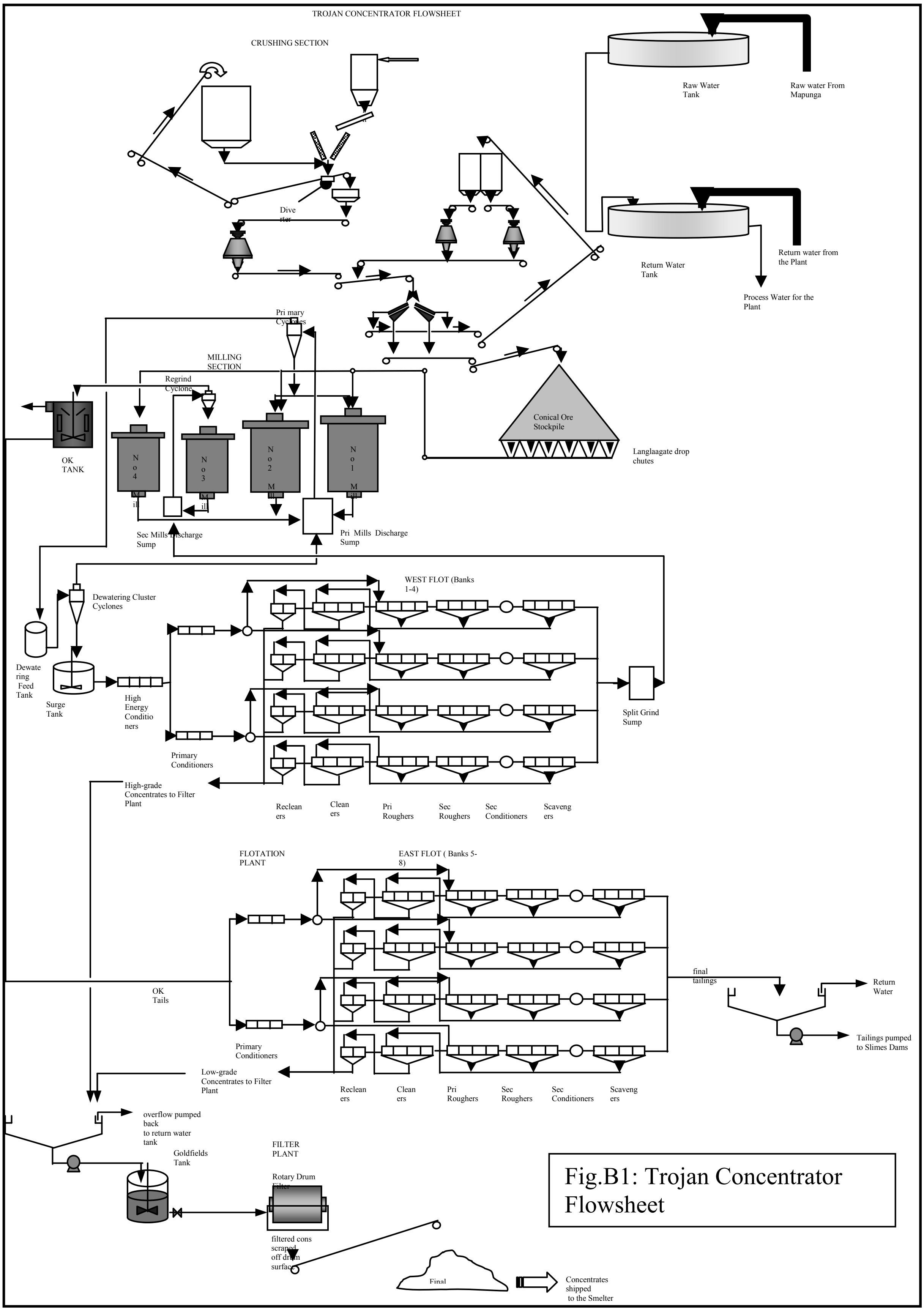

Fig.B1: Trojan Concentrator Flowsheet

Fig.B2: Mazowe Mine Processing Plant Flowsheet

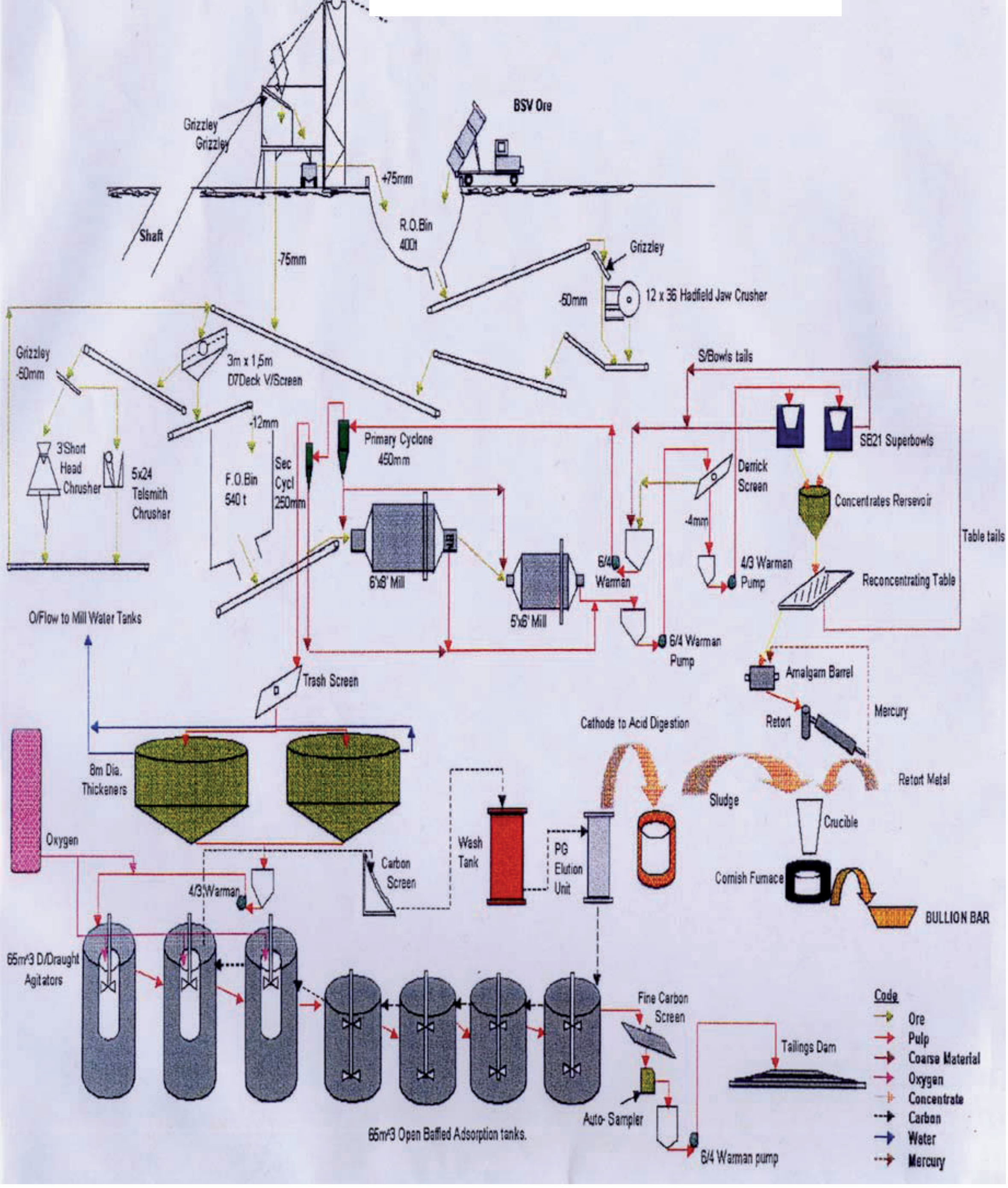

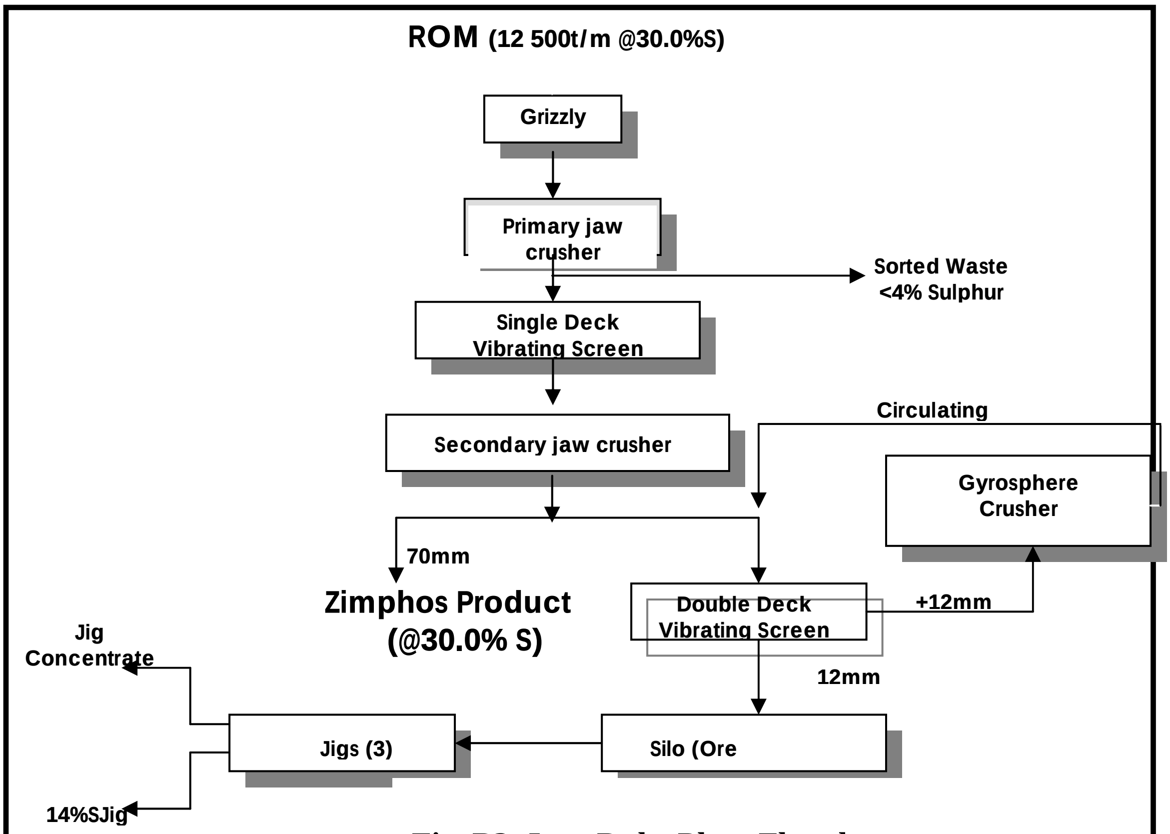

Fig. B3: Iron Duke Plant Flowsheet

Fig.B4: Trojan Nickel Mine (Site 1) Drainage Sampling Plan

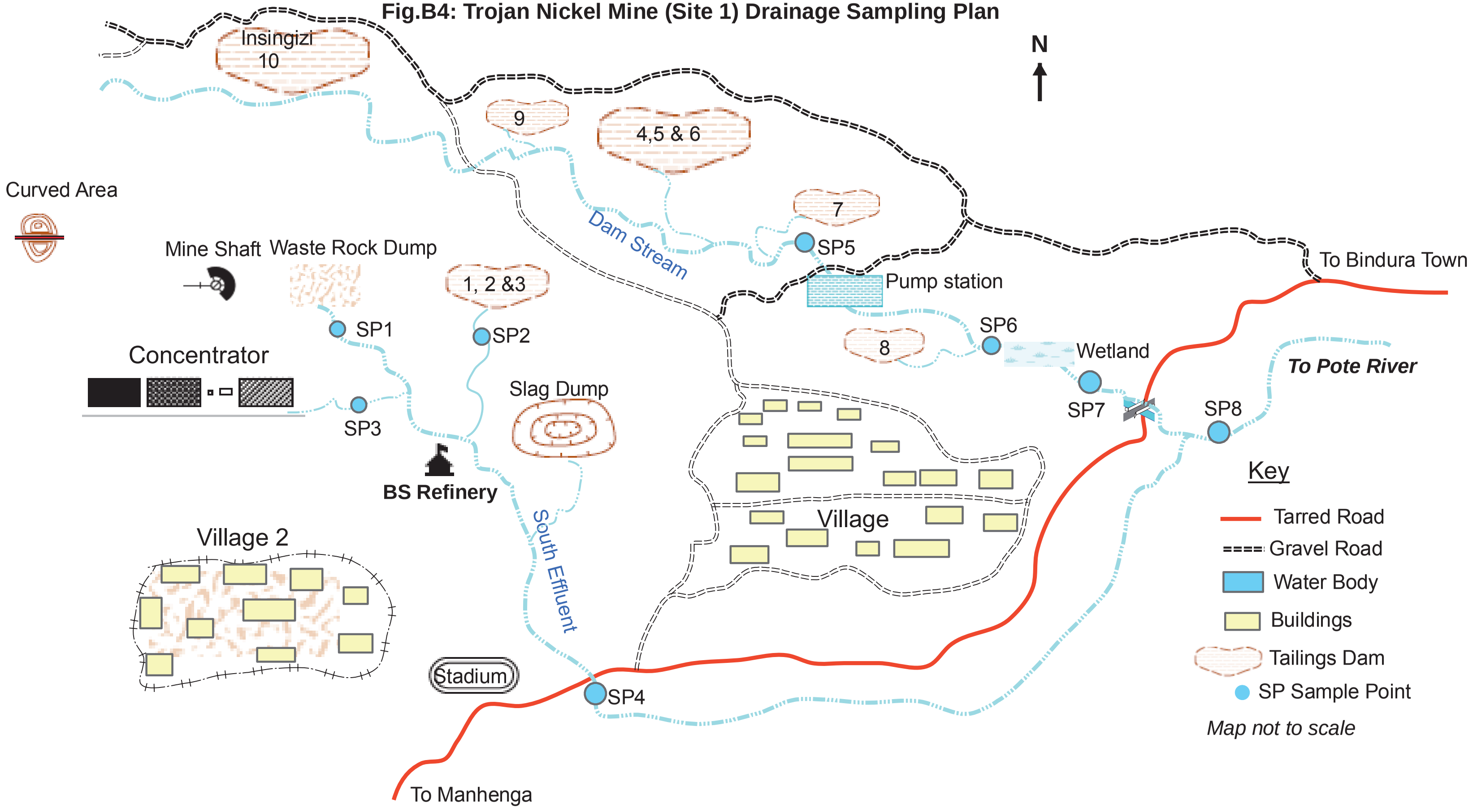

Fig. B5: Mazowe Mine (Site 2) Drainage Sampling Locations

(Adapted from site map originally drawn by Thomas Melsom Edvardsen, 2000)

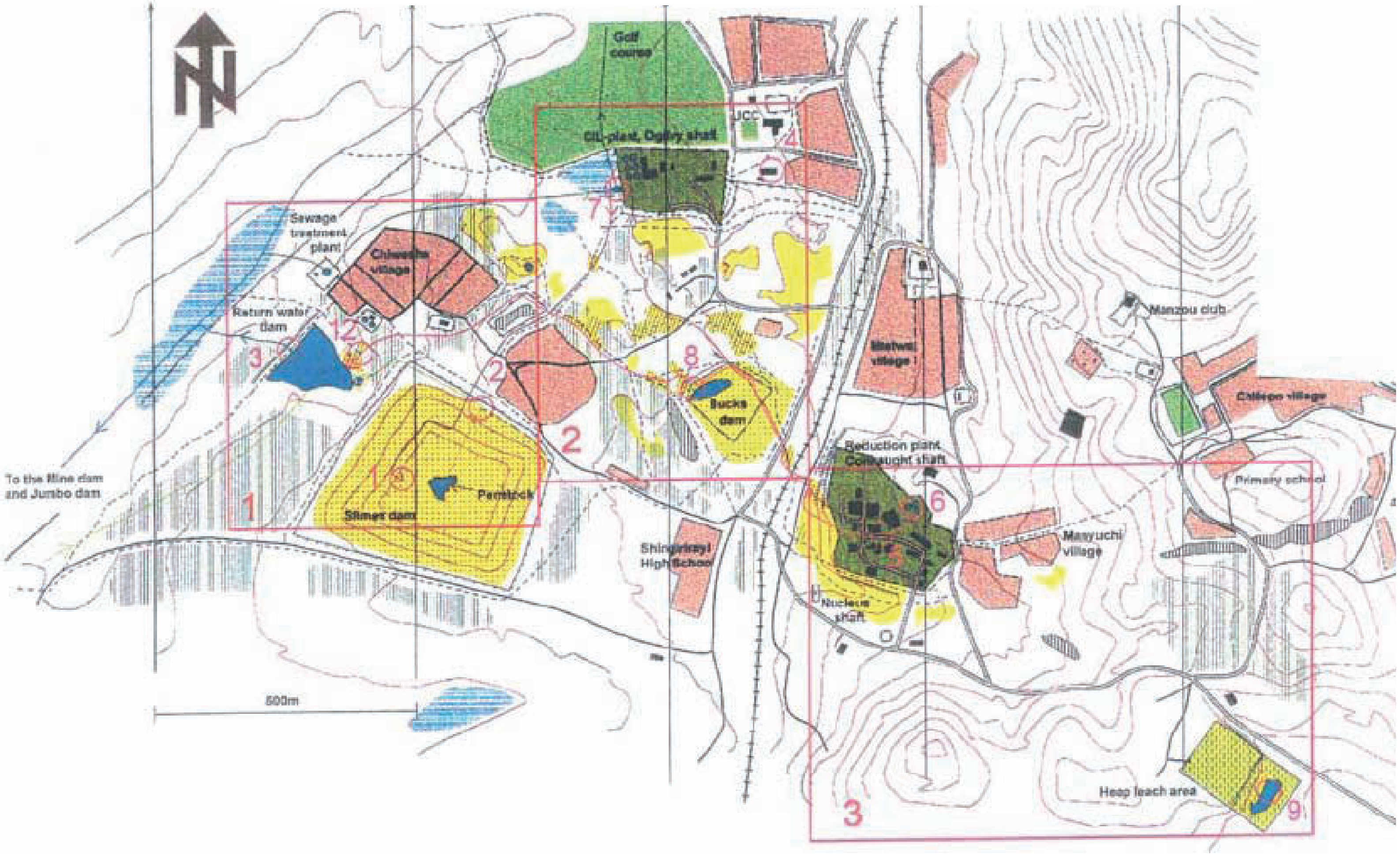

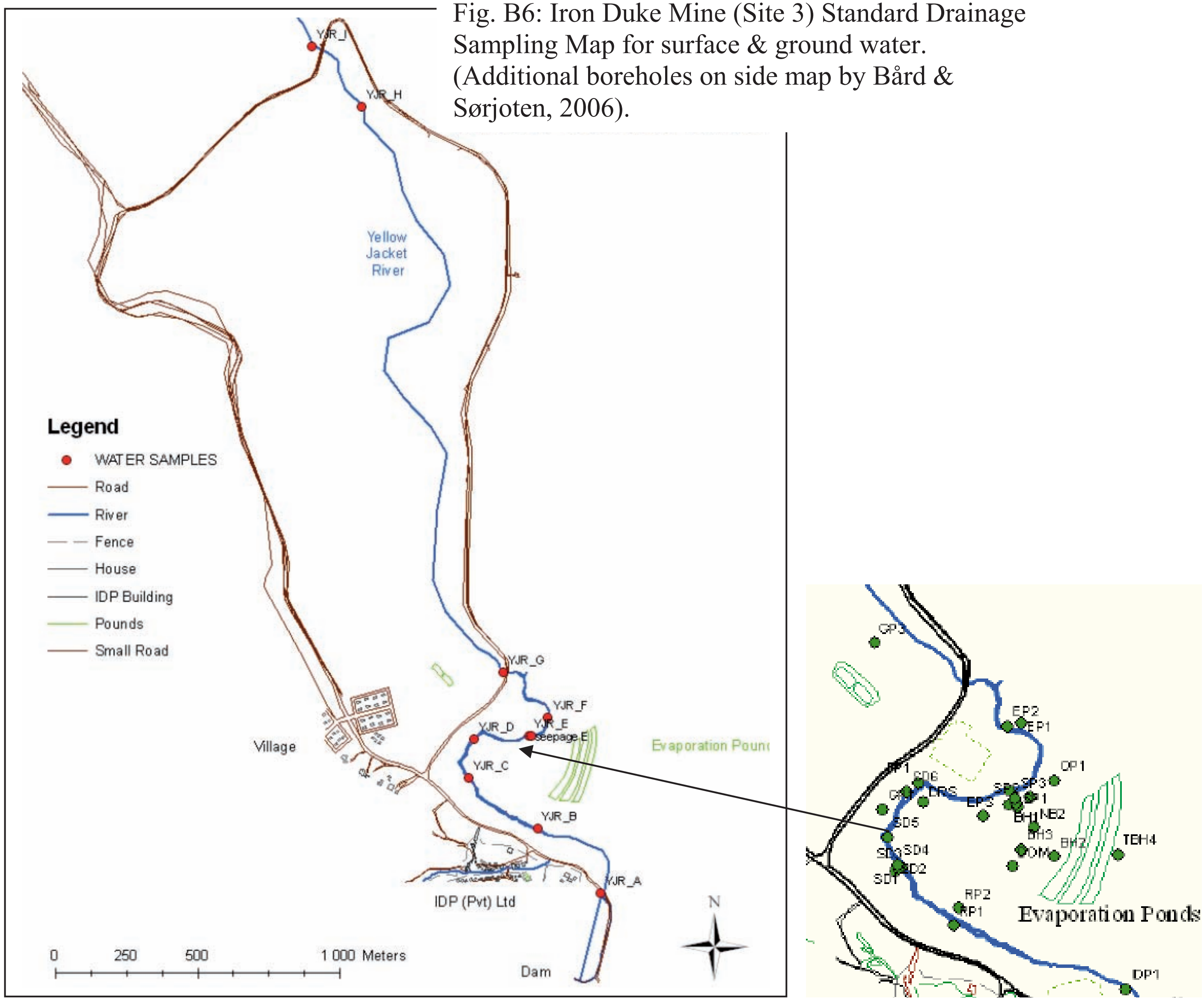

Fig. B6: Iron Duke Mine (Site 3) Standard Drainage Sampling Map for surface & ground water. (Additional boreholes on side map by Bård & Sørjoten, 2006).

APPENDIX C: Hydrochemical, ABA & Metals Data from monitoring program and laboratory geochemical prediction tests

ACID MINE DRAINAGE PROJECT - 2002 - 2006													
Iron Duke Mine Drainage Analysis													
Sample	Mine Water	MW	MW	MW	MW	MW	MW	MW	MW	MW	MW	MW	MW
Station	Site 3	Site 3	Site 3	Site 3	Site 3	Site 3	Site 3	Site 3	Site 3	Site 3	Site 3	Site 3	Site 3
Date Sampled		mai/ 04	jun/ 04	jul/ 04	aug/ 04	sep/ 04	okt/ 04	nov/ 04	des/ 04	jan/ 05	feb/ 05	mar/ 05	apr/ 05
Flow	m3/h	7.54	7.48	7.34	7.21	7.74	7.44	7.52	7.64	7.32	7.86	7.22	7.58
Temper	oC	21.40	16.50	15.80	22.70	25.20	24.80	25.70	23.20	25.80	24.70	24.60	26.20
pH		2.34	2.65	1.97	2.88	1.54	2.43	2.54	3.05	2.67	2.54	1.78	2.43
Eh	mV	78.50	38.50	27.40	96.40	77.80	84.20	96.30	101.40	95.60	112.80	85.60	92.10
Acidity	mg/l$_{CaCO3}$	17564.76	21498.90	18754.33	18425.48	19786.29	16842.49	14231.43	16759.44	14643.27	15354.98	17639.21	19265.42
TDS	mg/l	18603.30	18429.10	18102.40	15299.50	18507.90	13771.60	16588.90	16410.00	11843.70	15568.60	19642.90	14226.70
EC	uS/cm	21655.60	20987.80	22645.20	18376.40	19567.80	16489.60	17897.70	18321.10	14690.20	20909.60	22843.10	18456.20
SO42-	mg/l	11754.22	12647.87	11987.56	9354.78	11467.11	9067.84	11321.92	8494.65	7256.18	10124.12	13414.29	8847.33
Cl	mg/l	1237.04	703.41	926.42	548.77	1026.43	763.09	1107.82	921.47	653.28	736.11	892.46	713.19
NO3-	mg/l	287.26	192.38	276.53	167.41	107.59	211.37	184.73	190.16	148.66	173.43	228.47	265.88
Fe	mg/l	6172.45	6784.35	6805.76	4789.96	6432.24	4065.87	5935.22	4876.32	3478.45	5632.11	6784.92	4754.97
Mn	mg/l	88.45	95.67	78.98	102.54	103.46	89.74	99.87	92.88	84.65	67.54	104.77	98.55
Al	mg/l	161.43	144.16	136.77	108.87	156.43	102.76	160.25	149.76	96.98	121.89	117.94	147.48
Ni	mg/l	1.22	0.98	2.41	0.76	0.98	1.87	1.54	1.34	1.97	2.31	0.84	1.76
Cu	mg/l	0.34	0.25	0.17	0.46	0.31	0.08	0.26	0.38	0.45	0.37	0.42	0.26
Zn	mg/l	3.43	1.78	2.23	1.78	3.89	3.65	2.87	3.21	2.15	3.23	2.09	1.87
Ca	mg/l	2.13	0.98	1.27	2.54	0.56	0.33	1.96	2.01	2.56	1.18	2.05	2.17
Mg	mg/l	98.67	209.32	321.89	165.87	277.83	287.44	178.41	204.56	212.43	112.78	320.65	197.87
K	mg/l	14.32	9.17	11.87	6.84	12.34	17.18	15.49	13.87	7.69	11.43	10.06	13.84
Na	mg/l	67.24	51.33	58.76	40.12	42.87	46.88	61.23	54.79	36.45	42.17	58.32	41.89
Sum Cations meq/l		253.96	282.35	291.44	203.20	276.81	186.72	252.07	214.56	158.01	229.42	289.34	209.04
Sum Anions meq/l		284.25	286.27	280.18	212.95	269.44	213.73	269.95	205.92	171.90	234.35	308.15	208.61
Charge Balance %		-5.63	-0.69	1.97	-2.34	1.35	-6.74	-3.43	2.06	-4.21	-1.06	-3.15	0.10

UPSTREAM of mine Site 3													
Sample ID		YJR-A1	YJR-A2	YJR-A3	YJR-A4	YJR-A5	YJR-A6	YJR-A7	YJR-A8	YJR-A9	YJR-A10	YJR-A11	YJR-A12
Station		Site 3	Site 3	Site 3	Site 3	Site 3	Site 3	Site 3	Site 3	Site 3	Site 3	Site 3	Site 3
Date Sampled		mai/ 04	jun/ 04	jul/ 04	aug/ 04	sep/ 04	okt/ 04	nov/ 04	des/ 04	jan/ 05	feb/ 05	mar/ 05	apr/ 05
X		295048	295048	295048	295048	295048	295048	295048	295048	295048	295048	295048	295048
Y		8070522	8070522	8070522	8070522	8070522	8070522	8070522	8070522	8070522	8070522	8070522	8070522
Elevation		1179	1179	1179	1179	1179	1179	1179	1179	1179	1179	1179	1179
Flow	m3/h	37.50	35.00	28.50	26.50	23.50	22.50	35.50	36.00	40.50	44.50	45.50	41.50
Temper	oC	20.40	18.00	15.10	23.50	23.80	25.50	24.80	23.50	23.70	22.90	23.60	24.20
pH	Units	7.32	7.25	7.77	7.55	7.88	7.76	7.26	7.87	8.14	8.08	7.94	8.22
Eh	mV	216.00	215.00	220.00	216.00	237.00	223.00	236.00	242.00	238.00	241.00	234.00	230.00
Acidity	mg/lCaCO3	1.36	2.58	0.82	1.22	0.68	0.64	2.48	0.74	0.52	0.64	0.88	0.32
Alkalinit	mg/lHCO3	108.25	90.76	124.44	116.32	154.63	167.17	104.74	150.39	166.27	160.11	148.93	171.08
DO	mg/l	7.82	6.06	6.54	6.76	7.22	7.09	6.88	6.92	7.16	6.84	6.91	7.22
TDS	mg/l	183.90	200.60	227.00	217.40	237.50	228.90	215.80	227.40	276.50	258.10	221.70	230.40
EC	uS/cm	280.50	304.20	264.60	321.80	293.40	301.20	272.60	333.80	340.20	335.60	312.80	270.10
SO42-	mg/l	139.45	148.56	156.22	157.01	155.88	161.24	154.42	151.85	168.74	162.83	157.92	159.64
NO3-	mg/l	1.34	1.86	1.04	1.21	0.93	0.78	0.64	0.32	0.95	0.77	0.84	0.42
Cl-	mg/l	12.34	12.34	9.12	15.87	10.64	12.59	13.66	9.71	14.63	8.06	10.53	7.82
Fe	mg/l	0.87	0.75	0.46	0.66	0.39	0.36	1.09	0.75	0.46	0.37	0.49	0.33
Mn	mg/l	1.87	1.01	2.11	1.98	1.83	2.04	0.98	0.74	1.04	0.86	1.07	1.24
Al	mg/l	0.05	0.03	0.01	0.01	0.01	0.01	0.01	0.02	0.02	0.01	0.01	0.01
Ni	mg/l	0.04	0.04	0.02	0.01	0.01	0.01	0.01	0.01	0.01	0.01	0.01	0.01
Cu	mg/l	0.02	0.04	0.01	0.02	0.01	0.01	0.02	0.02	0.02	0.01	0.02	0.01
Zn	mg/l	0.61	1.95	0.92	2.32	0.53	1.75	0.85	0.72	1.38	1.54	0.64	1.03
Ca	mg/l	28.06	30.89	27.87	36.74	31.49	39.86	37.41	32.38	31.07	35.63	30.86	34.97
Mg	mg/l	29.04	22.89	26.74	20.11	33.21	26.05	28.02	30.36	33.54	32.64	32.07	32.92
K	mg/l	5.03	5.01	7.88	4.27	6.76	4.38	3.73	4.85	3.92	3.98	4.24	4.38
Na	mg/l	12.66	12.01	14.32	19.08	21.28	20.04	9.64	11.39	13.04	14.86	13.87	14.94
Sum Ca	meq/l	4.62	4.23	4.59	4.62	5.54	5.29	4.81	4.84	5.10	5.33	4.99	5.33
Sum An	meq/l	4.91	4.83	5.47	5.47	5.98	6.32	5.17	5.79	6.50	6.17	5.92	6.27
Charge	%	-3.03	-6.59	-8.77	-8.36	-3.78	-8.93	-3.58	-8.94	-12.07	-7.28	-8.50	-8.05

Chemical Composition at Seepage Point D													
Sample ID		YJR-D1	YJR-D2	YJR-D3	YJR-D4	YJR-D5	YJR-D6	YJR-D7	YJR-D8	YJR-D9	YJR-D10	YJR-D11	YJR-D12
Station		Site 3	Site 3	Site 3	Site 3	Site 3	Site 3	Site 3	Site 3	Site 3	Site 3	Site 3	Site 3
Date Sampled		mai/ 04	jun/ 04	jul/ 04	aug/ 04	sep/ 04	okt/ 04	nov/ 04	des/ 04	jan/ 05	feb/ 05	mar/ 05	apr/ 05
X		294196	294196	294196	294196	294196	294196	294196	294196	294196	294196	294196	294196
Y		8073298	8073298	8073298	8073298	8073298	8073298	8073298	8073298	8073298	8073298	8073298	8073298
Elevation		1151	1151	1151	1151	1151	1151	1151	1151	1151	1151	1151	1151
Flow	m3/h	37.50	35.00	28.50	26.50	23.50	22.50	35.50	36.00	40.50	44.50	45.50	41.50
Temper	oC	20.30	17.60	15.50	22.90	23.00	24.90	24.80	23.80	24.20	23.30	24.60	24.50
pH	Units	4.50	3.52	3.05	2.93	2.90	2.47	3.24	4.57	5.30	6.30	3.85	3.67
Eh	mV	214.00	218.00	216.00	227.00	226.00	225.00	223.00	226.00	221.00	220.00	220.00	230.00
Acidity	mg/lCaCO3	50.56	145.69	287.43	475.12	384.75	358.55	110.03	210.89	132.54	54.59	163.42	137.82
Alkalinit	mg/lHCO3	0.00	0.00	0.00	0.00	0.00	0.00	0.00	0.00	19.66	65.87	0.00	0.00
DO	mg/l	4.34	3.26	3.03	3.22	5.47	5.33	6.24	5.05	4.02	5.61	5.23	5.36
TDS	mg/l	425.50	965.80	1136.00	1222.00	1366.00	1592.00	1092.00	812.00	658.90	712.00	421.00	486.90
EC	uS/cm	627.10	1378.00	1605.00	1724.00	1911.00	2199.00	1191.00	1398.40	975.30	1090.00	573.50	678.20
SO42-	mg/l	408.43	624.87	896.44	1147.65	1376.81	1242.32	760.54	592.73	497.20	478.90	678.92	787.37
NO3-	mg/l	1.34	5.78	3.13	6.75	8.78	3.54	1.36	11.23	9.75	7.87	4.82	7.62
Cl-	mg/l	76.19	55.76	71.44	63.65	85.97	75.72	67.42	89.45	84.14	90.56	109.42	96.16
Fe	mg/l	3.56	1.64	1.74	2.66	3.65	3.87	0.78	4.33	3.98	0.97	2.04	4.28
Mn	mg/l	23.45	42.88	63.32	115.67	90.54	45.42	20.67	57.23	38.46	24.08	52.85	99.46
Al	mg/l	0.09	6.78	15.64	12.34	17.43	9.11	11.27	15.34	12.98	9.30	7.65	12.94
Ni	mg/l	0.53	0.78	0.82	1.44	1.38	0.76	0.32	1.43	0.97	0.43	0.78	0.98
Cu	mg/l	0.01	0.01	0.04	0.13	0.22	0.04	0.02	0.11	0.06	0.03	0.08	0.09
Zn	mg/l	0.25	0.41	0.45	1.03	2.19	0.54	0.22	2.19	0.87	0.34	1.84	1.79
Ca	mg/l	49.88	114.67	157.81	261.08	290.06	320.43	143.97	93.18	83.21	75.93	147.83	137.81
Mg	mg/l	39.89	72.75	76.83	101.22	96.45	78.90	82.45	77.04	70.09	73.20	73.07	82.77
K	mg/l	5.16	6.05	6.02	8.34	5.04	5.12	2.45	6.05	4.87	2.67	6.73	7.04
Na	mg/l	25.09	18.21	24.63	33.42	38.19	26.86	30.02	41.28	38.17	42.47	46.70	42.04
Sum Ca	meq/l	8.04	15.10	19.61	28.84	29.72	26.66	17.40	17.04	14.78	13.72	18.57	21.04
Sum Ar	meq/l	9.77	14.07	19.90	25.11	30.30	27.19	16.96	14.10	12.31	12.73	16.04	18.16
Charge	%	-9.70	3.54	-0.75	6.91	-0.97	-0.98	1.29	9.44	9.14	3.72	7.31	7.36

Mazowe River Regional Background Levels							
Sample ID		MZR-1	MZR-2	MZR-3	MZR-4	MZR-5	MZR-6
Station		Site 3	Site 3	Site 3	Site 3	Site 3	Site 3
Date Sampled		mai/ 04	jul/ 04	sep/ 04	nov/ 04	feb/ 05	mar/ 05
X		293017	293017	293017	293017	293017	293017
Y		8073383	8073383	8073383	8073383	8073383	8073383
Elevation		1149	1149	1149	1149	1149	1149
Flow	m3/h	67.50	55.00	57.50	76.50	93.50	102.50
Temper	oC	20.80	18.70	23.60	23.70	24.20	24.10
pH	Units	8.65	7.87	8.08	8.54	7.95	7.82
Eh	mV	230.00	240.00	232.00	241.00	234.00	239.00
Acidity	mg/lCaCO3	8.67	6.74	10.33	4.22	7.86	2.54
Alkalinit	mg/lHCO3	135.87	156.77	156.89	160.23	130.73	185.23
DO	mg/l	6.88	7.76	6.22	6.89	6.97	7.16
TDS	mg/l	412.00	315.20	380.00	321.80	412.40	335.80
EC	uS/cm	658.00	466.50	567.50	507.20	515.70	419.50
SO42-	mg/l	128.56	87.76	85.43	102.12	96.03	81.94
NO3-	mg/l	1.28	2.23	2.03	1.98	3.06	2.23
Cl-	mg/l	21.17	17.65	18.78	14.14	21.69	17.16
Fe	mg/l	0.82	0.67	0.85	0.57	0.98	0.75
Mn	mg/l	3.12	2.89	2.19	2.78	3.81	2.74
Al	mg/l	0.12	0.07	0.05	0.05	0.03	0.06
Ni	mg/l	0.02	0.05	0.01	0.01	0.02	0.02
Cu	mg/l	0.01	0.01	0.01	0.01	0.02	0.02
Zn	mg/l	0.02	0.02	0.01	0.02	0.02	0.01
Ca	mg/l	57.87	41.44	48.77	39.49	54.29	32.78
Mg	mg/l	20.34	18.78	23.76	17.98	15.69	26.93
K	mg/l	3.34	4.18	3.45	4.02	3.44	3.93
Na	mg/l	16.46	13.87	11.23	11.61	17.87	12.49
Sum Ca	meq/l	5.54	4.49	5.10	4.21	5.07	4.65
Sum Ar	meq/l	5.28	4.74	4.71	5.04	4.58	5.08
Charge	%	2.40	-2.77	4.00	-8.93	5.05	-4.39

Ground Water Samples														
Sample ID		BH1	BH2	BH3	BH4	BH1	BH2	BH3	BH4	BH1	BH2	BH3	BH4	Disused
Station		Site 3	Site 3	Site 3	Site 3	Site 3	Site 3	Site 3	Site 3	Site 3	Site 3	Site 3	Site 3	Site 3
Date Sampled		mai/ 04	mai/ 04	mai/ 04	mai/ 04	nov/ 04	nov/ 04	nov/ 04	nov/ 04	mar/ 05	mar/ 05	mar/ 05	mar/ 05	mai/ 04
X		294798	294845	294816	294887	294798	294845	294816	294887	294798	294845	294816	294887	294799
Y		8071046	8070997	8070952	8070948	8071046	8070997	8070952	8070948	8071046	8070997	8070952	8070948	8070920
Elevation		1177	1175	1175	1180	1177	1175	1175	1180	1177	1175	1175	1180	1168
Well De	m	2.55	6.46	4.54	4.40	2.65	6.56	4.68	4.75	2.25	6.23	4.30	4.25	4.90
Temper	oC	23.30	22.30	22.40	22.40	22.40	22.70	22.60	22.40	23.80	24.10	23.40	23.60	22.60
pH	Units	2.30	2.15	2.47	1.21	3.58	2.65	3.70	3.38	3.68	2.51	3.45	3.25	8.25
Eh	mV	221.00	241.00	239.00	236.00	234.00	243.00	241.00	230.00	231.00	238.90	237.80	233.10	236.00
Acidity	mg/lCaCO3	1520.44	1322.41	872.08	4324.06	764.12	976.41	603.45	710.25	684.12	803.84	734.91	837.09	0.00
Alkalinit	mg/lHCO3	0.00	0.00	0.00	0.00	0.00	0.00	0.00	0.00	0.00	0.00	0.00	0.00	243.77
DO	mg/l	4.86	5.74	4.54	5.34	3.82	4.87	4.22	5.04	4.06	4.15	4.72	4.64	5.66
TDS	mg/l	5657.00	7482.00	4099.00	8338.00	4876.40	4645.90	3639.20	7352.80	2765.20	3054.80	3174.30	5834.80	1057.00
EC	uS/cm	6970.00	8943.00	5181.00	9873.00	7012.30	6754.20	5758.70	10043.20	4128.60	4426.10	4408.30	7676.30	1388.00
SO42-	mg/l	2007.74	1952.88	1843.42	1564.22	1684.70	1702.10	1301.30	1604.80	1687.31	1709.22	1684.91	1692.06	156.64
NO3-	mg/l	78.54	43.38	65.78	42.04	45.65	48.77	98.33	56.09	47.76	48.21	51.79	48.96	3.54
Cl-	mg/l	201.45	128.77	122.89	143.73	287.34	132.98	176.88	232.17	301.55	308.42	299.03	286.77	10.03
Fe	mg/l	401.22	387.56	389.42	301.45	378.23	397.41	265.11	376.40	406.71	384.74	378.93	356.82	21.34
Mn	mg/l	231.35	164.86	149.23	203.64	245.03	162.44	199.28	211.08	226.94	187.46	164.92	175.08	27.43
Al	mg/l	3.56	2.13	0.98	1.23	2.45	1.87	0.46	0.67	2.27	1.09	1.15	0.96	0.09
Ni	mg/l	1.02	1.24	1.97	3.23	1.08	1.44	1.67	3.41	1.03	1.07	0.87	0.94	0.67
Cu	mg/l	0.31	0.48	0.53	0.37	0.42	0.35	0.47	0.44	0.38	0.42	0.39	0.37	0.04
Zn	mg/l	1.45	1.87	1.08	2.04	1.22	1.67	1.09	1.76	1.06	1.23	1.07	1.21	0.87
Ca	mg/l	243.12	265.70	249.43	210.56	254.38	178.93	182.97	230.40	247.82	268.44	261.47	250.46	43.65
Mg	mg/l	24.64	21.69	24.12	14.04	31.25	29.54	27.89	29.23	42.65	39.67	21.49	21.34	32.34
K	mg/l	5.76	8.76	3.05	5.08	6.43	7.78	6.30	4.98	7.22	7.68	6.37	6.53	2.65
Na	mg/l	35.21	28.49	16.18	30.47	27.07	21.04	17.98	24.63	28.31	27.83	29.34	28.05	19.28
Sum Ca	meq/l	39.15	36.79	34.83	31.68	39.47	32.98	29.31	36.55	40.49	38.92	36.07	35.02	7.59
Sum An	meq/l	47.27	43.96	42.22	36.07	41.00	38.96	32.72	38.74	41.34	41.92	41.36	41.24	7.52
Charge	%	-9.40	-8.88	-9.58	-6.49	-1.90	-8.31	-5.50	-2.91	-1.04	-3.71	-6.84	-8.15	0.44

Dissolved Pollutant Concentrations Along Yellow Jacket River											
Sample ID		YJR-A	YJR-B	YJR-C	YJR-D	YJR-E	YJR-F	YJR-G	YJR-H	YJR-I	Confluence
Station		Site 3	Site 3	Site 3	Site 3	Site 3	Site 3	Site 3	Site 3	Site 3	Site 3
Date Sampled: Average values for 12 sampling campaigns for each point											
X		295048	294816	294636	294604	294807	294906	294705	294196	294019	293717
Y		8070522	8070746	8070861	8071064	8071064	8071161	8071293	8073298	8073515	8073482
Elevation		1179	1168	1171	1169	1172	1171	1169	1151	1155	1146
Flow	m3/h	26.50	26.50	26.50	26.50	26.50	26.50	26.50	26.50	26.50	76.50
Temper	oC	24.43	25.27	24.50	24.30	23.97	23.63	23.70	24.50	23.93	23.87
pH	Units	7.66	7.52	6.46	4.95	3.86	3.95	3.66	3.75	5.58	7.66
Eh	mV	224.33	218.00	218.67	218.00	219.00	228.33	225.33	223.00	220.67	232.00
Acidity	mg/lCaCO3	0.95	1.55	18.05	51.83	209.80	245.53	261.75	211.65	80.33	8.95
Alkalinit	mg/lHCO3	135.77	141.42	97.87	11.46	3.08	7.03	0.00	6.55	27.40	97.83
DO	mg/l	7.19	6.64	5.79	5.32	4.20	4.49	5.13	4.85	5.88	6.69
TDS	mg/l	216.13	215.63	309.80	519.57	654.80	742.10	944.03	979.03	836.20	401.47
EC	uS/cm	279.50	309.07	517.20	875.03	1001.77	1136.90	1437.73	1500.73	1096.47	580.40
SO42-	mg/l	13.85	32.27	150.70	329.21	659.99	777.49	846.85	713.89	506.89	103.34
NO3-	mg/l	1.10	1.28	1.89	5.33	3.72	7.71	9.80	8.59	5.49	2.12
Cl-	mg/l	10.70	13.60	117.89	137.19	131.01	135.97	134.88	148.92	138.67	53.88
Fe	mg/l	0.57	0.59	2.55	1.43	1.97	3.57	4.14	4.20	1.00	0.88
Mn	mg/l	1.94	1.68	22.83	36.59	58.20	97.29	85.20	42.76	24.92	3.04
Al	mg/l	0.02	0.02	0.05	3.63	11.69	13.35	15.53	11.06	11.03	0.07
Ni	mg/l	0.02	0.02	0.45	0.91	0.86	1.22	1.29	0.82	0.43	0.02
Cu	mg/l	0.01	0.02	0.01	0.02	0.07	0.13	0.14	0.05	0.03	0.01
Zn	mg/l	0.02	2.01	1.50	0.87	0.99	1.27	2.02	0.86	0.44	0.02
Ca	mg/l	22.47	28.16	47.99	89.47	137.04	167.32	177.22	182.58	115.54	53.64
Mg	mg/l	11.00	15.68	39.95	52.03	79.85	89.18	79.02	75.16	78.70	23.26
K	mg/l	4.56	4.55	5.09	6.44	6.28	7.83	5.94	5.29	2.77	3.41
Na	mg/l	11.09	10.38	13.64	16.35	26.66	30.40	31.08	27.49	21.48	11.85
Sum Ca	meq/l	2.75	3.44	7.42	11.51	18.32	22.50	21.97	19.65	15.46	5.37
Sum An	meq/l	2.72	3.25	6.70	9.41	16.01	18.71	20.08	17.62	13.39	4.68
Charge	%	0.56	2.88	5.16	10.04	6.72	9.18	4.49	5.46	7.17	6.78

Site 2 Return Water Dam Overflow													
		mai/ 04	jun/ 04	jul/ 04	aug/ 04	sep/ 04	okt/ 04	nov/ 04	des/ 04	jan/ 05	feb/ 05	mar/ 05	apr/ 05
Flow	m^3/h	17.52	15.47	16.39	19.45	12.37	14.45	20.5	16.55	20.64	16.65	20.58	15.55
Temper	^oC	22.3	17.8	16.6	22.1	22.6	23.2	22.6	23.5	23.4	22.9	21.6	22.1
pH	Units	7.85	7.67	10.76	6.53	9.26	8.16	2.54	9.43	6.88	8.86	9.88	6.78
Eh	mV	294	292	295	296	294	289	286	295	298	296	294	296
Alkalinity	mg/lHCO3	76.08	84.06	109.56	43.76	76.84	81.23	97.84	87.42	67.93	68.41	109.06	85.66
DO	mg/l	5.76	4.88	5.87	5.23	5.44	5.43	5.21	5.87	5.77	5.84	5.78	6.05
TDS	mg/l	1276.9	1486.9	1453.4	1673.8	2165.7	1367.4	1043.7	1653.8	1874.2	2265.6	1875.2	1643.9
EC	uS/cm	1604.7	1652.6	1874.8	2274.1	2864.2	1748.4	2123.7	2002.6	2215.5	2758.1	2309.6	1974.7
SO_4^{2-}	mg/l	1048.44	1213.64	1087.42	1447.95	1304.63	975.42	876.83	1294.05	1231.07	1385.97	1186.93	1220.43
NO_3^-	mg/l	52.86	33.82	46.96	42.06	54.97	47.41	32.77	40.03	41.94	48.96	42.96	37.08
Cl^-	mg/l	30.04	12.09	28.11	32.19	31.53	27.08	19.36	21.74	29.87	30.48	24.07	27.93
CN	mg/l	0.01	0.03	0.01	0.02	0.06	0.03	0.04	0.03	0.01	0.05	0.03	0.04
As	mg/l	0.32	0.48	0.13	0.21	0.46	0.43	0.27	0.18	0.19	0.29	0.15	0.23
Fe	mg/l	1.81	5.64	2.84	1.97	3.64	2.67	2.09	4.65	1.18	2.13	5.67	2.18
Ni	mg/l	0.12	0.87	0.33	0.12	0.52	0.07	0.76	0.42	0.15	0.63	0.33	0.09
Cu	mg/l	0.01	0.04	0.04	0.01	0.05	0.01	0.04	0.08	0.03	0.03	0.05	0.03
Zn	mg/l	0.27	0.31	0.28	0.35	0.21	0.34	0.31	0.37	0.21	0.46	0.56	0.34
Ca	mg/l	296.03	285.79	254.18	298.32	306.13	275.97	269.08	304.76	338.95	331.84	325.09	277.41
Mg	mg/l	116.85	106.07	93.98	97.36	105.79	96.77	90.04	102.57	133.86	137.51	114.74	98.96
K	mg/l	14.76	24.66	23.97	16.94	22.53	23.12	24.79	23.78	17.98	27.41	21.33	25.86
Na	mg/l	61.38	78.12	74.07	87.96	106.94	74.73	85.08	97.92	96.71	98.09	87.84	98.56

Trojan (Site 1) Waste Rock South Effluent													
Sample Date		mai/ 04	jun/ 04	jul/ 04	aug/ 04	sep/ 04	okt/ 04	nov/ 04	des/ 04	jan/ 05	feb/ 05	mar/ 05	apr/ 05
Flow	m3/h	21.16	19.95	17.25	16.24	15.94	15.82	18.78	21.08	22.22	21.28	19.32	16.21
Temperatu	oC	21.50	22.30	21.70	22.70	23.90	18.40	16.20	20.70	22.80	23.50	22.60	23.80
pH	Units	8.13	8.25	8.09	7.85	8.12	7.94	8.18	8.05	7.94	7.88	8.09	8.16
Eh	mV	290.00	287.00	304.00	311.00	296.00	301.00	298.00	312.00	304.00	310.00	298.00	313.00
Alkalinity	mg/lHCO	91.43	108.26	96.43	112.74	145.42	128.60	125.02	119.42	132.84	119.04	128.48	137.42
DO	mg/l	5.42	6.21	5.75	5.62	5.44	4.95	5.28	5.07	5.03	5.12	4.97	5.86
TDS	mg/l	1185.40	976.60	918.40	1093.80	1207.40	985.20	847.20	926.40	1008.40	964.20	956.90	844.10
EC	uS/cm	1261.30	1108.90	1012.10	1408.40	1702.30	1248.50	1144.80	1208.20	1385.70	1279.40	1246.70	1185.30
SO42-	mg/l	423.86	350.65	280.08	376.42	438.50	375.21	352.84	330.41	294.80	326.80	287.48	275.49
NO3-	mg/l	0.00	0.00	0.00	0.00	0.00	0.01	0.00	0.00	0.00	0.00	0.01	0.00
Cl-	mg/l	76.36	82.69	92.46	98.04	102.42	94.28	97.42	112.08	97.53	126.63	87.09	98.54
Fe	mg/l	1.02	0.03	0.13	1.85	0.98	1.05	1.24	3.65	4.08	2.06	0.97	1.18
Mn	mg/l	0.43	0.31	0.22	0.52	0.79	0.84	0.92	0.77	0.64	0.85	0.72	0.92
Ni	mg/l	0.17	3.96	7.52	0.87	0.51	0.24	0.18	6.42	2.18	1.86	0.86	0.28
Cu	mg/l	0.08	0.04	0.06	0.15	0.03	0.04	0.14	0.08	0.04	0.03	0.03	0.02
Zn	mg/l	0.05	0.08	0.01	0.06	0.04	0.06	0.08	0.05	0.06	0.03	0.07	0.02
Ca	mg/l	58.43	73.24	64.21	72.88	64.17	58.27	48.08	58.19	60.04	53.92	46.27	43.18
Mg	mg/l	123.17	88.21	67.38	108.64	118.94	96.94	101.26	121.84	117.43	118.88	96.32	102.82
K	mg/l	1.01	1.27	2.11	2.75	2.16	3.04	2.94	3.16	2.75	3.19	3.47	3.28
Na	mg/l	26.88	27.64	33.04	31.08	36.08	39.42	42.04	44.84	37.16	39.49	44.51	48.93
Sum Cation	meq/l	14.31	12.30	10.52	14.13	14.71	12.77	12.74	15.36	14.61	14.46	12.37	12.93
Sum Anion	meq/l	12.48	11.41	10.02	12.45	14.40	12.58	12.14	12.00	11.07	12.33	10.55	10.77
Charge Bal	%	6.84	3.78	2.44	6.32	1.05	0.76	2.39	12.28	13.79	7.96	7.95	9.14

Trojan (Site 1) Tailings Dam Stream													
		mai/ 04	jun/ 04	jul/ 04	aug/ 04	sep/ 04	okt/ 04	nov/ 04	des/ 04	jan/ 05	feb/ 05	mar/ 05	apr/ 05
Flow	m3/h	32.55	31.83	28.68	22.05	27.16	31.95	32.37	37.44	32.64	35.68	26.66	23.69
Temperatu	oC	22.5	21.6	22.9	23.2	22.1	19.7	17.4	19.6	21.5	22.6	23.1	22.3
pH	Units	8.28	7.94	8.48	7.83	7.43	7.93	8.14	7.88	7.92	7.95	7.87	8.04
Eh	mV	287.00	294.00	296.00	292.00	293.00	287.00	290.00	294.00	286.00	298.00	301.00	287.00
Alkalinity	mg/lHCO	275.64	270.42	234.58	236.74	160.52	218.86	176.42	197.40	229.37	241.86	219.41	256.47
DO	mg/l	5.86	5.08	5.64	5.07	6.13	5.88	5.09	5.42	5.18	5.86	5.92	5.72
TDS	mg/l	471.80	1238.50	1057.60	1076.49	1360.60	1191.40	984.30	1085.70	1216.60	1120.40	984.80	998.70
EC	uS/cm	763.20	1387.40	1236.10	1289.60	1476.50	1277.90	1312.80	1396.40	1454.90	1408.60	1320.50	1325.80
SO42-	mg/l	590.21	322.86	863.42	426.96	420.11	450.08	508.17	617.54	907.42	518.80	621.63	580.28
NO3-	mg/l	0.00	0.01	0.00	0.00	0.00	0.00	0.01	0.01	0.00	0.01	0.00	0.00
Cl-	mg/l	120.22	52.38	106.21	49.07	66.07	68.25	52.18	67.84	72.14	69.36	56.29	52.81
Fe	mg/l	1.13	6.15	0.35	0.96	0.03	0.09	0.51	0.04	0.61	0.03	0.08	0.28
Mn	mg/l	0.11	0.25	0.26	0.25	0.40	0.21	0.15	0.22	0.31	0.39	0.41	0.38
Ni	mg/l	0.11	0.34	0.12	0.42	0.83	0.91	1.18	0.56	0.62	0.74	0.42	0.53
Cu	mg/l	0.01	0.02	0.03	0.03	0.16	0.01	0.04	0.02	0.01	0.04	0.06	0.05
Zn	mg/l	0.01	0.01	0.04	0.01	0.01	0.01	0.04	0.02	0.02	0.04	0.04	0.03
Ca	mg/l	87.54	75.28	160.81	87.44	64.32	77.04	64.82	66.19	74.28	70.04	58.19	62.38
Mg	mg/l	215.67	101.61	193.76	112.17	124.65	143.73	154.17	159.04	164.92	160.03	150.42	156.04
K	mg/l	2.07	3.28	1.06	1.84	4.55	3.04	2.38	2.86	4.25	3.08	3.19	4.04
Na	mg/l	48.54	49.64	37.85	47.53	49.06	63.42	52.06	44.08	66.86	58.24	60.07	59.08
Sum Catior	meq/l	24.34	14.62	25.67	15.78	15.79	18.57	18.32	18.43	20.37	19.34	18.03	18.69
Sum Anion	meq/l	20.20	12.63	24.82	14.15	13.24	14.88	14.94	18.01	24.69	16.72	18.13	17.77
Charge Bal	%	9.30	7.30	1.70	5.42	8.77	11.02	10.16	1.15	-9.57	7.25	-0.27	2.52

Trojan (Site 1) New Chihuri Monitoring Borehole													
		mai/ 04	jun/ 04	jul/ 04	aug/ 04	sep/ 04	okt/ 04	nov/ 04	des/ 04	jan/ 05	feb/ 05	mar/ 05	apr/ 05
Temperatu	oC	21.8	22.6	21.8	22.6	21.2	19.4	17.8	20.5	21.4	22.8	21.7	21.2
pH	Units	7.12	7.23	7.29	6.87	7.23	7.09	6.94	7.22	6.93	6.84	6.79	7.02
Eh	mV	234	279	276	265	271	242	254	238	263	241	261	258
Alkalinity	mg/lHCO	77.36	78.32	76.08	87.24	93.08	74.05	84.21	97.19	102.42	84.84	75.04	89.27
DO	mg/l	4.76	5.52	5.24	4.87	4.63	4.72	4.63	5.04	4.84	4.79	4.67	4.77
TDS	mg/l	1730.80	1855.16	1884.60	2425.30	1954.80	2370.70	2161.80	2201.90	2091.50	1874.70	1952.90	1608.60
EC	uS/cm	1946.40	1907.60	2001.40	3320.80	2875.30	3034.90	3007.50	3439.70	2976.40	2402.60	2867.80	2286.60
SO42-	mg/l	1050.27	925.58	823.40	940.41	1050.02	1200.56	850.27	918.24	1004.02	962.91	842.08	852.82
NO3-	mg/l	0.00	0.01	0.00	0.00	0.00	0.00	0.00	0.00	0.00	0.00	0.00	0.00
Cl-	mg/l	33.08	28.76	28.08	21.08	32.16	28.13	34.64	19.85	27.43	31.09	33.82	29.06
Fe	mg/l	0.46	0.97	0.48	2.37	0.78	6.31	5.95	0.82	0.44	0.67	0.28	1.27
Mn	mg/l	0.12	0.11	0.01	2.08	1.03	3.18	0.42	0.28	0.85	1.29	0.76	0.32
Ni	mg/l	0.11	0.01	0.12	0.01	0.01	0.02	0.02	0.01	0.02	0.02	0.01	0.01
Cu	mg/l	0.05	0.03	0.01	0.04	0.04	0.03	0.03	0.03	0.02	0.02	0.02	0.02
Zn	mg/l	0.04	0.09	0.16	2.83	0.78	0.07	0.24	0.13	0.28	0.05	0.15	0.31
Ca	mg/l	301.65	234.86	290.99	287.04	296.18	302.56	189.42	205.84	267.95	274.17	284.29	260.42
Mg	mg/l	129.47	125.21	68.97	119.63	107.37	90.41	86.49	93.15	82.47	86.04	90.17	77.83
K	mg/l	1.64	1.01	0.91	1.29	0.95	0.88	1.04	1.32	1.69	0.74	0.69	0.62
Na	mg/l	19.03	17.08	18.09	25.52	20.86	18.06	19.28	19.64	20.05	16.06	16.20	15.84
Sum Catio	meq/l	26.61	22.84	21.03	25.48	24.62	23.69	17.67	18.87	21.13	21.55	22.37	20.17
Sum Anion	meq/l	24.07	21.37	19.18	21.60	24.29	27.00	20.06	21.27	23.36	22.32	19.72	20.04
Charge Bal	%	5.02	3.33	4.60	8.23	0.66	-6.53	-6.33	-5.97	-5.00	-1.73	6.31	0.32

Trojan Nickel Mine (Site 1): TAILING DAM SAMPLES ABA DATA																
	PastepH	Rinse pH	EC	Moisture	Porosity	S(Total)	C(Total)	MPA	ANC	TotalCaNC	NAPP	NAGpH	NAGpH4.	NAGpH7.(	ANC/MPA	FizzRating
	(pHunits)	(pHunits)	uS/cm	%	%	(%)	(%)	kgH2SO4	kgCaCO3	(t CaCO3/1	(kgH2SO4	(pHunits)	kgH2SO4/	kgH2SO4/t		
	Measu	Measu	Measu	Measu	Measu	Measu	Measu	Calcu	Measu	Calcu	Calcu	Measu	Calcula	Calcul	Calcul	Observed
Sample ID		Sample Date: 17 October 2004														
TR-TL1	8.83	8.75	1264.30	4.62	36.93	0.57	0.07	17.81	48.19	5.43	-30.38	5.67	0.00	0.00	2.71	Moderate
TR-TL2	8.76	8.74	1187.10	4.05	35.21	0.75	0.04	23.44	49.77	3.57	-26.33	4.78	0.00	0.00	2.12	Moderate
TR-TL3	8.48	8.53	1196.40	4.96	34.08	0.52	0.01	16.25	51.27	1.24	-35.02	7.21	0.00	0.00	3.16	Moderate
TR-TL4	7.98	8.02	1327.90	4.72	30.27	0.62	0.01	19.38	42.76	0.65	-23.39	7.36	0.00	0.00	2.21	Slight
TR-TL5	8.04	7.89	1267.80	3.88	40.23	0.64	0.08	20.00	46.87	6.27	-26.87	4.84	0.00	0.00	2.34	Moderate
TR-TL6	8.77	8.64	1364.10	4.27	42.85	0.59	0.06	18.44	41.32	5.40	-22.88	7.16	0.00	0.00	2.24	Slight
TR-TL7	8.72	8.68	1189.50	4.84	39.46	0.61	0.04	19.06	44.24	3.55	-25.18	8.28	0.00	0.00	2.32	Slight
TR-TL8	9.04	8.77	1208.40	6.04	37.09	0.74	0.05	23.13	56.28	4.31	-33.16	4.29	2.05	3.77	2.43	Moderate
TR-TL9	8.73	8.74	1304.70	5.82	41.12	0.58	0.07	18.13	50.18	6.11	-32.06	5.73	0.00	0.00	2.77	Moderate
TR-TL10	9.22	9.05	1178.30	7.42	44.74	0.62	0.08	19.38	49.08	6.93	-29.71	5.84	0.00	0.00	2.53	Moderate
		Sample Date: 15 January 2005														
TR-TL1	8.62	8.47	1236.80	8.46	33.76	0.53	0.05	16.56	47.25	4.02	-30.69	6.74	0.00	0.00	2.85	Moderate
TR-TL2	7.86	7.89	1297.30	7.83	37.97	0.56	0.10	17.50	60.09	8.03	-42.59	5.63	0.00	0.00	3.43	Moderate
TR-TL3	8.23	8.17	1309.20	9.28	32.89	0.69	0.01	21.56	67.22	0.70	-45.66	4.37	1.86	3.08	3.12	Moderate
TR-TL4	8.17	8.21	1291.40	8.05	36.92	0.67	0.01	20.94	56.74	0.81	-35.80	4.06	2.38	5.37	2.71	Moderate
TR-TL5	7.72	7.71	1190.20	7.91	38.07	0.58	0.04	18.13	48.39	3.10	-30.27	5.17	0.00	0.00	2.67	Moderate
TR-TL6	8.42	8.39	1208.60	9.35	37.14	0.55	0.03	17.19	65.44	2.34	-48.25	6.28	0.00	0.00	3.81	Moderate
TR-TL7	8.61	8.58	1312.40	8.47	34.08	0.52	0.05	16.25	59.02	4.48	-42.77	6.32	0.00	0.00	3.63	Slight
TR-TL8	8.75	8.76	1272.10	8.78	37.12	0.69	0.07	21.56	62.83	5.74	-41.27	3.87	3.58	6.25	2.91	Moderate
TR-TL9	8.44	8.46	1390.40	9.24	38.46	0.61	0.07	19.06	59.06	6.19	-40.00	4.16	2.29	5.32	3.10	Moderate
TR-TL10	8.96	8.93	1289.70	11.03	39.05	0.69	0.06	21.56	58.29	5.09	-36.73	3.95	3.47	5.64	2.70	Moderate
		Sample Date: 21 March 2005														
TR-TL1	8.73	8.69	1199.20	5.64	36.94	0.51	0.04	15.94	64.95	3.40	-49.01	6.77	0.00	0.00	4.08	Moderate
TR-TL2	8.21	8.32	1282.60	5.92	40.21	0.54	0.05	16.88	58.28	4.31	-41.41	7.39	0.00	0.00	3.45	Slight
TR-TL3	8.14	8.12	1264.90	6.18	37.43	0.53	0.07	16.56	57.31	6.19	-40.75	6.83	0.00	0.00	3.46	Moderate
TR-TL4	8.22	8.19	1312.80	5.83	38.19	0.58	0.01	18.13	49.86	0.79	-31.74	8.17	0.00	0.00	2.75	Slight
TR-TL5	7.82	7.84	1277.30	6.07	35.23	0.57	0.08	17.81	53.08	6.87	-35.27	5.63	0.00	0.00	2.98	Moderate
TR-TL6	8.09	8.02	1269.30	5.92	36.47	0.54	0.07	16.88	63.27	6.10	-46.40	4.48	0.43	1.66	3.75	Moderate
TR-TL7	8.47	8.36	1302.10	6.01	37.08	0.67	0.06	20.94	58.72	5.07	-37.78	3.89	3.61	7.38	2.80	Moderate
TR-TL8	8.71	8.70	1159.30	5.59	34.28	0.59	0.08	18.44	61.94	6.30	-43.50	6.37	0.00	0.00	3.36	Moderate
TR-TL9	8.87	8.81	1286.50	5.37	33.96	0.62	0.08	19.38	59.23	6.89	-39.86	5.88	0.00	0.00	3.06	Moderate
TR-TL10	9.24	9.18	1218.70	8.42	36.18	0.66	0.06	20.63	56.17	5.16	-35.55	4.28	2.24	6.14	2.72	Moderate

Maximum	9.24	9.18	1390.40	11.03	44.74	0.75	0.10	23.44	67.22	8.03	-22.88	8.28	3.61	7.38	4.08	
Minimum	7.72	7.71	1159.30	3.88	30.27	0.51	0.01	15.94	41.32	0.65	-49.01	3.87	0.00	0.00	2.12	
Mean	8.50	8.45	1261.98	6.67	37.11	0.60	0.05	18.90	54.90	4.50	-36.01	5.71	0.73	1.49	2.94	
Standard De	0.41	0.38	57.66	1.87	3.00	0.07	0.03	2.07	7.09	2.10	7.38	1.33	1.25	2.49	0.51	
10 Percentil	7.97	7.89	1189.26	4.59	33.94	0.53	0.01	16.53	46.61	0.81	-45.73	4.05	0.00	0.00	2.31	
25 Percentil	8.18	8.18	1208.45	5.43	35.22	0.55	0.04	17.27	49.25	3.44	-41.37	4.40	0.00	0.00	2.68	
Median	8.55	8.50	1270.70	6.03	37.09	0.59	0.06	18.44	56.51	5.08	-35.67	5.70	0.00	0.00	2.83	
75 Percentil	8.76	8.74	1300.90	8.33	38.39	0.66	0.07	20.47	59.19	6.17	-30.46	6.76	1.50	2.73	3.31	
90 Percentil	8.97	8.82	1314.31	9.24	40.32	0.69	0.08	21.56	63.44	6.87	-26.22	7.36	2.49	5.69	3.64	
Count	30	30	30	30	30	30	30	30	30	30	30	30	30	30	30.00	
WASTE ROCK SAMPLES																
WRF10-04(	9.14	9.13	1178.50	_	_	3.26	0.06	101.88	92.67	5.13	9.21	3.26	4.27	5.73	0.91	Moderate
WRF10-04(	9.08	9.10	1206.30	_	_	2.91	0.05	90.94	112.07	4.57	-21.13	4.67	0.00	0.00	1.23	Moderate
WRF10-04(	8.93	9.02	1224.70	_	_	2.97	0.06	92.81	90.75	5.22	2.06	4.21	2.38	4.09	0.98	Moderate
WRW 01-05	8.64	8.72	1402.80	_	_	2.96	0.05	92.50	87.64	4.04	4.86	3.54	5.24	7.32	0.95	Moderate
WRW 01-05	8.79	8.78	1387.50	_	_	2.72	0.06	85.00	98.43	4.94	-13.43	5.08	0.00	0.00	1.16	Moderate
WRW 01-05	8.81	8.83	1391.90	_	_	2.78	0.06	86.88	119.27	5.14	-32.40	4.87	0.00	0.00	1.37	Moderate
Maximum	9.14	9.13	1402.80	0.00	0.00	3.26	0.06	101.88	119.27	5.22	9.21	5.08	5.24	7.32	1.37	
Minimum	8.64	8.72	1178.50	0.00	0.00	2.72	0.05	85.00	87.64	4.04	-32.40	3.26	0.00	0.00	0.91	
Mean	8.90	8.93	1298.62	#DIV/0!	#DIV/0!	2.93	0.06	91.67	100.14	4.84	-8.47	4.27	1.98	2.86	1.10	
Standard De	0.19	0.18	105.71	#DIV/0!	#DIV/0!	0.19	0.01	5.90	12.74	0.46	16.48	0.74	2.36	3.29	0.18	
Median	8.87	8.93	1306.10	#NUM!	#NUM!	2.94	0.06	91.72	95.55	5.04	-5.68	4.44	1.19	2.05	1.07	
Count	6	6	6	0	0	6	6	6	6	6	6	6	6	6	6	
Metals Data on Trojan Composite Samples																
%	Al	Ni	Ca	Mg	Co	Cr	Cu	Fe	Na	K	Mn	Pb	Sb	Zn	Cd	As
Sample ID		Sample date: March 2005														
TR-TL1	0.004	0.207	0.782	13.87	0.008	0.042	0.014	12.84	0.003	<0.001	ND	<0.001	ND	ND	<0.001	<0.001
TR-TL2	0.002	0.225	0.922	14.93	0.009	0.038	0.017	13.06	0.006	<0.001	ND	<0.001	ND	ND	<0.001	<0.001
TR-TL3	0.003	0.178	0.974	15.42	0.007	0.056	0.015	12.72	0.005	<0.001	ND	<0.001	ND	ND	<0.001	<0.001
TR-TL4	0.004	0.187	1.083	12.87	0.008	0.061	0.013	14.04	0.004	<0.001	ND	<0.001	ND	ND	<0.001	<0.001
TR-TL5	0.003	0.258	0.976	14.89	0.008	0.041	0.016	13.97	0.007	<0.001	ND	<0.001	ND	ND	<0.001	<0.001
TR-TL6	0.003	0.213	0.872	15.08	0.009	0.039	0.018	13.17	0.005	<0.001	ND	<0.001	ND	ND	<0.001	<0.001
TR-TL7	0.002	0.217	1.124	14.77	0.007	0.042	0.017	14.86	0.006	<0.001	ND	<0.001	ND	ND	<0.001	<0.001
TR-TL8	0.002	0.243	0.833	13.94	0.006	0.053	0.019	15.21	0.006	<0.001	ND	<0.001	ND	ND	<0.001	<0.001
TR-TL9	0.004	0.221	0.927	13.78	0.007	0.045	0.018	14.03	0.004	<0.001	ND	<0.001	ND	ND	<0.001	<0.001
TR-TL10	0.005	0.223	0.985	15.19	0.009	0.039	0.016	14.94	0.007	<0.001	ND	<0.001	ND	ND	<0.001	<0.001
TR-WASTE	0.009	0.314	2.044	21.61	0.008	0.065	0.032	17.61	0.014	<0.001	ND	<0.001	ND	ND	<0.001	<0.001
Maximum	0.005	0.258	1.124	15.42	0.009	0.061	0.019	15.21	0.007	0	0	0	0	0	0	0
Minimum	0.002	0.178	0.782	12.87	0.006	0.038	0.013	12.72	0.003	0	0	0	0	0	0	0
Mean	0.0032	0.2172	0.9478	14.474	0.0078	0.0456	0.0163	13.884	0.0053	#DIV/0!	#DIV/0!	#DIV/0!	#DIV/0!	#DIV/0!	#DIV/0!	#DIV/0!

Mazowe Mine (Site 2) ABA data																
SampleId.	PastepH	Rinse pH	EC	Moisture	Porosity	S(Total)	C(Total)	MPA	ANC	TotalCaNC	NAPP	NAGpH	NAGpH4.	NAGpH7.	ABAR	FizzRating
	(pHunits)	(pHunits)	uS/cm	%	%	(%)	(%)	kgH2SO4	kgCaCO3	(t CaCO3/1	(kgH2SO4	(pHunits)	kgH2SO4	kgH2SO4/t		
Sample date:May 2005																
Method	Measured	Measured	Measured	Measured	Measure	Measure	Measure	Calculate	Measured	Calculated	Calculated	Measured	Calculated	Calculated	Calculated	Observed
MZ-TL1	2.87	3.15	1847.70	12.64	26.74	4.38	0.09	136.88	128.84	7.80	8.04	3.48	11.04	19.84	0.94	Slight
MZ-TL2	6.29	6.27	1528.30	14.77	24.19	4.09	0.13	127.81	139.04	10.90	-11.23	7.43	0.00	0.00	1.09	Slight
MZ-TL3	8.36	8.21	1219.50	16.08	28.32	5.16	0.07	161.25	127.15	6.23	34.10	2.85	15.94	22.18	0.79	Slight
MZ-TL4	7.45	7.44	1208.60	11.53	23.47	5.25	0.06	164.06	130.78	5.20	33.28	2.61	15.09	21.97	0.80	Slight
MZ-TL5	9.52	9.46	1178.40	13.28	22.96	4.63	0.11	144.69	125.64	9.20	19.05	3.04	12.15	16.05	0.87	Slight
MZ-WASTE	6.83	6.71	1256.80	12.41	27.63	6.19	0.08	193.44	137.92	6.97	55.52	2.17	17.82	24.56	0.71	Slight
Maximum		9.52	9.46	1847.70	16.08	28.32	5.25	0.13	164.06	139.04	10.90	34.10	7.43	15.94	22.18	1.09
Minimum		2.87	3.15	1178.40	11.53	22.96	4.09	0.06	127.81	125.64	5.20	-11.23	2.61	0.00	0.00	0.79
Mean		6.90	6.91	1396.50	13.66	25.14	4.70	0.09	146.94	130.29	7.87	16.65	3.88	10.84	16.01	0.90
Standard Deviation		2.55	2.40	289.46	1.79	2.30	0.50	0.03	15.57	5.25	2.28	18.96	2.01	6.39	9.28	0.12
Median		7.45	7.44	1219.50	13.28	24.19	4.63	0.09	144.69	128.84	7.80	19.05	3.04	12.15	19.84	0.87
Count		5	5	5	5	5	5	5	5	5	5	5	5	5	5	5
Metals Data																
	Al	As	Ca	Cd	Co	Cr	Cu	Fe	K	Mg	Mn	Na	Ni	Pb	Sb	Zn
	%	%	%	%	%	%	%	%	%	%	%	%	%	%	%	%
MZ-TL1	0.001	0.06	3.84	0.004	<0.001	0.023	0.14	16.37	0.002	0.11	0.04	0.09	<0.001	ND	0.005	0.02
MZ-TL2	0.002	0.08	7.03	0.007	<0.001	0.017	0.09	14.08	0.001	0.18	0.06	0.08	<0.001	ND	0.006	0.05
MZ-TL3	0.001	0.12	5.48	0.006	<0.001	0.022	0.11	17.16	0.003	0.26	0.03	0.08	<0.001	ND	0.008	0.03
MZ-TL4	0.003	0.09	8.09	0.002	<0.001	0.018	0.07	13.84	0.003	0.22	0.04	0.08	<0.001	ND	0.003	0.02
MZ-TL5	0.002	0.07	8.12	0.004	<0.001	0.032	0.06	15.27	0.004	0.16	0.04	0.14	<0.001	ND	0.004	0.01
MZ-W ROC	0.004	0.16	3.54	0.003	<0.001	0.046	0.03	7.43	0.006	0.25	0.08	0.27	<0.001	ND	0.009	0.04
Maximum	0.003	0.120	8.120	0.007	0.000	0.032	0.140	17.160	0.004	0.260	0.060	0.140	0.000	0.000	0.008	0.050
Minimum	0.001	0.060	3.840	0.002	0.000	0.017	0.060	13.840	0.001	0.110	0.030	0.080	0.000	0.000	0.003	0.010
Mean	0.002	0.084	6.512	0.005	#DIV/0!	0.022	0.094	15.344	0.003	0.186	0.042	0.094	#DIV/0!	#DIV/0!	0.005	0.026
Standard De	0.001	0.023	1.840	0.002	#DIV/0!	0.006	0.032	1.433	0.001	0.057	0.011	0.026	#DIV/0!	#DIV/0!	0.002	0.015
Median	0.002	0.080	7.030	0.004	#NUM!	0.022	0.090	15.270	0.003	0.180	0.040	0.080	#NUM!	#NUM!	0.005	0.020
Count	5	5	5	5	0	5	5	5	5	5	5	5	0	0	5	5

Iron Duke Mine (Site 3) ABA Data															
Comments: Jig Plant Tailings															
	PastepH	Rinse pH	EC	Moisture	Porosity	S(Total)	C(Total)	MPA	ANC	TotalCaNC	NAPP	NAGpH	NAGpH4.	NAGpH7.	FizzRating
	(pHunits)	(pHunits)	uS/cm	%	%	(%)	(%)	kgH2SO4	kgCaCO3	(t CaCO3/1	(kgH2SO4	(pHunits)	kgH2SO4	kgH2SO4/t	
Date Sampled: June 2005															
	Measured	Measured	Measured	Measured	Measure	Measure	Measure	Calculate	Measured	Calculated	Calculated	Measured	Calculated	Calculated	Observed
JPT10	4.67	3.96	1674.80	19.42	27.18	12.26	0.09	383.13	27.09	7.37	356.04	1.72	163.43	287.41	Slight
JPT11	3.19	3.27	1827.60	21.87	31.42	10.47	0.08	327.19	30.41	6.80	296.78	2.45	136.19	241.63	Slight
JPT12	4.76	4.21	2096.50	25.94	24.53	14.56	0.10	455.00	22.86	8.13	432.14	2.08	140.43	200.78	Slight
JPT13	4.09	4.11	2114.50	24.06	29.56	9.73	0.07	304.06	32.81	5.44	271.25	2.36	138.77	196.42	Slight
JPT14	5.97	5.65	1848.20	17.22	23.68	8.75	0.08	273.44	26.19	6.35	247.25	2.20	140.48	193.08	Slight
JPT15	4.88	4.64	1738.40	19.35	26.11	13.48	0.08	421.25	25.66	6.86	395.59	1.95	148.43	233.26	Slight
JPT16	5.65	5.59	1863.70	23.81	27.08	12.95	0.09	404.69	31.73	7.73	372.96	2.64	119.47	241.11	Slight
JPT17	5.73	5.71	2054.30	21.49	24.28	14.84	0.04	463.75	30.89	3.72	432.86	2.19	137.28	174.92	Slight
Maximum	5.97	5.71	2114.50	25.94	31.42	14.84	0.10	463.75	32.81	8.13	432.86	2.64	163.43	287.41	
Minimum	3.19	3.27	1674.80	17.22	23.68	8.75	0.04	273.44	22.86	3.72	247.25	1.72	119.47	174.92	
Mean	4.87	4.64	1902.25	21.65	26.73	12.13	0.08	379.06	28.46	6.55	350.61	2.20	140.56	221.08	
Standard De	0.93	0.92	166.67	2.90	2.70	2.26	0.02	70.57	3.50	1.41	71.56	0.29	12.32	36.46	
Median	4.82	4.43	1855.95	21.68	26.60	12.61	0.08	393.91	28.75	6.83	364.50	2.20	139.60	217.02	
Count	8	8	8	8	8	8	8	8	8	8	8	8	8	8	

APPENDIX D: Trends in Drainage Chemistry at Iron Duke

Fig. AP6.1 Mine water pH, flow & Temperature

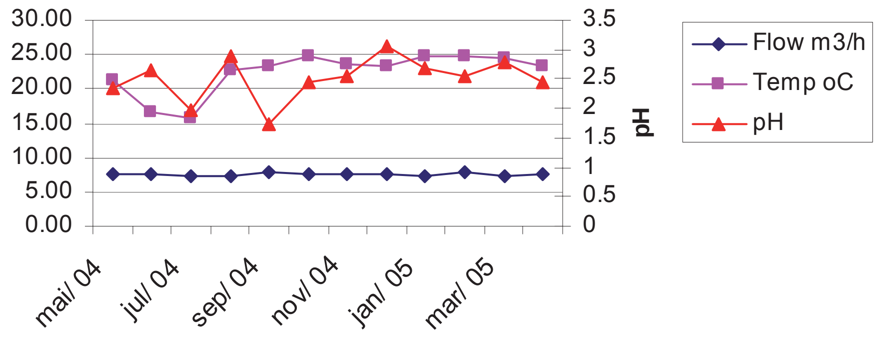

Fig.AP6.2 Mine water Acidity,TDS & EC

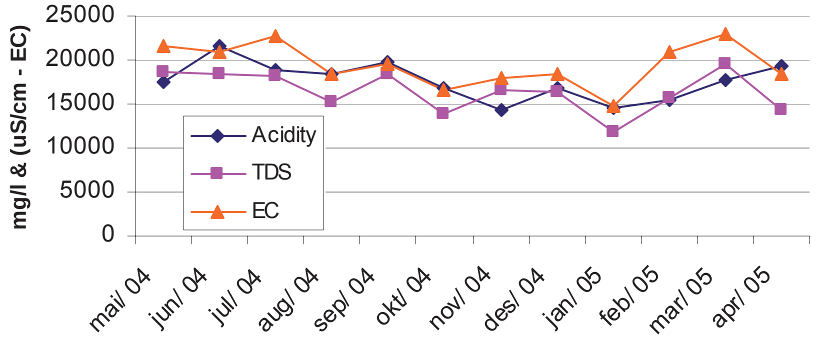

Fig.AP6.3 Mine Water Major Anions

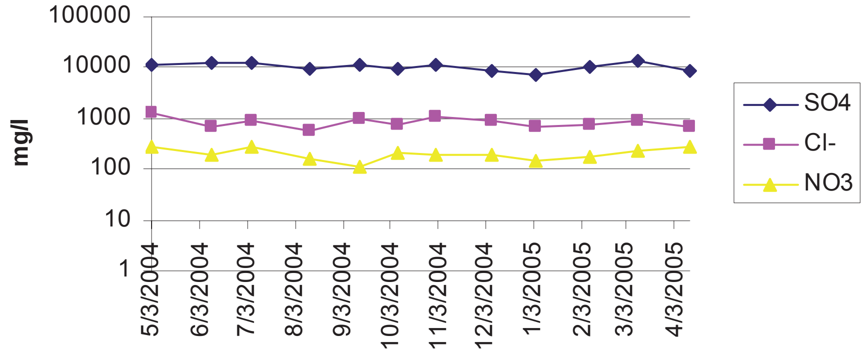

Fig.AP6.4 Mine water Cations

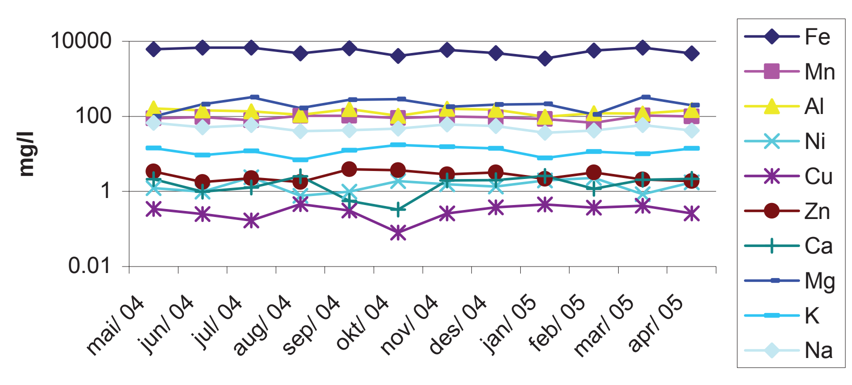

Fig.AP6.5 Ground water cheimistry for polluted aquifer

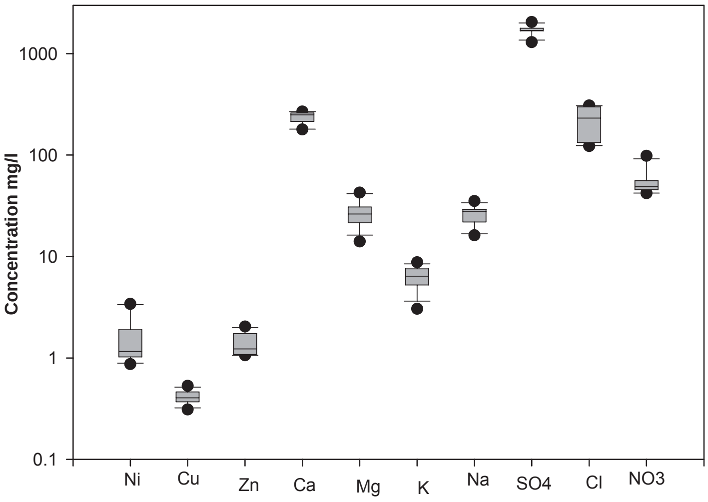

Fig.AP6.6 Seepage Zone (D) water Chemistry along Yellow Jacket

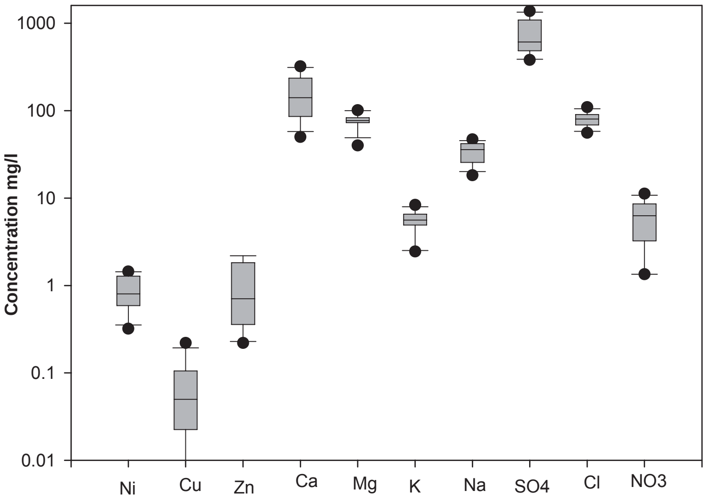

Fig.AP6.7 Background water chemistry upstream of seepage zone

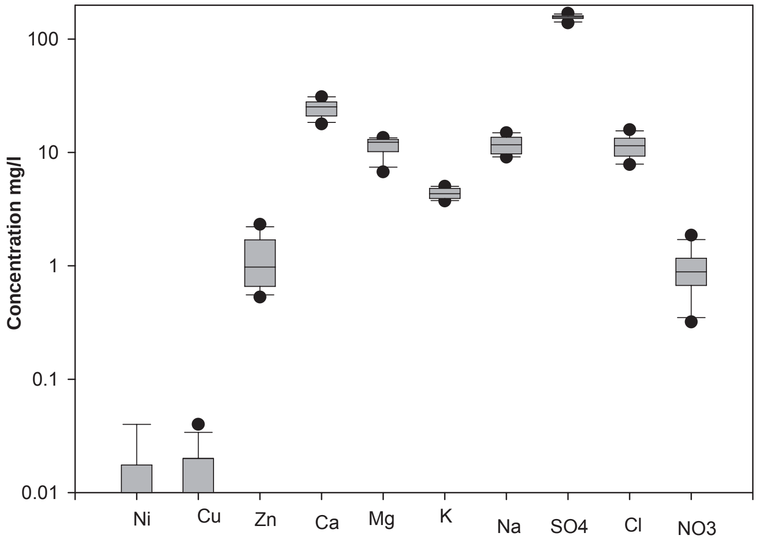

Fig.AP6.8 Mine components pH Profile

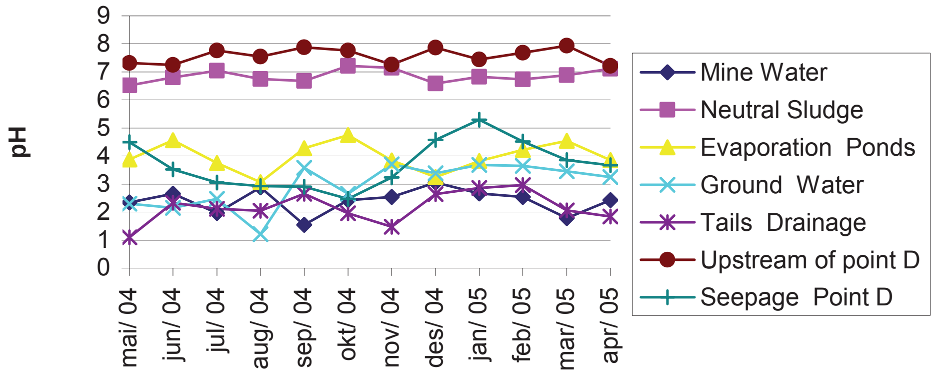

APPENDIX E: Phreeqc Geochemical Modelling Input and Output Files

Simulation Experiment 1:

```
TITLE Oxidation of AMD
SOLUTION 1 AMD        # Composition of Mine Water at Iron Duke
Mine
    units   mg/l;
    pH      2.34;       pe  4.60;      temp 21.4
    S(6)   11754.22 charge;    Mn  88.45;     Zn  3.43
    Cl     1237.04;     Al  161.43;    Ca  2.13
    N(5)   287.26;      Si  1.12;      Mg  98.67
    Fe     6172.45;     Cu  0.34;      K   14.32
    Na     67.24
    Alkalinity 0    as HCO3
REACTION 1
    O2(g)
    0.1 mole in 10 steps
    End
SOLUTION 2
    Units mg/l
    pH 3.225; pe 18.324
    S(6)   11754.22 charge;    Mn  88.45;     Zn  3.43
    Cl     1237.04;     Al  161.43;    Ca  2.13
    N(5)   287.26;      Si  1.12;      Mg  98.67
    Fe     6172.45;     Cu  0.34;      K   14.32
    Na     67.24
    Alkalinity 0    as HCO3
USE SOLUTION 2
REACTION 2
    Calcite
    CO2(g)
    0.3 moles in 10 steps
KINETICS 1 AMD Neutralisation with Calcite Dissolution
    Calcite
    -m 1.78e-2
    -m0 1.78e-2
    -parms 5.0 0.3
    -tol 1.e-8
    -steps 1000 2500 4500 5000 7500 8500 9500 10000 12000 15000
# seconds
    -step_divide 100
RATES
    Calcite
    -start
    1   rem M = current number of moles of calcite
    2   rem M0 = number of moles of calcite initially present
    3   rem PARM(1) = A/V, cm^2/L
    4   rem PARM(2) = exponent for M/M0
    10  si_cc = SI("Calcite")
    20  if (M<=0 and si_cc<0) then goto 200
    30  k1 = 10^(0.198-444.0/TK)
    40  k2 = 10^(2.84-2177.0/TK)
```

```
    50  if TC<=25 then k3 = 10^(-5.86-317.0/TK)
    60  if TC>25 then k3 = 10^(-1.1-1737.0/TK)
    70  t = 1
    80  if M0>0 then t = M/M0
    90  if t = 0 then t = 1
    100   moles = parm(1) * 0.1 * (t)^parm(2)
    110   moles = moles * (k1 * act("H+") + k2 * act("CO2") + k3
* act("H2O"))
   120   moles = moles * (1 - 10^(2/3*si_cc))
   130   moles = moles * time
   140  if (moles > m) then moles = m
   150 if (moles >= 0) then goto 200
   160  temp = tot("Ca")
   170  mc  = tot("C(4)")
   180  if mc < temp then temp = mc
   190  if -moles > temp then moles = -temp
   200 save moles
  -end
  SELECTED_OUTPUT
    -file AMDoxd3.csv
    -molalities Fe+2 Fe+3 Ca+2
    -saturation_indices O2(g) CO2(g) Anhydrite Calcite Gibbsite
Goethite Gypsum Jarosite-K Pyrolusite
  END
```

Simulation Experiment 2:

```
Title   # AMD Mixing with Yellow Jacket Stream Water
 SOLUTION 1 AMD # Composition of Mine water
    units   mg/l;
    pH      2.34;  pe           4.60;  temp    21.4
    S(6)   11754.22 charge;     Mn  88.45;     Zn  3.43
    Cl     1237.04;             Al  161.43;    Ca  2.13
    N(5)   287.26;              Si  1.12;      Mg  98.67
    Fe     6172.45;             Cu  0.34;      K   14.32
    Na     67.24
    Alkalinity 0    as HCO3
SELECTED_OUTPUT
    -file Mixing.csv
    -totals Al  Cu Fe  Mn  S(6) Zn
    -saturation_indices  Ferrihydrite  Goethite Gibbsite  Gypsum
Pyrolusite
End



SOLUTION 2 BGSW      # Composition of Background surface water
    units   mg/l;
    pH      7.32;           pe  12.63;     temp 20.4
    S(6)   139.45 charge;   Mn  1.87;       Zn  0.61
    Cl     12.34;           Al  0.05;       Ca  28.06
    N(5)   1.34;            Si  0.08;       Mg  29.04
    Fe     0.87;            Cu  0.02;        K   5.03
```

```
    Na     12.66
    Alkalinity 108.25    as HCO3

EQUILIBRIUM_PHASES
    CO2(g)  -3.5
    O2(g)   -0.68
End
MIX 1 mixing AMD and stream water
    1   1.0
    2   1.0
End
MIX 2  dry season
    1   1.0
    2   6.0
End
MIX 3
    1   1.0
    2   50
End
MIX 4   wet season
    1   1.0
    2   100
End
MIX 5   Floods
    1   1.0
    2   1000

SAVE SOLUTION 3
END

USE SOLUTION 3
PHASES; Ferrihydrite; Fe(OH)3 + 3H+ = Fe+3 + 3H2O; -log_k 2.0
EQUILIBRIUM_PHASES
 O2(g) -0.68             # P_O2 = 0.21 atm (log 0.21 = -0.68)
 Ferrihydrite 0.0 0.0     # SI = 0.0, initial amount = 0.0
 CO2(g) -3.5
SAVE SOLUTION 4
SAVE equilibrium_phases 2
END
USE SOLUTION 4
USE Equilibrium_phases 2
SURFACE 1
 Hfo_w Ferrihydrite 0.2 5.33e4      # weak sites, 0.2 mol/mol,
surface area 5.33e4 m2/mol
 Hfo_s Ferrihydrite 0.5e-2   # strong sites 2.5% of weak sites
 -equil 1
SURFACE_SPECIES
 Hfo_wOH + CO3-2 + H+ = Hfo_wCO3- + H2O; log_k 12.56
 Hfo_wOH + CO3-2 + 2H+= Hfo_wHCO3 + H2O; log_k 20.62

USER_PRINT
 -start
```

```
 10 print 'pH  Al_tot  Mn Zn'
 20 print -la("H+"), tot("Al") * 26.98e6, tot("Mn") * 54.94e6,
tot("Zn") * 65.39e6
 -end
END
```

Simulation Experiment 3:

```
Title # Acidification & Buffering in Aquifer
SOLUTION 1-50  # Fresh pore water in aquifer at start
 units mg/l
 pH 7.5; temp 21.4
 Na 19.28; K 2.65;   Mg 32.34;  Ca 43.65;  Al 0.09
 Cl 10.03; S(6) 156.64 charge; N(5) 3.54;  Mn 27.43; Cu 0.04;
 Zn 0.87; Alkalinity 197.55 as HCO3

EQUILIBRIUM_PHASES 1-50
Gibbsite 0.29; CO2(g) -3.5
SAVE solution 1-50
END
EXCHANGE 1-50
 X 0.08; -equilibrate 1
END
PRINT; -reset true
SOLUTION 0  # Seepage from evaporation ponds enters the aquifer
 units mg/l
 pH 4.5;       temp 23.5
 Na 16.85; K 19.18;   Mg 21.09;   Ca 28.17;  Fe 907.52
 Cl 78.16; S(6) 1850.86 charge; N(5) 28.96; Mn 106.26; Al 3.84
 Cu 1.18; Zn 1.87
END

TRANSPORT    # 8 yr flow, 7.5 m/yr, in 100 m
 -cells 50;              -length 2
 -time_step 2.52e8
 -flow_direction forward; -shifts 30
 -dispersivity 1;         -punch_frequency 30
USER_GRAPH
 -heading dist Al Mn Fe S(6) Alk
 -init false
 -plot_concentration_vs x
 -axis_titles "Distance / m" "mmol/L"
 -start
 10 graph_x dist
 20 graph_y tot("Al")*1e3, tot("Mn")*1e3, tot("Fe")*1e3,\
            tot("S(6)")*1e3, Alk*1e3
 -end
END
```

Simulation Experiment 4:

```
Title # Aquifer Injection with Uncontaminated Stream water
SOLUTION 1-4  # Groundwater in aquifer
```

```
units mg/l
pH 3.58; pe 13.89; temp 22.4
Na 27.07; K 6.43; Mg 31.25; Ca 254.38
Zn 1.22; Cu 0.42; Al 2.45; Mn 245.03
Fe 378.23; Cl 287.34; N(5) 45.65; S(6) 1684.7 charge

EXCHANGE_SPECIES
 Mg+2 + 2X- = MgX2; -log_k 0.54; -gamma 5.5 0.2
 Ca+2 + 2X- = CaX2; -log_k 0.78; -gamma 5.0 0.165
EXCHANGE 1-4
 X 0.08; -equilibrate 1
PRINT; -reset  false
END

SOLUTION 0   # Injected solution - uncontaminated stream water
 Units mg/l
 pH 7.32; pe 12.58; Na 12.66; K 5.03
 Mg 29.04; Ca 28.06; Zn 0.61; Cu 0.02
 Al 0.05; Mn 1.87; Fe 0.87; Cl 12.34
 N(5) 1.34; S(6) 139.45 charge

END

TRANSPORT
 -cells     4
 -shifts  330
 -length 19.24  13.83  12.94  12.48
 -dispersivity 1.0
 -punch     4
USER_GRAPH
 -headings Injected Cl S(6) Mn Fe
 -axis_scale  x_axis  100  100000  auto  auto  true   #  logarithmic
axes
 -axis_scale y_axis 0.1 160 auto auto true
 -plot_concentration_vs time
 -axis_titles "m^3 injected" "mmol/L"
 -start
 10 V0 = 300          # m3 of injected stream water into aquifer
 20 graph_x V0 * (step_no + 0.5)/cell_no
 30 graph_y 1e3 * tot("Cl"), 1e3 * tot("S(6)"), 1e3 * tot("Mn"),
1e3 * tot("Fe")
 -end
END
```

E1:Saturation Indices							
SOLUTION 1							
	Phase	**SI**	**log IAP**	**log KT**			
	Al(OH)3(a)	-8.24	2.8	11.04	Al(OH)3		
	Albite	-16.42	-34.66	-18.23	NaAlSi3O8		
	Alunite	-4.94	-5.89	-0.95	KAl3(SO4)2(OH)6		
	Anhydrite	-2.54	-6.88	-4.35	CaSO4		
	Anorthite	-30.42	-50.24	-19.82	CaAl2Si2O8		
	Ca-Montmorillonite	-18.88	-64.43	-45.55	Ca0.165Al2.33Si3.67O10(OH)2		
	Chalcedony	-1.09	-4.69	-3.59	SiO2		
	Chlorite(14A)	-70.67	-0.93	69.74	Mg5Al2Si3O10(OH)8		
	Chrysotile	-37.51	-4.86	32.65	Mg3Si2O5(OH)4		
	Fe(OH)3(a)	-8.1	-3.21	4.89	Fe(OH)3		
	Gibbsite	-5.51	2.8	8.31	Al(OH)3		
	Goethite	-2.34	-3.21	-0.87	FeOOH		
	Gypsum	-2.31	-6.89	-4.58	CaSO4:2H2O		
	H2(g)	-13.83	29.76	43.6	H2		
	H2O(g)	-1.6	0	1.6	H2O		
	Halite	-5.89	-4.32	1.57	NaCl		
	Hausmannite	-44.68	17.25	61.93	Mn3O4		
	Hematite	-2.69	-6.42	-3.73	Fe2O3		
	Illite	-22.6	-63.36	-40.76	K0.6Mg0.25Al2.3Si3.5O10(OH)2		
	Jarosite-K	-14.99	-23.92	-8.93	KFe3(SO4)2(OH)6		
	K-feldspar	-14.75	-35.6	-20.85	KAlSi3O8		
	K-mica	-20.18	-6.95	13.23	KAl3Si3O10(OH)2		
	Kaolinite	-11.52	-3.77	7.75	Al2Si2O5(OH)4		
	Manganite	-17.28	8.06	25.34	MnOOH		
	Melanterite	-1.3	-3.55	-2.25	FeSO4:7H2O		
	O2(g)	-56.67	-59.53	-2.87	O2		
	Pyrochroite	-14.08	1.12	15.2	Mn(OH)2		
	Pyrolusite	-26.96	15	41.96	MnO2:H2O		
	Quartz	-0.67	-4.69	-4.01	SiO2		
	Sepiolite	-26.91	-11.06	15.86	Mg2Si3O7.5OH:3H2O		
	Sepiolite(d)	-29.72	-11.06	18.66	Mg2Si3O7.5OH:3H2O		
	SiO2(a)	-1.95	-4.69	-2.74	SiO2		
	Talc	-36.05	-14.23	21.81	Mg3Si4O10(OH)2		
	Willemite	-21.37	-5.74	15.63	Zn2SiO4		
	Zn(OH)2(e)	-12.03	-0.53	11.5	Zn(OH)2		

Saturation Indices							
SOLUTION 2							
	Phase	**SI**	**log IAP**	**log KT**			
	Al(OH)3(a)	-1.06	10.05	11.1	Al(OH)3		
	Albite	-6.19	-24.49	-18.3	NaAlSi3O8		
	Alunite	-1.05	-1.87	-0.82	KAl3(SO4)2(OH)6		
	Anhydrite	-2.07	-6.42	-4.34	CaSO4		
	Anorthite	-5.36	-25.2	-19.85	CaAl2Si2O8		
	Aragonite	-0.91	-9.21	-8.31	CaCO3		
	Ca-Montmorillonite	-1.83	-47.52	-45.7	Ca0.165Al2.33Si3.67O10(OH)2		
	Calcite	-0.76	-9.21	-8.46	CaCO3		
	Chalcedony	-1.53	-5.14	-3.61	SiO2		
	Chlorite(14A)	-7.88	62.24	70.12	Mg5Al2Si3O10(OH)8		
	Chrysotile	-8.52	24.26	32.78	Mg3Si2O5(OH)4		
	CO2(g)	-2.33	-3.74	-1.41	CO2		
	Dolomite	-1.22	-18.2	-16.98	CaMg(CO3)2		
	Fe(OH)3(a)	2.97	7.86	4.89	Fe(OH)3		
	Gibbsite	1.67	10.05	8.37	Al(OH)3		
	Goethite	8.69	7.86	-0.83	FeOOH		
	Gypsum	-1.84	-6.42	-4.58	CaSO4:2H2O		
	H2(g)	-39.85	3.91	43.77	H2		
	H2O(g)	-1.63	0	1.63	H2O		
	Halite	-8.37	-6.8	1.57	NaCl		
	Hausmannite	7.45	69.64	62.19	Mn3O4		
	Hematite	19.37	15.72	-3.65	Fe2O3		
	Illite	-2.31	-43.21	-40.9	K0.6Mg0.25Al2.3Si3.5O10(OH)2		
	Jarosite-K	0.41	-8.44	-8.85	KFe3(SO4)2(OH)6		
	K-feldspar	-4.2	-25.13	-20.93	KAlSi3O8		
	K-mica	4.73	18.12	13.38	KAl3Si3O10(OH)2		
	Kaolinite	1.98	9.82	7.84	Al2Si2O5(OH)4		
	Manganite	4.52	29.86	25.34	MnOOH		
	Melanterite	-14.39	-16.66	-2.27	FeSO4:7H2O		
	O2(g)	-4.97	-7.83	-2.86	O2		
	Pyrochroite	-5.29	9.91	15.2	Mn(OH)2		
	Pyrolusite	7.69	49.81	42.13	MnO2:H2O		
	Quartz	-1.11	-5.14	-4.03	SiO2		
	Rhodochrosite	0.53	-10.58	-11.11	MnCO3		
	Sepiolite	-8.27	7.61	15.88	Mg2Si3O7.5OH:3H2O		
	Sepiolite(d)	-11.05	7.61	18.66	Mg2Si3O7.5OH:3H2O		
	Siderite	-8.59	-19.46	-10.86	FeCO3		
	SiO2(a)	-2.39	-5.14	-2.75	SiO2		
	Smithsonite	-1.27	-11.22	-9.95	ZnCO3		
	Talc	-7.94	13.99	21.93	Mg3Si4O10(OH)2		
	Willemite	-2.29	13.42	15.71	Zn2SiO4		
	Zn(OH)2(e)	-2.22	9.28	11.5	Zn(OH)2		

Saturation Indices							
SOLUTION 3							
	Phase	**SI**	**log IAP**	**log KT**			
	Al(OH)3(a)	-9.24	1.67	10.91	Al(OH)3		
	Albite	-18.09	-36.2	-18.11	NaAlSi3O8		
	Alunite	-9.38	-10.57	-1.19	KAl3(SO4)2(OH)6		
	Anhydrite	-0.71	-5.06	-4.35	CaSO4		
	Anorthite	-30.29	-50.05	-19.76	CaAl2Si2O8		
	Ca-Montmorillonite	-21.39	-66.66	-45.27	Ca0.165Al2.33Si3.67O10(OH)2		
	Chalcedony	-1.24	-4.81	-3.57	SiO2		
	Chlorite(14A)	-74.47	-5.45	69.02	Mg5Al2Si3O10(OH)8		
	Chrysotile	-38.65	-6.24	32.41	Mg3Si2O5(OH)4		
	Fe(OH)3(a)	-2.07	2.82	4.89	Fe(OH)3		
	Gibbsite	-6.54	1.67	8.21	Al(OH)3		
	Goethite	3.76	2.82	-0.94	FeOOH		
	Gypsum	-0.48	-5.06	-4.58	CaSO4:2H2O		
	H2(g)	-29.1	14.18	43.28	H2		
	H2O(g)	-1.55	0	1.55	H2O		
	Halite	-6.83	-5.25	1.58	NaCl		
	Hausmannite	-27	34.46	61.45	Mn3O4		
	Hematite	9.52	5.64	-3.88	Fe2O3		
	Illite	-25.73	-66.22	-40.5	K0.6Mg0.25Al2.3Si3.5O10(OH)2		
	Jarosite-K	1.97	-7.11	-9.08	KFe3(SO4)2(OH)6		
	K-feldspar	-16.53	-37.23	-20.7	KAlSi3O8		
	K-mica	-24	-11.05	12.95	KAl3Si3O10(OH)2		
	Kaolinite	-13.86	-6.27	7.58	Al2Si2O5(OH)4		
	Manganite	-9	16.34	25.34	MnOOH		
	Melanterite	-3.43	-5.66	-2.23	FeSO4:7H2O		
	O2(g)	-25.49	-28.37	-2.88	O2		
	Pyrochroite	-13.43	1.77	15.2	Mn(OH)2		
	Pyrolusite	-10.74	30.91	41.65	MnO2:H2O		
	Quartz	-0.82	-4.81	-3.98	SiO2		
	Sepiolite	-27.98	-12.17	15.8	Mg2Si3O7.5OH:3H2O		
	Sepiolite(d)	-30.83	-12.17	18.66	Mg2Si3O7.5OH:3H2O		
	SiO2(a)	-2.08	-4.81	-2.73	SiO2		
	Talc	-37.45	-15.85	21.59	Mg3Si4O10(OH)2		
	Willemite	-21.41	-5.94	15.47	Zn2SiO4		
	Zn(OH)2(e)	-12.06	-0.56	11.5	Zn(OH)2		

Saturation Indices							
SOLUTION 4							
	Phase	**SI**	**log IAP**	**log KT**			
	Al(OH)3(a)	-8.16	2.64	10.81	Al(OH)3		
	Albite	-16.81	-34.82	-18.01	NaAlSi3O8		
	Alunite	-6.9	-8.29	-1.39	KAl3(SO4)2(OH)6		
	Anhydrite	-0.59	-4.95	-4.36	CaSO4		
	Anorthite	-27.44	-47.15	-19.72	CaAl2Si2O8		
	Ca-Montmorillonite	-18.66	-63.7	-45.04	Ca0.165Al2.33Si3.67O10(OH)2		
	Chalcedony	-1.2	-4.75	-3.55	SiO2		
	Chlorite(14A)	-67.36	1.06	68.42	Mg5Al2Si3O10(OH)8		
	Chrysotile	-35.7	-3.49	32.21	Mg3Si2O5(OH)4		
	Fe(OH)3(a)	-3.44	1.45	4.89	Fe(OH)3		
	Gibbsite	-5.47	2.64	8.12	Al(OH)3		
	Goethite	2.44	1.45	-1	FeOOH		
	Gypsum	-0.37	-4.95	-4.58	CaSO4:2H2O		
	H2(g)	-31.6	11.42	43.01	H2		
	H2O(g)	-1.51	0	1.51	H2O		
	Halite	-7.35	-5.77	1.58	NaCl		
	Hausmannite	-25.09	35.97	61.05	Mn3O4		
	Hematite	6.9	2.9	-4	Fe2O3		
	Illite	-22.81	-63.09	-40.28	K0.6Mg0.25Al2.3Si3.5O10(OH)2		
	Jarosite-K	-2.68	-11.88	-9.2	KFe3(SO4)2(OH)6		
	K-feldspar	-15.2	-35.78	-20.58	KAlSi3O8		
	K-mica	-20.53	-7.82	12.72	KAl3Si3O10(OH)2		
	Kaolinite	-11.65	-4.21	7.44	Al2Si2O5(OH)4		
	Manganite	-8.08	17.26	25.34	MnOOH		
	Melanterite	-6.5	-8.71	-2.21	FeSO4:7H2O		
	O2(g)	-19.94	-22.83	-2.89	O2		
	Pyrochroite	-13.76	1.44	15.2	Mn(OH)2		
	Pyrolusite	-8.31	33.08	41.4	MnO2:H2O		
	Quartz	-0.79	-4.75	-3.96	SiO2		
	Sepiolite	-26	-10.24	15.76	Mg2Si3O7.5OH:3H2O		
	Sepiolite(d)	-28.9	-10.24	18.66	Mg2Si3O7.5OH:3H2O		
	SiO2(a)	-2.04	-4.75	-2.71	SiO2		
	Talc	-34.39	-12.98	21.41	Mg3Si4O10(OH)2		
	Willemite	-21.31	-5.97	15.34	Zn2SiO4		
	Zn(OH)2(e)	-12.11	-0.61	11.5	Zn(OH)2		

E2: Distribution of Species						
SOLUTION 1						
				Log	**Log**	**Log**
	Species	**Molality**	**Activity**	**Molality**	**Activity**	**Gamma**
	H+	5.83E-03	4.57E-03	-2.234	-2.34	-0.106
	OH-	2.44E-12	1.65E-12	-11.612	-11.782	-0.17
	H2O	5.55E+01	9.96E-01	1.744	-0.002	0
Al	6.10E-03					
	AlSO4+	3.78E-03	2.78E-03	-2.423	-2.556	-0.134
	Al(SO4)2-	1.77E-03	1.30E-03	-2.752	-2.885	-0.134
	Al+3	5.49E-04	6.11E-05	-3.26	-4.214	-0.954
	AlHSO4+2	3.74E-06	1.09E-06	-5.427	-5.961	-0.534
	AlOH+2	3.57E-07	1.04E-07	-6.447	-6.981	-0.534
	Al(OH)2+	1.76E-10	1.29E-10	-9.755	-9.888	-0.134
	Al(OH)3	2.95E-15	3.17E-15	-14.53	-14.5	0.03
	Al(OH)4-	1.69E-18	1.24E-18	-17.772	-17.906	-0.134
Ca	5.42E-05					
	Ca+2	2.98E-05	8.69E-06	-4.526	-5.061	-0.535
	CaSO4	2.36E-05	2.53E-05	-4.627	-4.598	0.03
	CaHSO4+	8.81E-07	6.48E-07	-6.055	-6.189	-0.134
	CaOH+	4.27E-16	3.14E-16	-15.369	-15.503	-0.134
Cl	3.56E-02					
	Cl-	3.47E-02	2.37E-02	-1.46	-1.625	-0.166
	FeCl+	8.50E-04	6.25E-04	-3.07	-3.204	-0.134
	MnCl+	3.67E-05	2.70E-05	-4.436	-4.569	-0.134
	ZnCl+	4.60E-07	3.38E-07	-6.337	-6.471	-0.134
	MnCl2	2.60E-07	2.79E-07	-6.584	-6.554	0.03
	ZnCl2	7.72E-09	8.27E-09	-8.112	-8.082	0.03
	MnCl3-	2.48E-09	1.82E-09	-8.606	-8.74	-0.134
	ZnCl3-	2.93E-10	2.15E-10	-9.533	-9.667	-0.134
	FeCl+2	1.30E-10	3.79E-11	-9.887	-10.421	-0.534
	ZnCl4-2	8.50E-12	2.49E-12	-11.07	-11.605	-0.534
	FeCl2+	6.13E-12	4.51E-12	-11.212	-11.346	-0.134
	FeCl3	9.98E-15	1.07E-14	-14.001	-13.971	0.03
Cu(1)	1.73E-08					
	Cu+	1.73E-08	1.12E-08	-7.762	-7.953	-0.191
Cu(2)	5.44E-06					
	Cu+2	2.99E-06	8.75E-07	-5.524	-6.058	-0.534
	CuSO4	2.45E-06	2.63E-06	-5.611	-5.581	0.03
	CuOH+	2.76E-12	1.91E-12	-11.559	-11.72	-0.161
	Cu(OH)2	8.10E-16	8.68E-16	-15.092	-15.062	0.03
	Cu(OH)3-	1.55E-26	1.14E-26	-25.81	-25.944	-0.134
	Cu(OH)4-2	1.69E-36	4.95E-37	-35.771	-36.306	-0.534
Fe(2)	1.13E-01					
	Fe+2	6.53E-02	1.91E-02	-1.185	-1.719	-0.534
	FeSO4	4.47E-02	4.79E-02	-1.35	-1.32	0.03
	FeHSO4+	1.94E-03	1.42E-03	-2.713	-2.847	-0.134
	FeCl+	8.50E-04	6.25E-04	-3.07	-3.204	-0.134
	FeOH+	1.36E-09	1.00E-09	-8.866	-8.999	-0.134

Fe(3)	1.76E-08					
	FeSO4+	1.23E-08	9.07E-09	-7.909	-8.042	-0.134
	Fe(SO4)2-	4.01E-09	2.95E-09	-8.397	-8.53	-0.134
	Fe+3	5.34E-10	5.95E-11	-9.272	-10.226	-0.954
	FeHSO4+2	3.81E-10	1.11E-10	-9.419	-9.953	-0.534
	FeOH+2	2.31E-10	6.75E-11	-9.636	-10.171	-0.534
	FeCl+2	1.30E-10	3.79E-11	-9.887	-10.421	-0.534
	FeCl2+	6.13E-12	4.51E-12	-11.212	-11.346	-0.134
	Fe(OH)2+	5.77E-12	4.24E-12	-11.239	-11.373	-0.134
	FeCl3	9.98E-15	1.07E-14	-14.001	-13.971	0.03
	Fe(OH)3	9.48E-17	1.02E-16	-16.023	-15.994	0.03
	Fe2(OH)2+4	1.95E-17	1.43E-19	-16.709	-18.846	-2.137
	Fe(OH)4-	2.37E-23	1.74E-23	-22.625	-22.759	-0.134
	Fe3(OH)4+5	3.86E-25	1.77E-28	-24.414	-27.753	-3.339
H(0)	1.76E-17					
	H2	8.79E-18	9.41E-18	-17.056	-17.026	0.03
K	3.74E-04					
	K+	3.42E-04	2.34E-04	-3.466	-3.632	-0.166
	KSO4-	3.16E-05	2.32E-05	-4.501	-4.634	-0.134
	KOH	1.65E-16	1.76E-16	-15.783	-15.753	0.03
Mg	4.14E-03					
	Mg+2	2.12E-03	6.73E-04	-2.674	-3.172	-0.498
	MgSO4	2.02E-03	2.17E-03	-2.694	-2.664	0.03
	MgOH+	5.21E-13	3.83E-13	-12.283	-12.417	-0.134
Mn(2)	1.64E-03					
	Mn+2	9.54E-04	2.79E-04	-3.021	-3.554	-0.534
	MnSO4	6.52E-04	6.98E-04	-3.186	-3.156	0.03
	MnCl+	3.67E-05	2.70E-05	-4.436	-4.569	-0.134
	MnCl2	2.60E-07	2.79E-07	-6.584	-6.554	0.03
	Mn(NO3)2	2.00E-07	2.14E-07	-6.699	-6.669	0.03
	MnCl3-	2.48E-09	1.82E-09	-8.606	-8.74	-0.134
	MnOH+	1.58E-12	1.16E-12	-11.801	-11.935	-0.134
Mn(3)	3.21E-24					
	Mn+3	3.21E-24	2.02E-25	-23.493	-24.695	-1.202
N(5)	2.09E-02					
	NO3-	2.09E-02	1.38E-02	-1.679	-1.859	-0.18
	Mn(NO3)2	2.00E-07	2.14E-07	-6.699	-6.669	0.03
Na	2.98E-03					
	Na+	2.78E-03	2.02E-03	-2.556	-2.695	-0.139
	NaSO4-	2.03E-04	1.49E-04	-3.693	-3.826	-0.134
	NaOH	2.71E-15	2.91E-15	-14.566	-14.536	0.03
O(0)	0.00E+00					
	O2	0.00E+00	0.00E+00	-59.561	-59.531	0.03
S(6)	1.25E-01					
	SO4-2	5.95E-02	1.51E-02	-1.226	-1.822	-0.596
	FeSO4	4.47E-02	4.79E-02	-1.35	-1.32	0.03
	HSO4-	8.43E-03	6.20E-03	-2.074	-2.208	-0.134
	AlSO4+	3.78E-03	2.78E-03	-2.423	-2.556	-0.134
	MgSO4	2.02E-03	2.17E-03	-2.694	-2.664	0.03

	FeHSO4+	1.94E-03	1.42E-03	-2.713	-2.847	-0.134
	Al(SO4)2-	1.77E-03	1.30E-03	-2.752	-2.885	-0.134
	MnSO4	6.52E-04	6.98E-04	-3.186	-3.156	0.03
	NaSO4-	2.03E-04	1.49E-04	-3.693	-3.826	-0.134
	KSO4-	3.16E-05	2.32E-05	-4.501	-4.634	-0.134
	CaSO4	2.36E-05	2.53E-05	-4.627	-4.598	0.03
	ZnSO4	2.00E-05	2.14E-05	-4.7	-4.67	0.03
	Zn(SO4)2-2	9.22E-06	2.70E-06	-5.035	-5.569	-0.534
	AlHSO4+2	3.74E-06	1.09E-06	-5.427	-5.961	-0.534
	CuSO4	2.45E-06	2.63E-06	-5.611	-5.581	0.03
	CaHSO4+	8.81E-07	6.48E-07	-6.055	-6.189	-0.134
	FeSO4+	1.23E-08	9.07E-09	-7.909	-8.042	-0.134
	Fe(SO4)2-	4.01E-09	2.95E-09	-8.397	-8.53	-0.134
	FeHSO4+2	3.81E-10	1.11E-10	-9.419	-9.953	-0.534
Si	1.90E-05					
	H4SiO4	1.90E-05	2.04E-05	-4.721	-4.691	0.03
	H3SiO4-	7.86E-13	5.78E-13	-12.104	-12.238	-0.134
	H2SiO4-2	2.32E-23	6.77E-24	-22.635	-23.169	-0.534
Zn	5.35E-05					
	Zn+2	2.39E-05	6.22E-06	-4.622	-5.206	-0.584
	ZnSO4	2.00E-05	2.14E-05	-4.7	-4.67	0.03
	Zn(SO4)2-2	9.22E-06	2.70E-06	-5.035	-5.569	-0.534
	ZnCl+	4.60E-07	3.38E-07	-6.337	-6.471	-0.134
	ZnCl2	7.72E-09	8.27E-09	-8.112	-8.082	0.03
	ZnCl3-	2.93E-10	2.15E-10	-9.533	-9.667	-0.134
	ZnCl4-2	8.50E-12	2.49E-12	-11.07	-11.605	-0.534
	ZnOH+	1.53E-12	1.13E-12	-11.814	-11.948	-0.134
	Zn(OH)2	3.47E-18	3.72E-18	-17.46	-17.43	0.03
	Zn(OH)3-	3.48E-27	2.56E-27	-26.458	-26.592	-0.134
	Zn(OH)4-2	3.03E-37	8.84E-38	-36.519	-37.054	-0.534